Stony Brook University

Molecular Movie Magic: Real-time Picosecond to Microsecond Structural Dynamics of Photoactive Flavoproteins

A Dissertation Presented

by

Richard Brust

to

The Graduate School

in Partial Fulfillment of the

Requirements

for the Degree of

Doctor of Philosophy

In

Chemistry

Stony Brook University

August 2013

Stony Brook University

The Graduate School

Richard Brust

We, the dissertation committee for the above candidate for the

Doctor of Philosophy degree, hereby recommend

acceptance of this dissertation.

Peter J. Tonge – Dissertation Advisor
Professor of Chemistry

Erwin London – Chair of Defense
Professor of Biochemistry and Cell Biology

Orlando Schärer – Committee Member of Defense
Professor of Chemistry

Mark Bowen – External Committee Member of Defense
Professor of Physiology and Biophysics, Stony Brook University

This dissertation is accepted by the Graduate School

Charles Taber
Interim Dean of the Graduate School

Abstract of the Dissertation

Molecular Movie Magic: Real-time Picosecond to Microsecond Structural Dynamics of Photoactive Flavoproteins

by

Richard Brust

Doctor of Philosophy

in

Chemistry

Stony Brook University

August 2013

Femtosecond (fs) excitation of photoreceptors results in protein structural changes that occur on the microsecond to millisecond timescale or longer. It is thus of fundamental interest to understand how these fast timescale events dictate large scale protein dynamics that occur on much longer (10^6 orders of magnitude) timescales. AppA is a blue light using FAD (BLUF) protein which acts as a transcriptional antirepressor in *Rhodobacter sphaeroides*. The ultrafast photocycle and IR spectra are well characterized and involve a near instantaneous (<100 fs) response of the protein matrix that surrounds the chromophore. While there has been extensive study on the ultrafast time scales there has never been an observation of the kinetics of the light induced structural changes in the protein. Here we investigated the ultrafast (ps) to ms structural dynamics through transient IR. The data show that significant structural changes occur on the sub microsecond timescale following photoactivation.

In addition our work has expanded to other BLUF proteins. BlsA is a BLUF protein found in the pathogenic bacterium *Acinetobacter baumannii*. Vibrational data together with homology modeling identify significant differences in β5 strand caused by photoactivation, a region of BLUF photoreceptors proposed to be essential for signal modulation, that are unique for BlsA. In addition, the BLUF protein PixD, from *Synechocystis*, was characterized by transient IR, where photoexcitation results in radical pair formation, an event not observed in AppA. Transient IR also revealed that light state formation is complete within nanoseconds for PixD, suggesting a unique mechanism for single and multidomain BLUF systems.

Dedication Page

To Lana, for never losing faith in me.

Table of Contents

List of Figures/Tables

Chapter 1

Chapter 2

Chapter 3

Chapter 4

Chapter 5

Chapter 6

List of Abbreviations

Ala (A)	Alanine
Amp	Ampicillin
AppA	Activation of photopigment and puc expression
$AppA_{BLUF}$	AppA blue light using FAD domain
$AppA_{\Delta C}$	AppA construct of residues 1-378
$AppA_{FULL}$	AppA full length protein
Arg (R)	Arginine
Asn (N)	Asparagine
Asp (D)	Aspartic acid
BlsA	blue light sensing protein A
BLUF	Blue light using FAD
BN-PAGE	Blue native polyacrylamide gel electrophoresis
C	Celcius
cAMP	Cyclic Adenosine Monophosphate
CCD	Charge coupled device
cm	Centimeter
cm^{-1}	Wavenumbers
Cys (C)	Cysteine
D	Deuterium
Da	Dalton
dAppA	Dark AppA
ES	Excited state
ET	Electron transfer

FAD	Flavin adenine dinucleotide
FDA	Food and drug administration
FMN	Flavin mononucleotide
fs	Femtosecond
FTIR	Fourier transform infrared
g	Grams
Gln (Q)	Glutamine
Glu (E)	Glutamic acid
Gly (G)	Glycine
GS	Ground state
H-Bond	Hydrogen bond
HOMO	Highest occupied molecular orbital
His (H)	Histidine
Ile (I)	Isoleucine
IPTG	Isopropyl-beta-D-thiogalactopyranoside
IR	Infrared
L	Liter
lAppA	Light AppA
LB	Luria-Bertani broth
Leu (L)	Leucine
LOV	Light oxygen voltage
LUMO	Lowest unoccupied molecular orbital
Lys (K)	Lysine
Met (M)	Methionine
mg	Milligram

ms	Millisecond
min	Minute
mL	Milliliter
mM (mmol)	Millimolar
MS	Mass spectrometry
MW	Molecular weight
MWCO	Molecular weight cut off
nm	Nanometer
ns	Nanosecond
NTA	Nitrilotriacetic acid
OD600	Optical density at 600 nm
OPA	Optical parametric amplifier
PAC	Photoactivated adenylyl cyclase
PAGE	Polyacrylamide gel electrophoresis
PCET	Proton coupled electron transfer
PDB	Protein Database
Phe (F)	Phenylalanine
PixD	positive phototaxis protein D
PixE	positive phototaxis protein E
PMSF	Phenylmethanesulfonylfluoride
Pro (P)	Proline
ps	Picosecond
PT	Proton transfer
RPM	Revolutions per minute
SDS	Sodium dodecyl sulfate

Ser (S)	Serine
SCHIC	Sensor containing heme in place of cobalamin
Slr1693	S-locus related 1693
Slr1694	S-locus related 1694
Thr (T)	Threonine
TRIR	Time resolved infrared
TRMPS	Time resolved multiple probe spectroscopy
Trp (W)	Tryptophan
Tyr (Y)	Tyrosine
UV	Ultraviolet
Val (V)	Valine
Vis	Visible
WT	Wild-type

Acknowledgments

John, Paul, George and Ringo taught me that "I get by with a little help from my friends." And that is certainly the case with this dissertation. This was easily the most difficult thing I have ever done, and the only way I got through it was with the support I received from so many people. To start, I want to thank my advisor, Prof. Peter Tonge, for allowing me to work in his lab and for his patience and wisdom. Your patience and wisdom have been greatly appreciated. I would also like to say thank you to Prof Stephen Meech for your guidance and assistance these last few years.

I also want to say thank you to my committee: Prof Erwin London and Prof Orlando Schärer. Thank you for your insightful questions and for pushing me to be a better researcher. I would also like to thank Prof. Mark Bowen for taking the time out to serve as my outside member.

During my time at Stony Brook I've been able to forge some lasting friendships with the brightest minds the university has to offer. I would like to thank my various mentors: Dr. Deborah Stoner-Ma, Dr. Eduard Melief, and Dr. Allison Haigney, for all your help throughout this ordeal. I would also like to thank Agnieszka Gil, Dr. Eleanor Allen, and Dr. Kanishk Kapilashrami for your assistance with editing. I would also like to thank my collaborators: Dr. Andras Lukacs, Dr Adelbert Bacher.Dr. Mike Towrie, Dr. Greg Greetham and Dr. Ian Clark for all they have done.

Thank you to my parents, for your support and for never saying "so you not going to be a 'real' doctor, right?" And, most importantly, thank you to the love of my life, Lana. Without your unwavering support I would have never gotten through this. You are an inspiration to me as a scientist and a person, and I am so happy to have you in my life.

List of Publications

Allison Haigney, Andras Lukacs, **Richard Brust**, Rui-Kun Zhao, Michael Towrie, Greg Greetham, Ian Clark, Boris Illarionov, Adelbert Bacher, RR Kim, Markus Fischer, Stephen Meech, Peter Tonge. *Vibrational assignment of the ultrafast infrared spectrum of the photoactivatable flavoprotein AppA.* J Phys Chem B, 2012, Sep 6;116(35):10722-9.

Andras Lukacs, Rui-Kun Zhao, Allison Haigney, **Richard Brust**, Greg Greetham, Mike Towrie, Peter Tonge, Stephen Meech. *Excited state structure and dynamics of the neutral and anionic flavin radical revealed by ultrafast transient mid IR to visible spectroscopy.* J. Phys. Chem. B 2012, 116, 5810−5818

Andras Lukacs, Allison Haigney, **Richard Brust**, Rui-Kun Zhao, Allison Stelling, Ian Clark, Mike Towrie, Greg Greetham, Stephen Meech, Peter Tonge. *Photoexcitation of the blue light using FAD photoreceptor AppA results in ultrafast changes to the protein matrix.* J Am Chem Soc. 2011 Oct 26;133(42):16893-900.

Rui- Kun Zhao, Andras Lukacs, Allison Haigney, **Richard Brust**, Greg Greetham, Mike Towrie, Peter Tonge, Stephen Meech. *Ultrafast transient mid IR to visible spectroscopy of full reduced flavins.* Phys Chem Chem Phys. 2011 Oct 21;13(39):17642-8.

Allison Haigney, Andras Lukacs, Rui-Kun Zhao, Allison Stelling, **Richard Brust**, RR Kim, Minako Kondo, Ian Clark, Greg Greetham, Boris Illarionov, Adelbert Bacher, Warner Romisch-Margl, Marcus Fisher, Stephen Meech, Peter Tonge. *Ultrafast infrared spectroscopy of an isotope-labeled photoactivatable flavoprotein.* Biochemistry. 2011 Mar 1;50(8):1321-8.

Chapter 1

Introduction to Photoreceptors, the BLUF domain, and AppA.

1.1. An Overview of Photoreceptors

The ability to sense and respond to light stimuli is a trait shared by all organisms. Light is used for a wide range of biological processes including photosynthesis, phototropism, or visual signal transduction. Based on their needs, numerous organisms have evolved to encode for a system of photoreceptors, which are used to regulate a number of mechanisms essential for the survival of the organism [1-4].

Photoreceptors are the molecules which detect light and relay a signal as a result of light stimulation. Although their functions vary, photoreceptors follow the same basic mechanism: a chromophore detects light which causes a structural change. It is common for this structural change to be a significant one [5]. Such is the case in photoproteins such as the rhodopsins and phytochromes, which feature cis-trans photoisomerization of their chromophores upon absorption [5]. Xanthopsins bind a trans-coumaric acid via thioester linkage of a conserved cysteine, which undergo *trans-cis* isomerization upon excitation with blue light [6]. Phytochromes bind porphryin-like bilin chromophores that regulate photoperiodism in a variety of plants [7].

A common theme amongst all photoreceptor proteins is that the surrounding protein matrix must be able to sense and respond to the photoexcited chromophore. In systems where large structural changes, such as *cis-trans* isomerization, occur, the mechanism is fairly well characterized [3, 5, 8]. However, in systems where the chromophore cannot undergo large scale structural changes, different methods of detection must be used to understand how the protein

environment senses these events. Flavin binding photoreceptors are a unique subset of photoreceptors. The isoalloxazine ring of the flavin chromophore cannot undergo large scale structural rearrangement as a result of the structure of the flavin chromophore: flavin binding photoreceptors have evolved to sense subtle changes in the electronic structure of the flavin as a result of photoexcitation. There are three classes of flavoprotein photoreceptors: light-oxygen-voltage (LOV) [9], photoylase-like cryptochomes [10, 11] and blue-light using flavin adenosine dinucleotide (FAD) (BLUF) domain proteins [1, 2, 4, 12]. Structural changes induced by photoexcitation are possible because of the flavin's unique ability to adopt multiple redox states [13, 14]. For example, LOV domain proteins form cysteinyl-flavin adducts [15]. Cryptochromes undergo one electron transfer, which reduces the flavin to a neutral radical semiquinone intermediate [10]. BLUF domain proteins undergo small structural changes, in particular to residues surrounding the flavin, upon photoexcitation [16].

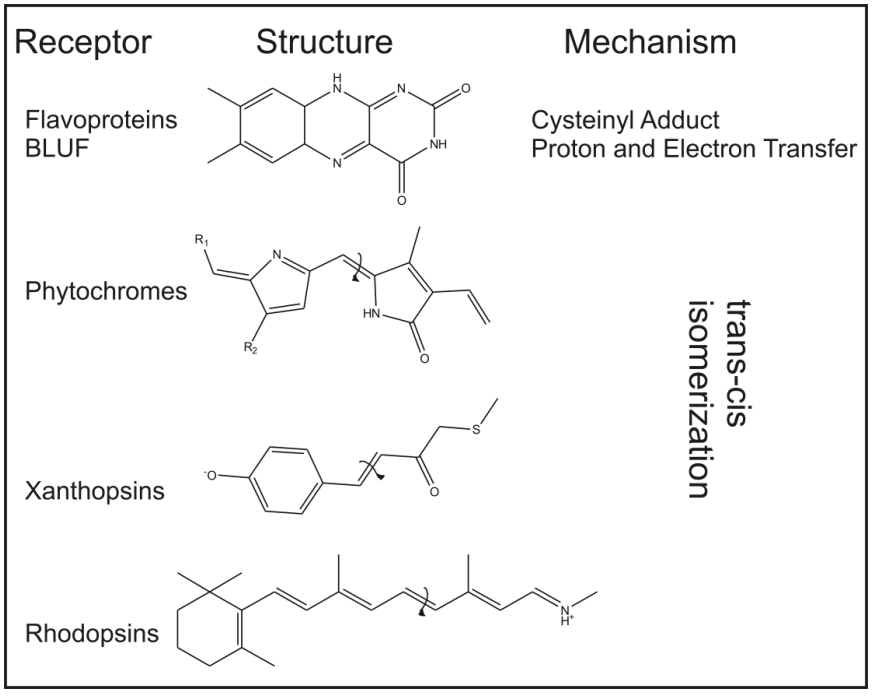

Figure 1.1. Examples of photoreceptors.

1.2. The BLUF Domain

The BLUF proteins undergo rearrangement of the H-bonding network encompassing the flavin which leads to formation of the signaling state of the protein [5], in contrast to the rhodopsins, xanthopsins and phytochromes describded in 1.1. BLUF domain proteins exist in many species with a variety of functions. An estimated 1 in 10 sequenced bacteria have been discovered to encode for a BLUF protein [2], and because of their widespread use in nature these photoreceptors are promising candidates as optogenetic tools [17, 18]. One example of a multidomain protein is photoactivated adenylyl cyclase (PAC), a modular protein in *Euglena gracilis* where regulation of cAMP biosynthesis is controlled by blue light. The N-terminal BLUF domain enables PAC to act as a photoreceptor in order to regulate photophobic, phototaxic responses and to synthesize cAMP depending upon light conditions [19]. Simple BLUF proteins consist of a single domain responsible for sensing blue light but have the potential to communicate this blue light signal to protein binding partners where multidomain proteins communicate through a single system [20, 21]. BlrB1, a standalone BLUF protein from *Rhodobacter sphaeroides*, is a 136 amino acid BLUF protein that contains a short, C-terminal tail currently of unknown function [22, 23]. The PixD proteins are examples of standalone BLUF proteins and are found in cyanobacteria. Two such examples are Tll0078 from *Thermosynechococcus elongates* and Slr1694 from *Synechocystis,* which regulate phototaxis via a blue light signaling mechanism [20, 21, 24, 25].

There are a number of crystal structures for BLUF proteins and each exhibits a conserved βαββαββ, ferrodoxin-like fold (Figure 1.2) [26-29]. The flavin isoalloxazine ring is non-covalently bound between the two α-helices [26-29]. Surrounding the flavin is an intricate

hydrogen bonding network involving a conserved glutamine and tyrosine that have been shown to be essential for blue light sensing [30, 31].

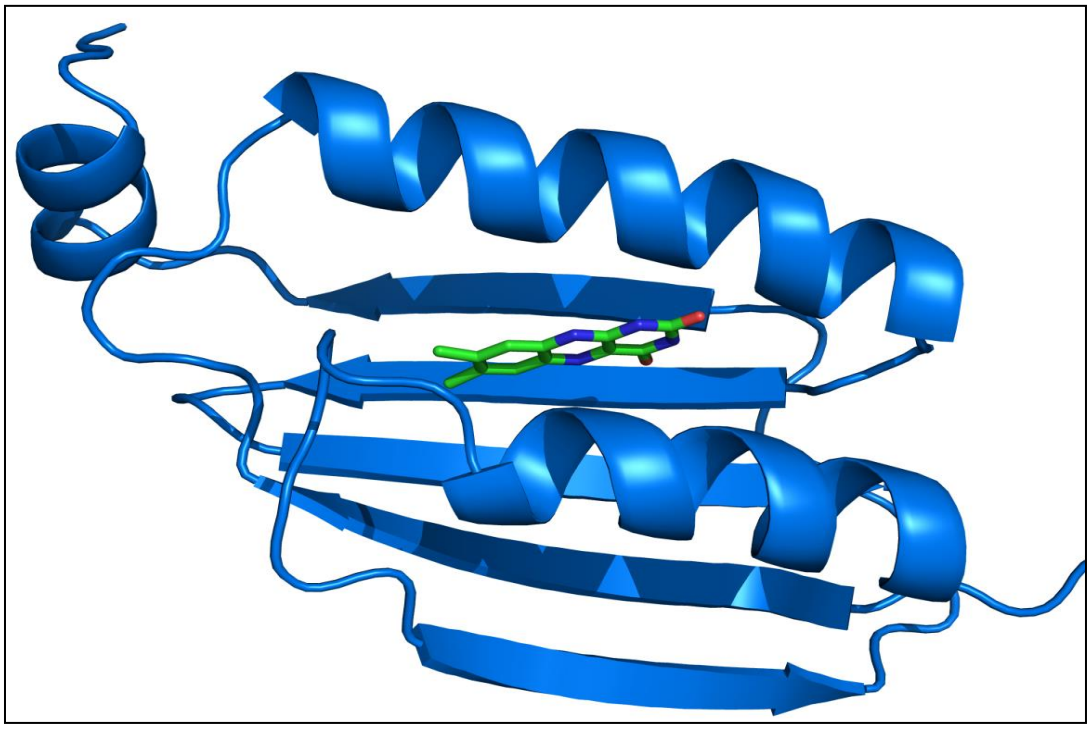

Figure 1.2 The x-ray crystal structure of a BLUF protein. The isoalloxazine ring is shown in green. PDB ID 1YRX [26].

BLUF proteins exhibit a two state photocycle that can be monitored using absorption spectroscopy. Photoexcitation of the pre-irradiated, or dark, state results in a 10 nm red shift of the flavin λ_{max} (Figure 1.3) and is indicative of formation of the signaling, or light state.[12, 16, 32]. The light adapted state is not an excited state but rather a new ground state and will recover back to the dark state if removed from the blue light source. The stability of the light state varies in different BLUF systems, but typically recovery back to the dark state is on the order of a few seconds to a few minutes [12, 22, 24, 32-34].

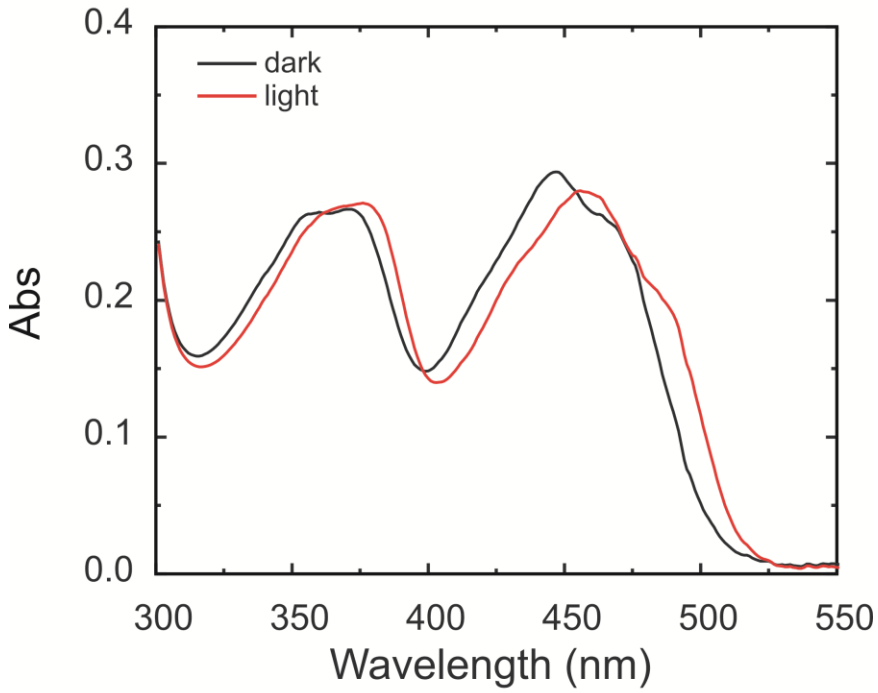

Figure 1.3. Example of the change in flavin absorption in BLUF proteins. Photoexcitation of 400 nm light leads to light state and a 10 nm red shift in UV spectrum. Protein concentration is 50 μM.

1.3. AppA, the First Discovered BLUF Protein

The first BLUF protein to be discovered was AppA from in *Rhodobacter sphaeroides*. AppA is a 450 residue multidomain protein responsible for regulation of photosystem biosynthesis [35]. The N-terminal BLUF domain is responsible for the light sensing while the C-terminal serves as both an oxygen sensor and the binding site for the transcription factor, PpsR [36-38]. AppA regulates photosystem biosynthesis by responding to both light excitation and oxygen concentration (Figure 1.4). In low light, low oxygen environments, AppA forms a complex with PpsR. This allows for the production of purple photopigment clusters that serve as the source of photosynthesis. Upon blue light excitation under semi-aerobic conditions, AppA undergoes a conformational change and releases PpsR, which binds to the gene cluster encoding the photopigment clusters responsible for photosynthesis in the bacterium, blocking RNA

polymerase binding, and thus inhibiting photosystem biosynthesis [12]. An important aspect of studying AppA involves the mechanism for how blue light excitation of the N-terminal domain results in a structural change of the C-terminal domain, resulting in the release of PpsR.

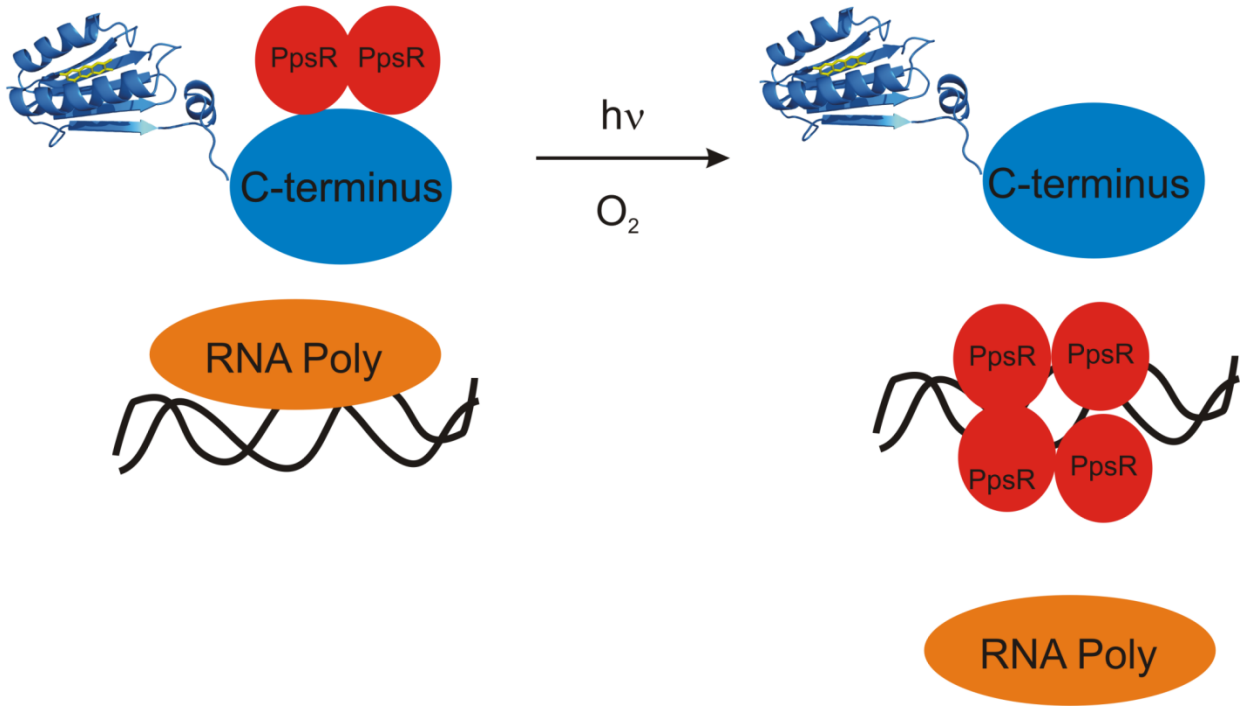

Figure 1.4. The biological role of AppA. In low light, low oxygen environments AppA binds 2 PpsR molecules. Photoirradation of blue light or increase in O2 in the atmosphere results in a conformational change, releasing PpsR, which forms a tetramer and binds to DNA, inhibiting transcription of photosynthetic genes.

1.4. Initial Characterization of $AppA_{BLUF}$

The photocycle of the BLUF domain of AppA, $AppA_{BLUF}$, has been studied using both steady state and time resolved spectroscopy. The red shift in UV-Vis absorption spectra of the flavin indicates there are two states of AppA. They are referred to as $dAppA_{BLUF}$ (pre-excitation) and $lAppA_{BLUF}$ (post-excitation). The quantum yield for the photoconversion was measured by time resolved fluorescence and was shown to be 0.24 (Figure 1.5) [39]. The

process of signaling state formation is reversible, with recovery back to the dark state 30 minutes upon removal of the blue light source. This is unusual for BLUF systems, which typically recover on a faster timescale (seconds to a few minutes) [16].

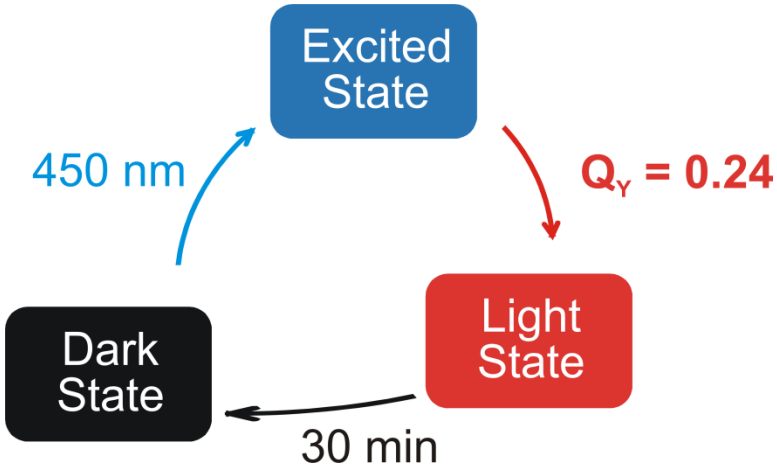

Figure 1.5. The photocycle of AppA. Irradiation of blue light excites the flavin, which is sensed by the surrounding protein resulting in a conformational change yielding the light state with a quantum yield of 0.24. Recovery back to the dark state is observed in 30 minutes.

The X-ray crystal of $AppA_{BLUF}$ reveals an intricate hydrogen bonding network surrounding the flavin (Figure 1.6) [26, 27]. Residues where direct contact with the flavin can be observed are Q63, Y21, N45, and H44. Q63 forms a hydrogen bond with the N5 of the flavin ring and a conserved tyrosine (Y21), which are well established to be essential for photoactivity [30, 31]. Methionine at position 106 is conserved in all BLUF proteins, and while not essential for photoactivity in AppA [40], this methionine has been shown to be essential in other BLUF systems for signal output [41]. The asparagine at position 45 is conserved in all BLUF proteins, and is found to H-bond with the C4=O flavin in both dark and light adapted states. Histidine at position 44, however, is only found in $AppA_{BLUF}$. In other BLUF proteins, this position is occupied either by an asparagine or arginine.

The position of tryptophan at position 104 is intriguing. There are two crystal structures of $AppA_{BLUF}$ [26, 27]. The side chain of W104 can be seen either in the "Trp_{out}" (Figure 1.6A) or the "Trp_{in}" position (Figure 1.5B). This has led to a model for light excitation where W104 motion results in transferring the signal from the N-terminus to C-terminus [40]. Recent NMR data suggests a minimal role for W104 [42, 43], however further investigation is necessary to fully elucidate the role of this residue.

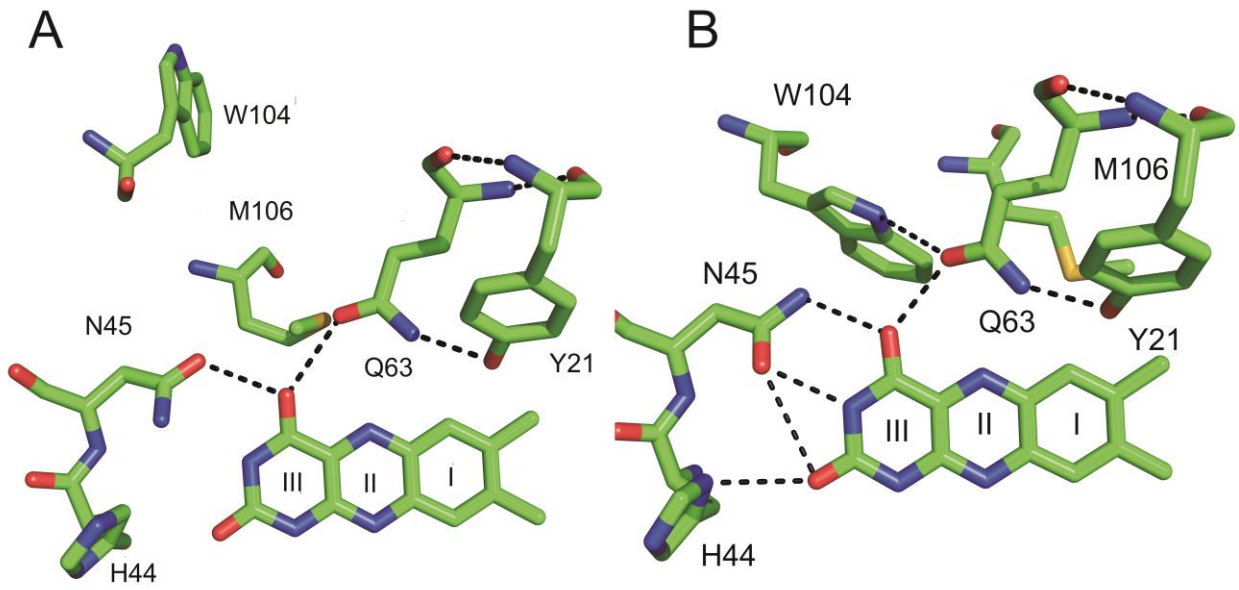

Figure 1.6. Comparison of $AppA_{BLUF}$ crystal structures. Tryptophan at position 104 can be seen in Trp_{out} (PDB 2IYG [27]) in **A** and Trp_{in} (PDB 1YRX [26]) in **B**.

The present hypothesis for light state formation involves the conserved glutamine. Discussed in detail below, vibrational spectroscopy has revealed that an increase in H-bonding to the C4=O flavin carbonyl upon photoexcitation. Based on this information, and the position of Q63 in the crystal structure, photoexcitation of the flavin chromophore induces rearrangement of the surrounding protein environment, culminating with the rotation of the Q63 side chain and forming a new hydrogen bond to the C4=O of the flavin (Figure 1.7).

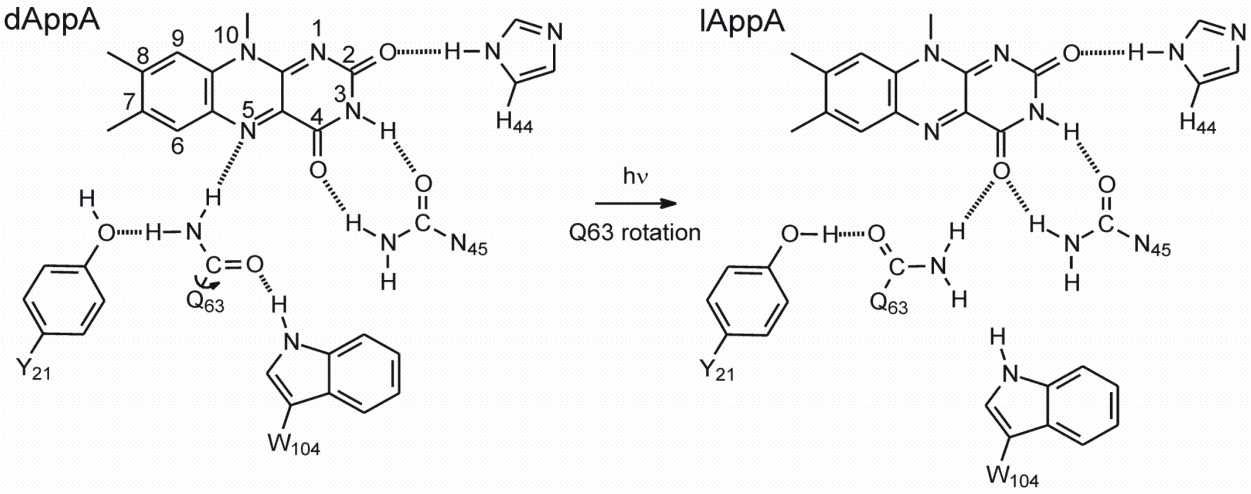

Figure 1.7. Initial proposed mechanism for formation of lAppA. Photoexcitation of the flavin chromophore results in rotation of the Q63 amide side chain, which forms a new H-bond to the C4=O flavin carbonyl.

1.4.1. Raman Spectroscopy of $AppA_{BLUF}$

Raman spectroscopy has been used to study the small changes in hydrogen bonding around the flavin of AppA caused by photoexcitation. Steady state Raman spectroscopy has also been used to characterize the mechanism of photoactivation in AppA, revealing key structural changes as a result of altering the H-bonding network surrounding the flavin [44, 45]. The vibrational spectrum is sensitive to structure and environment and can be used to probe changes as a result of blue light excitation. Analysis of the steady state Raman spectra generated for $AppA_{BLUF}$ reveal modes (1348, 1405, 1500, 1549 and 1580 cm^{-1}) present in free flavin [46, 47]. The intense band at 1668 cm^{-1} is absent in free flavin and has been assigned as the protein amide I mode while bands in the 1150-1340 cm^{-1} region are assigned to amide III [44]. One such feature that is different in the two states of AppA is a 10 cm^{-1} red shift in the shoulder at 1700 cm^{-1} to 1690 cm^{-1} (Figure 1.8), which has been associated with an increase in hydrogen bonding to the C4=O of the flavin [44].

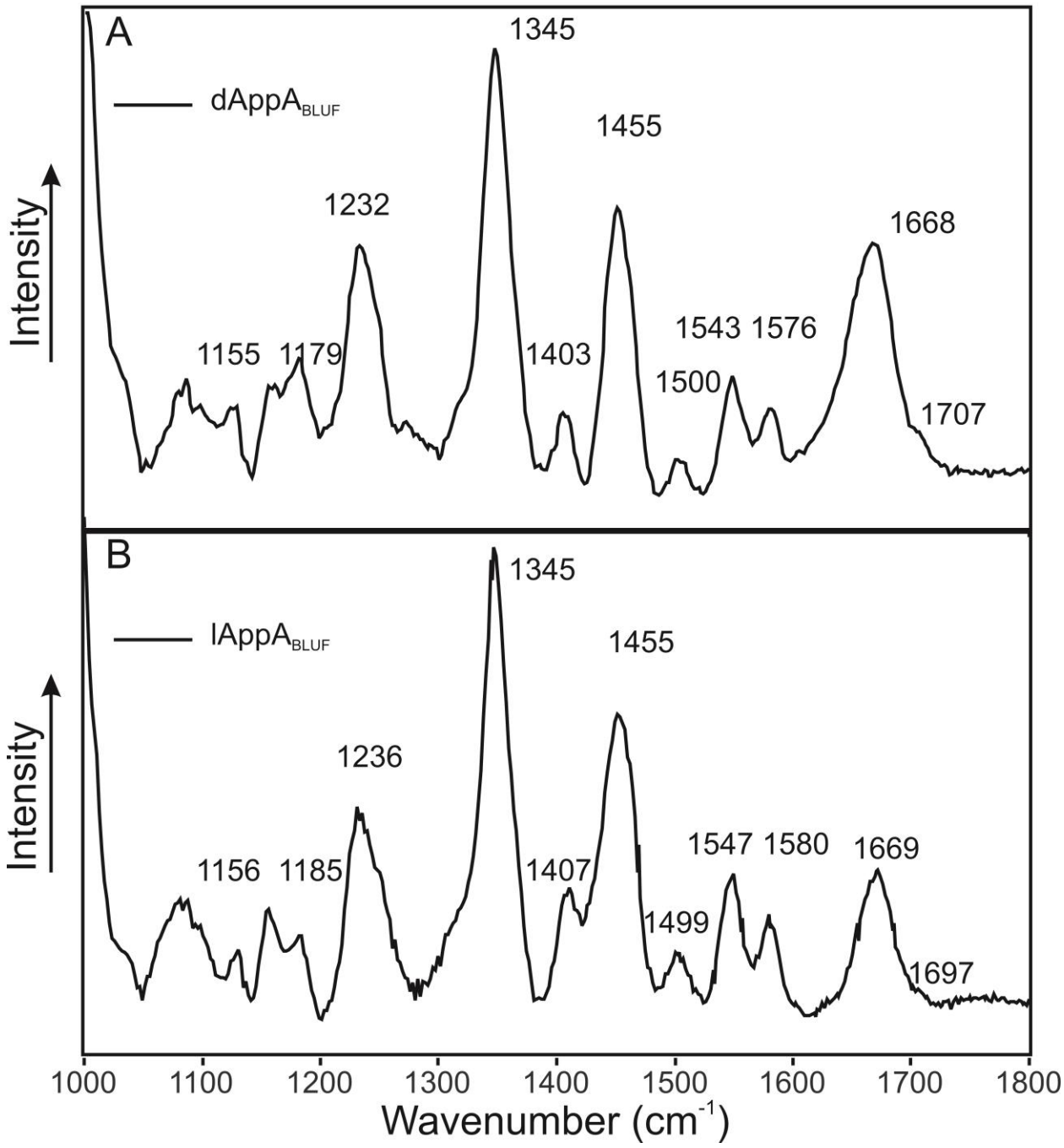

Figure 1.8. Raman Spectroscopy of AppA$_{BLUF}$. Steady state Raman spectrum of dAppA$_{BLUF}$ (**A**) and lAppA$_{BLUF}$ (**B**) using a 752 nm laser source. Spectra were generated by recording 300 scans at 2 s acquisition.

1.4.2. FTIR Spectroscopy of $AppA_{BLUF}$

FTIR spectroscopy has proven to be an essential tool for monitoring structural changes as a result of photoexcitation. The major caveat to using FTIR spectroscopy is the strong signals from the protein which overlap with key flavin modes [48, 49]. Therefore, it is difficult to monitor small changes in flavin and protein structure from the amide peak alone. This is overcome by generating difference spectra. The light adapted state was generated by irradiation of 460 nm light and subsequently subtracted from the dark spectrum. For $AppA_{BLUF}$, two difference modes are observed at 1622 (-)/1632 (+) cm^{-1} and at 1688 (+)/1700(-) cm^{-1} (Figure 1.9). Isotopic labeling enabled assignment of the 1688 (+)/1700 (-) cm^{-1} mode to the C4=O carbonyl of the flavin while the 1622(-)/1632(+) cm^{-1} mode was assigned to changes of the protein matrix [50].

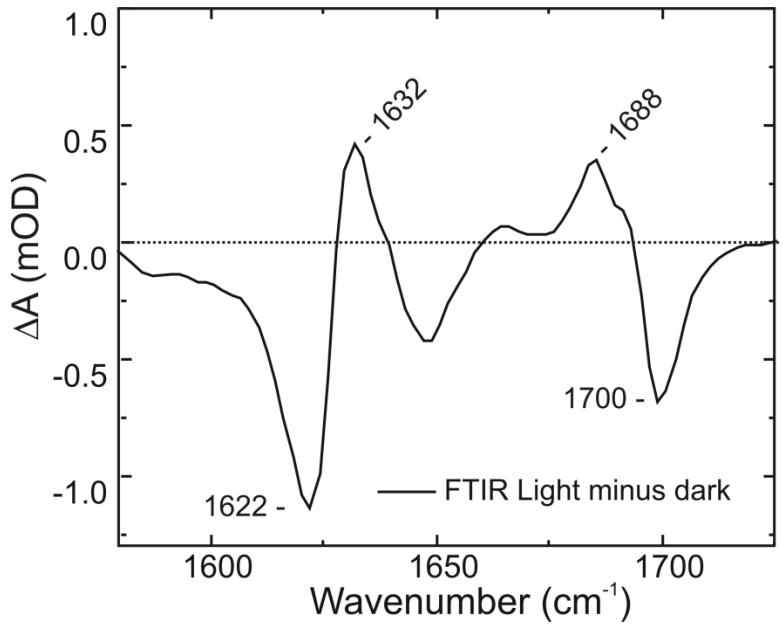

Figure 1.9. FTIR light minus dark difference spectra of $AppA_{BLUF}$. The light state was generated by 3 minute irradiation with 460 nm light. The pre-irradiated spectrum was then subtracted from the post-irradiated spectrum.

1.4.3. Time Resolved IR Spectroscopy of $AppA_{BLUF}$

Ultrafast time resolved spectroscopy enables the characterization of the primary steps immediately after photoexcitation (fs to ns). Spectra are recorded using carefully aligned lasers that operate on sub-picosecond time intervals; therefore we can monitor excited state structures. The time resolved infrared (TRIR) method reports the evolution of the pump-on minus pump-off transient difference spectra following excitation of the flavin chromophore with a 100 fs visible (450 nm) pulse. Using a pump-on-pump off technique, excited state IR signals are subtracted from ground state IR signals. The subsequent difference spectrum then contains information on excited and ground state changes. Transients (positive ΔA) are excited state modes formed as a result of photoexcitation while bleaches (negative ΔA) are the result of the depopulation of ground state modes.

Time resolved infrared spectra have been reported for $dAppA_{BLUF}$, $lAppA_{BLUF,}$ and free flavin [46, 51, 52]. Key flavin modes at 1547, 1580, 1650 and 1700 cm^{-1} have all been assigned by isotope incorporation [52, 53]. Photoexcitation results in a 10 cm^{-1} red shift in the 1700 cm^{-1} mode in dAppA to 1690 cm^{-1} in lAppA and has been assigned as the flavin C4=O carbonyl [52], in agreement with FTIR data [50]. The appearance of a transient at 1670 cm^{-1} in $dAppA_{BLUF}$ is perhaps the most significant finding [51]. This mode is absent in both free flavin and photoconverted protein and does not shift with isotope labeling of the flavin and can therefore be assigned to the protein [51-53]. Based on its position it has been proposed to arise from the amide side chain of Q63, which upon irradiation ultimately results in an increase in hydrogen bonding to the flavin observed in $lAppA_{BLUF}$.

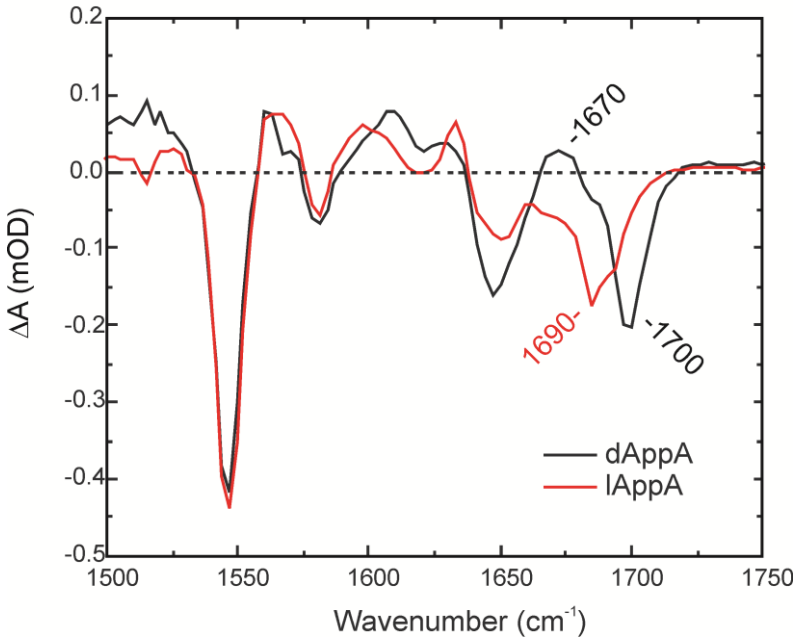

Figure 1.10. TRIR spectra of AppA. TRIR spectra of dAppA (black) and lAppA (red) taken 3 ps post-excitation [13].

1.5. Current Hypothesis on Light State Formation in AppA

The mechanism of signaling state formation in AppA is not fully understood, but it is proposed to involve rearrangement of the H-bonding network surrounding the flavin [33, 43, 54]. A proposed mechanism using ultrafast transient absorption spectroscopy has been proposed involving fast electron transfer and subsequent proton transfer from Y21 to the flavin in its excited state [51, 55]. At present time, current TRIR studies show no evidence of PT or ET intermediates in photoactivation of $dAppA_{BLUF}$. In one proposed mechanism, proton transfer disrupts the H-bonding network between the hydroxyl of Y21 with the amide side chain of Q63, which allows for free rotation of Q63. Q63 then forms a new hydrogen bond with O4 of the light excited flavin [44, 50, 51]. This model is consistent with current FTIR and NMR studies, which show a change in the hydrogen bonding of O4 following blue light excitation [42, 43]. Using a more theoretical approach, a competing hypothesis was proposed stating that upon light

excitation Q63 forms a stable tautomer which alters the hydrogen bonding network around the flavin [56, 57].

A more recent hypothesis was generated using an inactive mutant, Q63E. While this mutation results in an inactive mutant, a red shift in the UV-Vis spectra is observed when compared to dAppA (450 nm versus 445 nm) [55, 58]. In addition, this mutation is unable to bind PpsR, suggesting a light-like structure [58]. Upon further investigation using TRIR, a unique spectrum was observed for the Q63E mutant (Figure 1.11). The TRIR spectrum of Q63E possesses 3 bleaches at 1650 cm^{-1} together with well-resolved bleaches at 1662 and 1685 cm^{-1}. Based on their position with wild type spectra, they have been assigned as the C2=O and C4=O, respectively.

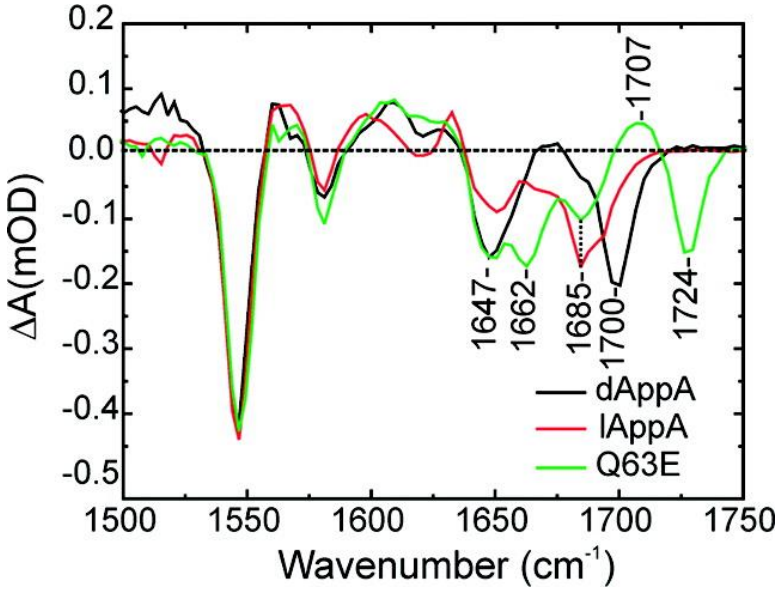

Figure 1.11. TRIR of AppA and Q63E. TRIR spectra of $dAppA_{BLUF}$ (black), $lAppA_{BLUF}$ (red), and Q63E $AppA_{BLUF}$ (green) bound to FAD reported by Lukacs et al. [55].

Unique to the Q63E spectrum is the bleach and transient observed at 1724 and 1707 cm^{-1}, respectively. Isotopic labeling of the protein allowed for assignment of these modes as the neutral carboxylic acid side chain of Q63E. And since these modes are observed within the time

resolution of the instrument (< 100 fs) [59], these data indicate that the protein responds instantaneously to blue light excitation. With this in mind, a model where the equilibrium of keto-enol tautomerism of the glutamine side chain is altered by photoexcitation was proposed [55].

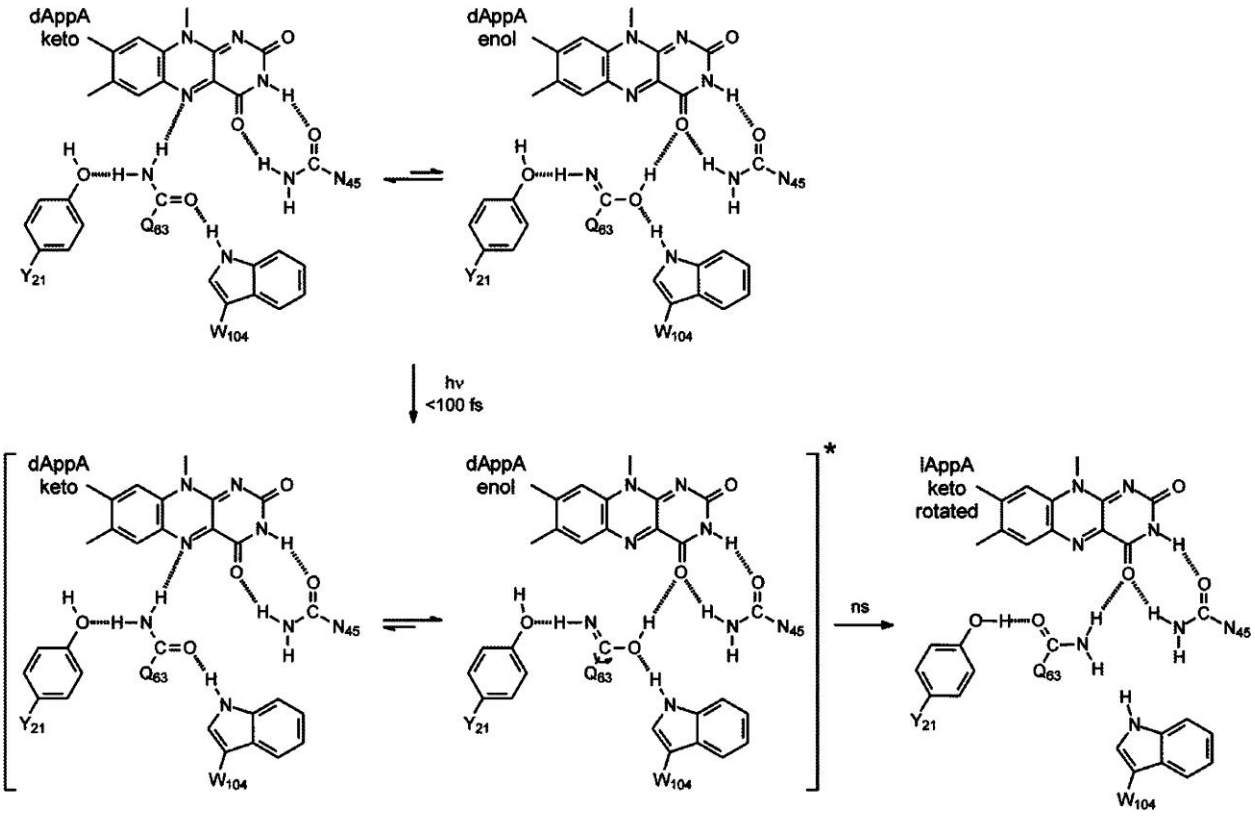

Figure 1.12. The current proposed model for formation of lAppA. Q63 is in equilibrium with its keto-enol forms, favoring the keto form initially. Photoexcitation results in a shift to the enol form, which ultimately results in rotation of the amide side chain. This model was proposed by Lukacs et al. [55].

1.6. Optogenetics

Optogenetics is an emerging field in synthetic biology, where photoreceptor proteins are genetically incorporated into a host system in such a way to allow control of a particular biological event by light [60]. The ability to regulate cellular response with light has been of particular interest in the field of neural science [60-62]. The first application of optogenetics was

in *Drosophila melanogaster*, where stimulation of neural transmitters was activated by light. This was achieved by genetically incorporating a rhodopsin linked retinal, in other terms tethering a photoresponse protein to a photoreceptor, to specific regions of neural cells [63]. Subsequent studies have employed channelrhodopsin (Ch2) from *Chlamydomonas reinhardtii*, a gated ion channel that responds to light excitation [64]. To date, the most successful BLUF protein as an optogenetic sensor is photoactivated adenylyl cyclase from *Euglena gracilis,* although there are concerns of its use, in particular the mass of the photoreceptors chosen and their poor solubility [65]. As such, there is interest in developing different BLUF proteins for optogenetic purposes [17]. However, in order to fully utilize the potential of BLUF proteins, such as AppA, the mechanisms of photoactivation must be fully characterized.

1.7. Specific Aims

There are 5 specific aims for this work.

1. **Analysis of S41 and its mutants.** To fully understand the mechanism of photoactivation in AppA the role of key amino acids adjacent to the flavin must be elucidated. Serine at position 41 has been proposed to be an important residue in light state formation. Mutations to S41 significantly alter the electronic absorption of the flavin. Here, mutants of S41 were characterized by vibrational spectroscopy.

2. **Initial characterization of BlsA, a BLUF protein from the pathogenic bacterium *Acinetobacter baumannii*.** To understand the mechanism of BLUF proteins work must be expanded into other BLUF systems. The pathogenic bacterium *Acinetobacter baumannii* was shown to be sensitive to blue light by encoding for a BLUF protein, named BlsA. Initial characterization of BlsA was performed using steady state and

ultrafast vibrational spectroscopy, revealing a mechanism that is unique among BLUF proteins.

3. **Monitoring dynamics from pico- to milliseconds of the BLUF domain of AppA.** Protein dynamics can occur over many decades of time. To monitor longer timescale changes we used a new technique, TRMPS, which utilizes the same system as the ultrafast IR method described but is capable of measuring from femtoseconds to milliseconds post-excitation. The W104A mutant was also characterized, revealing its importance for the *in vivo* function of AppA.

4. **Expansion to the full length protein.** As a multidomain photoreceptor, AppA has evolved to modulate signal from N-terminus to C-terminus upon blue light excitation. Photoexcitation of the N-terminal domain results in conformational changes in the C-terminal domain, resulting in the release of PpsR. Therefore, to fully understand the mechanism of photoactivation the full length protein must be investigated. Here, initial characterization of the vibrational spectra of the full length protein, $AppA_{FULL}$, was performed.

5. **Characterization of PixD, from the cyanobacterium *Synechocystis*.** PixD has become the model stand-alone BLUF protein. Here, vibrational spectroscopy was performed to better understand the mechanism of signal output from PixD. Key differences in the mechanism from AppA were observed in both the primary (ps to ns) and latter stages (ns to μs) post-excitation. In addition, initial characterization of the PixD-PixE complex was performed.

1.8. References

1. Losi, A. and W. Gärtner, *The evolution of flavin-binding photoreceptors: An ancient chromophore serving trendy blue-light sensors.* Annu Rev Plant Biol, 2012. **63**(1): p. 49-72.
2. Losi, A. and W. Gartner, *Bacterial bilin- and flavin-binding photoreceptors.* Photochem Photobiol Sci, 2008. **7**(10): p. 1168-1178.
3. Losi, A., *The bacterial counterparts of plant phototropins.* Photochem. Photobiol. Sci., 2004. **3**(6): p. 566-574.
4. Losi, A. and W. Gärtner, *Old chromophores, new photoactivation paradigms, trendy applications: Flavins in blue light-sensing photoreceptors.* Photochem Photobiol, 2011. **87**(3): p. 491-510.
5. van der Horst, M.A. and K.J. Hellingwerf, *Photoreceptor proteins, "star actors of modern times": a review of the functional dynamics in the structure of representative members of six different photoreceptor families.* Acc Chem Res, 2004. **37**(1): p. 13-20.
6. Kort, R., W.D. Hoff, M. Van West, A.R. Kroon, S.M. Hoffer, K.H. Vlieg, W. Crielaand, J.J. Van Beeumen, and K.J. Hellingwerf, *The xanthopsins: a new family of eubacterial blue-light photoreceptors.* EMBO J, 1996. **15**(13): p. 3209-18.
7. Rockwell, N.C., Y.S. Su, and J.C. Lagarias, *Phytochrome structure and signaling mechanisms.* Annu Rev Plant Biol, 2006. **57**: p. 837-58.
8. Losi, A., E. Polverini, B. Quest, and W. Gärtner, *First evidence for phototropin-related blue-light receptors in prokaryotes.* Biophys J, 2002. **82**(5): p. 2627-2634.

9. Kottke, T., P. Hegemann, B. Dick, and J. Heberle, *The photochemistry of the light-, oxygen-, and voltage-sensitive domains in the algal blue light receptor phot.* Biopolymers, 2006. **82**(4): p. 373-378.

10. Chaves, I., R. Pokorny, M. Byrdin, N. Hoang, T. Ritz, K. Brettel, L.-O. Essen, G.T.J. van der Horst, A. Batschauer, and M. Ahmad, *The cryptochromes: Blue light photoreceptors in plants and animals.* Annu Rev Plant Biol, 2011. **62**(1): p. 335-364.

11. Li, Q.-H. and H.-Q. Yang, *Cryptochrome signaling in plants.* Photochem Photobiol, 2007. **83**(1): p. 94-101.

12. Gomelsky, M. and G. Klug, *BLUF: a novel FAD-binding domain involved in sensory transduction in microorganisms.* Trends Biochem Sci, 2002. **27**(10): p. 497-500.

13. Kao, Y.-T., C. Saxena, T.-F. He, L. Guo, L. Wang, A. Sancar, and D. Zhong, *Ultrafast dynamics of flavins in five redox states.* J Am Chem Soc, 2008. **130**(39): p. 13132-13139.

14. Rieff, B., S. Bauer, G. Mathias, and P. Tavan, *IR Spectra of flavins in solution: DFT/MM description of redox effects.* J Phys Chem B, 2011. **115**(9): p. 2117-2123.

15. Briggs, W.R., *The LOV domain: a chromophore module servicing multiple photoreceptors.* J Biomed Sci, 2007. **14**(4): p. 499-504.

16. Masuda, S., *Light detection and signal transduction in the BLUF photoreceptors.* Plant Cell Physiol, 2013. **54**(2): p. 171-179.

17. Christie, J.M., J. Gawthorne, G. Young, N.J. Fraser, and A.J. Roe, *LOV to BLUF: Flavoprotein contributions to the optogenetic toolkit.* Mol Plant, 2012. **5**(3): p. 533-544.

18. Yin, T. and Y. Wu, *Guiding lights: recent developments in optogenetic control of biochemical signals.* Pflugers Archiv, 2013. **465**(3): p. 397-408.

19. Iseki, M., S. Matsunaga, A. Murakami, K. Ohno, K. Shiga, K. Yoshida, M. Sugai, T. Takahashi, T. Hori, and M. Watanabe, *A blue-light-activated adenylyl cyclase mediates photoavoidance in Euglena gracilis.* Nature, 2002. **415**(6875): p. 1047-51.

20. Okajima, K., Y. Fukushima, H. Suzuki, A. Kita, Y. Ochiai, M. Katayama, Y. Shibata, K. Miki, T. Noguchi, S. Itoh, and M. Ikeuchi, *Fate determination of the flavin photoreceptions in the cyanobacterial blue light receptor TePixD (Tll0078).* J Mol Biol, 2006. **363**(1): p. 10-8.

21. Tanaka, K., Y. Nakasone, K. Okajima, M. Ikeuchi, S. Tokutomi, and M. Terazima, *A way to sense light intensity: Multiple-excitation of the BLUF photoreceptor TePixD suppresses conformational change.* FEBS Lett, 2011. **585**(5): p. 786-790.

22. Zirak, P., A. Penzkofer, T. Schiereis, P. Hegemann, A. Jung, and I. Schlichting, *Photodynamics of the small BLUF protein BlrB from Rhodobacter sphaeroides.* J Photochem Photobiol B, 2006. **83**(3): p. 180-194.

23. Mathes, T., I.H.M. van Stokkum, C. Bonetti, P. Hegemann, and J.T.M. Kennis, *The hydrogen-bond switch reaction of the Blrb BLUF domain of Rhodobacter sphaeroides.* J Phys Chem B, 2011. **115**(24): p. 7963-7971.

24. Okajima, K., S. Yoshihara, Y. Fukushima, X. Geng, M. Katayama, S. Higashi, M. Watanabe, S. Sato, S. Tabata, Y. Shibata, S. Itoh, and M. Ikeuchi, *Biochemical and functional characterization of BLUF-type flavin-binding proteins of two species of Cyanobacteria.* J Biochem, 2005. **137**(6): p. 741-750.

25. Yuan, H., V. Dragnea, Q. Wu, K.H. Gardner, and C.E. Bauer, *Mutational and structural studies of the PixD BLUF output signal that affects light-regulated interactions with PixE.* Biochemistry, 2011. **50**(29): p. 6365-6375.

26. Anderson, S., V. Dragnea, S. Masuda, J. Ybe, K. Moffat, and C. Bauer, *Structure of a novel photoreceptor, the BLUF domain of AppA from Rhodobacter sphaeroides.* Biochemistry, 2005. **44**(22): p. 7998-8005.

27. Jung, A., J. Reinstein, T. Domratcheva, R.L. Shoeman, and I. Schlichting, *Crystal structures of the AppA BLUF domain photoreceptor provide insights into blue light-mediated signal transduction.* J Mol Biol, 2006. **362**(4): p. 717-732.

28. Wu, Q. and K.H. Gardner, *Structure and insight into blue light-induced changes in the BlrP1 BLUF domain.* Biochemistry, 2009. **48**(12): p. 2620-2629.

29. Yuan, H., S. Anderson, S. Masuda, V. Dragnea, K. Moffat, and C. Bauer, *Crystal structures of the Synechocystis photoreceptor Slr1694 reveal distinct structural states related to signaling.* Biochemistry, 2006. **45**(42): p. 12687-12694.

30. Laan, W., M.A. van der Horst, I.H. van Stokkum, and K.J. Hellingwerf, *Initial characterization of the primary photochemistry of AppA, a blue-light-using flavin adenine dinucleotide-domain containing transcriptional antirepressor protein from Rhodobacter sphaeroides: a key role for reversible intramolecular proton transfer from the flavin adenine dinucleotide chromophore to a conserved tyrosine?* Photochem Photobiol, 2003. **78**(3): p. 290-7.

31. Grinstead, J.S., M. Avila-Perez, K.J. Hellingwerf, R. Boelens, and R. Kaptein, *Light-induced flipping of a conserved glutamine sidechain and its orientation in the AppA BLUF domain.* J Am Chem Soc, 2006. **128**(47): p. 15066-15067.

32. Masuda, S., K. Hasegawa, A. Ishii, and T.-a. Ono, *Light-induced structural changes in a putative blue-light receptor with a novel FAD binding fold sensor of blue-light using*

FAD (BLUF); Slr1694 of Synechocystis sp. PCC6803. Biochemistry, 2004. **43**(18): p. 5304-5313.

33. Laan, W., M. Gauden, S. Yeremenko, R. van Grondelle, J.T.M. Kennis, and K.J. Hellingwerf, *On the mechanism of activation of the BLUF domain of AppA.* Biochemistry, 2005. **45**(1): p. 51-60.

34. Kita, A., K. Okajima, Y. Morimoto, M. Ikeuchi, and K. Miki, *Structure of a cyanobacterial BLUF protein, Tll0078, containing a novel FAD-binding blue light sensor domain.* J Mol Biol, 2005. **349**(1): p. 1-9.

35. Masuda, S. and C.E. Bauer, *AppA Is a blue light photoreceptor that antirepresses photosynthesis gene expression in Rhodobacter sphaeroides.* Cell, 2002. **110**(5): p. 613-623.

36. Pandey, R., D. Flockerzi, Marcus J.B. Hauser, and R. Straube, *Modeling the light- and redox-dependent interaction of PpsR/AppA in Rhodobacter sphaeroides.* Biophys J, 2011. **100**(10): p. 2347-2355.

37. Kim, S.K., J.T. Mason, D.B. Knaff, C.E. Bauer, and A.T. Setterdahl, *Redox properties of the Rhodobacter sphaeroides transcriptional regulatory proteins PpsR and AppA.* Photosynth. Res., 2006. **89**(2-3): p. 89-98.

38. Pandey, R., D. Flockerzi, M.J.B. Hauser, and R. Straube, *An extended model for the repression of photosynthesis genes by the AppA/PpsR system in Rhodobacter sphaeroides.* FEBS J, 2012. **279**(18): p. 3449-3461.

39. Gauden, M., S. Yeremenko, W. Laan, I.H. van Stokkum, J.A. Ihalainen, R. van Grondelle, K.J. Hellingwerf, and J.T. Kennis, *Photocycle of the flavin-binding*

photoreceptor AppA, a bacterial transcriptional antirepressor of photosynthesis genes. Biochemistry, 2005. **44**(10): p. 3653-62.

40. Masuda, S., K. Hasegawa, and T.-a. Ono, *Tryptophan at position 104 is involved in transforming light signal into changes of β-sheet structure for the signaling state in the BLUF domain of AppA.* Plant Cell Physiol, 2005. **46**(12): p. 1894-1901.

41. Masuda, S., K. Hasegawa, H. Ohta, and T.-a. Ono, *Crucial role in light signal transduction for the conserved Met93 of the BLUF protein PixD/Slr1694.* Plant Cell Physiol, 2008. **49**(10): p. 1600-1606.

42. Dragnea, V., A.I. Arunkumar, H. Yuan, D.P. Giedroc, and C.E. Bauer, *Spectroscopic studies of the AppA BLUF domain from Rhodobacter sphaeroides: Addressing movement of tryptophan 104 in the signaling state.* Biochemistry, 2009. **48**(42): p. 9969-9979.

43. Grinstead, J.S., S.-T.D. Hsu, W. Laan, A.M.J.J. Bonvin, K.J. Hellingwerf, R. Boelens, and R. Kaptein, *The solution structure of the AppA BLUF domain: Insight into the mechanism of light-induced signaling.* ChemBioChem, 2006. **7**(1): p. 187-193.

44. Unno, M., R. Sano, S. Masuda, T.A. Ono, and S. Yamauchi, *Light-induced structural changes in the active site of the BLUF domain in AppA by Raman spectroscopy.* J Phys Chem B, 2005. **109**(25): p. 12620-6.

45. Unno, M., S. Kikuchi, and S. Masuda, *Structural refinement of a key tryptophan residue in the BLUF photoreceptor AppA by ultraviolet resonance Raman spectroscopy.* Biophys J, 2010. **98**(9): p. 1949-1956.

46. Kondo, M., J. Nappa, K.L. Ronayne, A.L. Stelling, P.J. Tonge, and S.R. Meech, *Ultrafast vibrational spectroscopy of the flavin chromophore.* J Phys Chem B, 2006. **110**(41): p. 20107-20110.

47. Bowman, W.D. and T.G. Spiro, *Normal mode analysis of lumiflavin and interpretation of resonance Raman spectra of flavoproteins.* Biochemistry, 1981. **20**(11): p. 3313-3318.

48. Venyaminov, S.Y. and N.N. Kalnin, *Quantitative IR spectrophotometry of peptide compounds in water (H2O) solutions. II. Amide absorption bands of polypeptides and fibrous proteins in α-, β-, and random coil conformations.* Biopolymers, 1990. **30**(13-14): p. 1259-1271.

49. Barth, A., *Infrared spectroscopy of proteins.* Biochim Biophys Acta, 2007. **1767**(9): p. 1073-1101.

50. Masuda, S., K. Hasegawa, and T.-a. Ono, *Light-induced structural changes of apoprotein and chromophore in the sensor of blue light using FAD (BLUF) domain of AppA for a signaling state* Biochemistry, 2005. **44**(4): p. 1215-1224.

51. Stelling, A.L., K.L. Ronayne, J. Nappa, P.J. Tonge, and S.R. Meech, *Ultrafast structural dynamics in BLUF domains: Transient infrared spectroscopy of AppA and its mutants.* J Am Chem Soc, 2007. **129**(50): p. 15556-15564.

52. Haigney, A., A. Lukacs, R.-K. Zhao, A.L. Stelling, R. Brust, R.-R. Kim, M. Kondo, I. Clark, M. Towrie, G.M. Greetham, B. Illarionov, A. Bacher, W. Romisch-Margl, M. Fischer, S.R. Meech, and P.J. Tonge, *Ultrafast infrared spectroscopy of an isotope-labeled photoactivatable flavoprotein.* Biochemistry, 2011. **50**(8): p. 1321-1328.

53. Haigney, A., A. Lukacs, R. Brust, R.-K. Zhao, M. Towrie, G.M. Greetham, I. Clark, B. Illarionov, A. Bacher, R.-R. Kim, M. Fischer, S.R. Meech, and P.J. Tonge, *Vibrational assignment of the ultrafast infrared spectrum of the photoactivatable flavoprotein AppA.* J Phys Chem B, 2012. **116**(35): p. 10722-10729.

54. Toh, K.C., I.H.M. van Stokkum, J. Hendriks, M.T.A. Alexandre, J.C. Arents, M.A. Perez, R. van Grondelle, K.J. Hellingwerf, and J.T.M. Kennis, *On the signaling mechanism and the absence of photoreversibility in the AppA BLUF domain.* Biophys J, 2008. **95**(1): p. 312-321.

55. Lukacs, A., A. Haigney, R. Brust, R.K. Zhao, A.L. Stelling, I.P. Clark, M. Towrie, G.M. Greetham, S.R. Meech, and P.J. Tonge, *Photoexcitation of the blue light using FAD photoreceptor AppA results in ultrafast changes to the protein matrix.* J Am Chem Soc, 2011. **133**(42): p. 16893-900.

56. Domratcheva, T., B.L. Grigorenko, I. Schlichting, and A.V. Nemukhin, *Molecular models predict light-induced glutamine tautomerization in BLUF photoreceptors.* Biophys J, 2008. **94**(10): p. 3872-3879.

57. Sadeghian, K., M. Bocola, and M. Schultz, *A conclusive mechanism of the photoinduced reaction cascade in blue light using dlavin photoreceptors.* J Am Chem Soc, 2008. **130**(37): p. 12501-12513.

58. Dragnea, V., A.I. Arunkumar, C.W. Lee, D.P. Giedroc, and C.E. Bauer, *A Q63E Rhodobacter sphaeroides AppA BLUF domain mutant is locked in a pseudo-light-excited signaling state.* Biochemistry, 2011. **49**(50): p. 10682-10690.

59. Greetham, G.M., P. Burgos, Q. Cao, I.P. Clark, P.S. Codd, R.C. Farrow, M.W. George, M. Kogimtzis, P. Matousek, A.W. Parker, M.R. Pollard, D.A. Robinson, Z.-J. Xin, and M. Towrie, *ULTRA: A unique instrument for time-resolved spectroscopy.* Appl Spectrosc, 2009. **64**(12): p. 1311-1319.

60. Fenno, L., O. Yizhar, and K. Deisseroth, *The development and application of optogenetics.* Annu Rev Neurosci, 2011. **34**(1): p. 389-412.

61. Boyden, E.S., F. Zhang, E. Bamberg, G. Nagel, and K. Deisseroth, *Millisecond-timescale, genetically targeted optical control of neural activity.* Nat Neurosci, 2005. **8**(9): p. 1263-1268.

62. Gradinaru, V., M. Mogri, K.R. Thompson, J.M. Henderson, and K. Deisseroth, *Optical deconstruction of Parkinsonian neural circuitry.* Science, 2009. **324**(5925): p. 354-359.

63. Zemelman, B.V., G.A. Lee, M. Ng, and G. Miesenböck, *Selective photostimulation of genetically chARGed neurons.* Neuron, 2002. **33**(1): p. 15-22.

64. Berthold, P., S.P. Tsunoda, O.P. Ernst, W. Mages, D. Gradmann, and P. Hegemann, *Channelrhodopsin-1 initiates phototaxis and photophobic responses in Chlamydomonas by iImmediate light-induced depolarization.* Plant Cell, 2008. **20**(6): p. 1665-1677.

65. Schroder-Lang, S., M. Schwarzel, R. Seifert, T. Strunker, S. Kateriya, J. Looser, M. Watanabe, U.B. Kaupp, P. Hegemann, and G. Nagel, *Fast manipulation of cellular cAMP level by light in vivo.* Nat Meth, 2007. **4**(1): p. 39-42.

Chapter 2

Mechanistic Studies of S41 Mutants in $AppA_{BLUF}$

NOTE: The contents of this work are in preparation for publication. Authors for this manuscript are as follows: Andras Lukacs, Allison Haigney, Agnieszka Gil, Michael Towrie, Gregory M. Greetham, Ian P. Clark, Peter J. Tonge and Stephen R. Meech.

2.1. Introduction

Flavin binding photoreceptors are a unique group of photoreceptor proteins due to their inability to undergo large scale structural changes as a result of photoexcitation [1-4]. There is a growing interest in understanding how these flavin binding photoreceptors respond to light activation, in part because of their potential as optogenetic tools [4-7].

BLUF proteins are flavin binding photoreceptors that regulate numerous biological processes [2-4, 8, 9]. In contrast to other flavoproteins [3], the FAD is intact and fully oxidized in both dark and signaling states, and as such the protein has evolved to sense subtle changes in electronic structure of the flavin produced by photoexcitation. The best characterized BLUF protein is AppA from *R. sphaeroides,* a 450 residue multidomain protein responsible for regulation of photosystem biosynthesis [10]. A multidomain protein, AppA contains an N-terminal BLUF protein that responds to blue light and a C-terminal domain that functions as both an oxygen sensor and binds the transcription factor, PpsR [11-13]. AppA regulates photosystem biosynthesis by responding to both light excitation and oxygen concentration. In low light, low oxygen environments, AppA sequesters PpsR, allowing for production of the biochemical machinery responsible for photosynthesis. Blue light excitation or increase in O_2 stimulates a conformational change resulting in the release of PpsR, which binds to the gene cluster encoding

the photopigments responsible for photosynthesis, blocking RNA polymerase binding, and thus inhibiting photosystem biosynthesis [8]. The mechanism for light state formation is still under debate, however, it is well established that photoexcitation results in rearrangement of the H-bonding network around the flavin chromophore (Figure 2.1) [14-17]. Recent time resolved IR data have shown that the protein environment instantaneously responds to blue light in a mechanism involving keto-enol tautomerization of a conserved glutamine (Q63) side chain followed subsequently by rotation [18].

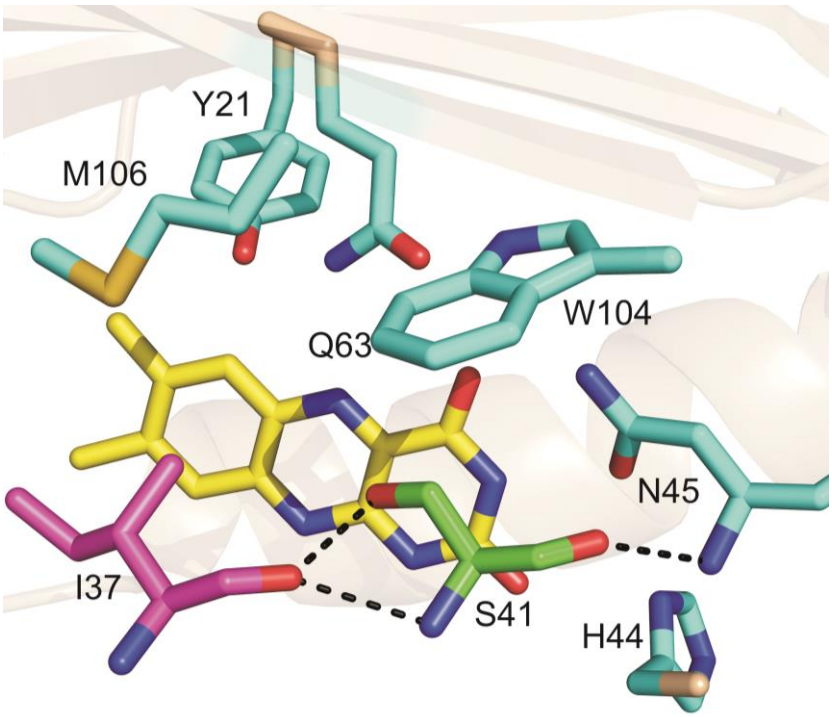

Figure 2.1. X-ray structure of $AppA_{BLUF}$ highlighting S41. Crystal structure of the flavin binding pocket, highlighting key residues Y21, H44 N45, Q63, W104 and M106 (blue). S41 is shown in green and I37 in magenta. Polar contacts involving S41 and the backbone amides of I37 and N45 are shown as dashes. The Figure was made using Pymol [19] with PDB 1YRX [20].

Rearrangement of the H-bonding interactions from the protein to the flavin must propagate to more global structural change(s) linked to PpsR dissociation, and we are interested in probing the interactions between the amino acids that directly contact the flavin and

surrounding residues. Besides Q63 and Y21, two other conserved residues interact with the flavin: N45 and H44.To date, emphasis on the characterization of photoactivation in AppA has involved looking at the residues directly involved in the H-bonding network of the flavin. Clearly, residues surrounding the flavin binding pocket must also be important for signal modulation. The backbone of N45 is H-bonded to the backbone of a Ser residue (S41 in AppA), that is conserved in 43% of BLUF proteins [21], which in turn H-bonds to a conserved isoleucine (I37) located outside the flavin binding pocket (Figure 2.1) [20]. Sequence analysis reveals a conserved IxxxS motif, suggesting an important role of I37 and its interaction with S41 for photoactivity [21]. While it has been shown to not be essential for photoactivity, the S41A mutation resulted in a 15 nm red shift in the UV-Vis absorption in both the dark and light states [21]. Computational analysis provided a mechanism where S41 "flips" upon light excitation, and this event along with rotation of the Q63 side chain stimulates light state formation, although the exact mechanism has not been experimentally tested (Figure 2.2) [21].This result was based on evidence of two possible steps involving formation of the red shift in flavin absorption: Q63 rotation/enol formation and motion of W104. Their computational evidence supported a model where either in addition to or just before W104 moves, S41 rotates to a new conformation. Restraining the temperature to <50 K, the authors reported seeing only the Q63-W104 H-bond broken. At <200 K, the S41 side chain adopts a new conformation, where the side chain –OH moves away from W104 and towards I37 (Figure 2.2). This orientation of the –OH side chain was observed in the solution NMR structure reported for $AppA_{BLUF}$ [22].

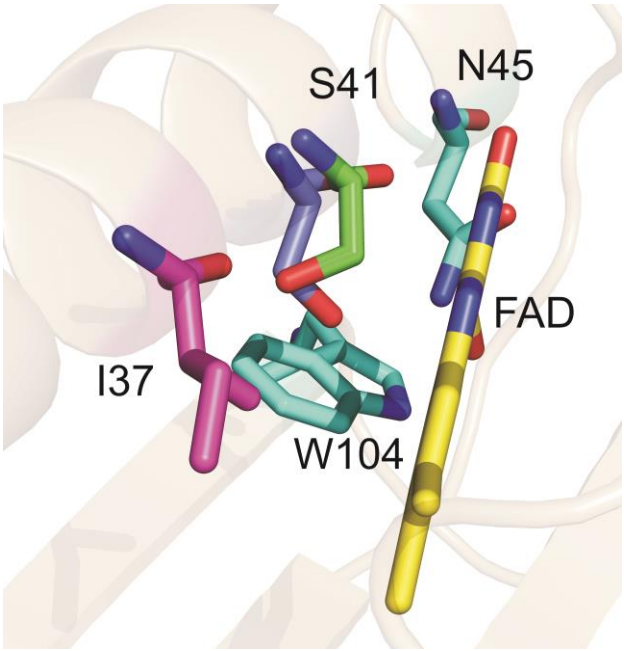

Figure 2.2. Flipping of S41 side chain. The –OH side chain can be seen in two conformations. The –OH can either be seen pointing towards W104 (blue, PDB 1YRX [20]) or I37 (green, PDB 2BUN [22]).

To further understand the role of this residue, transient absorption measurements on a homologous mutant, S28A, in the BLUF protein PixD from *Synechocystis*, were performed. These results indicated no significant difference between wild type and mutant data in terms of quantum yield of light state formation or photoactivation and the authors suggested that S28 was not essential [23]. However, these results only focused on the initial and final steps and provided no insight into the mechanism and how Ser in this position affects the photocycle. Because of its proximity to the flavin and high level of conservation in BLUF proteins, we sought to probe the origins of the red shift and the interactions between S41 and the flavin. This was achieved by measuring the ultrafast time resolved infrared (TRIR) spectra. We generated four mutants, S41A, S41T, S41C, and S41Y. These mutants were characterized using steady state and ultrafast vibrational spectroscopy. Here, we report key structural differences between wild type and the S41 mutants, revealing key interactions between S41 and N45.

2.2. Experimental Methods

2.2.1. Site-Directed Mutagenesis

Site directed mutagenesis was performed using pfu turbo (Agilent) and the primers listed in Table 2.1. Here, a pET-15B encoding for $AppA_{BLUF}$ and an N-terminal His_6 tag was used as the template.

Table 2.1. Primer design for S41 mutants.

Mutant	Forward Primer Sequence
S41A forward	5'-GACATCGTCGAGACCGCGCAGGCGCACAATGCC-3'
S41A reverse	5'-GGCATTGTGCGCCTGCGCGGTCTCGACGATGTC-3'
S41T forward	5'-GACATCGTCGAGACCACCCAGGCGCACAATGCC-3'
S41T reverse	5'- GGCATTGTGCGCCTGGGTGGTCTCGACGATGTC-3'
S41C forward	5'-GACATCGTCGAGACCTGCCAGGCGCACAATGCC-3'
S41C reverse	5'- GGCATTGTGCGCCTGGCAGGTCTCGACGATGTC-3'
S41Y forward	5'-GACATCGTCGAGACCTATCAGGCGCACAATGCC-3'
S41Y reverse	5'- GGCATTGTGCGCCTGATAGGTCTCGACGATGTC-3'

2.2.2. Protein Expression and Purification

Plasmids were transformed into BL21 (DE3) competent cells. Cells were grown at 30°C at 250 rpm in LB media until an OD600 of 0.8 was achieved. Induction was performed overnight with 0.8 mM IPTG at 18°C in the dark. The following morning, cells were harvested by centrifugation (5000 rpm, 4°C) and cell pellets were stored at -20°C until needed. Thawed cell pellets were then resuspended in 40 mL of lysis buffer (10 mM sodium chloride, 50 mM sodium phosphate, pH 8) to which 200 μL of 50 mM PMSF was added. After lysis by sonication, cell debris was removed by ultracentrifugation (33000 rpm for 90 min). A 1 mL solution of 10 mg/mL FAD was added to the supernatant and incubated for 45 min at 4°C. Purification was

performed using Ni-NTA chromatography (Qiagen) with 10 mM sodium chloride, 50 mM sodium phosphate, pH 8 (wash buffer).The column was then washed with 0, 10 and 20 mM imidazole and ultimately eluted with 250 mM imidazole. Fractions containing protein were pooled (~15-20 mL) and dialyzed in 3L of wash buffer overnight. The purity and yield were determined using SDS-PAGE and UV-Vis absorption spectroscopy and stored at 4°C.

2.2.3. Photoconversion Experiments

Steady state absorption spectra were recorded using a Cary 100 (Varian) UV-Vis spectrometer at 25°C. Light state samples were generated by irradiation with 20 mW of 460 nm light for 3 min.

2.2.4. Raman Spectroscopy

Steady state Raman spectra were recorded using a model 890 Ti:sapphire laser (Coherent, Santa Clara, CA), pumped by an Innova 308C argon ion laser (Coherent), providing 550 mW at 752 nm. Spectra were measured by focusing the beam on the base of a 2 mm by 2 mm quartz cuvette containing a solution of 80 µL of 1.5 mM protein and were collected at 90°. Rayleigh scattered light was removed with a super notch plus holographic filter (Kaiser Optical Systems, Inc.). Data were collected for 300 accumulations with an exposure time of 2 seconds. Buffer spectra were collected at the same conditions and were subtracted from the protein spectra. The system was calibrated using cyclohexanone as a standard at a resolution of 8 cm^{-1} [24].

2.2.5. FTIR Spectroscopy

FTIR spectroscopy was performed on a Vertex 80 (Bruker) IR spectrometer. The sample chamber and optics were purged with dry air and 64 scans were taken at 1 cm^{-1} resolution in a 50 µm path length cell containing CaF_2 windows. Protein samples at a concentration of 1.5 mM in deuterated buffer (50 mM sodium phosphate, 10 mM sodium chloride, pD 8) were irradiated with a 460 nm high mount LED (Prizmatix) for 3 minutes. Light minus dark difference spectra were generated by subtracting the irradiated spectrum from the non-irradiated spectrum.

2.2.6. TRIR Spectroscopy

Ultrafast time resolved infrared (TRIR) spectroscopy was performed at the STFC Central Laser Facility (CLF) using the apparatus and methods previously described [25]. Measurements on both dark and light states were performed using a 10 kHz amplified Ti:sapphire system pumping OPAs. Transient IR spectra were recorded as pump on minus pump off difference spectra with excitation wavelength set to 450 nm at 200 nJ per pulse. Dark state measurements were performed with samples flowed at a rate of 1.5 mL/min to minimize photoconversion during the measurement. All samples were rastered to minimize sample degradation. Protein samples were prepared at concentrations of 1.5 mM in deuterated buffer (50 mM sodium phosphate, 10 mM sodium chloride, pD 8). The TRIR setup was operated and maintained by the CLF (Dr. Greg Greetham, Dr. Ian Clark, Dr. Mike Towrie).

2.3. Results and Discussion

2.3.1. Photoconversion Data

Formation of the signaling state of $AppA_{BLUF}$ results in a ~10 nm red shift in the flavin absorption band at 445 nm (to 456 nm). This subsequently returns to the dark state in a light-independent reaction in 30 min (Table 2.2). This has been proposed to be the result of rearrangement of the protein matrix surrounding the flavin, as indicated by the vibrational spectra of the flavin C4=O carbonyl [14, 26]. To elucidate a possible role for S41 in the photocycle, initial characterization was performed using UV-Vis absorption spectroscopy. The S41A mutation resulted in a red shift (Table 2.2) in the UV-Vis absorption spectrum of the flavin (Figure 2.3A). Photorecovery experiments revealed minimal effect on the light to dark recovery time. Both of these results are in good agreement with published data [21]. The absorption data for the S41C $AppA_{BLUF}$ mutant resulted in a 5 nm red shift in flavin absorbance for both the dark and light adapted states along with a ~4-fold faster rate of dark state recovery (Figure 2.3B, Table 2.2) In contrast, for S41T (Figure 2.3C), the absorption spectra revert to that observed for $wtAppA_{BLUF}$. However, the rate of dark state recovery is increased by ~8-fold (Table 2.2). The S41Y mutant did not bind flavin and therefore no further studies were performed. The lack of binding is presumably due to a potential steric clash with the bulky phenol side chain now present in the S41Y mutant that occupies part of the flavin binding pocket.

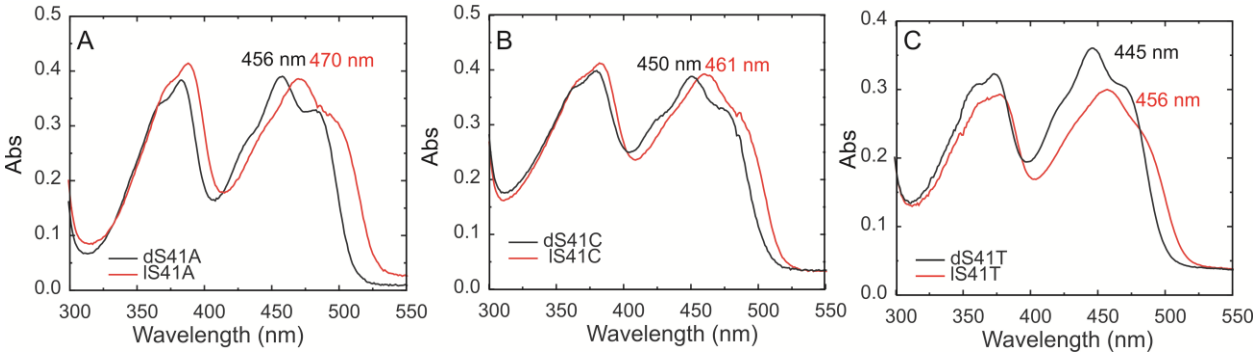

Figure 2.3. Photoconversions of S41 mutants. Absorption spectra of the flavin in S41A (**A**), S41C (**B**) and S41T (**C**). Dark adapted states are in black and light adapted states are in red. Light adapted states were generated by 3 minute irradiation of 460 nm light.

Table 2.2. Light to dark photorecovery data for S41 mutants.

Sample	Dark Abs (nm)	Light Abs (nm)	ΔAbs (nm)	t ½ (min)
wtAppA$_{BLUF}$	445	456	11	13.7 ± 0.1
S41A	456	470	14	12.7 ± 0.2
S41T	450	461	11	1.8 ± 0.1
S41C	445	456	11	3.1 ± 0.1

Photorecovery data revealed an interesting result for the S41 mutations. Removing the hydroxyl side chain resulted in a red shift in the λ_{MAX} of the flavin, yet moving the hydroxyl side chain did not. While eliminating a potential H-bond partner in the S41A mutation did not significantly affect photorecovery, the S41C and S41T resulted in a faster relaxing signaling state. Increasing the size of the side chain (S41C) resulted in a faster recovering mutant, and moving the hydroxyl diminished the recovery even more. In addition to the shifted –OH side chain, a methyl group is present in the S41T mutant that may perturb interactions surrounding the flavin. Computational analysis of S41 revealed an important role for this residue. It was shown that the molecular orbital contributing primarily to the S1 transition shows contribution of the S41 side chain, where considerable electron density was observed on the hydroxyl side chain

of S41 [21]. By delocalizing electron density away from the flavin, the authors suggest that the presence of S41 lowers the energy of the HOMO but does not affect the LUMO (Figure 2.4). The S41A mutant, therefore, would increase the energy of the HOMO without disrupting the LUMO. This would ultimately result in a lower energy HOMO to LUMO transition in S41A, and is indicated by the red shift in flavin absorption from in both dark (445 nm to 456 nm) and light (456 to 470 nm) states. The –OH side chain in the S41T mutant is also capable of delocalizing electron density away from the flavin, which would result in a similar electronic absorption spectrum, as observed in Figure 2.3B. However, the addition of the methyl group may introduce steric clashes that destabilize the light adapted state. For the S41C, based on the absorption data it can be concluded that the thiol side chain is in some intermediate state, where some electron density is delocalized away from the flavin yet not to the extent observed in wild type.

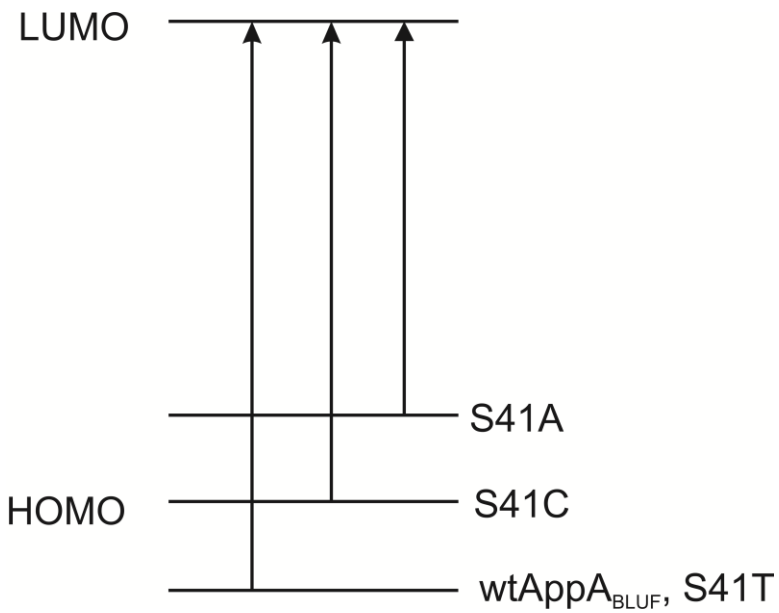

Figure 2.4. Electronic transitions in S41 mutants. Delocalization of electron density away from the flavin stabilizes the HOMO (lower energy). This stabilization is reduced in the S41C mutant and gone in the S41A mutant. The LUMO is unaffected. By stabilizing the HOMO, a higher energy (i.e. lower wavelength) electronic transition is observed.

2.3.2. FTIR Spectroscopy

To further characterize structural changes upon photoactivation, we performed steady state FTIR spectroscopy. The spectra are reported as light minus dark difference spectra in Figure 2.5. In agreement with previously published results, two difference modes are present for wtAppA_{BLUF} at 1688(+)/1700(-) cm^{-1}, assigned to a shift in the C4=O carbonyl vibration of the flavin, and a lower mode at 1622(-)/1631(+) cm^{-1}, which has been assigned to vibrations of the protein backbone, in particular the β5 strand [14, 16]. This band is greatly diminished in W104 mutants, a residue found on the β5 strand that has been proposed to function as the modulator of the photoexcitation signal from the N-terminal domain to the C-terminal domain [27-29]. The 1688(+)/1700(-) cm^{-1} mode, assigned as the C4=O carbonyl of the flavin [14], is unaffected by mutations to S41. These results would indicate that the primary effect of the S41 mutations is not on the position of Q63.

The S41A mutant appears to have little or no effect on the protein difference band. A 15 nm red shift in absorbance is observed in both dark and light adapted S41A, however, the FTIR difference spectra reported in Figure 2.4, and show that the S41A mutant resembles that of wtAppABLUF. These results indicate a possible contribution of the ES to the red shift in the flavin absorbance for S41A (Figure 2.3, Table2.2). In addition to the red shift observed in S41A, a 5 nm red shift in flavin absorption (Table 2.2) is observed in the S41C mutant. A slight difference is observed in the FTIR light minus dark difference spectrum at the positive mode at 1665 cm^{-1} compared to wtAppA_{BLUF}, indicating a difference between the light state of AppA_{BLUF} and S41C. The assignment of this mode was performed by Masuda et al by uniform ^{13}C-labeling of the protein. Isotopic labeling of the protein resulted in this mode shifting, by approximately 40 cm^{-1}, indicating that is was a protein mode and was tentatively assigned to CN vibrations of the

protein backbone [14]. Based on its position, it is possible that this mode has some contributions from turns and some disordered regions, with possible minor contributions from α-helices [30], both of which can be found in the flavin binding pocket of $AppA_{BLUF}$ (Figure 2.1). Therefore, one can conclude that minor perturbations to secondary structure occur as a result of the S41C mutation which are absent in the S41A mutant, presumably due to steric interactions.

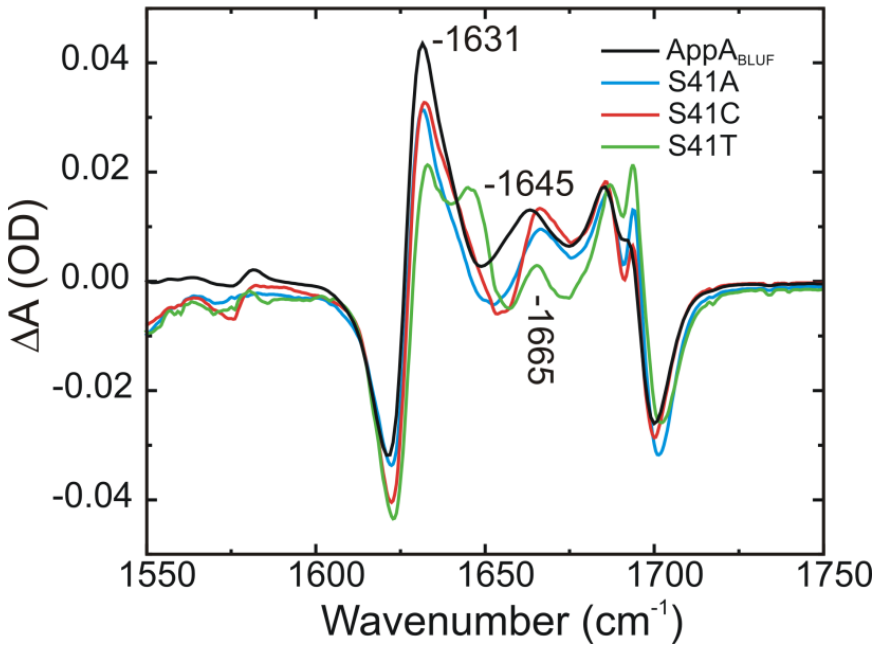

Figure 2.5. FTIR spectra of S41 mutants. FTIR light minus dark spectra of $AppA_{BLUF}$ (black), S41A (green), S41T (red), and S41C (blue). Light states were formed followed by 3 min of excitation with 460 nm light.

Comparison of the spectra for wild type and S41T revealed differences in the 1620(-)/1631(+) cm^{-1} mode. This vibration is disrupted in the S41T mutant, where a new shoulder is observed at 1645 cm^{-1}. The observed 1620/1631 cm^{-1} mode in $AppA_{BLUF}$ is indicative of a loss of β-sheet character [30]. The W104A mutant in AppABLUF was shown to suppress formation of the protein modes while also greatly increasing the rate of dark state recovery [27]. The role of W104 will be discussed in greater detail in Chapter 4. It is possible that the S41T mutant introduces unwanted steric clashes with W104, which is producing the altered protein modes.

The shoulder observed at 1645 cm^{-1}, however, is in a unique position. This band is in a region where one would expect to see α-helical structures, which are not observed in wild type or the other S41 mutants. This mode is also positive, indicating that this difference is present in the light adapted state. An 8-fold difference in recovery was observed for the S41T mutant compared to wild type (Table 2.2). The S41T mutant exhibits a decrease in intensity in the protein mode at 1665 cm^{-1}. These results suggest that the S41T alters the secondary structure of the protein, in particular the β5 strand near the flavin.

2.3.3. Raman Spectroscopy

Further characterization of the S41 mutants was performed using Raman spectroscopy. Raman spectroscopy has been well established as a method for monitoring structural changes in BLUF proteins [26, 28, 31]. Raman spectroscopy also allows for improved characterization of flavin specific modes, where in FTIR these modes overlap with the much stronger amide I and II vibrations of the protein backbone. These experiments are also capable of being performed in H_2O, while in FTIR water has a significant absorption in 1500-1700 cm^{-1} region. Figure 2.6 shows the spectra measured for the S41 mutants overlaid with wt$AppA_{BLUF}$. The intense mode at 1668 cm^{-1} is absent in free flavin and has been assigned as the amide I mode. Bands at 1345, 1500 and 1543 cm^{-1} are present in free flavin and have all been assigned to CC and CN vibrations of the flavin chromophore while bands at 1452 and 1403 cm^{-1} were assigned to methyl deformation [26, 32]. The intense band observed at 1232 cm^{-1} has been assigned to three overlapping bands, two arising from FAD and the third from amide III. An intense band is observed at 1668 cm^{-1} in all the spectra that is absent in free flavin and has been assigned as arising from the amide I vibrations of the protein. Bands at 1155 and 1179 cm^{-1} are weak flavin modes assigned to vibrations in the xylene ring of the flavin chromophore [33].

Initial comparisons of the S41 mutant spectra with wild type indicate few differences in the flavin modes (Figure 2.6). These results indicate the flavin is not substantially perturbed in the binding pocket. Characterization of secondary structure has been well described in the literature using Raman spectroscopy [34-37]. Differences between mutant and wild type spectra are observed in the protein modes, in particular the amide I vibration. In the dS41T spectrum, a less broad peak is observed; losing some intensity on the lower wavenumber side of the peak, where one would expect to see contributions from α-helices [35]. This is not observed in the lS41T spectrum, indicating an increase in α-helical structure as a result of photoexcitation and is in agreement with FTIR data presented above (Figure 2.5). The amide band of S41C in both the dark and light adapted spectra both are at a much higher intensity than wild type. Protein amide I bands increase in intensity with increasing depolarization ratio [38], and thiols are more polarizable than hydroxyls. Therefore, it is possible that the addition of the more polarizable thiol side chain increases the magnitude of the amide I; however, this mode does not shift.

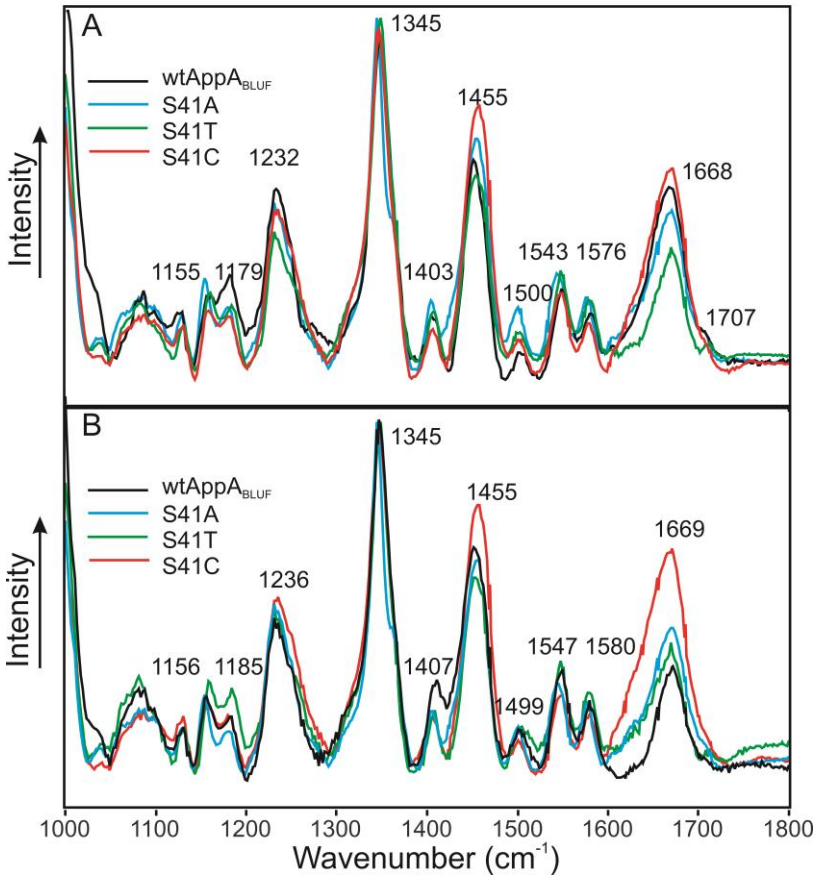

Figure 2.6. Steady state Raman spectra of S41 Mutants. Raman spectra for wtAppA (black), S41A (blue), S41T (green) and S41C (red) measured with 752 nm light. A. Spectra of dark states. B. Spectra of light states.

2.3.4. TRIR Spectroscopy

The steady state FTIR data reveal that the structural rearrangements which accompany light state formation are largely unperturbed in the S41 mutants. To gain insight into the initial steps of photoactivation, we employed time resolved infrared (TRIR) spectroscopy. Bleaches observed at 1547 cm^{-1}, 1585 cm^{-1}, 1650 cm^{-1}, and 1700 cm^{-1} have all been assigned as flavin based on the TRIR spectra of free flavin in solution [38]. For dAppA$_{BLUF}$, a transient at 1670 cm^{-1} is observed absent in free flavin and light adapted AppA$_{BLUF}$ along with a 10 cm^{-1} shift in the 1700 cm^{-1} band to 1690 cm^{-1} in lAppA$_{BLUF}$ [15, 16, 40]. These modes have all been proposed to be indicators of a photoactive species.

Characterization of the TRIR spectra for S41A revealed important structural differences relative to wtAppA$_{BLUF}$. In the dS41A (Figure 2.7A) and lS41A (Figure 2.7B) spectra, there is a slight shift is observed in the 1547 cm^{-1} flavin mode to 1541 cm^{-1}. This bleach has been assigned primarily as the C10a-N1 vibration, with a contribution to the C4a-N5 stretch and is normally unaffected by signaling state formation [40]. The two highest frequency bleaches have been assigned to the C2=O and C4=O of the flavin are observed at 1650 and 1700 cm^{-1}, respectively; these bands do not shift with the S41A mutation. The 1700 cm^{-1} mode is shifted by 10 cm^{-1} on formation of lS41A which is consistent with previous findings on wtAppA$_{BLUF}$ [15, 16]. A transient feature at 1670 cm^{-1} (assigned as Q63 side chain [16]) in dAppA$_{BLUF}$ is present also in S41A, suggesting no perturbation of the Q63 side chain in the S41A mutant. A more prominent feature at 1630 cm^{-1} is also observed in both dS41A and lS41A in comparison to d and lAppA, as well as a stronger bleach at 1625 cm^{-1} for lS41A. In our previous work this mode shifted upon ^{13}C labeling of the protein, revealing it to be a protein mode [18]. These results indicate protein modes surrounding the flavin are altered as a result of the S41A mutation. Based on its position, potential residues for this assignment are H44 and N45, which have vibrational modes at ~1630 cm^{-1} [41, 42]. Rotation of the Q63 side chain alters the H-bonding network, resulting in formation of the light adapted state. The formation of a new H-bond to the C4=O which is proposed to result from these changes would decrease electron density around the flavin C4=O, and thus weaken the interaction to N45. As a consequence this may allow additional freedom of motion in this side chain. Immediately adjacent to N45 is H44, which forms an H-bond to the C2=O of the flavin. The loss of the hydroxyl side chain in the S41A mutation would result in the loss of H-bonding interactions to the backbone amides of H44 and N45. Based on these results we propose changes are due to the loss of stabilizing interactions between S41 and H44/N45.

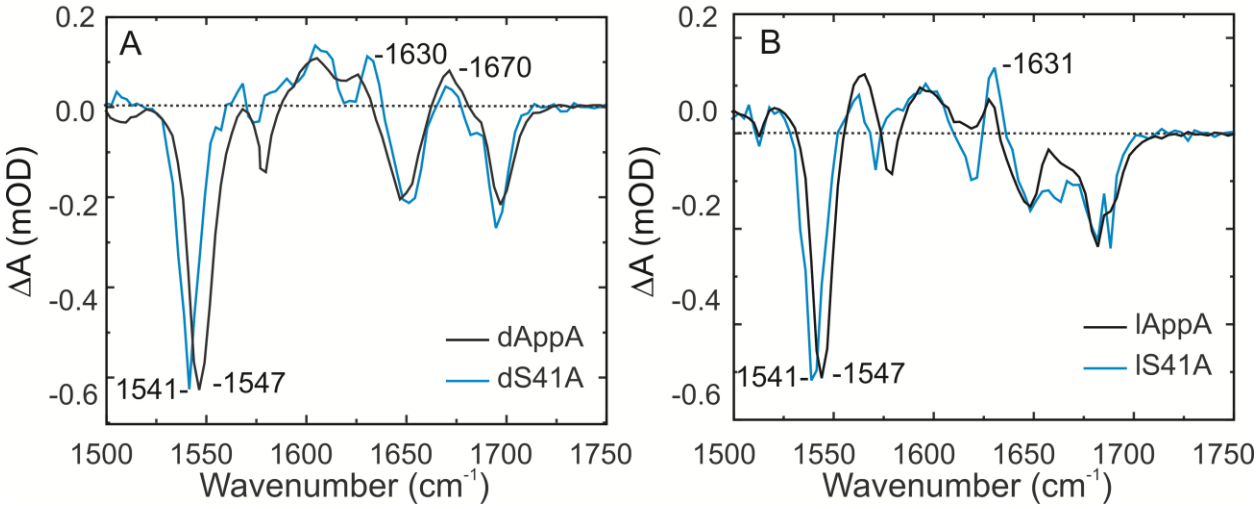

Figure 2.7. TRIR spectra of S41A. TRIR spectra of AppA (black) and S41A (blue) taken 3 ps post-excitation. **A.** Spectra of dark adapted states. **B.** Spectra of light adapted states.

In addition to the shift in the main bleach of the flavin, splitting of the flavin carbonyl bleaches can be observed in lS41A (Figure 2.7B). This is observed in the wild type spectrum for the C4=O, albeit to a much lesser extent than the mutant spectrum. The splitting of the C2=O carbonyl is intriguing. The Removal of the –OH group in the S41A mutant results in the loss of H-bonding interactions between S41 and the backbone H44/N45 amide (Figure 2.1), which have been proposed to form H-bonds with the flavin C2=O and C4=O carbonyls, respectively. These results signify key differences in the H-bonding network surrounding the flavin.

TRIR spectra measured for the dark and light adapted state of S41T reveal similar features to those observed in wtAppA$_{BLUF}$, in particular in the 1500 – 1600 cm^{-1} region (Figure 2.8A and 2.8B). Unlike that observed in the S41A mutant, no shift in the 1547 cm^{-1} bleach is present. The S41T mutation does not exhibit a red shift in the flavin absorption spectrum, which is observed for the S41A mutation. For dS41T, no transient is observed at 1670 cm^{-1}. This band was previously proposed to be a marker for photoactivity [16]. However, a 10 cm^{-1} shift in the flavin C4=O is observed in lS41T. The 10 cm^{-1} shift is to be expected based on steady state FTIR

analysis (Figure 2.5), however, the loss of the 1670 cm^{-1} transient is surprising. At 1670 cm^{-1} one would not expect to see a hydroxyl side chain; if this mode did in fact arise from the S41 side chain it should not be present in other S41 mutants. In order to understand what has happened, one must consider the structure of the flavin binding pocket. There are two amide side chains present in the flavin binding pocket; Q63 and N45. Structural data indicate that S41 can interact with N45. Interactions between S41 and N45 could stabilize interactions between N45 and the flavin. The S41A mutation revealed that this interaction is not required, yet with its loss, the electrostatic interactions between the protein environment and the flavin are altered, as exhibited by the shift in the flavin absorption spectrum. However, if the incorrect interactions are formed, the H-bonding network would be altered and ultimately the formation of the light state. Disrupting the interaction between S41 and N45 would also disrupt interactions between N45 and the flavin, as evidenced by both the loss of the 1670 cm^{-1} transient in dS41T compared to $dAppA_{BLUF}$. Therefore, we can potentially modify our previous assignment of the 1670 cm^{-1} as arising from contributions of N45 and not exclusively from Q63.

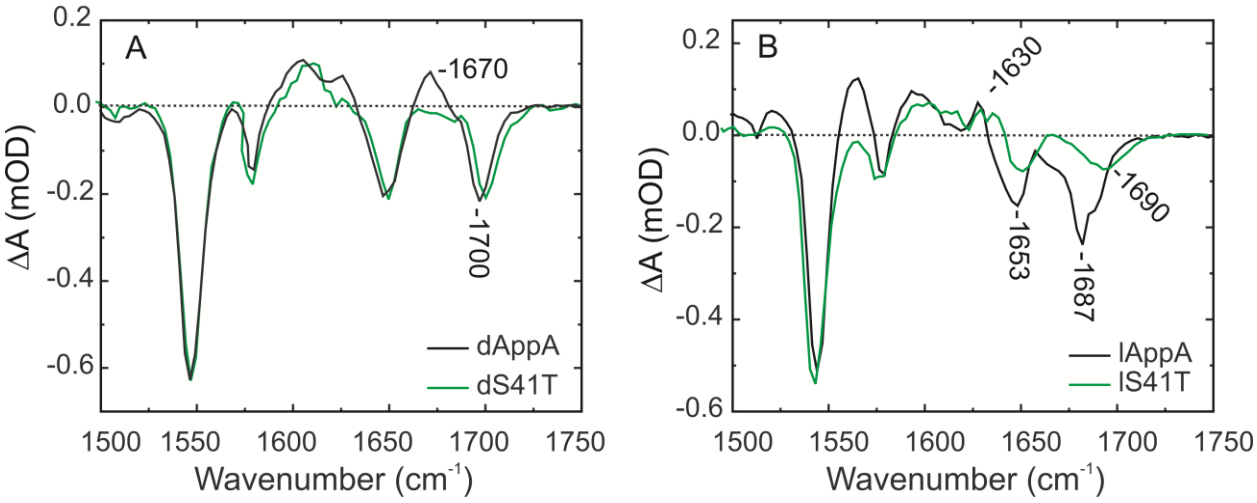

Figure 2.8. TRIR spectra of S41T. TRIR spectra of AppA (black) and S41T (green) taken 3 ps post-excitation. **A.** Spectra of dark adapted states. **B.** Spectra of light adapted states.

Another potential hypothesis is that formation of the 1670 cm^{-1} transient is disrupted as a result of the S41T mutant. Based on the FTIR and Raman spectra above for S41T, one can clearly see the protein matrix is disrupted. This results in a photoactive species with a 7.6 fold increase in photorecovery. Therefore, it is possible the reason for the absence of this mode is a kinetic one. By overlaying multiple spectra (Figure 2.9), one can see while no transient is formed at 1670 cm^{-1}, a small positive feature can be seen forming at 1689 cm^{-1}. This mode appears in the steady state FTIR spectrum, and is assigned as the red-shifted C4=O flavin carbonyl [14]. This is rather surprising, since it was reported that formation of the light state occurs within 1 ns [43]. If this is in fact the formation of the light state, this is occurring on a much faster timescale. These results clearly indicate that S41T disrupts the mechanism of photoactivation, indicating the importance of S41 in $AppA_{BLUF}$.

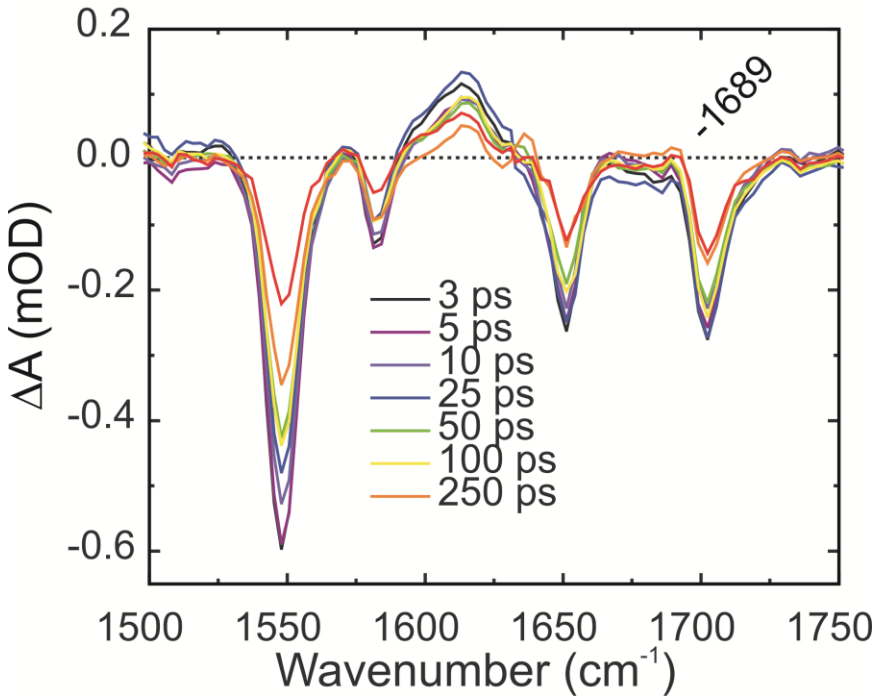

Figure 2.9. Overlay of dS41T. TRIR spectra of dS41T at 3 (black) 5 (purple), 10 (violet), 25 (blue), 50 (green) 100 (orange) and 250 ps (red).

The S41C mutation increased the rate of dark state recovery while also shifting the absorption spectrum by 5 nm; however, no structural differences were observed by FTIR spectroscopy. In both d and lS41C, the main bleach that is typically observed at 1547 cm^{-1} is shifted down to 1543 cm^{-1} (Figure 2.10) while the absorption spectrum of the flavin shifts from 445 nm to 450 nm (Figure 2.3B). These results correlate with what is observed in S41A and S41T. For S41A, an 11 nm red shift is observed in the UV-Vis absorption spectrum of the flavin (Figure 2.3A) and a 6 cm^{-1} blue shift on the main bleach associated with the flavin (from 1547 to 1541 cm^{-1}). In the S41T absorption spectrum, no shift is observed (Figure 2.3C) and no shift is observed in the main bleach (Figure 2.8). These results show a correlation between the main flavin bleach with the absorption spectrum.

Apart from the 1543 cm^{-1} bleach, the TRIR spectrum for dS41C is very similar to $dAppA_{BLUF}$ (Figure 2.10A), with the exception of the transient observed at 1670 cm^{-1} in wtAppA; for dS41C this mode is now at 1665 cm^{-1} (Figure 2.10A). This mode has not been observed to shift with any other mutant before. For lS41C, an interesting result is observed at the 1652 cm^{-1} bleach, previously assigned as the C2=O flavin carbonyl which was shown to be unaffected by light state formation (Figure 2.10B) [15]. This mode is weakened upon light state formation. Disrupting the interactions between N45 and the flavin would also affect those between H44 and the flavin. It is plausible the thiol side chain would alter interactions to H44 and N45. Based on these results and the 5 cm^{-1} shift in the 1670 cm^{-1} mode to 1665 cm^{-1} in dS41C, it can be concluded that the S41C mutation disrupts the H-bonding interactions of H44 and N45 to the flavin in both the dark and light state.

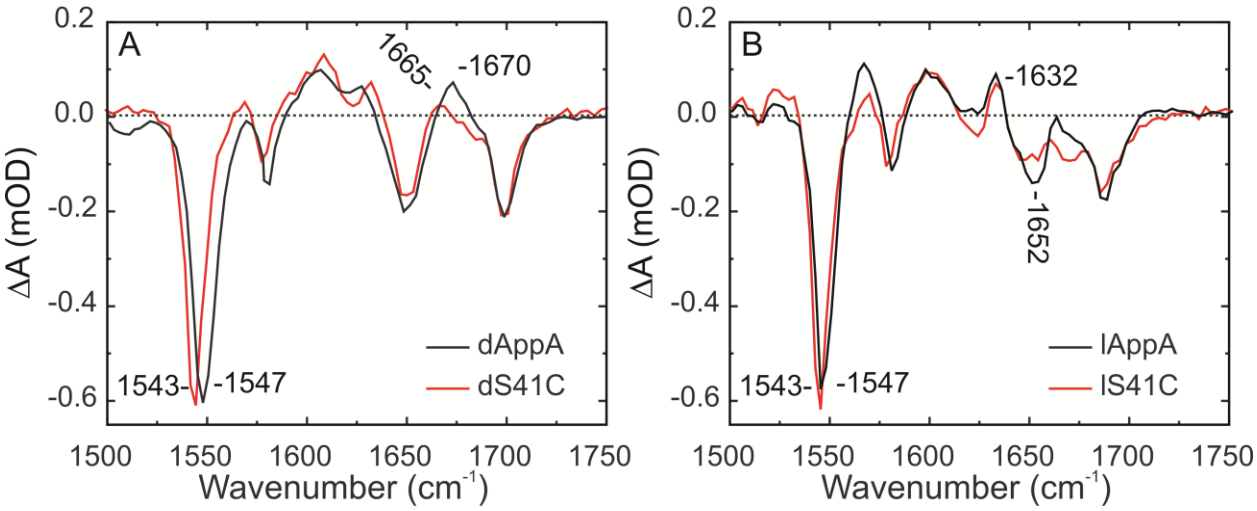

Figure 2.10. TRIR spectra of S41C. TRIR spectra of AppA (black) and S41C (red) taken 3 ps post-excitation. **A.** Spectra of dark adapted states. **B.** Spectra of light adapted states.

An interesting trend that is observed in the S41 mutants involves the main flavin bleach that is observed in wtAppA_{BLUF} in both the dark and light adapted states at 1547 cm^{-1}. In Figure 2.11, the λ_{max} of the flavin in both the dark and light adapted states was converted to wavenumbers and compared with the frequency of the main flavin bleach. A linear correlation can be seen between flavin absorbance and the frequency of this vibrational mode. This mode is a bleach and can be assigned to the ground state of the flavin and indicates that a ground state stabilization contributes to the red shift in flavin absorbance observed in the S41A (Figure 2.3A) and S41C (Figure 2.3B) mutants.

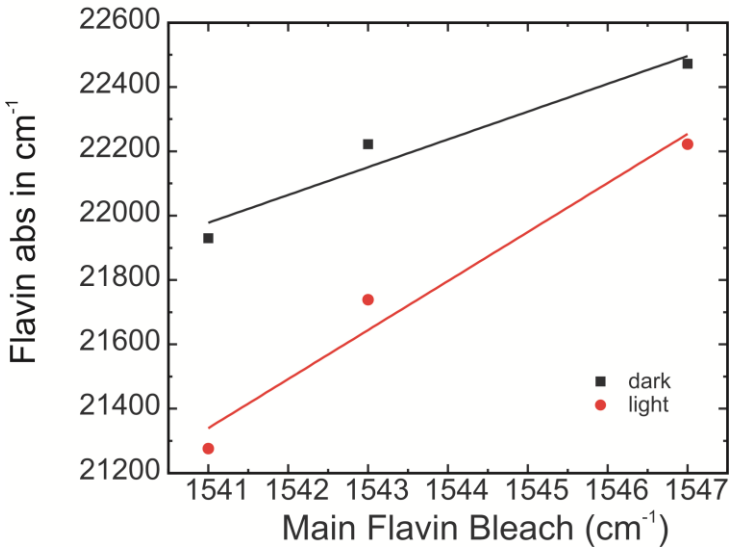

Figure 2.11. Overlay of main flavin bleach and UV-Vis absorption. Overlay of the main flavin bleach for the S41 mutants with the flavin absorption in wavenumbers reveals a linear correlation. For the dark states (black), an R^2 of 0.90 is reported with a slope of 86 ± 20 and for the light states (red) an R^2 of 0.94 is reported with a slope of 152 ± 27 was calculated.

Ground state recovery kinetics were measured for AppA and the S41 mutants by recording the kinetics at 1547 cm^{-1}; the results are summarized in Table 2.3. Non-single exponential decay was observed for wild type and for the S41 mutants, in agreement with previous results [15, 18]. Analysis of the average lifetimes recovered from a bi-exponential fit reveal mutations to S41 increases the ground state recovery in the dark states by a factor of 1.8 (S41A), 3.1 (S41T), and 1.7 (S41C). A more modest increase in recovery is observed in the light adapted states of 1.36 (S41A), 1.45 (S41T). For lS41C, there is a slight decrease in rate of recovery compared to wild type (1.07 fold). These values indicate the S41 mutations affect the initial events upon photoexcitation but yield little effect once the light adapted state is formed in terms of ground state recovery.

Table 2.3. GS recovery kinetics for S41 mutants

Sample	α1	τ1 (ps)	α2	τ2 (ps)	<τ> (ps)
dAppA	0.51	34 ± 4	0.49	473 ± 73	249
lAppA	0.72	11 ± 1	0.28	134 ± 24	45
dS41A	0.64	26 ± 3	0.36	204 ± 12	140
lS41A	0.68	8 ± 0.5	0.32	86 ± 10	33
dS41T	0.38	6 ± 1	0.62	202 ± 44	80
lS41T	0.33	8 ± 2	0.67	77 ± 26	31
dS41C	0.46	38 ± 3	0.54	244 ± 21	149
lS41C	0.29	10 ± 1	0.71	141 ± 12	48

2.5. Conclusions

While not an essential residue for photoactivity, S41 does play an important role in the photocycle of AppA. The S41A and S41C mutants resulted in red shifts in the UV-Vis absorption of the flavin, while the S41T mutation drastically altered dark state recovery. Light minus dark FTIR difference and steady state Raman spectra implicate the S41 residue as being essential for ensuring proper secondary structures are formed in both dark and light adapted states. The TRIR data showed several differences which all point to an indirect role for S41 in the H-bond network around the flavin. The S41 mutants reveal a correlation between the main bleach of the flavin along with a transient associated with the protein and the absorption of the flavin (Figure 2.10). Linear correlations can be seen in both dark and light adapted states, albeit to different magnitudes. A nearly 2-fold larger slope is observed in the light states compared to the dark states (152 versus 86).

These data highlight the importance of S41 in orienting the surrounding residues for optimal interactions with the flavin. The most significant finding is that seen in the TRIR spectrum of dS41T, where the absence of the 1670 cm^{-1} transient, previously proposed to be a

marker of photoactivity, is absent and does not form within the first 2 ns. Therefore, this mode can tentatively be assigned to include N45.

2.6. References

1. Losi, A., *The bacterial counterparts of plant phototropins.* Photochem. Photobiol. Sci., 2004. **3**(6): p. 566-574.
2. Losi, A. and W. Gartner, *Bacterial bilin- and flavin-binding photoreceptors.* Photochem Photobiol Sci, 2008. **7**(10): p. 1168-1178.
3. Losi, A. and W. Gärtner, *Old chromophores, new photoactivation paradigms, trendy applications: Flavins in blue light-sensing photoreceptors.* Photochem Photobiol, 2011. **87**(3): p. 491-510.
4. Losi, A. and W. Gärtner, *The evolution of flavin-binding photoreceptors: An ancient chromophore serving trendy blue-light sensors.* Annu Rev Plant Biol, 2012. **63**(1): p. 49-72.
5. Christie, J.M., J. Gawthorne, G. Young, N.J. Fraser, and A.J. Roe, *LOV to BLUF: Flavoprotein contributions to the optogenetic toolkit.* Mol Plant, 2012. **5**(3): p. 533-544.
6. Yin, T. and Y. Wu, *Guiding lights: recent developments in optogenetic control of biochemical signals.* Pflugers Archiv, 2013. **465**(3): p. 397-408.
7. Mitra, D., X. Yang, and K. Moffat, *Crystal structures of aureochrome1 LOV suggest new design strategies for optogenetics.* Structure, 2012. **20**(4): p. 698-706.
8. Gomelsky, M. and G. Klug, *BLUF: a novel FAD-binding domain involved in sensory transduction in microorganisms.* Trends Biochem Sci, 2002. **27**(10): p. 497-500.
9. Masuda, S., *Light detection and signal transduction in the BLUF photoreceptors.* Plant Cell Physiol, 2013. **54**(2): p. 171-179.

10. Masuda, S. and C.E. Bauer, *AppA Is a blue light photoreceptor that antirepresses photosynthesis gene expression in Rhodobacter sphaeroides.* Cell, 2002. **110**(5): p. 613-623.

11. Pandey, R., D. Flockerzi, Marcus J.B. Hauser, and R. Straube, *Modeling the light- and redox-dependent interaction of PpsR/AppA in Rhodobacter sphaeroides.* Biophys J, 2011. **100**(10): p. 2347-2355.

12. Kim, S.K., J.T. Mason, D.B. Knaff, C.E. Bauer, and A.T. Setterdahl, *Redox properties of the Rhodobacter sphaeroides transcriptional regulatory proteins PpsR and AppA.* Photosynth. Res., 2006. **89**(2-3): p. 89-98.

13. Pandey, R., D. Flockerzi, M.J.B. Hauser, and R. Straube, *An extended model for the repression of photosynthesis genes by the AppA/PpsR system in Rhodobacter sphaeroides.* FEBS J, 2012. **279**(18): p. 3449-3461.

14. Masuda, S., K. Hasegawa, and T.-a. Ono, *Light-induced structural changes of apoprotein and chromophore in the sensor of blue light using FAD (BLUF) domain of AppA for a signaling state* Biochemistry, 2005. **44**(4): p. 1215-1224.

15. Haigney, A., A. Lukacs, R.-K. Zhao, A.L. Stelling, R. Brust, R.-R. Kim, M. Kondo, I. Clark, M. Towrie, G.M. Greetham, B. Illarionov, A. Bacher, W. Romisch-Margl, M. Fischer, S.R. Meech, and P.J. Tonge, *Ultrafast infrared spectroscopy of an isotope-labeled photoactivatable flavoprotein.* Biochemistry, 2011. **50**(8): p. 1321-1328.

16. Stelling, A.L., K.L. Ronayne, J. Nappa, P.J. Tonge, and S.R. Meech, *Ultrafast structural dynamics in BLUF domains: Transient infrared spectroscopy of AppA and its mutants.* J Am Chem Soc, 2007. **129**(50): p. 15556-15564.

17. Unno, M., R. Sano, S. Masuda, T.-a. Ono, and S. Yamauchi, *Light-Induced Structural Changes in the Active Site of the BLUF Domain in AppA by Raman Spectroscopy.* J. Phys. Chem. B, 2005. **109**(25): p. 12620-12626.

18. Lukacs, A., A. Haigney, R. Brust, R.-K. Zhao, A.L. Stelling, I.P. Clark, M. Towrie, G.M. Greetham, S.R. Meech, and P.J. Tonge, *Photoexcitation of the blue Light Using FAD Photoreceptor AppA results in ultrafast changes to the protein matrix.* J Am Chem Soc, 2011. **133**(42): p. 16893–16900.

19. *The PyMOL molecular graphics system, Version 1.2r3pre, Schrödinger, LLC.*

20. Anderson, S., V. Dragnea, S. Masuda, J. Ybe, K. Moffat, and C. Bauer, *Structure of a novel photoreceptor, the BLUF domain of AppA from Rhodobacter sphaeroides.* Biochemistry, 2005. **44**(22): p. 7998-8005.

21. Götze, J. and P. Saalfrank, *Serine in BLUF domains displays spectral importance in computational models.* J Photochem Photobiol B, 2009. **94**(2): p. 87-95.

22. Grinstead, J.S., S.-T.D. Hsu, W. Laan, A.M.J.J. Bonvin, K.J. Hellingwerf, R. Boelens, and R. Kaptein, *The solution structure of the AppA BLUF domain: Insight into the mechanism of light-induced signaling.* ChemBioChem, 2006. **7**(1): p. 187-193.22.

23. Bonetti, C., M. Stierl, T. Mathes, I.H.M. van Stokkum, K.M. Mullen, T.A. Cohen-Stuart, R. van Grondelle, P. Hegemann, and J.T.M. Kennis, *The role of key amino acids in the photoactivation pathway of the Synechocystis Slr1694 BLUF domain.* Biochemistry, 2009. **48**(48): p. 11458-11469.

24. Bell, A.F., X. He, R.M. Wachter, and P.J. Tonge, *Probing the ground state structure of the green fluorescent protein chromophore using Raman spectroscopy.* Biochemistry, 2000. **39**(15): p. 4423-31.

25. Greetham, G.M., P. Burgos, Q. Cao, I.P. Clark, P.S. Codd, R.C. Farrow, M.W. George, M. Kogimtzis, P. Matousek, A.W. Parker, M.R. Pollard, D.A. Robinson, Z.-J. Xin, and M. Towrie, *ULTRA: A unique instrument for time-resolved spectroscopy.* Appl Spectrosc, 2010. **64**(12): p. 1311-1319.

26. Unno, M., R. Sano, S. Masuda, T.A. Ono, and S. Yamauchi, *Light-induced structural changes in the active site of the BLUF domain in AppA by Raman spectroscopy.* J Phys Chem B, 2005. **109**(25): p. 12620-6.

27. Masuda, S., K. Hasegawa, and T.-a. Ono, *Tryptophan at position 104 is involved in transforming light signal into changes of β-sheet structure for the signaling state in the BLUF domain of AppA.* Plant Cell Physiol, 2005. **46**(12): p. 1894-1901.

28. Unno, M., S. Kikuchi, and S. Masuda, *Structural refinement of a key tryptophan residue in the BLUF photoreceptor AppA by ultraviolet resonance Raman spectroscopy.* Biophys J, 2010. **98**(9): p. 1949-1956.

29. Masuda, S., Y. Tomida, H. Ohta, and K.-i. Takamiya, *The critical role of a H-bond between Gln63 and Trp104 in the blue-light sensing BLUF domain that controls AppA activity.* J Mol Biol, 2007. **368**(5): p. 1223-1230.

30. Barth, A., *Infrared spectroscopy of proteins.* Biochim Biophys Acta, 2007. **1767**(9): p. 1073-1101.

31. Kennis, J.T. and M.L. Groot, *Ultrafast spectroscopy of biological photoreceptors.* Curr Opin Struct Biol, 2007. **17**(5): p. 623-30.

32. Kim, M. and P.R. Carey, *Observation of a carbonyl feature for riboflavin bound to riboflavin-binding protein in the red-excited raman spectrum.* J Am Chem Soc, 1993. **115**(15): p. 7015-7016.

33. Bowman, W.D. and T.G. Spiro, *Normal mode analysis of lumiflavin and interpretation of resonance Raman spectra of flavoproteins.* Biochemistry, 1981. **20**(11): p. 3313-3318.

34. Pelton, J.T. and L.R. McLean, *Spectroscopic methods for analysis of protein secondary structure.* Anal Biochem, 2000. **277**(2): p. 167-176.

35. Maiti, N.C., M.M. Apetri, M.G. Zagorski, P.R. Carey, and V.E. Anderson, *Raman spectroscopic characterization of secondary structure in natively unfolded proteins: α-synuclein.* J Am Chem Soc, 2004. **126**(8): p. 2399-2408.

36. Barron, L.D., *Structure and behaviour of biomolecules from Raman optical activity.* Curr Opin Struct Biol, 2006. **16**(5): p. 638-643.

37. Roach, C.A., J.V. Simpson, and R.D. JiJi, *Evolution of quantitative methods in protein secondary structure determination via deep-ultraviolet resonance Raman spectroscopy.* Analyst, 2012. **137**(3): p. 555-562.

38. Measey, T., A. Hagarman, F. Eker, K. Griebenow, and R. Schweitzer-Stenner, *Side chain dependence of intensity and wavenumber position of amide I' in IR and visible Raman spectra of XA and AX dipeptides.* J Phys Chem B, 2005. **109**(16): p. 8195-8205.

39. Kondo, M., J. Nappa, K.L. Ronayne, A.L. Stelling, P.J. Tonge, and S.R. Meech, *Ultrafast vibrational spectroscopy of the flavin chromophore.* J Phys Chem B, 2006. **110**(41): p. 20107-20110.

40. Haigney, A., A. Lukacs, R. Brust, R.-K. Zhao, M. Towrie, G.M. Greetham, I. Clark, B. Illarionov, A. Bacher, R.-R. Kim, M. Fischer, S.R. Meech, and P.J. Tonge, *Vibrational assignment of the ultrafast infrared spectrum of the photoactivatable flavoprotein AppA.* J Phys Chem B, 2012. **116**(35): p. 10722-10729.

41. Venyaminov, S.Y. and N.N. Kalnin, *Quantitative IR spectrophotometry of peptide compounds in water (H2O) solutions. I. Spectral parameters of amino acid residue absorption bands.* Biopolymers, 1990. **30**(13-14): p. 1243-1257.

42. Barth, A., *The infrared absorption of amino acid side chains.* Prog Biophys Mol Biol, 2000. **74**(3–5): p. 141-173.

43. Laan, W., M. Gauden, S. Yeremenko, R. van Grondelle, J.T.M. Kennis, and K.J. Hellingwerf, *On the mechanism of activation of the BLUF domain of AppA.* Biochemistry, 2006. **45**(1): p. 51-60.

Chapter 3

Ultrafast Structural Dynamics of BlsA, from *Acinetobacter baumannii*

NOTE: The contents of this chapter have been adapted from a manuscript which is in preparation for submission with the same title as this chapter. The authors are as follows: Richard Brust, Allison Haigney, Andras Lukacs, Agnieszka Gil, Shahrier Hossain, Kiri Addison, Cheng-Tsung Lai, Michael Towrie, Gregory M. Greetham, Ian P. Clark, Boris Illarionov, Adelbert Bacher, Ryu-Ryun Kim, Markus Fischer, Carlos Simmerling, Stephen R. Meech, and Peter J. Tonge.

3.1. Introduction to *Acinetobacter baumannii* and BlsA

Acinetobacter baumannii is a Gram-negative opportunistic pathogen that has become of interest because of its ability to survive in unfit environments and its emerging presence in nosocomial infections in the US [1, 2]. Symptoms are observed in patients with compromised immune systems [3]. The pathogen typically targets moist tissue such as mucous membranes and open wound infections, commonly at sites of catheter insertion, which appears orange in color and rough to the touch [4]. Infection by *A. baumannii* can also lead to pneumonia and meningitis [5]. If left unattended to, the bacterium will spread and begin to induce necrosis and sepsis, leading to death of the patient. Given the high number of incidences in coalition troops during Operation Iraqi Freedom, *A. baumannii* was notoriously given the moniker “Iraqibacter” [5, 6].

It has been well established that *A. baumannii* has developed the ability to sense and adapt to the surrounding environment [1, 5, 7]. For example, *A. baumannii* can respond to iron levels in the host organism, an essential cog in the immune system machinery, and begin to express iron scavenging systems [8-10], eliminating the host’s immune response. In addition, the ability of the pathogen to survive in harsh environments has been attributed to the bacterium’s

capability to form biofilms on abiotic surfaces [11]. Biofilms are formed when a large cluster of cells adhere to a surface, releasing a dense extracellular matrix composed of proteins, DNA, and sugars that acts as a protective barrier and has been attributed to the bacterium's survival in harsh conditions, antibiotics and the host's immune system [12-16]. Increasing rates of nosocomial infections along with the emergence of extensively drug resistant (sensitive only to colistin or tigecycline [3, 17, 18]) and pandrug resistant (resistant to all FDA approved antibiotics [18]) strains have led to the pressing need to understand how *A. baumannii* responds to its external environment.

It was only recently discovered that *A. baumannii* exhibited the ability to sense and respond to blue light irradiation [19], a trait that was determined to be conserved within the *Acinetobacter* genus [20]. Currently of unknown function, it was shown that the *blsA* gene is responsible for photosensitive cell motility at room temperature [21]. Initial characterization of the b*lsA* gene was carried out in on "motility plates," due to the bacterium's lack of flagella. While the bacterium does not have flagella, it has been shown to "twitch" or "wiggle," allowing for some motility [22]. Cells with and without the *blsA* gene were grown at 24°C and 37°C while either in the dark or in under blue light illumination. Under blue light illumination at 24°C, cell motility was greatly diminished. However, although cell morphology was unaffected by temperature, blue light sensitivity is greatly diminished at 37°C. A 5-fold reduction of *blsA* mRNA levels was observed at 37°C when compared to that observed at 24°C, revealing a temperature response previously unobserved in the pathogen [19].

Sensing of blue light is achieved by the encoding of a BLUF protein, named blue light sensing A, or BlsA. BLUF proteins have been found in numerous organisms [23-26], where they are either directly fused within a multidomain protein that is tethered to an output domain, or as

standalone single domain that interacts with a binding partner [25]. BlsA falls into the latter category, and currently the identity of the protein binding partner(s) for BlsA are unknown.

To understand the mechanism of photoactivation in BlsA we employed site-directed mutagenesis. To compare BlsA to other BLUF proteins first one must look at the sequence alignment and to look for significant deviations. Due to the extensive work previously performed [27-31], AppA was chosen based on the available amount of information and experience with the protein (Figure 4.1). Using BLAST, a 35% sequence identity and 50% sequence similarity between $AppA_{5\text{-}125}$ and BlsA as well as PixD and BlsA was calculated. In particular the flavin binding pocket is well conserved with one significant difference. In place of H44 in AppA, BlsA has F32. While differences in the position has been reported in the standalone BLUF proteins BlrB1 (Lys) [32] and PixD (Asn) [33-35], to date there is no report of a phenylalanine at this position. This is particularly interesting since at this position one anticipates finding H-bonding partners in BLUF proteins, yet for BlsA this is not the case. To further investigate this, site directed mutagenesis was performed for BlsA at F32.

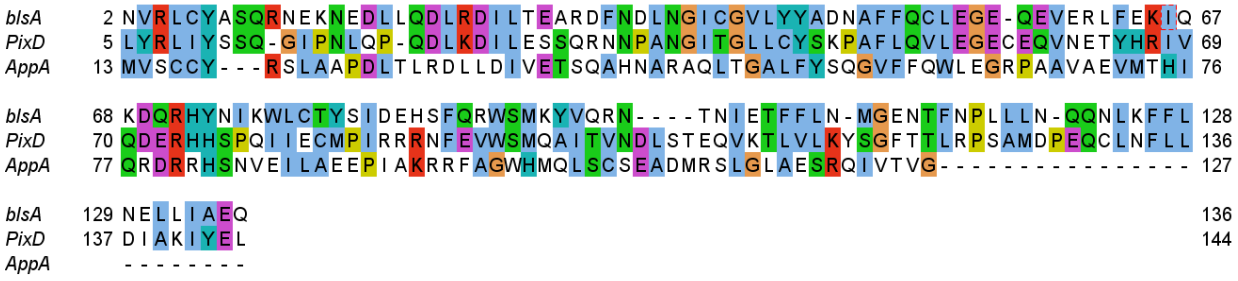

Figure 3.1. Sequence alignment of BlsA. The sequence alignment of BlsA compared to that of PixD from *Synechocystis* and AppA from *Rhodobacter sphaeroides*. This Figure was generated using Jalview [36, 37].

3.2. Experimental Methods

3.2.1. Protein Expression and Purification

The gene encoding BlsA was cloned from genomic DNA (ATCC 17978) and then inserted into a pET-15b vector so that an N-terminal His_6 tag was encoded. Protein expression was performed using *E. coli* BL21(DE3)cells. Following transformation and selection using ampicillin, a single colony was used to inoculate 10 mL of LB-amp which was the incubated overnight at 37°C. This overnight culture was then used to inoculate 1 L of LB to which 1 mL of a 200 mg/mL stock solution of ampicillin was added and shaken at 30°C until an OD600 of 0.6 – 0.8 was reached. The temperature was then lowered to 18°C and 0.8 mM IPTG was added. After overnight induction in the dark, cells were harvested by centrifugation (5000 rpm, 20 min, and 4°C) and stored at -20°C. After thawing, cells were resuspended in 50 mM sodium phosphate buffer pH 8 containing 10 mM sodium chloride (wash buffer), and lysed by sonication. Cell debris was removed by ultracentrifugation (33000 rpm for 90 min) and the supernatant was then incubated with 1 mL of a 10 mg/mL solution of FAD for 45 min at 4°C. Subsequently, BlsA was purified using a Ni-NTA (Novagen) column. After washing the column with wash buffer containing increasing concentrations of imidazole (0 mM, 10 mM, 20 mM), BlsA was eluted using wash buffer containing 250 mM imidazole. Fractions containing BlsA were pooled and the imidazole was removed by dialysis in 3 L of wash buffer. Protein purity and yield were determined using SDS-PAGE and UV-Vis spectroscopy.

3.2.2. Preparation of F32 mutants

Site directed mutagenesis was performed using pfu turbo (Agilent) for F32N and F32H using the primers reported in Table 3.1. Following digestion of the template DNA using Dpn1,

the reaction mixture was transformed into Xl1 blue cells. Following confirmation of the mutant strain through sequencing, the plasmids were transformed into BL21(DE3) and prepared using the same protocol as described in 3.2.1.

Table 3.1. Primer design of F32 mutants.

Mutant	Primer Design
F32H forward	5'-CTGACAGAAGCTCGTGATCATAACGATTTAAACGGGATTTGT-3'
F32H reverse	5'-AATCCCGTTTAAATCGTTATGATCACGAGCTTCTGTCAGAAT-3'
F32N forward	5'-CTGACAGAAGCTCGTGATAATAACGATTTAAACGGGATTTGT-3
F32N reverse	5'- AATCCCGTTTAAATCGTTATTATCACGAGCTTCTGTCAGAAT-3'
A29S forward	5'- GATATTCTGACAGAATCTCGTGATTTCAACGAT-3'
A29S reverse	5'- ATCGTTGAAATCACGAGATTCTGTCAGAATATC-3'

3.2.3. Photoconversion Experiments

Steady state absorption spectra were recorded using a Cary 100 (Varian) UV-Vis spectrometer at 25°C. Light state samples were generated by irradiation with 20 mW of 460 nm light for 3 min.

3.2.4. Uniform ^{13}C Labeling

Uniform ^{13}C protein labeling was performed by expressing BlsA in BL21(DE3) *E. coli* cells that were grown on minimal media containing [U-$^{13}C_6$]-D-glucose (Cambridge Isotopes) as the sole carbon source. The method used to label the protein was identical to that reported previously for $AppA_{BLUF}$ [38]. Single colonies containing plasmids for BlsA that had been grown on LB/Amp plates were streaked on M9 minimal media/glucose/ampicillin plates containing 200 mg/mL ampicillin, and 5 mg/mL glucose. This process has been hypothesized to acclimatize the cells to growth in minimal media, leading to improved protein expression. A single colony from an M9 plate was used to inoculate 500 mL of M9/ampicillin minimal media in a 4 L flask that

contained 4 g of glucose and 5 mL of 100x MEM vitamins (Sigma). The cells were grown to an OD_{600} of approximately 0.5 at 30°C, which were then pelleted and resuspended in fresh media with [U-$^{13}C_6$] glucose in place of unlabeled glucose. After 30 min at 18°C, 0.8 mM IPTG was added to induce protein expression, and the culture was shaken in the dark for 24 h to maximize the yield of protein. Purification followed the same protocol described in 3.2.1.

3.2.5. Incorporation of Labeled FAD

[2-$^{13}C_1$]-FAD was prepared according to Tishler et al. [39] by first generating riboflavin isotopologues and subsequently converting them enzymatically to the FAD isotopologues. The [2-$^{13}C_1$]-FAD isotopologue was incorporated into BlsA by incubating a 1 mM solution of the purified protein with 3 mM [2-$^{13}C_1$]-FAD. This protein flavin mixture was then washed with buffer using a 10 kDa Amicon filter (Millipore) until free flavin was no longer detectable. The protein sample (~1 mM) was then incubated a second time with 3 mM [2-$^{13}C_1$]-FAD 3 mM, followed by repeated washing until no free flavin could be detected in the flow through. Using this method, the final percent isotope incorporation was estimated to be 94%. Synthesis of the labeled FAD samples was prepared by Prof Adelbert Bacher, Boris Illarionov, Ryu-Ryun Kim, and Markus Fischer.

3.2.6. FTIR Spectroscopy

FTIR spectroscopy was performed on a Bruker Vertex 80 spectrometer. Proteins were prepared in deuterated buffer (50 mM sodium phosphate, 10 mM sodium chloride, pD 8) at concentrations of 1.5 mM and FTIR spectra were obtained using a demountable liquid cell with a 50 µm spacer where 64 scans were accumulated at 1 cm^{-1} resolution. The light state of BlsA was generated by irradiation of the sample *in situ* for 5 min with a 460 nm high mount LED

(Prizmatix) set to 200 mW. Difference spectra were obtained by subtracting the spectrum of the dark adapted protein from the light adapted protein.

3.2.7. TRIR Spectroscopy

TRIR experiments were performed at STFC Central Laser facility. The TRIR system has been described in detail elsewhere [31]. Excitation pulses were set to 450 nm with a power set to 200 nJ and a spot size radius of 100 μm. Samples were prepared in deuterated buffer (50 mM sodium phosphate, 10 mM sodium chloride, pD 8) at 1.5 mM concentration. Dark state measurements were rastered and flowed at a rate of 1.5 mL/min in a 50 μm path length transmission cell of CaF_2 to minimize photobleaching and sample degradation. The IR probe recorded transient difference spectra (pump on-pump off) at time delays between 1 ps and 2000 ps. After the measurements were recorded, the extent of photoconversion was shown to be negligible using absorption spectroscopy. The probe beam was measured by two carefully matched 128 pixel detectors at a resolution of 3 cm^{-1} per pixel. Spectra were calibrated relative to the IR transmission of a pure polystyrene standard. Light-adapted samples were prepared by irradiation at 380 nm using a high mount LED illuminator (ThorLabs). Photoconversion was monitored using UV-Vis spectroscopy and was found to be complete within 5 min. The TRIR setup was operated and maintained by the CLF (Dr. Greg Greetham, Dr. Ian Clark, and Dr. Mike Towrie).

3.2.8. Homology Modeling

The primary sequence of BlsA was aligned with the BLUF protein PixD (Slr1694). PixD was found to have the highest sequence identity to BlsA and subsequently the structure of PixD (PDB code: 2HFN) [35] was used as the template based on the sequence alignment using the

SWISS-MODEL server, which subsequently generated the homology model [40-43]. The homology model was generated by Cheng-Tsung Lai.

3.3. Results and Discussion

3.3.1. UV-Vis Spectroscopy

Initial characterization of BlsA revealed a characteristic BLUF photocycle [19]. A 13 nm red shift in the dark (456 nm) and light (470 nm) states were observed when compared to $AppA_{BLUF}$ (Figure 3.2). Comparison of the primary sequences of $AppA_{BLUF}$ and BlsA reveal an alanine (A29) in the homologous position to S41 in $AppA_{BLUF}$. Chapter 2 revealed that the S41A mutant resulted in a red shift in flavin absorption in both the dark and light adapted states [44], and is consistent with the spectra reported for BlsA in Figure 3.2. Dark state recovery was measured, and a half-life of 7.6 min was observed (Table 3.2). This is similar to that observed in $AppA_{BLUF}$ (τ of 15 min), and longer than other previously reported stand-alone BLUF proteins [32, 33]. To further verify that the red shift in flavin absorbance in both dark and light state was due to A29, the A29S mutant was made. A dark (445 nm) and light (460 nm) λ_{max} similar to $AppA_{BLUF}$, in good agreement with the S41A data (Figure 3.3).

In order to further explore the role of F32 we mutated this position to a His and Asn, which are present in AppA and PixD, respectively. AppA exhibits the longest reported photocycle of any reported BLUF protein, whereas PixD has a photorecovery of 4 s [34]. Therefore it was hypothesized that mutations to F32 would alter the photocycle in such a way to mimic that of the homologous BLUF protein: His would increase the rate of photorecovery while Asn would decrease the rate of photorecovery. Mutations to F32 do not result in a photoinactive species. The absorption spectra of BlsA, F32N, and F32H overlay quite well (Figure 3.4).

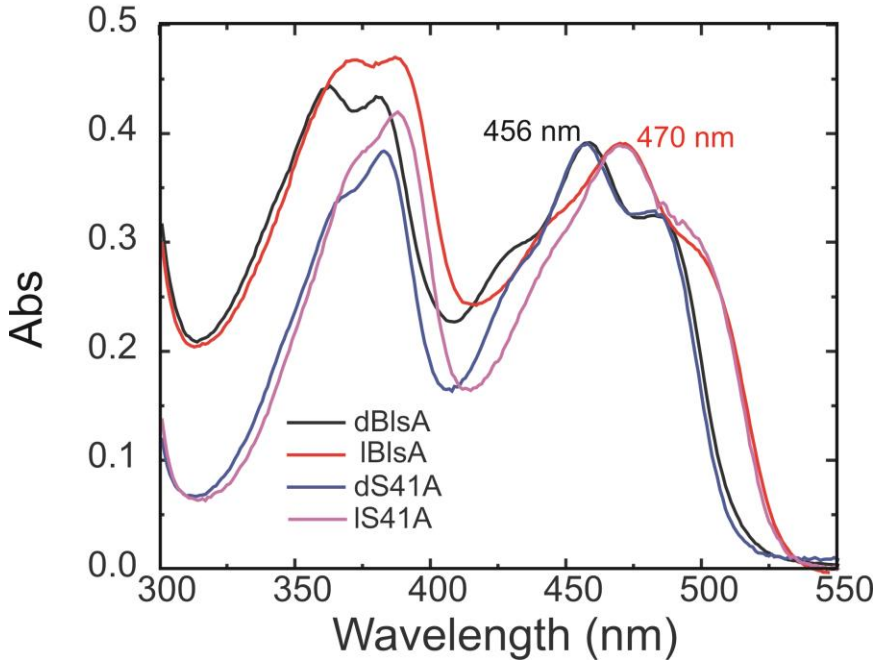

Figure 3.2. Photoconversion of BlsA and S41A AppA$_{BLUF}$. UV-Vis spectroscopy of dS41A AppA$_{BLUF}$ (black), lS41A AppA$_{BLUF}$ (red), dBlsA (blue) and lBlsA (magenta). Light adapted spectra were generated by 3 minute irradiation of 460 nm light.

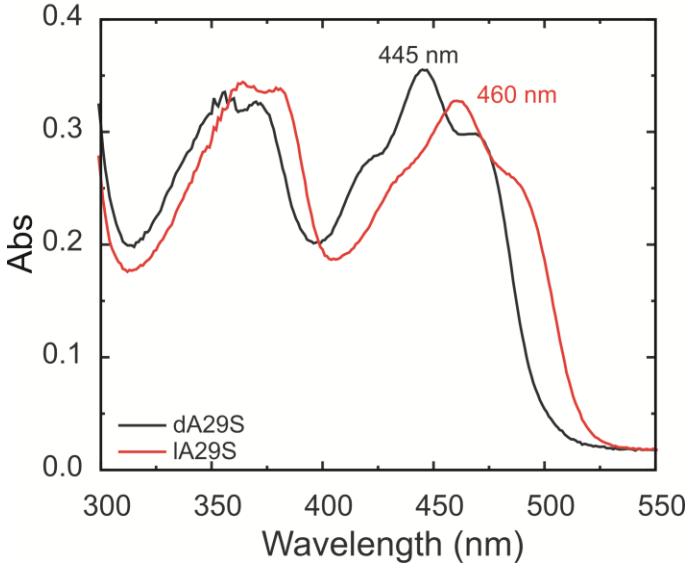

Figure 3.3. Absorption spectra of A29S. UV-Vis absorption data for dA29S (black) and lA29S (red). Light adapted spectrum was generated by 3 min irradiation with 460 nm light.

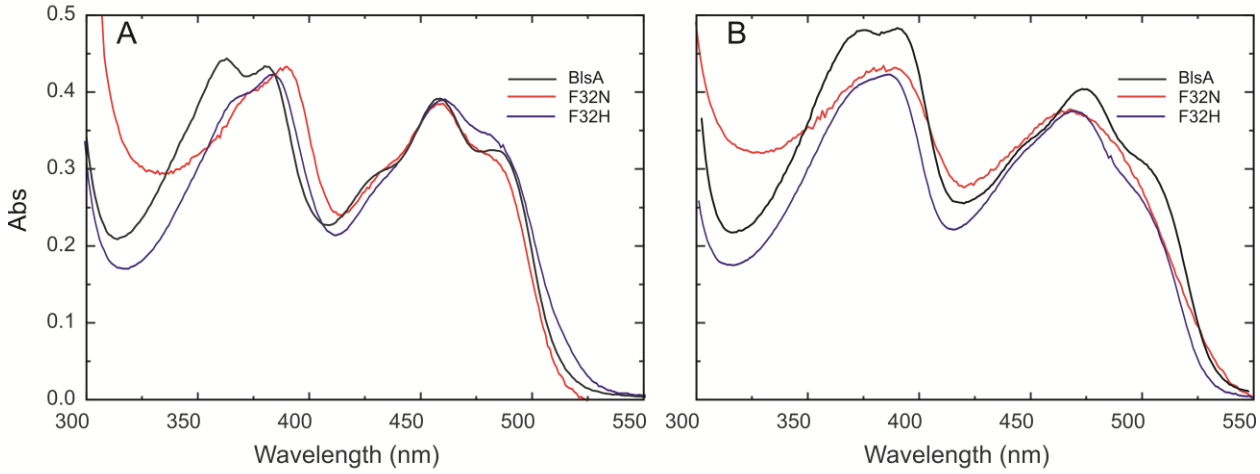

Figure 3.4. Absorption spectra of F32 mutants. UV-Vis absorption data of BlsA (black), F32N (red) and F32H (blue). **A.** Spectra reported pre-irradiation (dark states). **B.** Spectra recorded 3 min after irradiation with 460 nm light (light adapted states).

The light to dark photorecovery data for BlsA and its mutants are reported in Table 3.2. The F32N and F32H clearly affect the photocycle, as can be observed in the rates of dark state recoveries. As predicted, the F32N mutation resulted in a faster recovering protein by 4.5 fold, albeit still longer than PixD [33]. However, the F32H also decreased dark state recovery by 2.7 fold. AppA is known to exhibit the slowest dark state recovery [45]; however, the F32H mutant increases the rate of dark state recovery. These results reveal that BlsA has evolved to prefer the bulky phenyl side chain of F32 in place of H-bonding partners as observed in other BLUF systems. In addition, similar to the S41A mutant in $AppA_{BLUF}$, the A29S mutant does not produce a significant effect on light to dark recovery.

Table 3.2. Light to dark recovery data for BlsA and its mutants.

Sample	Dark Abs (nm)	Light Abs (nm)	ΔAbs (nm)	$t_{½}$ (min)
$AppA_{BLUF}$	445	456	11	13.7 ± 0.1
S41A $AppA_{BLUF}$	456	470	14	12.7 ± 0.2
BlsA	456	470	14	7.6 ± 0.1
F32N BlsA	453	471	17	1.7 ± 0.1
F32H BlsA	460	472	12	2.8 ± 0.1
A29S BlsA	445	460	15	7.0 ± 0.1

3.3.2. FTIR Spectroscopy

To provide additional information on the structural change accompanying light state formation, we measured the light minus dark steady state FTIR difference spectrum of BlsA and compared it to the analogous spectrum obtained for $AppA_{BLUF}$ (Figure 3.5). Both spectra exhibit the 1688(+)/1700(-) cm^{-1} difference band assigned to changes in H-bonding to the flavin C4=O associated with rotation of Q63 (Q51 in BlsA) between dark and light states of $AppA_{BLUF}$ [29]. In addition, photoexcitation also leads to formation of a 1634(5)/1620 cm^{-1} difference band in both $AppA_{BLUF}$ and BlsA in a region where β-sheet secondary structure can be observed, but is not observed in the ps timescale [46, 47]. Significantly, this difference mode has opposite signs in $AppA_{BLUF}$ 1635(+)/1620(-) cm^{-1} and BlsA 1634(-)/1620(+) cm^{-1}, revealing that the secondary structure content of dBlsA resembles that of l$AppA_{BLUF}$, and vice versa. This is a unique feature compared to all characterized BLUF proteins. In $AppA_{BLUF}$, the 1635(+)/1620(-) cm^{-1} difference mode has been attributed to structural rearrangement of the BLUF β-sheet, consistent with the notion that the β-sheet, and β-strand 5 in particular, is involved in signal transduction [34, 48, 49]. In AppA, the N-terminal residue of β-strand 5 is a conserved tryptophan (W104; W91 in BlsA) which is hypothesized to adopt a new conformation upon light state formation [49, 50], and significantly the 1635(+)/1620(-) cm^{-1} difference mode is absent in the W104A photoactive $AppA_{BLUF}$ mutant [34]. Based on its position it could be proposed that, in contrast to the AppA and PixD, an increase in β-sheet character is occurring.

To further elucidate the role of F32 in the photocycle of BlsA, FTIR spectroscopy was employed for the F32H and F32N mutants (Figure 3.6). The F32 mutants exhibit the characteristic red shift of the C4=O flavin carbonyl at 1688(+)/1700(-) cm^{-1}, as expected for a photoactive BLUF protein. The 1634(-)/1620(+) cm^{-1} mode indicated that the dark spectra of

BlsA resembled that of light adapted $AppA_{BLUF}$. The F32 mutants also exhibit this feature, and overlay quite well with wild type (Figure 3.5), revealing that F32 is not the main contributor to the altered secondary structure of BlsA compared to other BLUF proteins.

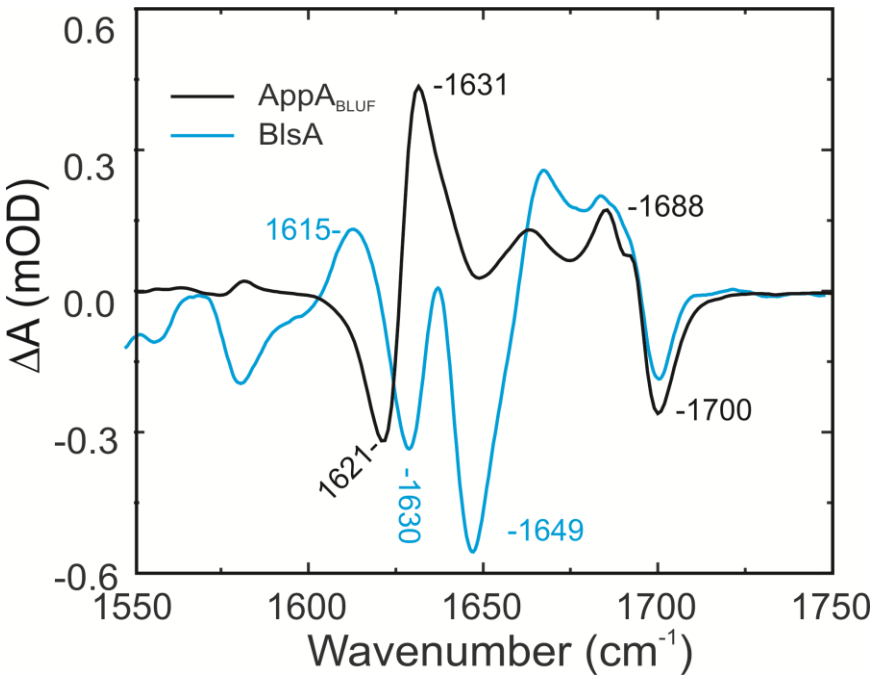

Figure 3.5. FTIR spectra of $AppA_{BLUF}$ and BlsA. FTIR difference spectra of $AppA_{BLUF}$ (black) and BlsA (blue). Light adapted spectra were generated by 3 minute irradiation of 460 nm light.

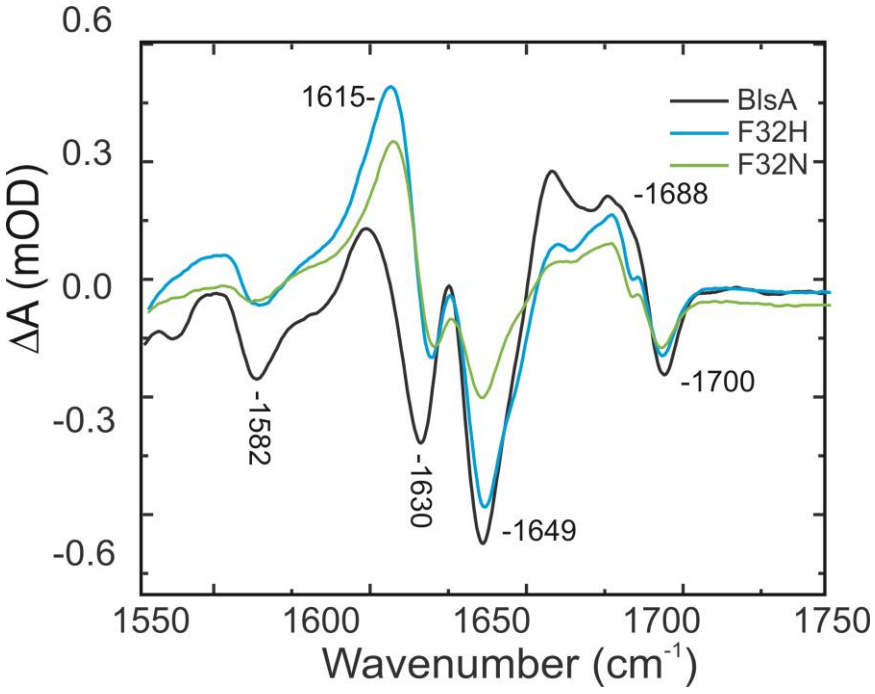

Figure 3.6. FTIR spectra of BlsA and F32 mutants. FTIR light minus dark difference spectra of wtBlsA (black), F32N (green) F32H (blue). Light adapted spectra were generated by 3 minute irradiation of 460 nm light.

3.3.3. TRIR Spectroscopy

To investigate structural similarities and differences between BlsA and $AppA_{BLUF}$, we used ultrafast time resolved IR (TRIR) spectroscopy to probe the primary structural changes associated with photoexcitation of dBlsA. Spectra reported for BlsA at 3 ps are compared to $AppA_{BLUF}$ (Figure 3.7A and B). Similar spectra are observed in the 1500-1650 cm^{-1} region, where modes associated with the flavin are primarily seen [29, 31], for BlsA and $AppA_{BLUF}$. In contrast to what was previously reported for the S41A mutant (Chapter 2), where this mutation led to a blue shift in the 1547 cm^{-1} bleach of $AppA_{BLUF}$ to 1541 cm^{-1} in S41A, the main bleach is unshifted in BlsA. The S41 mutant data described in Chapter 2 for $AppA_{BLUF}$ indicated that GS stabilization could be attributed to the red shift in flavin absorbance. Here, no GS stabilization is observed, indicating that for BlsA the red shift is due to stabilization of the flavin ES.

A key difference between the spectra of BlsA and $AppA_{BLUF}$ is that the transient at 1670 cm^{-1} observed in $dAppA_{BLUF}$, which is absent in dBlsA (Figure 3.7A). This mode is absent in free flavin, $lAppA_{BLUF}$ and photoinactive mutants of $AppA_{BLUF}$, and has proposed to be from the conserved glutamine (Q63 in AppA) [28, 51]. Since BlsA is a photoactive BLUF protein and also has the conserved glutamine (Q51) it is surprising that this mode is absent. Interestingly, in addition to the lack of a positive feature in the dark state of dBlsA, a new bleach is observed in lBlsA at 1670 cm^{-1} that does not appear to share any similarity to the reported spectrum of $lAppA_{BLUF}$. The two carbonyl modes in FAD have been well characterized in $AppA_{BLUF}$ [29, 31], so the presence of this new mode is surprising.

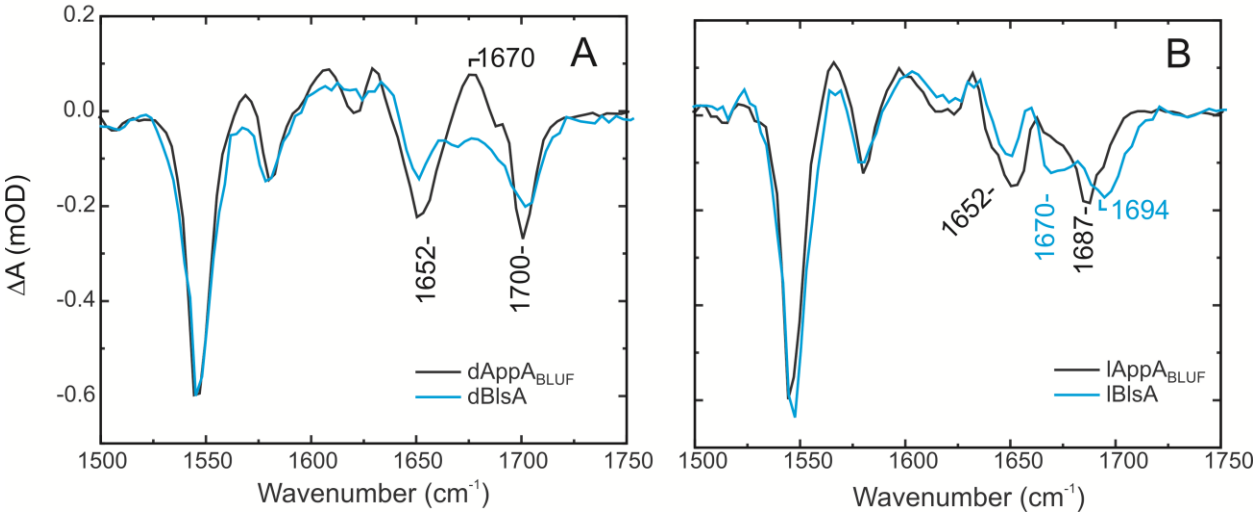

Figure 3.7. TRIR spectra of BlsA. TRIR spectra of $AppA_{BLUF}$ (black), BlsA (blue) taken 3 ps post excitation. **A.** Spectra of dark adapted states. **B.** Spectra of light adapted states.

The position of the new bleach at 1670 cm^{-1} in lBlsA is intriguing. The carbonyl region of the flavin TRIR spectra has been well characterized, where 2 flavin carbonyl modes are observed that can be assigned as either the C2=O (~1650 cm^{-1}) or the C4=O carbonyl (~1700 cm^{-1}, ~1690 cm^{-1} for light adapted samples) [29, 31, 51]. Therefore one could propose that this new bleach arises from the protein and not the flavin. Uniform ^{13}C of the protein yielded little effect

on the carbonyl region of the spectra (Figure 3.8A and 3.8B) although an unusual enhancement of the 1580 cm^{-1} mode previously assigned to flavin is observed. These results indicate that the 1670 cm^{-1} bleach in lBlsA and the bleach observed in both d and lBlsA do not arise from the protein, meaning they must be flavin modes.

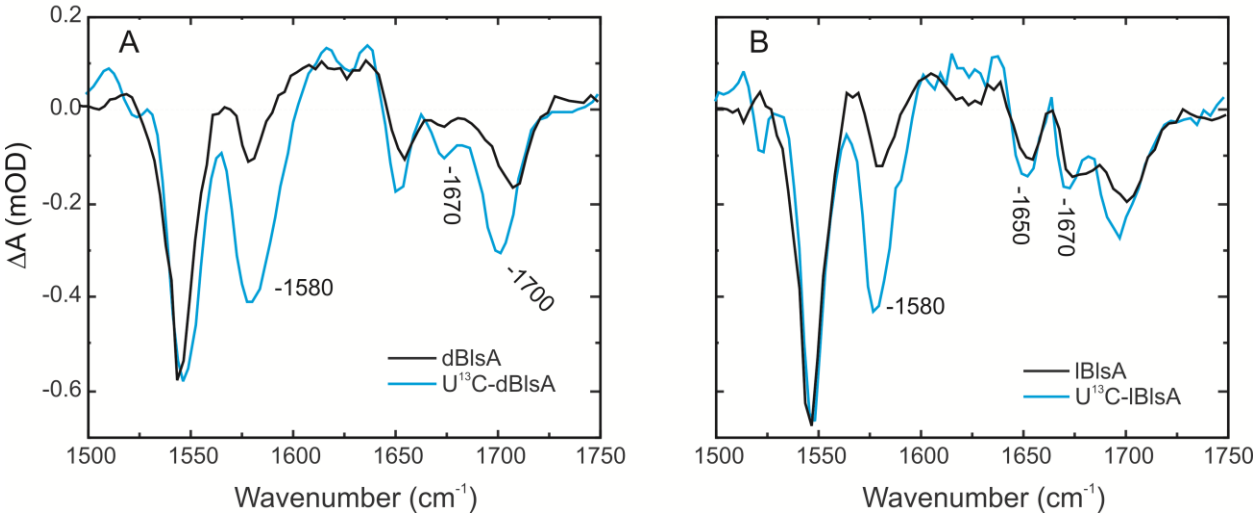

Figure 3.8. TRIR spectra of ^{13}C-BlsA. TRIR spectra of BlsA (black) and ^{13}C-BlsA (blue) taken 3 ps post excitation. **A.** Spectra of dark adapted states. **B.** Spectra of light adapted states.

Since uniform ^{13}C labeling of the protein did not result in any spectral shift of the 1670 cm^{-1} bleach, isotopic labeling was performed on the flavin chromophore (Figure 3.9). Incorporation of 2-[$^{13}C_1$-FAD] into the protein using a protocol previously described for $AppA_{BLUF}$ [29, 31]. 2-[$^{13}C_1$-FAD] incorporated dBlsA did not produce a significant effect on the observed TRIR spectra (Figure 3.9A), however, minor changes can be observed in the carbonyl region of the spectra. It could be proposed that the absence of the transient at 1670 cm^{-1} in dBlsA that is typically observed in dark state spectra is the presence of the bleach seen at 1670 cm^{-1} in lBlsA. If this mode were present in both dark and light adapted spectra, then it would directly overlap with the transient seen only in the dark state. Therefore, if one were to shift either mode then the other should appear. In the uniform ^{13}C labeled protein dark spectrum, a weak bleach is

observed at 1670 cm^{-1}, yet no transient is observed in the 2-[$^{13}C_1$]-FAD dark spectrum. In the light adapted 2-[$^{13}C_1$]-FAD incorporated BlsA spectrum, the 1670 cm^{-1} mode is shifted to 1652 cm^{-1}. This shift in vibration in the light adapted state reveals that this mode to be the C2=O of the flavin and is consistent with previous isotopic labeling experiments [31]. The fact that the transient is absent in the dark spectra suggests that the spectral shift was not profound enough to result in the appearance of the transient, or that the transient does not occur in BlsA.

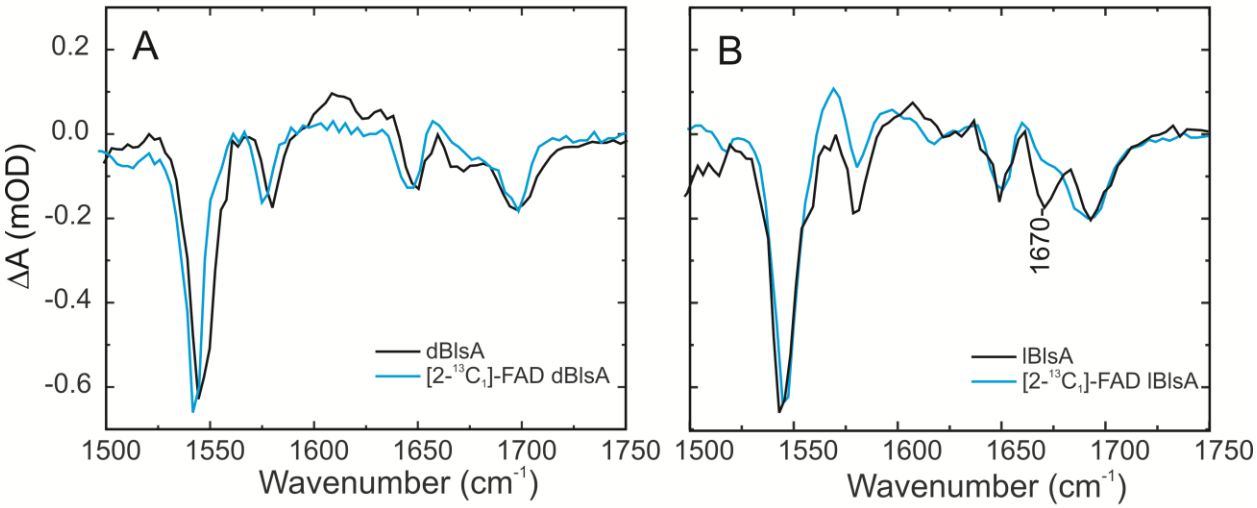

Figure 3.9. TRIR spectra of [2-$^{13}C_1$]-FAD BlsA. TRIR spectra of BlsA (black) and [2-$^{13}C_1$]-FAD BlsA (blue) taken 3 ps post excitation. **A.** Spectra of dark adapted states. **B.** Spectra of light adapted states.

The red shift in flavin absorption in the S41 mutants in $AppA_{BLUF}$ was shown to be correlated with the red shift in the flavin main bleach (C=C, C=N vibrations) in Chapter 2. To further investigate this in BlsA, the TRIR spectra for the A29S mutant were measured (Figure 3.10). No shift in the main flavin bleach (1547 cm^{-1}) is observed, in contrast to what was observed in $AppA_{BLUF}$ (Chapter 2). In addition, a transient at 1675 cm^{-1} is observed in dA29S that is absent in dBlsA (Figure 3.10A). For the light adapted mutant, the spectra overlays well with wild type with the exception of an increase in intensity of the flavin C4=O carbonyl in

lA29S at 1687 cm^{-1} (Figure 3.10B). These results suggest a slightly disrupted H-bonding network in the dark state, resulting in the appearance of a protein mode at 1675 cm^{-1} that is typically observed in photoactive BLUF proteins, which suggests two possible conformations for the Ser side chain in the A29S mutant in BlsA, in agreement with computational data reported for $AppA_{BLUF}$ [44].

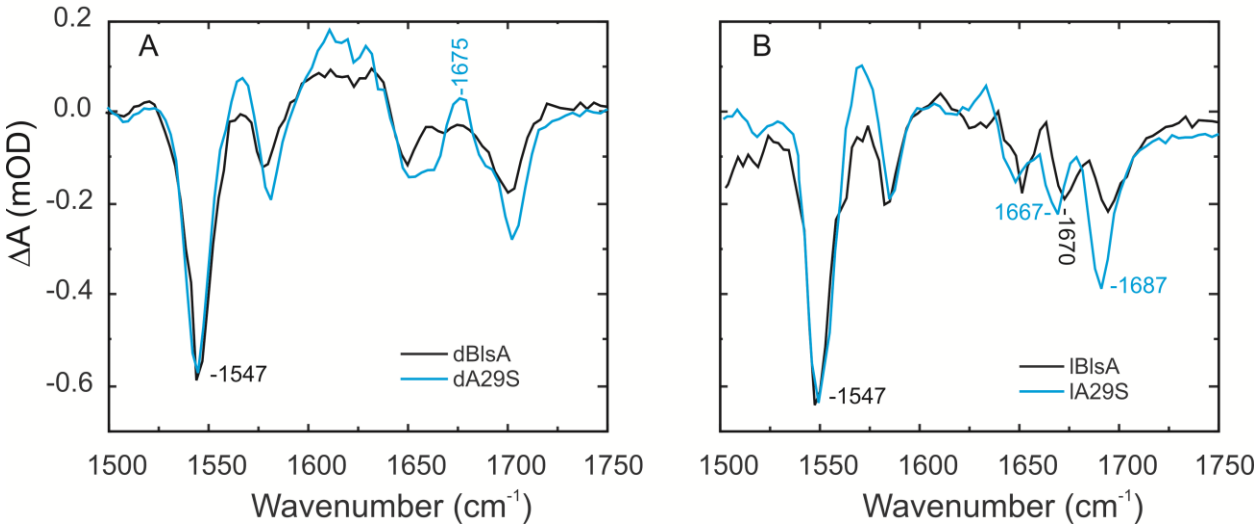

Figure 3.10. TRIR spectra of A29S mutant. TRIR spectra of BlsA (black) and A29S (blue) taken 3 ps post excitation. **A.** Spectra of dark adapted states. **B.** Spectra of light adapted states.

Isotopic labeling of the flavin has assigned the C2=O of the flavin as the 1670 cm^{-1} bleach in light adapted BlsA. Based on sequence alignment, it can be proposed that adjacent to the C2=O in BlsA is F32, a residue whose side chain cannot undergo H-bonding. As a residue that is incapable of forming H-bonds, it could be postulated that being so near the flavin carbonyl mode would result in a blue-shift. To test this hypothesis, TRIR spectra for F32N and F32H were recorded. Replacing the phenylalanine side chain with either Asn or His introduces a potential H-bond donor for the flavin C2=O carbonyl. Figure 3.11A and 3.11B report the TRIR spectra of F32H overlaid with wild type BlsA. Spectra overlay quite well; no spectral shift of the 1670 cm^{-1} bleach in lF32H is observed.

TRIR spectra for F32N reveal spectral similarities to wild type BlsA (Figure 3.11 C and D). In addition, a new transient is observed at 1662 cm^{-1} that is absent in d and lBlsA as well as lF32N. This mode is shifted by 8 cm^{-1} to that reported for here $AppA_{BLUF}$ in Figure 3.7, and is in the expected region where one would expect a transient for a photoactive BLUF protein. In addition, a 1642(3) cm^{-1} bleach is observed in d and lF32N. This position is similar to the vibration of the C2=O observed in $AppA_{BLUF}$, and is unaffected by ^{13}C labeling of the protein, indicating it is a flavin mode. However, the bleach observed at 1670 cm^{-1} in lBlsA is absent in both d and lF32N. Isotopic editing of the flavin chromophore revealed the 1670 cm^{-1} bleach to be the C2=O carbonyl. The absence of the 1670 cm^{-1} C2=O carbonyl bleach indicates that the C2=O mode is altered in the F32N Mutant. If the amide side chain of the F32N mutant is H-bonding with the C2=O, a red shift would be expected. This is what is observed, a red shift of the C2=O carbonyl to 1643 cm^{-1}. In addition, this mode is also shifted by ~7 cm^{-1} compared to the TRIR spectra of $AppA_{BLUF}$ (Figure 3.7), indicating stronger H-bonding interactions in the F32N mutant than compared to $AppA_{BLUF}$. Shifting this residue down in frequency also allows for the protein transient observed in photoactive BLUF proteins to be seen, here at 1662 cm^{-1}. These results would indicate that a His side chain near the C2=O flavin carbonyl cannot undergo H-bonding, providing new insight into the role of this position in both $AppA_{BLUF}$ and BlsA.

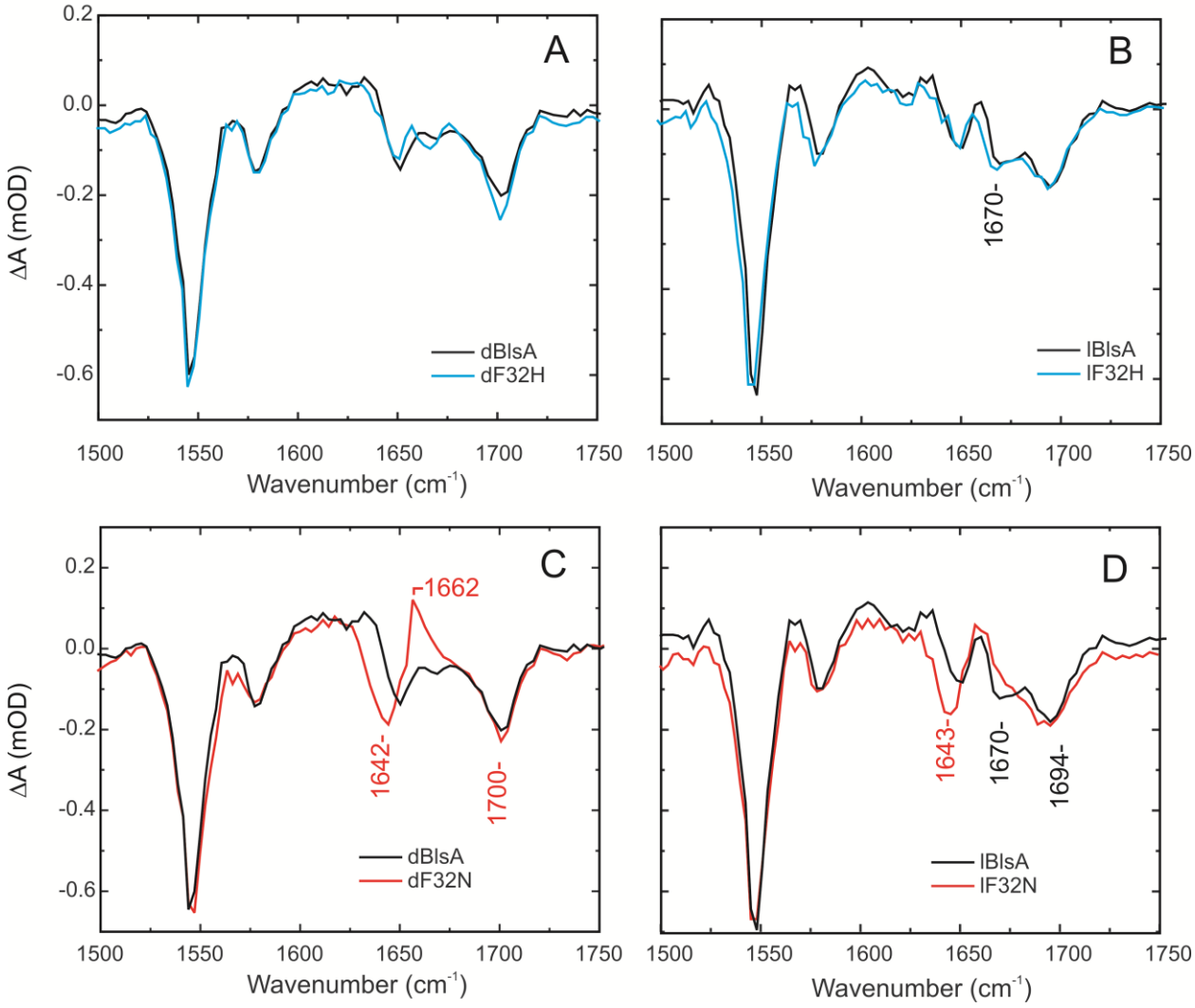

Figure 3.11. TRIR spectra of F32 mutants. TRIR spectra of BlsA (black), F32H (blue) and F32N (red) taken 3 ps post excitation. **A** and **C** are spectra of dark adapted states. **B** and **D** are spectra of light adapted states.

Analysis of the ES dynamics can be conducted by plotting at the main bleach at 1547 cm^{-1}. Fitting to a biexponential yielded the results in Table 3.3. Average lifetimes for AppA and BlsA are in good agreement with each other. The F32 mutants exhibited roughly a 2 fold increase in rate of GS recovery for the dark states. A slight increase is observed in GS recovery for the light adapted states: 1.4 fold for lF32N and 1.1 fold for F32H. These results suggest a weak destabilization of the ES with the F32 mutants compared to wtBlsA. GS recovery is also

significantly affected by the A29S mutant in the dark state (2 fold increase in lifetime), with minimal effect on the light state. This result, in addition with the flavin bleach at 1547 cm^{-1} being unshifted, suggests an ES stabilization in BlsA contributing to the red shift in the electronic absorption spectrum of the flavin when compared to $AppA_{BLUF}$.

Table 3.3. GS recovery kinetics of BlsA and its mutants.

Sample	α1	τ1 (ps)	α2	τ2 (ps)	<τ> (ps)
dAppA	-0.51	34 ± 4	-0.49	473± 73	249
lAppA	-0.78	11± 1	-0.22	134± 24	45
dBlsA	-0.40	11 ± 1	-0.60	310 ± 15	200
lBlsA	-0.73	12 ± 1	-0.27	145 ± 16	48
dF32N	-0.35	7 ± 1	-0.65	152 ± 9	99
lF32N	-0.67	11 ± 1	-0.37	166 ± 26	69
dF32H	-0.23	10 ± 2	-0.77	150 ± 8	116
lF32H	-0.70	11 ± 1	-0.30	178 ± 27	53
dA29S	-0.42	26 ± 2	-0.58	736 ± 64	437
lA29S	-0.36	12 ± 4	-0.64	56 ± 9	40

3.3.4. Homology Modeling of BlsA

To gain some structural insight as to why the C2=O of the flavin is shifted, we employed homology modeling using the BLUF protein PixD (Slr1694) from *Synechocystis* PCC6803 (PDB 2HFN [35]) as a template. PixD was chosen based on sequence identity to BlsA (Figure 3.1) and generated using SWISS-Model (Figure 3.10) [40-43]. For comparison, the homology model was overlaid with the structure of AppA (PDB 1YRX [52]). While several important conserved

residues adopt similar positions in both structures including Y7 (Y21), Q51 (Q63), W91 (W104) and N33 (N45), residue H44 in AppA is replaced with F32 in BlsA. Since H44 in AppA is within H-bonding distance to the flavin C2=O, the homology modeling agrees with the vibrational data presented above for the F32 mutants: replacement of H44 with a phenylalanine places the C2=O in a more nonpolar environment, causing a blue shift of the C2=O vibration to 1670 cm^{-1}.

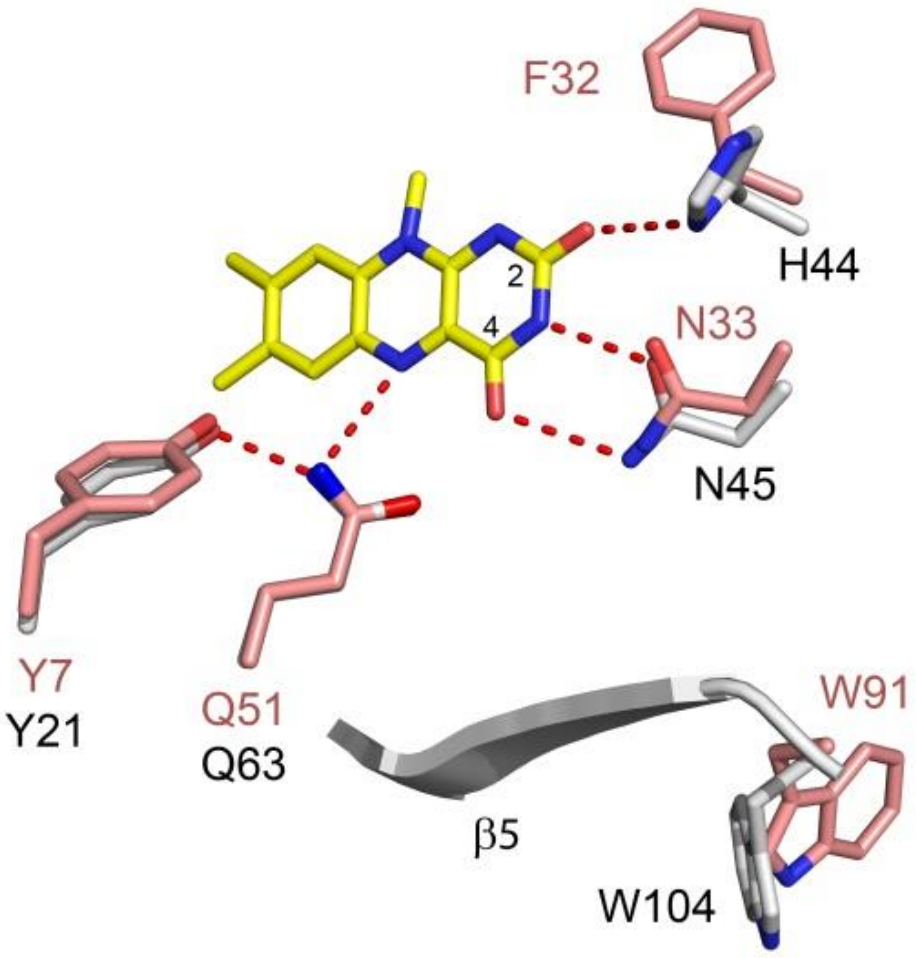

Figure 3.11. Homology model of BlsA. Structure of AppA overlaid with the homology model of BlsA. AppA (2IYG) is in grey and BlsA is in pink. The figure was made using Pymol.

3.4. Conclusions

Photoexcitation leads to formation of a 1634(5)/1620 cm^{-1} difference band in both AppA and BlsA in a region where β-sheet secondary structure can be observed, but with opposite signs. In AppA the 1635(+)/1620(-) cm^{-1} difference mode has been attributed to structural rearrangement of the BLUF β-sheet, consistent with the notion that the β5 strand. In AppA the N-terminal residue of β-strand 5 is a tryptophan (W104; W91 in BlsA) which is hypothesized to move upon light state formation [49, 50], and significantly the 1635(+)/1620(-) cm^{-1} difference mode is absent in the W104A photoactive AppA mutant [34]. Based on its position it could be proposed that the position of W91 is opposite that of AppA. Mutations to F32 result in shorted lived photoactivated species but do not affect the stationary state IR spectra, indicating that the overall structure of the mutants is similar to wild type. Uniform ^{13}C labeling of the protein and incorporation of 2-[$^{13}C_1$-FAD] allowed for unambiguous assignment of the 1670 cm^{-1} bleach in lBlsA to be the C2=O carbonyl. To date, this makes BlsA the most unique BLUF protein in terms of its infrared spectra.

Although it is not clear how changes in β5 strand in AppA modulate the structure of the C-terminal domain of this protein, it is known that in the related BLUF protein PixD, photoactivation leads to dissociation of PixD from the output protein PixE [53]. PixD and AppA have similar FTIR difference spectra in the 1620-1635 cm^{-1} region [54], with PixD showing the characteristic 1635(+)/1620(-) cm^{-1} difference mode. We propose that the weakening of H-bonding in the β-sheet that occurs upon photoactivation in PixD is directly related to dissociation of PixE from PixD. Conversely then, the strengthening of H-bonding in the BlsA β-sheet upon photoactivation, revealed by the change in sign of the β-strand marker mode, supports a model

for BlsA photoreceptor function in which photoactivation leads to *formation* of a complex with the downstream target protein rather than dissociation.

3.5. References

1. Giamarellou, H., A. Antoniadou, and K. Kanellakopoulou, *Acinetobacter baumannii: a universal threat to public health?* Int J Androl, 2008. **32**(2): p. 106-119.
2. Tomaras, A.P., M.J. Flagler, C.W. Dorsey, J.A. Gaddy, and L.A. Actis, *Characterization of a two-component regulatory system from Acinetobacter baumannii that controls biofilm formation and cellular morphology.* Microbiol, 2008. **154**(11): p. 3398-3409.
3. Kallen, Alexander J.M.D.M.P.H., M.D. Alicia I. Hidron, J.P. Patel, and A.M.D. Srinivasan, *Multidrug Resistance among Gram-Negative Pathogens That Caused Healthcare-Associated Infections Reported to the National Healthcare Safety Network, 2006–2008.* Infect. Control Hosp. Epidemiol., 2010. **31**(5): p. 528-531.
4. Sebeny, P.J., M.S. Riddle, and K. Petersen, *Acinetobacter baumannii skin and soft-tissue infection associated with war trauma.* Clin Infect Dis, 2008. **47**(4): p. 444-449.
5. Howard, A., M. O'Donoghue, A. Feeney, and R.D. Sleator, Acinetobacter baumanni*: An emerging opportunistic pathogen.* Virulence, 2012. **3**(3): p. 243-250.
6. *Acinetobacter baumannii infections among patients at military medical facilities treating injured U.S. service members, 2002-2004.* MMWR Morb Mortal Wkly Rep, 2004. **53**(45): p. 1063-6.
7. Peleg, A.Y., H. Seifert, and D.L. Paterson, *Acinetobacter baumannii: Emergence of a successful pathogen.* Clin Microbiol Rev, 2008. **21**(3): p. 538-582.

8. Zimbler, D., W. Penwell, J. Gaddy, S. Menke, A. Tomaras, P. Connerly, and L. Actis, *Iron acquisition functions expressed by the human pathogen Acinetobacter baumannii.* BioMetals, 2009. **22**(1): p. 23-32.

9. Daniel, C., S. Haentjens, M.-C. Bissinger, and R.J. Courcol, *Characterization of the Acinetobacter baumannii Fur regulator: cloning and sequencing of the fur homolog gene.* FEMS Microbiol Lett, 1999. **170**(1): p. 199-209.

10. Charnot-Katsikas, A., A.H. Dorafshar, J.K. Aycock, M.Z. David, S.G. Weber, and K.M. Frank, *Two cases of necrotizing fasciitis due to Acinetobacter baumannii.* J Clin Microbiol, 2009. **47**(1): p. 258-263.

11. McQueary, C. and L. Actis, *Acinetobacter baumannii biofilms: Variations among strains and correlations with other cell properties.* J Microbiol, 2011. **49**(2): p. 243-250.

12. Mah, T.-F.C. and G.A. O'Toole, *Mechanisms of biofilm resistance to antimicrobial agents.* Trends Microbiol., 2001. **9**(1): p. 34-39.

13. Thurlow, L.R., M.L. Hanke, T. Fritz, A. Angle, A. Aldrich, S.H. Williams, I.L. Engebretsen, K.W. Bayles, A.R. Horswill, and T. Kielian, *Staphylococcus aureus biofilms prevent macrophage phagocytosis and attenuate inflammation in vivo.* J Immunol, 2011. **186**(11): p. 6585-6596.

14. Schommer, N.N., M. Christner, M. Hentschke, K. Ruckdeschel, M. Aepfelbacher, and H. Rohde, *Staphylococcus epidermidis uses distinct mechanisms of biofilm formation to interfere with phagocytosis and activation of mouse macrophage-like cells 774A.1.* Infect Immun, 2011. **79**(6): p. 2267-2276.

15. Gaddy, J.A., A.P. Tomaras, and L.A. Actis, *The Acinetobacter baumannii 19606 OmpA protein plays a role in biofilm formation on abiotic surfaces and in the interaction of this pathogen with eukaryotic cells.* Infect Immun, 2009. **77**(8): p. 3150-3160.

16. Gaddy, J.A. and L.A. Actis, *Regulation of Acinetobacter baumannii biofilm formation.* Future Microbiol, 2009. **4**(3): p. 273-278.

17. Marc S. Hoffmann, M.D., B.S.E. Michael R. Eber, and P.M.P.H. Ramanan Laxminarayan, *Increasing resistance of Acinetobacter species to imipenem in United States hospitals, 1999–2006* Infect Control Hosp Epidemiol, 2010. **31**(2): p. 196-197.

18. Lin, L., B. Tan, P. Pantapalangkoor, T. Ho, B. Baquir, A. Tomaras, J.I. Montgomery, U. Reilly, E.G. Barbacci, K. Hujer, R.A. Bonomo, L. Fernandez, R.E.W. Hancock, M.D. Adams, S.W. French, V.S. Buslon, and B. Spellberg, *Inhibition of LpxC protects mice from resistant Acinetobacter baumannii by modulating inflammation and enhancing phagocytosis.* mBio, 2012. **3**(5).

19. Mussi, M.A., J.A. Gaddy, M. Cabruja, B.A. Arivett, A.M. Viale, R. Rasia, and L.A. Actis, *The opportunistic human pathogen Acinetobacter baumannii senses and responds to Llight.* J Bacteriol, 2010. **192**(24): p. 6336-6345.

20. Golic, A., M. Vaneechoutte, A. Nemec, A.M. Viale, L.A. Actis, and M.A. Mussi, *Staring at the cold sun: Blue light regulation is distributed within the genus Acinetobacter.* PLoS ONE, 2013. **8**(1): p. e55059.

21. Mussi, M.A., J.A. Gaddy, M. Cabruja, B.A. Arivett, A.M. Viale, R. Rasia, and L.A. Actis, *The Opportunistic Human Pathogen Acinetobacter baumannii Senses and Responds to Light.* J. Bacteriol. **192**(24): p. 6336-6345.

22. Clemmer, K.M., R.A. Bonomo, and P.N. Rather, *Genetic analysis of surface motility in Acinetobacter baumannii*. Microbiology, 2011. **157**(9): p. 2534-2544.

23. Losi, A. and W. Gartner, *Bacterial bilin- and flavin-binding photoreceptors.* Photochem Photobiol Sci, 2008. **7**(10): p. 1168-1178.

24. Masuda, S., *Light detection and signal transduction in the BLUF photoreceptors.* Plant Cell Physiol, 2013. **54**(2): p. 171-179.

25. Losi, A. and W. Gärtner, *Old chromophores, new photoactivation paradigms, trendy applications: Flavins in blue light-sensing photoreceptors.* Photochem Photobiol, 2011. **87**(3): p. 491-510.

26. Losi, A. and W. Gärtner, *The evolution of flavin-binding photoreceptors: An ancient chromophore serving trendy blue-light sensors.* Annu Rev Plant Biol, 2012. **63**(1): p. 49-72.

27. Tonge, P., G.R. Moore, and C.W. Wharton, *Fourier-transform infra-red studies of the alkaline isomerization of mitochondrial cytochrome c and the ionization of carboxylic acids.* Biochem J, 1989. **258**(2): p. 599-605.

28. Stelling, A.L., K.L. Ronayne, J. Nappa, P.J. Tonge, and S.R. Meech, *Ultrafast structural dynamics in BLUF domains: Transient infrared spectroscopy of AppA and its mutants.* J Am Chem Soc, 2007. **129**(50): p. 15556-15564.

29. Haigney, A., A. Lukacs, R.-K. Zhao, A.L. Stelling, R. Brust, R.-R. Kim, M. Kondo, I. Clark, M. Towrie, G.M. Greetham, B. Illarionov, A. Bacher, W. Romisch-Margl, M. Fischer, S.R. Meech, and P.J. Tonge, *Ultrafast infrared spectroscopy of an isotope-labeled photoactivatable flavoprotein.* Biochemistry, 2011. **50**(8): p. 1321-1328.

30. Lukacs, A., A. Haigney, R. Brust, R.K. Zhao, A.L. Stelling, I.P. Clark, M. Towrie, G.M. Greetham, S.R. Meech, and P.J. Tonge, *Photoexcitation of the blue light using FAD photoreceptor AppA results in ultrafast changes to the protein matrix.* J Am Chem Soc, 2011. **133**(42): p. 16893-900.

31. Haigney, A., A. Lukacs, R. Brust, R.-K. Zhao, M. Towrie, G.M. Greetham, I. Clark, B. Illarionov, A. Bacher, R.-R. Kim, M. Fischer, S.R. Meech, and P.J. Tonge, *Vibrational assignment of the ultrafast infrared spectrum of the photoactivatable flavoprotein AppA.* J Phys Chem B, 2012. **116**(35): p. 10722-10729.

32. Zirak, P., A. Penzkofer, T. Schiereis, P. Hegemann, A. Jung, and I. Schlichting, *Photodynamics of the small BLUF protein BlrB from Rhodobacter sphaeroides.* J Photochem Photobiol B, 2006. **83**(3): p. 180-194.

33. Masuda, S., K. Hasegawa, A. Ishii, and T.-a. Ono, *Light-induced structural changes in a putative blue-light receptor with a novel FAD binding fold sensor of blue-light using FAD (BLUF); Slr1694 of Synechocystis sp. PCC6803.* Biochemistry, 2004. **43**(18): p. 5304-5313.

34. Hasegawa, K., S. Masuda, and T.-a. Ono, *Spectroscopic analysis of the dark relaxation process of a photocycle in a sensor of blue light using FAD (BLUF) protein Slr1694 of the cyanobacterium Synechocystis sp. PCC6803.* Plant Cell Physiol, 2005. **46**(1): p. 136-146.

35. Yuan, H., S. Anderson, S. Masuda, V. Dragnea, K. Moffat, and C. Bauer, *Crystal structures of the Synechocystis photoreceptor Slr1694 reveal distinct structural states related to signaling.* Biochemistry, 2006. **45**(42): p. 12687-12694.

36. Clamp, M., J. Cuff, S.M. Searle, and G.J. Barton, *The Jalview Java alignment editor.* Bioinformatics, 2004. **20**(3): p. 426-427.

37. Waterhouse, A.M., J.B. Procter, D.M.A. Martin, M. Clamp, and G.J. Barton, *Jalview Version 2—a multiple sequence alignment editor and analysis workbench.* Bioinformatics, 2009. **25**(9): p. 1189-1191.

38. Lukacs, A., A. Haigney, R. Brust, R.-K. Zhao, A.L. Stelling, I.P. Clark, M. Towrie, G.M. Greetham, S.R. Meech, and P.J. Tonge, *Photoexcitation of the Blue Light Using FAD Photoreceptor AppA Results in Ultrafast Changes to the Protein Matrix.* J. Am. Chem. Soc., 2011. **133**(42): p. 16893–16900.

39. Tishler, M., K. Pfister, R.D. Babson, K. Ladenburg, and A.J. Fleming, *The Reaction between o-aminoazo compounds and barbituric acid. A new synthesis of riboflavin.* J Am Chem Soc, 1947. **69**(6): p. 1487-1492.

40. Arnold, K., L. Bordoli, J.r. Kopp, and T. Schwede, *The SWISS-MODEL workspace: a web-based environment for protein structure homology modelling.* Bioinformatics, 2006. **22**(2): p. 195-201.

41. Geux, N., Peitsch, Manuel C., *SWISS-MODEL and the Swiss-PdbViewer: An environment for comparative protein modelling.* Electrophoresis, 1997. **18**: p. 2714-2723.

42. Kiefer, F., K. Arnold, M. KÃ¼nzli, L. Bordoli, and T. Schwede, *The SWISS-MODEL epository and associated resources.* Nuc Acids Res, 2009. **37**(suppl 1): p. D387-D392.

43. Schwede, T., J. Kopp, N. Guex, and M.C. Peitsch, *SWISS-MODEL: an automated protein homology-modeling server.* Nucl. Acids Res., 2003. **31**(13): p. 3381-3385.

44. Götze, J. and P. Saalfrank, *Serine in BLUF domains displays spectral importance in computational models.* J Photochem Photobiol B, 2009. **94**(2): p. 87-95.

45. Masuda, S. and C.E. Bauer, *AppA Is a blue light photoreceptor that antirepresses photosynthesis gene expression in Rhodobacter sphaeroides.* Cell, 2002. **110**(5): p. 613-623.

46. Decatur, S.M., *Elucidation of residue-level structure and dynamics of polypeptides via isotope-edited infrared spectroscopy.* Acc Chem Res, 2006. **39**(3): p. 169-175.

47. Strasfeld, D.B., Y.L. Ling, R. Gupta, D.P. Raleigh, and M.T. Zanni, *Strategies for extracting structural information from 2D IR spectroscopy of amyloid: Application to islet amyloid polypeptide.* J Phys Chem B, 2009. **113**(47): p. 15679-15691.

48. Masuda, S., K. Hasegawa, and T.-a. Ono, *Tryptophan at position 104 is involved in transforming light signal into changes of β-sheet structure for the signaling state in the BLUF domain of AppA.* Plant Cell Physiol, 2005. **46**(12): p. 1894-1901.

49. Grinstead, J.S., M. Avila-Perez, K.J. Hellingwerf, R. Boelens, and R. Kaptein, *Light-induced flipping of a conserved glutamine sidechain and its orientation in the AppA BLUF domain.* J Am Chem Soc, 2006. **128**(47): p. 15066-15067.

50. Masuda, S., K. Hasegawa, and T.-a. Ono, *Light-induced structural changes of apoprotein and chromophore in the sensor of blue light using FAD (BLUF) domain of AppA for a signaling state* Biochemistry, 2005. **44**(4): p. 1215-1224.

51. Kondo, M., J. Nappa, K.L. Ronayne, A.L. Stelling, P.J. Tonge, and S.R. Meech, *Ultrafast vibrational spectroscopy of the flavin chromophore.* J Phys Chem B, 2006. **110**(41): p. 20107-20110.

52. Jung, A., J. Reinstein, T. Domratcheva, R.L. Shoeman, and I. Schlichting, *Crystal structures of the AppA BLUF domain photoreceptor provide insights into blue light-mediated signal transduction.* J Mol Biol, 2006. **362**(4): p. 717-732.

53. Yuan, H. and C.E. Bauer, *PixE promotes dark oligomerization of the BLUF photoreceptor PixD.* Proc. Nat. Acad. Sci., 2008. **105**(33): p. 11715-11719.

54. Masuda, S., K. Hasegawa, H. Ohta, and T.-a. Ono, *Crucial role in light signal transduction for the conserved Met93 of the BLUF protein PixD/Slr1694.* Plant Cell Physiol, 2008. **49**(10): p. 1600-1606.

Chapter 4

Time Resolved Multiple Probe Spectroscopy of AppA

NOTE: The contents of this chapter have been adapted from a recently submitted manuscript entitled "Proteins in Action: Real time fs to ms Dynamics of a Photoactive Flavoprotein."The authors are as follows: Richard Brust, Andras Lukacs, Allison Haigney, Agnieszka Gil, Kiri Addison, Michael Towrie, Gregory M. Greetham, Ian P. Clark, Peter J. Tonge and Stephen R. Meech.

4.1. Introduction

The underlying mechanism of protein function involves time dependent changes in structure occurring on multiple time scales, from sub-picosecond to seconds [1-3]. These processes are mediated by photoreceptors in which the initial ultrafast ($<10^{-13}$ s) absorption of light by a photoreceptor chromophore is coupled to structural events resulting in a downstream response of the organism. Since the rate of protein motion occurs on the ns-ms (or longer) timescales [4-6], it follows that photoreceptors must function over many decades of time. In this chapter, the structural evolution of the photoreceptor AppA from the sub-ps excitation to ms time scale using time resolved infrared (TRIR) will be discussed.

Important progress in time resolved structural dynamics has been made through the study of photoreceptor proteins. The application of pulsed laser setups to such systems provides an ideal setup for monitoring real time structural dynamics. Time resolved X-ray diffraction has provided detailed insights into photo-induced structural dynamics in a number of photoactive proteins [7-14]. For example, formation of the signaling state of the photoactive yellow protein (PYP) has been recorded on a 100 ps to ms time scale. However, X-ray diffraction requires the

protein to be studied in a crystalline environment [7, 9, 14], which may not accurately depict or permit structural dynamics. To overcome this, solution phase X-ray scattering has been performed to study PYP dynamics [12, 13]. Unfortunately, scattering data yields less microscopic structural detail than diffraction. As such, there is a need to develop new methods for monitoring protein structural dynamics.

BLUF domain proteins exhibit a two state, reversible photocycle characterized by a 10 nm red shift in the absorption spectrum of the isoalloxazine ring of FAD, which remains intact and fully oxidized in both dark and signaling states [15]. The red shift occurs within 1 ns and the photocycle is completed by recovery of the dark adapted (dAppA) ground state in 30 minutes [16]. There are two solved X-ray crystal structures for the N-terminal BLUF domain of AppA ($AppA_{BLUF}$), revealing an intricate H-bonding network surrounding the chromophore (Figure 4.1) [17, 18]. Studies of the structure of $dAppA_{BLUF}$ and its light adapted signaling state ($lAppA_{BLUF}$) suggest a key step in forming the signaling state involves rotation of the conserved glutamine (Q63 in AppA) adjacent to the isoalloxazine ring; in-line with this, Q63 is found to be an essential residue for photoactivity [19]. Based on previous work and our study of the photoinactive mutant Q63E, we proposed a refinement to this model in which tautomerization of Q63 precedes rotation, leading to the formation of a new H-bond to the flavin C4=O carbonyl (Figure 4.2) [20, 21]. This is consistent with stationary state vibrational spectra, where a red shift in the C4=O stretch mode (indicative of stronger H-bonding) is observed between dark and light adapted states [18, 22]. Other conserved residues critical to photoactivation include Y21 and W104 [23]. The W104A mutant has been well characterized, resulting in a system where blue light sensitivity is diminished and large scale protein events are abolished, leading to a number of

models where W104 has been proposed to serve as the source of signal modulation from N-terminus to C-terminus in AppA [19, 24-26].

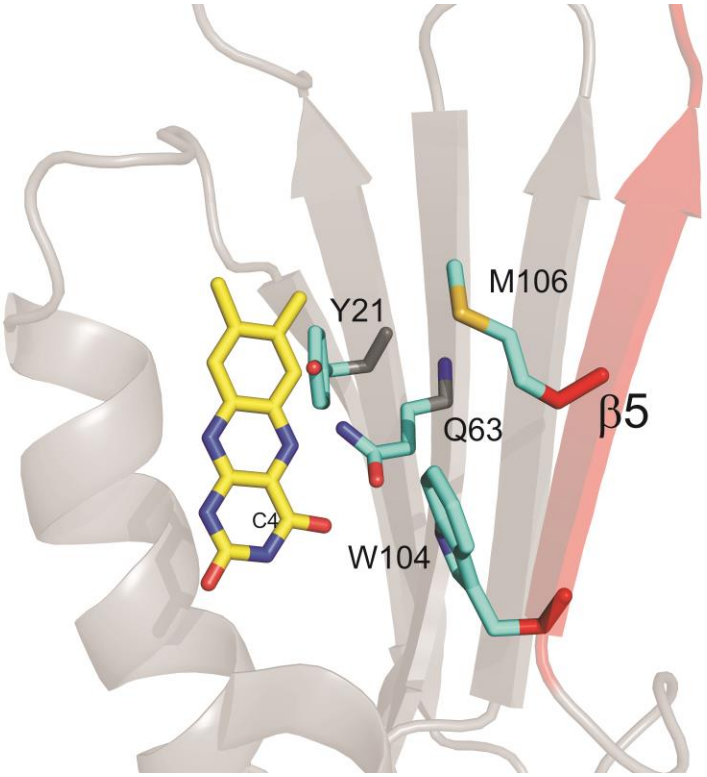

Figure 4.1. Structure of FAD in AppA$_{BLUF}$. Crystal structure of AppA$_{BLUF}$ showing flavin bound. The H-bonding network around the flavin includes key residues Y21, Q63, W104, and M106. The Figure was made using Pymol [27], and the structure 1YRX.pdb [18].

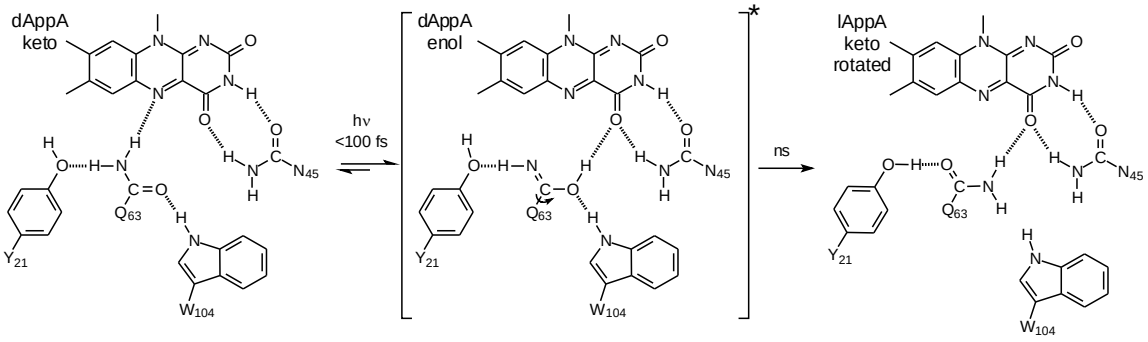

Figure 4.2 H-bonding network in AppA$_{BLUF}$. Details of the proposed H-bonding network changes in AppA$_{BLUF}$ as a result of photoexcitation.

In this chapter, the photoinduced structural dynamics over a very wide time range, from 100 fs to 1 ms of $dAppA_{BLUF}$ and two of its mutants (W104A and M106A) as they evolve post-excitation. In these experiments, protein dynamics are recovered from measurements of the TRIR difference spectra, which are sensitive to structural changes in both the chromophore and the surrounding protein. To achieve this, the recently developed method of ultrafast time resolved multiple probe spectroscopy (TRMPS), will be used [28, 29].

4.2. Experimental Methods

4.2.1. Site Directed Mutagenesis

Table 4.1 lists the different primers used for the various mutants generated. Site directed mutagenesis was performed using pfu Turbo (Invitrogen). After amplification, Dpn1 was used to cleave template DNA, and 20 μL of the reaction mixture was then transformed into 100 μL of XL1-blue cells.

4.2.2. Protein Expression and Purification

Plasmids were expressed in BL21(DE3) *E. coli* cells and grown in 10 mL cultures containing LB media with 200 μg/mL ampicillin at 37°C at 250 rpm and used to inoculate 1 L LB/ampicillin media was performed using these cultures and grown to an OD600 of about 1 at 30°C for 5 hours. Induction was performed by adding 0.8 mM IPTG at 18°C, followed by overnight incubation in the dark. Cells were harvested at 5000 rpm at 4 °C and stored at -20 °C until needed.

Purification of wild type and the various mutants were performed in the dark. Thawed cell pellets were resuspended in 40 mL of wash buffer (10 mM NaCl, 50 mM $Na_2H_2PO_4$, pH 8.0), to which 200 μL of 50 mM PMSF was added to inhibit endogenous protease activity. Cells were lysed by sonication and cell debris was removed by ultracentrifugation (33000 rpm

for 90 minutes). The cell pellet was discarded, and to the soluble fraction 10mg/mL FAD was added and incubated for 45 minutes on ice. The protein was then purified by Ni-NTA affinity chromatography using wash buffer. The bound protein was then washed using the wash buffer and increasing amounts of imidazole and finally eluted with 250 mM imidazole. The fractions were then dialyzed overnight in the dark in the wash buffer. Protein purity and yield were determined using UV-Vis spectroscopy and SDS-PAGE.

Table 4.1 Primer design of W104 and M106 mutants.

Mutant	Forward Primer Sequence
W104A forward	5'-TTTGCGGGAGCGCACATGCAGCTCTCCTGCTCG-3'
W104A reverse	5' CGAGCAGGAGAGCTGCATGTGCGCTCCCGCAAA-3'
M106A forward	5'-TTTGCGGGATGGCACGCGCAGCTCTCCTGCTCG-3'
M106A reverse	5'- CGAGCAGGAGAGCTGCGCGTGCCATCCCGCAAA-3'
M106F forward	5'-TTTGCGGGATGGCACTTTCAGCTCTCCTGCTCG-3'
M106F reverse	5'- TTTGCGGGATGGCACTTTCAGCTCTCCTGCTCG-3'

4.2.3. Uniform ^{13}C labeling

Uniform ^{13}C protein labeling was performed by expressing BlsA in BL21(DE3) *E. coli* cells that were grown on minimal media containing [U-$^{13}C_6$]-D-glucose (Cambridge Isotopes) as the sole carbon source. Single colonies containing plasmids for AppA that had been grown on LB/Amp plates were streaked on M9 minimal media/glucose/ampicillin plates containing 200 mg/mL ampicillin, and 5 mg/mL glucose. This process has been hypothesized to acclimatize the cells to growth in minimal media, leading to improved protein expression. The cells were grown to an OD_{600} of approximately 0.5 at 30 °C, which were then pelleted and resuspended in fresh media with [U-$^{13}C_6$] glucose in place of unlabeled glucose. After 30 min at 18°C, 0.8 mM IPTG was added to induce protein expression, and the culture was shaken in the dark for 24 h to maximize the yield of protein. Purification followed the same protocol described in 4.2.2.

4.2.4. Photoconversion Experiments

AppA photoconversion experiments were recorded using a Cary 100 UV-Vis spectrometer (Varian) at 25 °C. Protein concentrations were typically around 40-60 μM in 10 mM NaCl, 50 mM NaH_2PO_4, pH 8.0. A handheld UV illuminator was used, emitting about 20 mW of 365 nm light for 3 minutes.

4.2.5. FTIR Spectroscopy

Light minus dark FTIR spectra were obtained on a Vertex 80 FTIR spectrometer (Bruker). Here, 80 μL of 2 mM protein was placed between two CaF_2 plates equipped with a 50 μm spacer were 64 scans were accumulated at a 3 cm^{-1} resolution. The light state was generated by 3 minute irradiation using a 460 nm high mount LED (Prizmatix) inserted into the sample compartment.

4.2.6. TRIR Spectroscopy

TRIR experiments were performed at STFC Central Laser facility. The TRIR system has been described in detail elsewhere [30]. Using the system with a repetition rate of 10 kHz with a high signal to noise, resolution of about 100 fs can be achieved. Excitation pulses were set to 450 nm at 200 nJ with a spot size radius of 100 μm. Dark state measurements were rastered and flowed at a rate of 1.5 mL/min, to minimize photobleaching and sample degradation during the measurement, in a 50 μm path length transmission cell using CaF_2 windows. The IR probe recorded transient difference spectra (pump on-pump off) at time delays between 1 ps and 2000 ps. Photoconversion was shown to be minimal by steady state absorption spectroscopy. The probe beam was measured by two carefully matched 128 pixel CCD detectors, yielding a resolution of 3 cm^{-1} per pixel. Spectra were calibrated relative to the IR transmission of a polystyrene standard. Light-adapted samples were prepared by irradiation at 380 nm high mount

LED (Thorlabs). Photoconversion was monitored using UV-Vis absorption spectroscopy and was found to be complete within 3 min. The TRIR setup was operated and maintained by the CLF (Dr. Greg Greetham, Dr. Ian Clark, Dr. Mike Towrie).

4.2.7. TRMPS

The TRMPS method utilizes the impressive signal-to-noise and stable pulse to pulse timing of the ULTRA laser setup described in 4.2.2. [30]. A 1 kHz visible pump laser (450 nm) at 1 µJ is synchronized with the 65 MHz (15×10^{-9} s^{-1}) repetition rate of the titanium sapphire seed laser and is automatically locked to the 10 kHz pulses of the ULTRA amplifier. The delay between 100 ps and 15 ns is achieved by varying an optical stage delay. The times between 10 ns and 100 µs are controlled by using the oscillator seed pulses to add multiples of 15 ns to the pump laser delay. For times between 100 µs and 1 ms the 10 kHz pulses are synchronized with the 1 kHz pump laser, providing a data point every 0.1 ms. In this way the timing is extended but the detection apparatus is identical, allowing transient IR difference data to be recorded every 100 µs with high signal-to-noise. The TRMPS setup was operated and maintained by the CLF (Dr. Greg Greetham, Dr. Ian Clark, Dr. Mike Towrie).

4.3. Results and Discussion

Two crystal structures have been solved for the N-terminal BLUF domain of AppA, revealing an intricate H-bonding network surrounding the flavin chromophore [17, 18]. A key aspect to all the models for formation of the light adapted state is the importance of the conserved glutamine (Q63 in AppA), an essential residue for photoactivity [17-19, 31, 32]. Structural data characterized by Anderson and co-workers proposed a model where Q63 rotation upon light absorption results in the formation of a new H-bond to the flavin O4 carbonyl oxygen

(Figure 4.1) [18]. This is in good agreement with vibrational spectroscopy, where a shift of 10 cm^{-1} in the C4=O is observed both in steady state and ultrafast IR spectroscopy [20, 21, 33]. In addition a conserved tryptophan residue (W104), located on β5 strand, may also be directly involved in photoactivation, where motion of the W104 side chain results in signal transduction [20, 25, 26].

The β5 strand is of particular interest due to its potential role in signal modulation from the N-terminus of AppA to the C-terminus. Residues W104 and M106 are found on the β5 strand. In the Anderson et al. BLUF crystal structure, W104 is located near the flavin where the W104 forms an H-bond with Q63 [18]. In the Jung et al. structure, the W104 side chain is about 10 Å away than in the Anderson structure and is partially solvent exposed (Figure 4.3) [17]. In place of W104 is M106, whose side chain occupies a similar space as the W104 side chain does in the Anderson structure. A crystal structure of the BLUF protein PixD from *Synechocystis* shows that PixD forms a 10-subunit complex in which 9 subunits have the equivalent tryptophan (W91) is "out" of the flavin binding pocket and the remaining subunit exhibits the "$W91_{in}$" conformation [32]. Here we sought to better understand the roles of these residues through site-directed mutagenesis. Previous work has been performed on two W104 mutants; W104A and W104F. Mutations to W104 alter the FTIR spectra when compared to wild type, revealing an important role for this residue. Further characterization of the W104A mutant along with the M106A and M106F mutant was necessary to better understand the β5 strand.

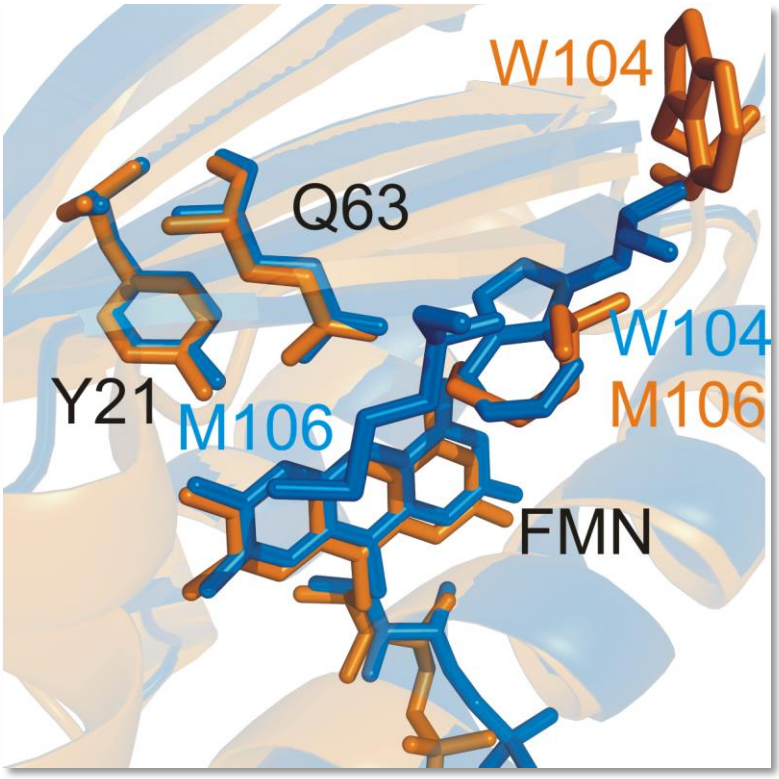

Figure 4.3. Crystal structure comparison of $AppA_{BLUF}$. Comparison of the two possible conformations for W104 in the two solved crystal structure of AppA: PDB 2IYG (orange) [17] and 1YRX (blue) [18].

4.3.1. Photorecovery of W104 and M106 Mutants

Compared to the wild type protein, the W104A mutant is known to dramatically increase rate of dark state recovery (80 fold) while the M106A exhibits only 1.5 fold faster rate [23, 34]. M106 is also conserved in BLUF proteins, however mutations to M106 have only a minimal effect on the rate of dark state recovery (23 min versus 30 min for wild-type) [34]. The M106F mutation was performed to see if the addition of another bulky aromatic side chain would have on photorecovery. The M106F mutant exhibited similar absorption spectra to wild type $AppA_{BLUF}$ (Figure 4.4A), with a recovery of 14 ± 0.2 minutes.

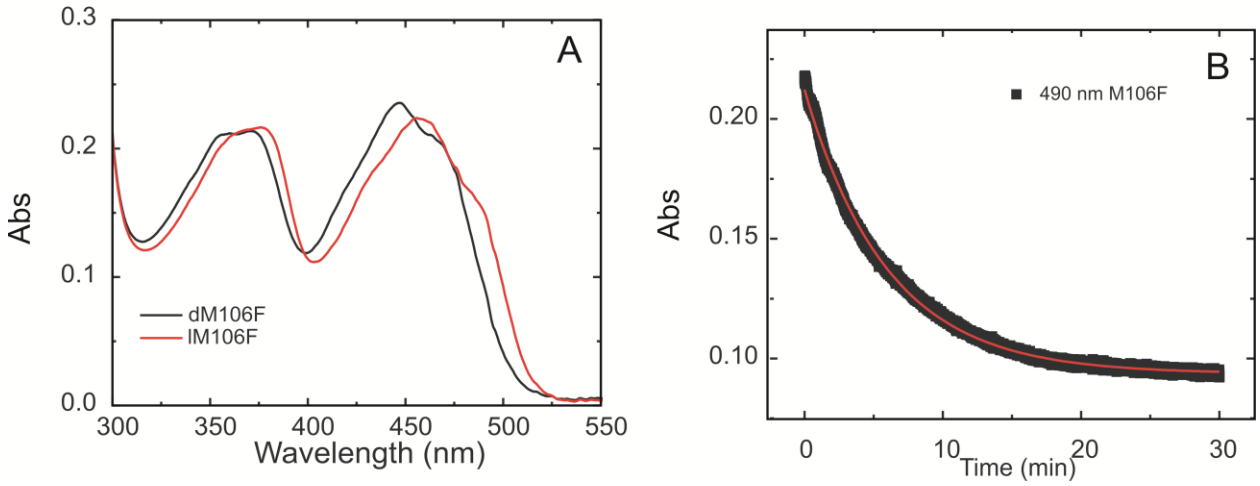

Figure 4.4. The photocycle of M106F. A. UV-Vis absorption spectra of pre irradiated (dM106F) and post-irradiated (lM106F). **B.** Kinetic trace recorded at 490 nm.

4.3.2. FTIR of W104 and M106 Mutants

FTIR spectroscopy has proven to be a valuable tool to monitor structural changes in BLUF proteins. For $AppA_{BLUF}$ two difference modes are observed at 1622(-)/1632(+) cm^{-1} and at 1688(+)/1700(-) cm^{-1} (Figure 4.4 and 4.5). The 1688(+)/1700(-) cm^{-1} mode was assigned to rearrangement of the H-bonding network surrounding the flavin resulting in an increase in H-bonding from the protein to the C4=O flavin carbonyl. The difference mode observed at 1622(-)/1632(+) cm^{-1} was associated with changes to the protein matrix, particularly the β5 strand [24]. To further characterize the role of W104 and M106 in $AppA_{BLUF}$, analysis by FTIR was performed. The difference spectrum generated for M106F (Figure 4.5) revealed little difference to $wtAppA_{BLUF}$. The characteristic mode at 1620(-)/1630(+) cm^{-1} is still present in M106F and M106A (Figure 4.5), however in W104A this is absent (Figure 4.6), in agreement with previous results [24].

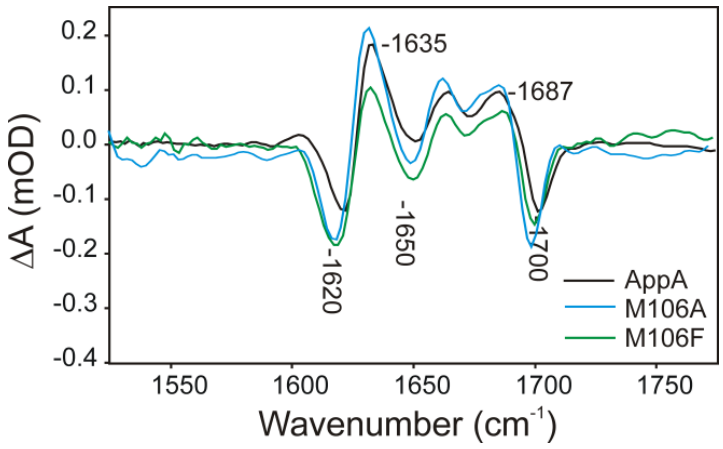

Figure 4.5. FTIR spectra of AppA and M106 mutants. Light minus dark FTIR spectra of $AppA_{BLUF}$ (black), M106A (blue) and M106F (green).

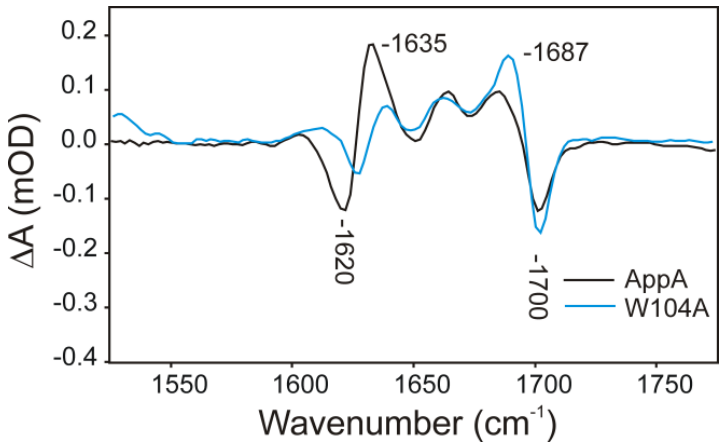

Figure 4.6. FTIR spectra of AppA and W104A. Light Minus Dark FTIR spectrum of $AppA_{BLUF}$ (black) and W104A (blue).

4.3.3. TRIR Spectroscopy

4.3.3.1. W104Mutants

The relative positions of W104 and M106 are essential in designing a mechanism for light state formation. For this reason we undertook time resolved IR spectroscopy as a method for elucidating the structure. The W104A mutation results in a singifican increase in photorecovery of the dark state [24]. In comparing the TRIR of the dark state of wild type with

W104A one sees minimal perturbation of the infrared spectrum reported in both the dark and light states (Figure 4.7). Characteristic bands at 1547, 1585, 1650 and are observed in both states of the W104A mutant. The 1700 cm^{-1} band in dW104A shifts down by 10 cm^{-1} to 1690 cm^{-1} in lW104A, consistent with an increase in H-bonding to the C4=O, a mechanism observed in photoactive BLUF proteins. In addition, a transient is observed at 1668 cm^{-1} in dW104A absent in lW104A, again in agreement with what is observed in $dAppA_{BLUF}$ [20]. Light adapted spectra are in good agreement. FTIR data suggest an altered protein structure as indicated by the mode observed at ~1620/1630 cm^{-1}. Here, the TRIR spectra reveal instantaneous interactions around the flavin. While W104 clearly affects the photocycle, TRIR spectra indicate a minimal effect on the H-bonding network surrounding the flavin.

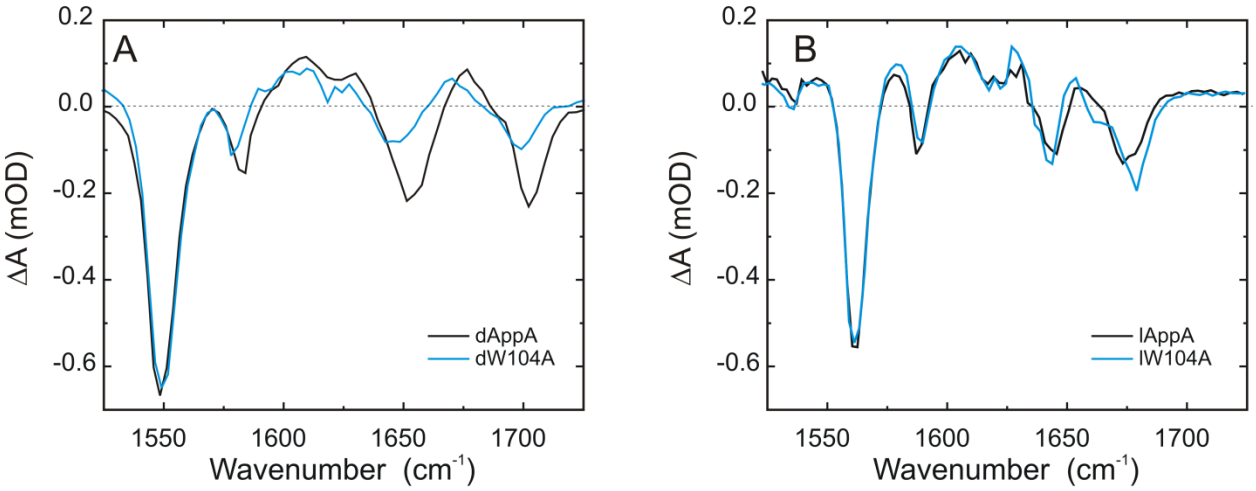

Figure 4.7. TRIR spectra of $AppA_{BLUF}$ and W104A. TRIR spectra of $AppA_{BLUF}$ (black) and W104A (blue) recorded at 3 ps post excitation. **A.** Spectra of dark state. **B.** Spectra of photoconverted species.

4.3.3.2. M106 Mutants

In the proposed models of signal formation, M106 and W104 play an essential role in modulation [24, 25, 35-37]. Both are present in the β5 strand, which has been shown to be very

fluid and has been proposed to relay the signal. To understand the effects on an ultrafast timescale, we measured TRIR on M106A and M106F. The M106A/F mutations altered the photocycle by reducing the dark state recovery by ~2 fold, however no significant difference is observed in the steady state FTIR spectra (Figure 4.5). Comparison to wild type of the M106 mutants revealed spectra similar to wild type (Figure 4.8). In dAppA there are four main bleaches associated with the flavin (1547, 1582, 1652 and 1700 cm^{-1}) [33]. In addition to the bleaches, there is a broad transient present in the unbound chromophore at 1610 cm^{-1}, and a transient present in the dark state but absent in the light adapted state and in free flavin, tentatively assigned as the side chain amide of Q63 [20, 33]. In addition to the absence of the 1670 cm^{-1} transient, in $lAppA_{BLUF}$ a 10 cm^{-1} red shift of the 1700 cm^{-1} mode, assigned as the C4=O. In d and l M106A and d and l M106F, one does not see a significant change structurally when compared to wild type. These data suggest these mutations do not alter the structure of either the ground or excited states.

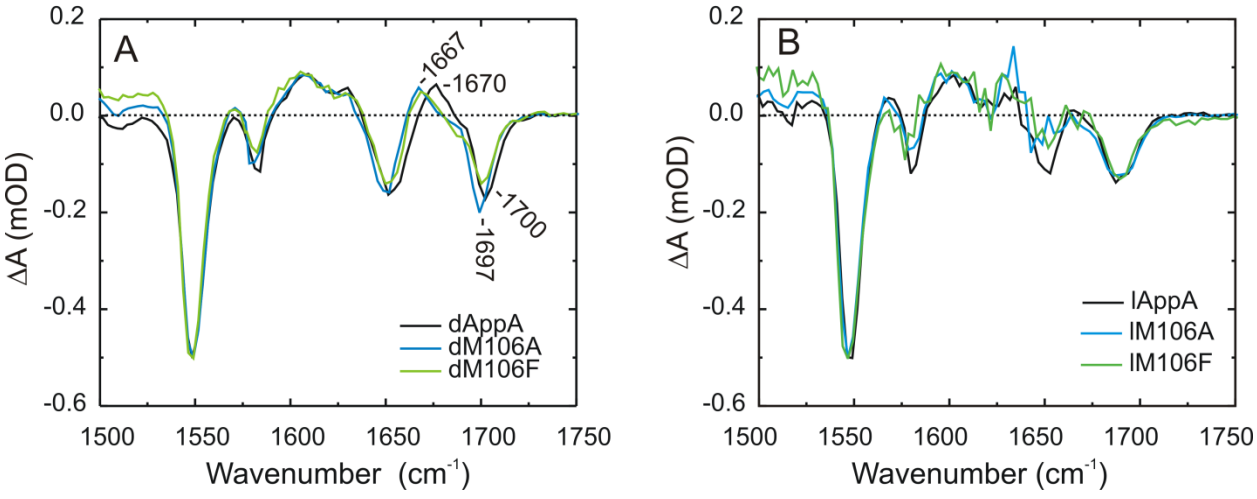

Figure 4.8. TRIR spectra of $AppA_{BLUF}$ and M106 mutants. TRIR spectra of $AppA_{BLUF}$ (black), M106A (blue), and M106F (green) recorded at 3 ps post excitation. **A.** Spectra of dark state. **B.** Spectra of photoconverted species.

4.3.3.3. Ultrafast Kinetics of W104 and M106 Mutants

Kinetics of the main bleach in the TRIR spectra for $AppA_{BLUF}$ and the W104 and M106 mutants are reported in Table 4.2. As previous reported [20, 21], the decay of the bleach at 1547 cm^{-1} on this time scale can be fit to a bi-exponential. Analysis of the average lifetimes indicates minimal effects on the rate of recovery of the W104 mutant. The M106 mutants exhibit a modest increase the ES lifetime of the dark (~1.2 fold) and light (~1.1 fold) state. This suggests a possible quenching effect for M106, although based on these results this effect would be minimal.

Table 4.2. Kinetics of ground state recovery of $AppA_{BLUF}$ and its mutants.

Sample	α1	τ1	α2	τ2	<τ>
dAppA	-0.51	34 ± 4 ps	-0.49	473 ± 73 ps	249 ps
lAppA	-0.78	11 ± 1 ps	-0.22	134 ± 24 ps	45 ps
dW104A	-0.42	18 ± 1 ps	-0.58	393 ± 18 ps	236 ps
lW104A	-0.64	11 ± 1 ps	-0.36	91 ± 8 ps	40 ps
dM106A	-0.39	68 ± 29 ps	-0.61	446 ± 50 ps	298 ps
lM106A	-0.73	11 ± 1 ps	-0.27	150 ± 20 ps	49 ps
dM106F	-0.39	70 ± 24 ps	-0.61	450 ± 43 ps	301 ps
lM106F	-0.72	12 ± 1 ps	-0.28	145 ± 19 ps	49 ps

4.3.4. TRMPS

4.3.4.1. FMN

Initial characterization of the system was performed on FMN. FMN was chosen over FAD as in aqueous solutions there is a reaction between the flavin ring and the adenine which is absent in the protein. In the TRMPS spectra recorded for FMN (Figure 4.9), one can clearly see that by 10 ns the initially excited singlet state has completely relaxed as indicated by the 1383 cm^{-1} transient mode assigned to the S_1 singlet excited state. However, the ground state has not

completely recovered based on the localized modes at 1547 and 1700 cm^{-1}) and a weak transient was formed at 1438 cm^{-1}. A plausible candidate for the appearance of this mode is flavin triplet state. Triplet states in flavin binding photoreceptors are well characterized, in particular the LOV domain, and occur on microsecond timescales [38-41]. Kennis et al. reported the observation of a band at 1438 cm^{-1} forming in 1.5 ns in the LOV2 domain of *Avena sativa*, but were unable to determine lifetime due to the time resolution of the IR system used [40]. Monoexponential formation was observed from 2 ps to 100 ns, a rise time component of 3.6 ± 0.3 ns is reported at 1440 cm^{-1} with monoexponential decay 100 ns to 50 μs with a time component of 1.4 ± 0.1 μs. Formation of the light state of $AppA_{BLUF}$ has been reported to be within 1 ns, as indicated by the shift in λmax of the flavin absorption spectrum by 10 nm [16], which is on a similar timescale to triplet state formation of FMN proposed here. These results indicate the possibility of a triplet state flavin in the mechanism of signaling state formation in $AppA_{BLUF}$.

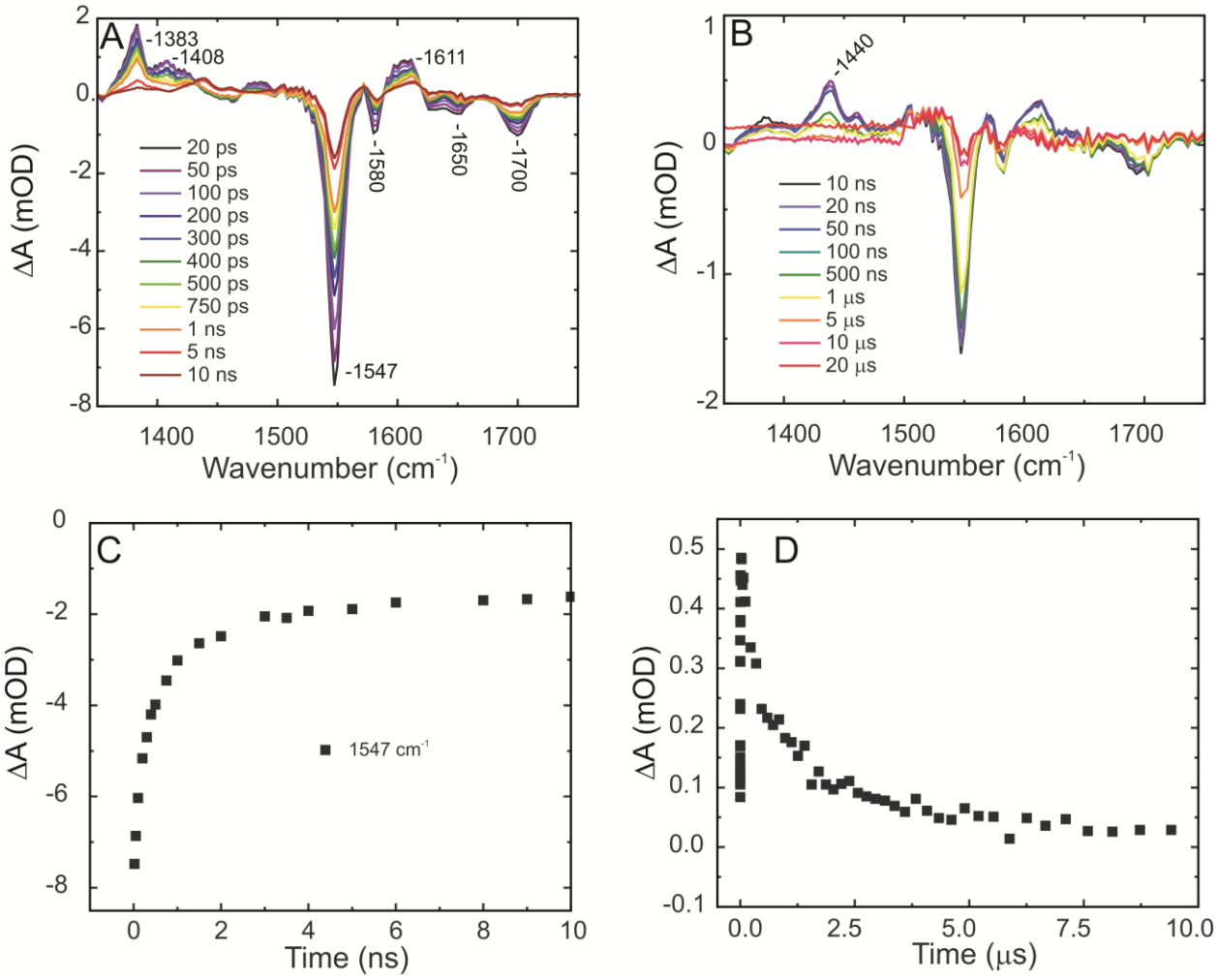

Figure 4.9. TRMPS IR difference spectra for FMN. A. Transient IR difference spectra recorded between 20 ps and 10 ns after excitation of the flavin in aqueous solution at 450 nm. **B.** Relaxation in the FMN spectrum between 10 ns and 20 μs after excitation. **C.** Kinetics at 1547 cm^{-1}, highlighting non-exponential decay. **D.** Kinetics at 1440 cm^{-1}. This mode is tentatively assigned to the triplet state, which has completely decayed in < 5 μs. The observation of this mode for FMN in aqueous solution suggests the need to consider triplet contributions in wtAppA.

4.3.4.2. TRMPS of $AppA_{BLUF}$

A considerable amount of effort has been performed on free flavin for the ps to ns time domain [33, 42]. Figure 4.10A shows the TRIR spectra for $dAppA_{BLUF}$ between 2 ps and 10 ns after 450 nm excitation of the flavin. The dominant sub-nanosecond relaxation is well fit by a

biexponential function with the time components consistent with previously reported sub-nanosecond data (34 ± 4 ps, 473 ± 73 ps) [20, 21, 42].

The two high frequency bleach modes at 1700 and 1650 cm^{-1} are associated with two carbonyl stretches of the FAD ground state, and are sensitive to the H-bond environment [33, 43]. The intense bleach at 1547 cm^{-1} and the weaker one at 1580 cm^{-1} are FAD ring modes. The two positive peaks at 1410 cm^{-1} and 1383 cm^{-1} are not assigned to specific vibrational modes, but are associated with the excited state of the flavin ring rather than shifted protein modes based on their presence in the free flavin spectra (Figure 4.8).

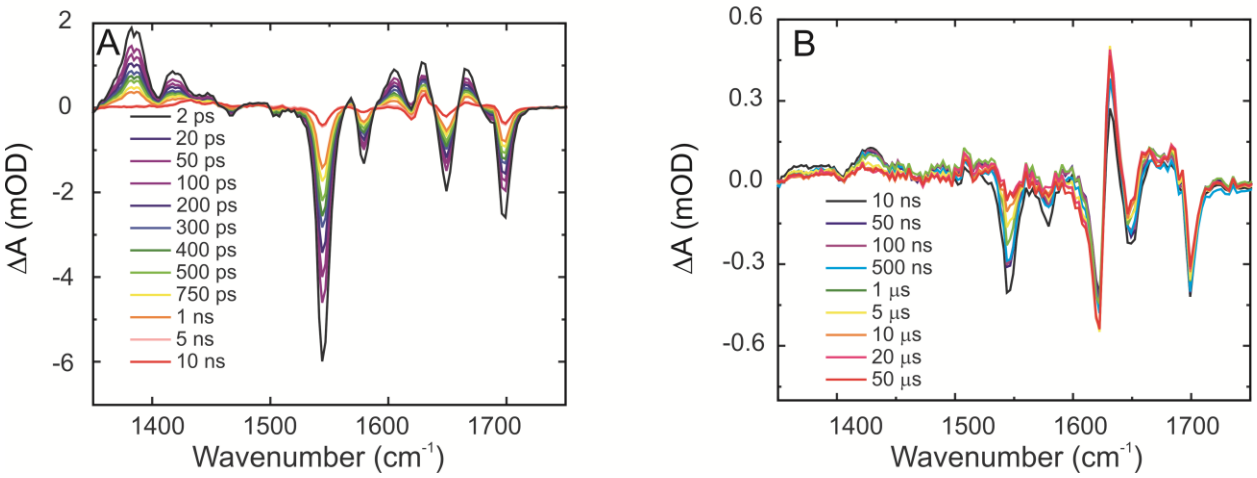

Figure 4.10. TRMPS IR difference spectra for $dAppA_{BLUF}$. **A.** TRIR spectra recorded between 2 ps and 10 ns after excitation of the flavin at 450 nm. The fast and complete decay of the singlet excited state is evident in the transient flavin modes at 1380 cm^{-1}. However, the ground state recovery is incomplete e.g. at 1547 cm^{-1} and some transient (probably triplet) state is formed. **B.** Relaxation in the $dAppA_{BLUF}$ TRIR spectrum between 10 ns and 50 µs after excitation. The electronic ground state recovers fully (1547 cm^{-1}) but formation of a new environment is indicated by the shift and incomplete recovery in the carbonyl mode at 1703 cm^{-1}. The temporal evolution in the 1622/1631 cm^{-1} pair of protein modes is also evident.

The fast kinetics in Figure 4.10A reflects the excited state chemistry of AppA. The primary photochemical step in the reaction is controversial. Transient absorption spectroscopy previously assigned the primary step to an electron transfer reaction between excited FAD and

tyrosine 21 (Figure 4.1) followed by proton transfer on a longer time scale [44-47]. The change in electronic structure is proposed to lead to rearrangement of the H-bonding network prior to recovery of oxidized flavin. Assignment of intermediates in the proposed ET and PT steps were based on analysis of the complex kinetics and on observations of a radical-like spectrum in the transient visible absorption of a related BLUF domain protein, PixD [48]. However, an alternative mechanism was proposed where excitation of FAD itself is sufficient to induce changes in the H-bonding network, giving rise to keto-enol tautomerization in Q63, which leads in-turn to the required structure change (Figure 4.2). This assignment was based on the absence of spectral features consistent with flavin radical states in the sub-nanosecond TRIR spectra of AppA (Figure 4.9A), and the observed perturbation of the protein network on excitation and the quenching rate of FAD [20, 21]. There is theoretical support for both mechanisms [49-51]. Both agree that a light induced structure change in the network of amino acids surrounding FAD occurs within 1 ns, which ultimately leads to formation of the signaling state.

While considerable amount of work has been performed to understand the initial steps in the mechanism, little is still known about the latter processes that ultimately result in the release of PpsR *in vivo*. To understand these processes, analysis of the TRIR spectra beyond 1 ns had to be performed. Although it is evident from Figure 4.10A that at least 80 % of the populated ES has returned to the ground state within 10 ns, small signals remain. Exploiting a high signal-to-noise apparatus with a 10 kHz data acquisition rate and the ability to measure structural changes from 100 fs to 1 ms [29], it has been proved possible to time resolve the data beyond 10 ns (Figure 4.9B). It is already evident from Figure 4.9A that by 10 ns the FAD excited state has completely relaxed based on the the 1383 cm^{-1} transient mode (FAD S_1 state) but the ground

state has not completely recovered (localized FAD modes at 1547 and 1700 cm^{-1}). This result immediately proves the existence of intermediate protein structures in the photocycle.

Figure 4.10B probes relaxation on the longer timescale and shows complete ground state recovery for the 1547 cm^{-1} chromophore ground state mode occurs on the microsecond timescale (Figure 4.10A), while the mode associated with the C4=O carbonyl at 1700 cm^{-1} recovers with the same rate (Table 4.3), but to a non-zero bleach level, i.e. the mode has not fully recovered even in 50 μs. Data beyond the 50 μs measurement (out to 1 ms) showed no further change in the TRMPS spectrum associated with either the chromophore or protein structure. These data point to microsecond dynamics refilling the original ground state, while the latter feature indicates the spectrum associated with the formation of light adapted AppA, with a shifted C4=O mode, due to altered H-bond interactions [36], has been formed. In addition, a weak band at 1440 cm^{-1} is present in the Figure 4.10B that is similar to what is observed in free flavin, indicating the possibility of triplet state in the photocycle of AppA. At present time the kinetics are not resolvable, but this appears to be the first reported evidence of flavin triplet state and its importance in the BLUF photocycle.

Further slow dynamics are evident in the complex dispersive band structure between 1600 and 1640 cm^{-1}, which continue to evolve after FAD recovers its electronic ground state. Since there are no strong chromophore modes in this region of the spectrum, these changes are assigned to structural evolution in the surrounding protein matrix. This result shows the sensitivity of vibrational spectroscopy to protein dynamics; in the electronic spectrum no evolution was detected between 10 ns and 15 μs [52]. The assignment of the 1622/1631 cm^{-1} dispersive band shape to protein modes was confirmed by repeating the experiment in uniformly ^{13}C labeled protein, U-^{13}C $dAppA_{BLUF}$; TRIR data recorded after 10 ns and 20 μs are shown in

Figure 4.11A. Both the positive and negative band are red-shifted by 36 ± 2 cm^{-1} from the unlabeled spectrum, consistent with labeling of a protein backbone [53, 54]; modes assigned to the FAD chromophore are unshifted [21, 33, 43]. The assignment of the dispersive band to the protein agrees with the stationary state IR difference spectra of Masuda and co-workers, who proposed on the basis of the observed frequencies that these changes arose from a C=O (amide) mode of the β-sheet structure, which is linked to the FAD bound in the α-helix region by the key residues W104, Q63 and Y21 (Figure 4.1) [36]. In Figure 4.11B, the TRIR spectra recorded at 20 μs is compared with steady state IR difference spectrum recorded with the same 3 cm^{-1} resolution as the TRIR data. The latter two spectra show that the structural dynamics associated with these protein modes are essentially complete within 20 μs, with no further TRIR spectral changes observed in the measurements out to 1 ms. Formation of the signaling state in 20 μs is longer than the nanosecond timescale previously proposed [52].

The microsecond timescale observed is significant with regards to NMR studies of light and dark adapted forms of the BLUF domain, which suggested that the structure changes which occur are of small scale but take place at residues relatively remote from the flavin chromophore, including in the β-sheet (Figure 4.1) [55]. The present data shows that structural changes in proteins, which take place at distances in excess of 10 Å, can occur on the microsecond timescale.

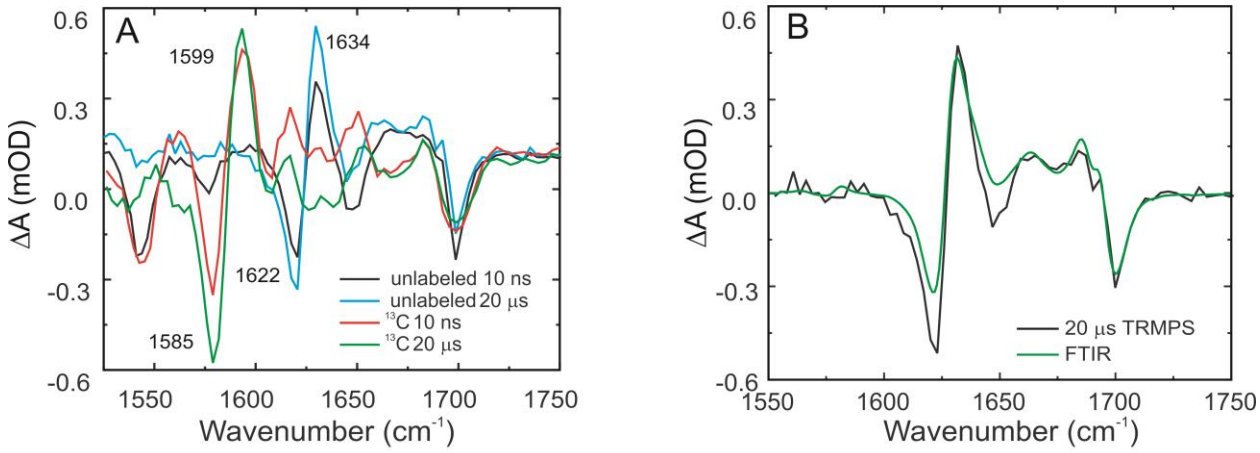

Figure 4.11. Assignments of $AppA_{BLUF}$ TRMPS spectra. A. Effect of ^{13}C isotope exchange in $AppA_{BLUF}$ measured 10 ns and 20 µs after excitation **B.** Comparison of the TRIR spectra recorded 20 µs after excitation with the stationary state IR difference spectrum for the light minus dark states.

Further detail can be recovered from analysis of the kinetics between 10 ns and 50 µs after excitation (Figure 4.12). For the 1622/1631 cm^{-1} dispersive pair associated with protein bleach and absorption respectively the kinetics are presented in Figure 4.11A. A striking result is that these bands are kinetically distinct and not linked by the monotonic blue shift of a single protein mode. The transient absorption at 1631 cm^{-1} rises in 1.5 µs and is reproducibly faster than the 2.1 µs development of the 1622 cm^{-1} bleach. This result is not unexpected, as the structural changes between the light and dark states are known to be spread over a number of residues [55], each of which may have a slightly different vibrational frequencies associated with the amide backbone. The kinetics associated with changes occurring on more than one residue are expected to be more complex than a simple first order process [56]. Unfortunately, the present signal-to-noise does not permit the extraction of anything more than a characteristic timescale for the dynamics associated with each mode.

The weak transient feature at 1688 cm^{-1} develops on a longer timescale than the protein modes (Table 4.3), but on the same timescale as the partial bleach recovery at 1700 cm^{-1}. This

mode is well characterized and assigned as the increase in H-bonding from the protein to the flavin C4=O carbonyl. The present results thus suggest a phase in protein structural reorganization slower than seen in the protein modes in Figure 4.12A. Significantly, the slower structural reorganization occurs in protein residues in the H-bonding network of the flavin chromophore. This contrasts with the faster changes assigned to the more remote residues in the β-sheet (Figure 4.12A), indicating there is no simple relationship between the timescale of the protein response to electronic excitation and distance from the chromophore.

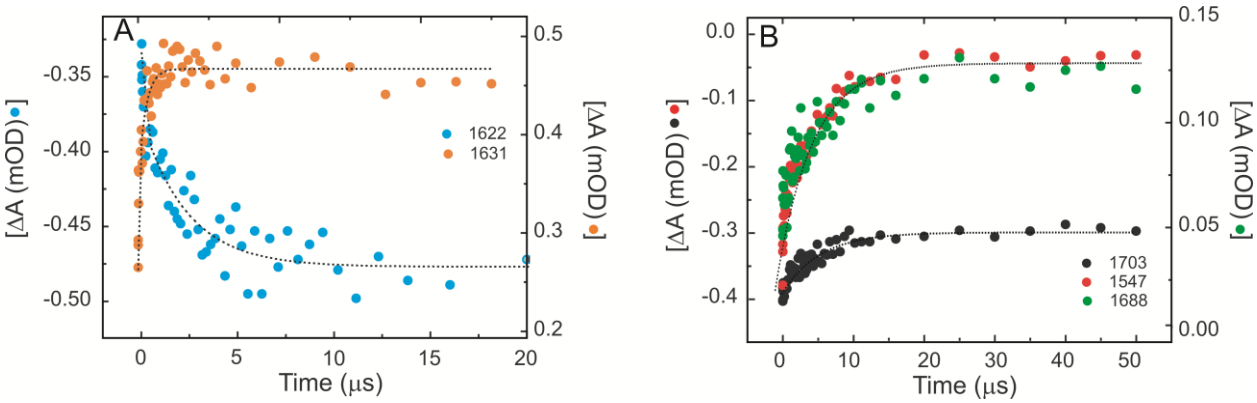

Figure 4.12. Comparison of protein and chromophore mode kinetics A. Kinetics of protein modes, showing that the linked pair at 1622/1631 cm^{-1} exhibit distinct kinetics. The growth of the transient occurs more rapidly than the evolution of the bleach. **B.** Kinetics associated with the recovery of the chromophore modes at 1547 cm^{-1} (complete recovery) and 1703 cm^{-1} (partial recovery (Figure 4.10B)) and the growth of the 1688 cm^{-1} transient. The slower dynamics associated with the chromophore recovery and growth of the light adapted state compared to the protein modes in **A.** is apparent. The relevant optical density axes are indicated by the symbol color.

4.3.4.3. TRMPS of a Photoinactive Mutant

The comparison between the relaxation times associated with the protein and recovery times of the FAD chromophore modes (Figure 4.12, Table 4.3) is informative. The recovery of the ground state population of FAD (exemplified by the complete recovery at 1547 cm^{-1}) occurs with a characteristic time of 5.4 μs, slower than either of the times associated with protein mode

dynamics (Table 4.3). It is possible that the FAD recovery reflects an additional slow channel, independent of the light activated protein structure change, for example due to the decay of a triplet state populated through intersystem crossing from the singlet excited state. To test this, we studied the photoinactive Q63E mutant of $AppA_{BLUF}$. The subnanosecond TRIR difference spectrum, whose subnanosecond time components have already been reported at 1547 cm^{-1} (47 ± 6 ps, 252 ± 30 ps [21]), reveals perturbation of the protein structure occurring instantaneously (Figure 4.13A). This result was highlighted by the blue shifted carbonyl mode at 1725 cm^{-1} that is formed within the instrument response (<100 fs) and indicates instantaneous response of the protein matrix to photoexcitation [21]. However, for this photoinactive mutant the dominant part of the relaxation after 10 ns occurs on a sub-microsecond time scale for both the chromophore and the perturbed protein. Note that in this Q63E mutant the protein modes seen in AppA at 1622 cm^{-1} and 1632 cm^{-1} and the flavin modes at 1688 cm^{-1} and 1700 cm^{-1} do not develop (Figure 4.13B). In addition, no 1440 cm^{-1} transient was observed which indicates that no triplet state is being formed in the inactive Q63E. The recovery of the flavin ground state (Figure 4.13C) was markedly faster in Q63E (750 ± 150 ns) than in $AppA_{BLUF}$ (5.4 ± 0.5 μs), so this result cannot rule out a contribution from the triplet state in $AppA_{BLUF}$.

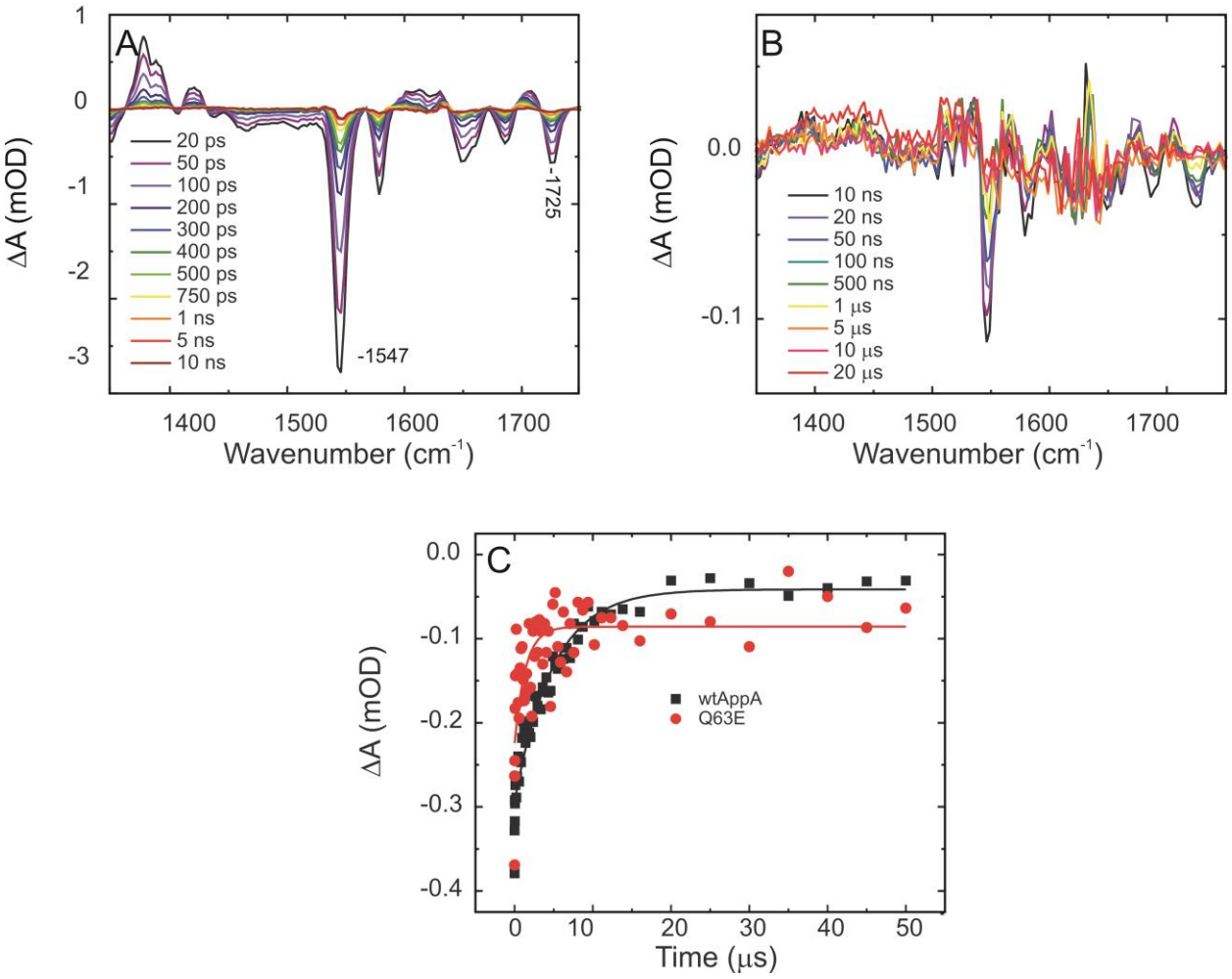

Figure 4.13. TRMPS spectra for the photoinactive mutant, Q63E. A. Time resolved IR difference spectra for Q63E $AppA_{BLUF}$ recorded between 20 ps and 10 ns after excitation of FAD at 450 nm. **B.** Relaxation in the Q63E $AppA_{BLUF}$ spectrum between 10 ns and 10 μs after excitation taken at 1547 cm^{-1}. **C**. Transient kinetics on the microsecond timescale for wt$AppA_{BLUF}$ and Q63E.

Evidently, the microsecond kinetics associated with ground state recovery of FAD in d$AppA_{BLUF}$ (Figure 4.10B) reflects slow dynamics of the photoactive protein in the vicinity of the chromophore. Since FAD is in its ground electronic state, these changes must be occurring in the H-bonding environment of the flavin. The observation of faster dynamics associated with changes in the protein β-sheet than with modes of the chromophore (Figure 4.10, Table 4.3)

suggests there is not a simple relation between the timescale of the proteins response to electronic excitation and distance from the chromophore.

4.3.4.4. TRMPS of W104A and M106A

To further characterize the mechanism of light state formation in $AppA_{BLUF}$ the microsecond dynamics were measured for two photoactive mutants which both show the red-shift in FAD absorption between dark and light adapted states: W104A and M106A. W104 and M106 are located on β5 strand (Figure 4.1), which is proposed to change conformation upon light activation [19, 34]. Compared to the wild type protein, the W104A mutant is known to dramatically increase rate of dark state recovery (80 fold) while the M106A exhibits only 1.5 fold faster rate [23, 34]. In addition, the W104A mutation significantly reduces the primary protein difference mode (1620/1631 cm^{-1}) observed in the FTIR light minus dark steady state difference spectrum (Figure 4.6) [24], leading to a model in where motion of W104 is essential for modulating the signal produced as a result of photoexcitation. M106 is also conserved in BLUF proteins, however, mutations to M106 have only a minimal effect on the rate of dark state recovery (23 min versus 30 min for wild-type), and do not impact steady state difference FTIR spectra or the picosecond time-resolved IR spectra. Thus, we chose M106A $AppA_{BLUF}$ as a useful control for the W104A variant.

There are distinct differences between the TRMPS data for W104A and $dAppA_{BLUF}$ between 2 ps to 10 ns (Figure 4.14). The most significant finding is that while the flavin ground state recovers (1547 cm^{-1}) , a red-shifted C4=O transient species (1688 cm^{-1}) along with a bleach at 1700 cm^{-1} develop simultaneously on the ns timescale (Figure 5.14C). The 1688 cm^{-1} mode is assigned to a rearrangement in H-bonding between the protein and the isoalloxazine ring [24]

and only appears on the microsecond timescale in dAppA$_{BLUF}$ (Figure 4.10A); evidently this rearrangement has very different dynamics in W104A. A second striking difference is in the kinetics associated with the protein mode at 1620 cm^{-1}/1630cm^{-1} on the nanosecond to millisecond time scale (Figure 4.13B). In W104A, the positive feature (1631 cm^{-1}) appears immediately and shows no further evolution, while the negative feature (1620 cm^{-1}) does grow over time but is much weaker than in dAppA$_{BLUF}$.

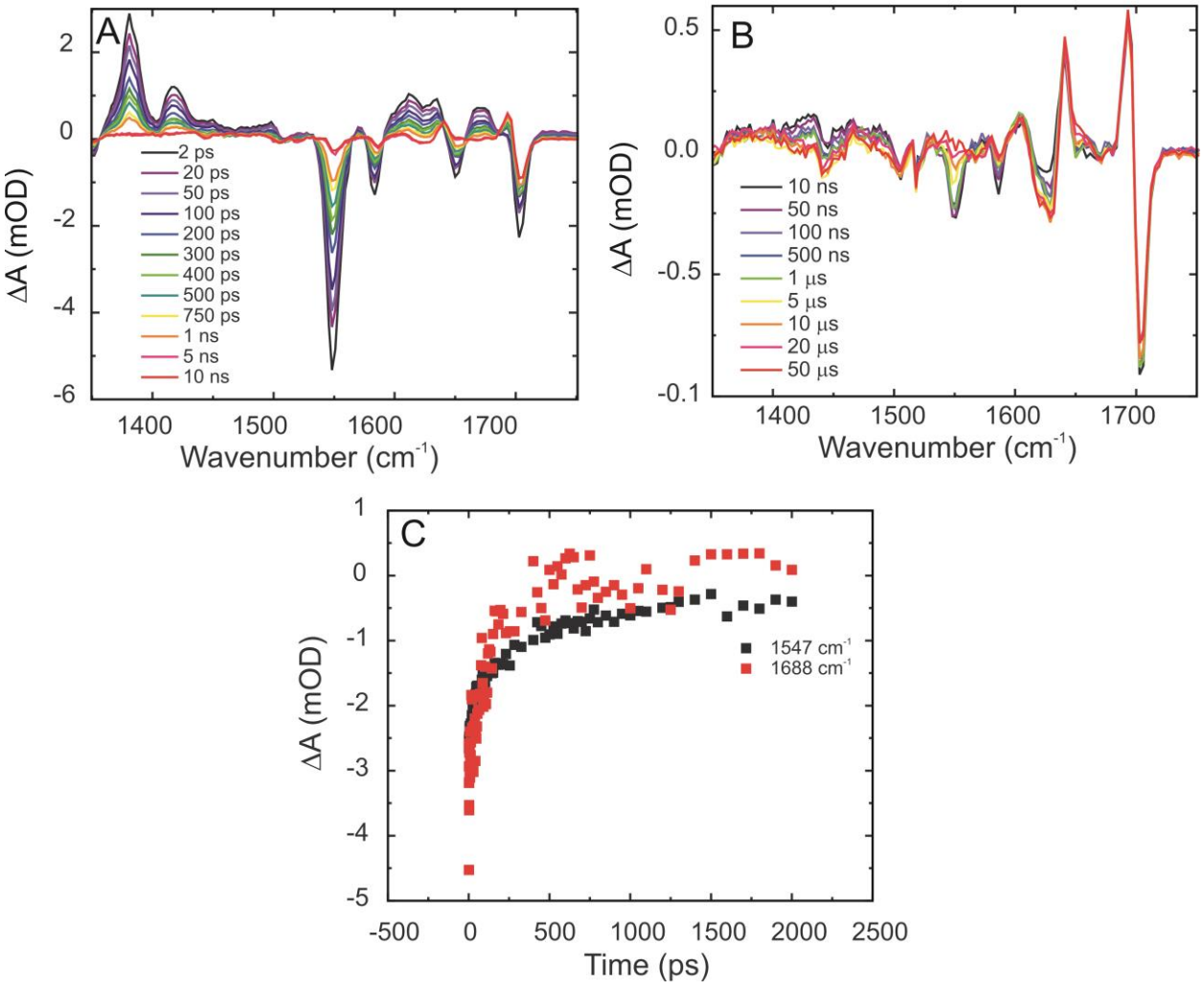

Figure 4.14. Transient IR spectra for W104A. A. Femtosecond to nanosecond TRIR of W104A. **B.** Microsecond dynamics of W104A. **C.** Comparison of the kinetics at 1547 cm^{-1} (black) and 1688 cm^{-1} (red), indicating that they are both occurring on a similar timescale.

This is further illustrated by the comparison for the transient spectra for W104A, M106A and $dAppA_{BLUF}$ at 10 ns and 20 μs (Figures 4.15). In Figure 4.15A, the prompt (sub-nanosecond) appearance of the 1688 and 1631 cm^{-1} features is apparent, while Figure 4.14B shows that there is little development of the transient bleach (1620 cm^{-1}) in W104A, while $dAppA_{BLUF}$ and M106A are very similar, and in particular both show the development of the 1688 cm^{-1} transient and the protein modes occur on the microsecond timescale (Table 4.3, Figure 4.16). Further investigation of the kinetics associated with each mode (Figure 4.16) confirms the lack of development beyond 10 ns for most modes in W104A and shows that the 1620 cm^{-1} bleach mode develops more rapidly than in M106A and wtAppA, which are in every respect similar.

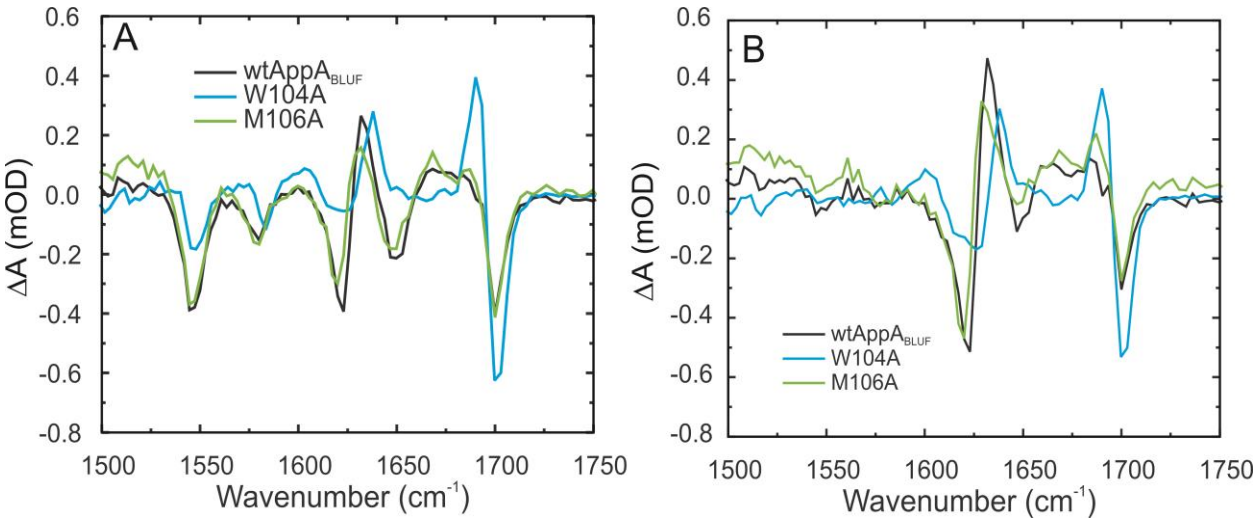

Figure 4.15 Transient IR spectra for $dAppA_{BLUF}$ and two mutants. Comparison of TRIR spectra of $AppA_{BLUF}$ (black), W104A (blue) and M106A (green) at 10 ns (**A**) and 20 μs (**B**).

Table 4.3. Kinetic analysis of TRMPS measurements for $AppA_{BLUF}$, W104A and M106A.

Peak	$AppA_{BLUF}$	W104A	M106A
1547 cm^{-1}	5.4 ± 0.5 µs	5.2 ± 0.6 µs	4.5 ± 0.5 µs
1622 cm^{-1}	2.1 ± 0.3 µs	2.6 ± 0.6 µs	2.2 ± 0.4 µs
1631 cm^{-1}	1.5 ± 0.3 µs	N.D.	1.2 ± 0.4 µs
1688 cm^{-1}	5.6 ± 0.8 µs	N.D.	6.3 ± 1.1 µs
1700 cm^{-1}	5.3 ± 0.7 µs	N.D.	5.8 ± 0.8 µs

N.D. = Not Determined

These data confirm that W104 is a key residue in communicating the electronic excitation of flavin to the protein backbone [24]. It was established in steady state IR difference measurements that mutations in W104 suppress the appearance of protein modes [24]. The present data show this is a mechanistic change rather than a kinetic one, i.e. for W104A a substantial photoinduced change in protein structure never occurs rather than occurs and rapidly relaxes. It is significant that W104A forms the red shifted flavin carbonyl associated with the signaling state (Figure 4.15), and this mode forms on the nanosecond time scale (Figure 4.15A, 4.16). Here it is proposed that in W104A, the structural evolution revealed in the microsecond TRIR of $dAppA_{BLUF}$ is 'short circuited,' meaning there is a light induced change in the local H-bonding environment of the FAD chromophore, which leads to the nanosecond spectral shift in the C4=O mode, but allosteric structural changes observed in $wtAppA_{BLUF}$, and critical for protein function, do not develop. Instead, the ground state structure recovers on a time scale slightly longer than $AppA_{BLUF}$ (Table 4.3). Such a short range change in structure is consistent with the 80 fold increase in the rate of dark state recovery in W104A, compared to $dAppA_{BLUF}$ and with biochemical measurements of AppA antirepressor activity, which showed much lower activity for W104A than for $dAppA_{BLUF}$ [23]. Evidently, a spectral shift alone is not sufficient to indicate a photoactive state of the BLUF domain.

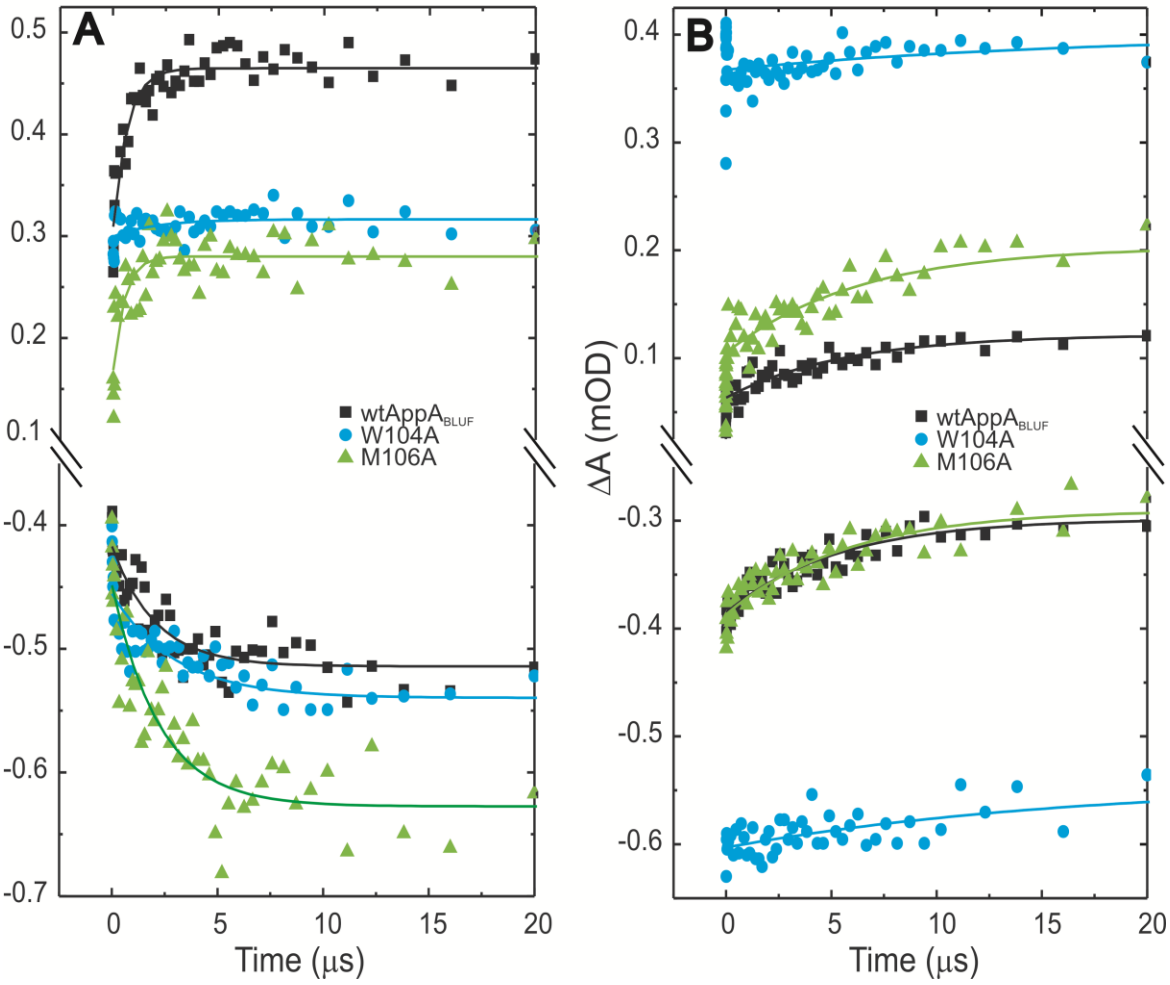

Figure 4.16. Transient kinetics associated with protein and C4=O modes. A. Transient dynamics in the protein modes at 1622 (bottom) and 1631 cm^{-1} (top) showing the similarity of timescales for $dAppA_{BLUF}$ and M106A and the distinct kinetics for W104A. **B.** Transient dynamics at mode associated with reorganization about the C4=O carbonyl chromophore modes 1688 cm^{-1} (top) and 1703 cm^{-1} (bottom) for the $dAppA_{BLUF}$ and the two mutants.

4.5. Conclusions

To further investigate the biological roles of key amino acids on the β5 strand in $AppA_{BLUF}$, infrared measurements beyond 2 ns had to be performed. TRMPS has revealed the timescale and pathway of structural dynamics in a BLUF domain. Structural dynamics were probed on the 100 fs to 1 ms time scale. Following electronic excitation, the primary events are

associated with relaxation of the flavin excited electronic state which occurs on a sub-nanosecond timescale. These events mainly result in recovery of the initial ground state, with a minor fraction of excited states leading to perturbation of the local structure of the protein and possibly some triplet state formation. The secondary steps involve protein structural dynamics which convert these local perturbations into the changes eventually form the signaling state, releasing the repressor molecule. The time scale for these protein structural dynamics is 1-5 μs. The fastest steps communicate optical excitation to the protein via the W104 residue in 1-2 μs, and more than one residue is involved, such that different protein modes present different response times. There are also slower dynamics that reflect relaxation in the vicinity of the chromophore, showing that the rate of structural change is not simply related to distance from the chromophore. In the W104A mutant, communication to the protein is suppressed, but fast H-bond rearrangements occur around the chromophore, suggesting changes in the chromophore spectrum are not necessarily a good measure of photoactivity.

4.6. References

1. Agarwal, P.K., S.R. Billeter, P.T. Rajagopalan, S.J. Benkovic, and S. Hammes-Schiffer, *Network of coupled promoting motions in enzyme catalysis.* Proc Natl Acad Sci U.S.A., 2002. **99**(5): p. 2794-9.
2. Yang, H., G. Luo, P. Karnchanaphanurach, T.M. Louie, I. Rech, S. Cova, L. Xun, and X.S. Xie, *Protein conformational dynamics probed by single-molecule electron transfer*. Science, 2003. **302**(5643): p. 262-6.
3. Lange, O.F., N.A. Lakomek, C. Fares, G.F. Schroder, K.F. Walter, S. Becker, J. Meiler, H. Grubmuller, C. Griesinger, and B.L. de Groot, *Recognition dynamics up to*

microseconds revealed from an RDC-derived ubiquitin ensemble in solution. Science, 2008. **320**(5882): p. 1471-5.

4. Mulder, F.A.A., N.R. Skrynnikov, B. Hon, F.W. Dahlquist, and L.E. Kay, *Measurement of slow (μs−ms) time scale dynamics in protein side chains by 15N relaxation dispersion NMR spectroscopy: Application to Asn and Gln residues in a cavity mutant of T4 lysozyme.* J Am Chem Soc, 2001. **123**(5): p. 967-975.
5. Boehr, D.D., H.J. Dyson, and P.E. Wright, *An NMR perspective on enzyme dynamics.* Chem Rev, 2006. **106**(8): p. 3055-3079.
6. Henzler-Wildman, K.A., M. Lei, V. Thai, S.J. Kerns, M. Karplus, and D. Kern, *A hierarchy of timescales in protein dynamics is linked to enzyme catalysis.* Nature, 2007. **450**(7171): p. 913-916.
7. Cho, H.S., N. Dashdorj, F. Schotte, T. Graber, R. Henning, and P. Anfinrud, *Protein structural dynamics in solution unveiled via 100-ps time-resolved x-ray scattering.* Proc Natl Acad Sci U S A, 2010. **107**(16): p. 7281-6.
8. Ihee, H., S. Rajagopal, V. Srajer, R. Pahl, S. Anderson, M. Schmidt, F. Schotte, P.A. Anfinrud, M. Wulff, and K. Moffat, *Visualizing reaction pathways in photoactive yellow protein from nanoseconds to seconds.* Proc Natl Acad Sci U S A, 2005. **102**(20): p. 7145-50.
9. Schotte, F., H.S. Cho, V.R. Kaila, H. Kamikubo, N. Dashdorj, E.R. Henry, T.J. Graber, R. Henning, M. Wulff, G. Hummer, M. Kataoka, and P.A. Anfinrud, *Watching a signaling protein function in real time via 100-ps time-resolved Laue crystallography.* Proc Natl Acad Sci U S A, 2012. **109**(47): p. 19256-61.

10. Ihee, H., M. Lorenc, T.K. Kim, Q.Y. Kong, M. Cammarata, J.H. Lee, S. Bratos, and M. Wulff, *Ultrafast x-ray diffraction of transient molecular structures in solution.* Science, 2005. **309**(5738): p. 1223-7.

11. Kim, K.H., S. Muniyappan, K.Y. Oang, J.G. Kim, S. Nozawa, T. Sato, S.Y. Koshihara, R. Henning, I. Kosheleva, H. Ki, Y. Kim, T.W. Kim, J. Kim, S. Adachi, and H. Ihee, *Direct observation of cooperative protein structural dynamics of homodimeric hemoglobin from 100 ps to 10 ms with pump-probe X-ray solution scattering.* J Am Chem Soc, 2012. **134**(16): p. 7001-8.

12. Kim, T.W., J.H. Lee, J. Choi, K.H. Kim, L.J. van Wilderen, L. Guerin, Y. Kim, Y.O. Jung, C. Yang, J. Kim, M. Wulff, J.J. van Thor, and H. Ihee, *Protein structural dynamics of photoactive yellow protein in solution revealed by pump-probe X-ray solution scattering.* J Am Chem Soc, 2012. **134**(6): p. 3145-53.

13. Ramachandran, P.L., J.E. Lovett, P.J. Carl, M. Cammarata, J.H. Lee, Y.O. Jung, H. Ihee, C.R. Timmel, and J.J. van Thor, *The short-lived signaling state of the photoactive yellow protein photoreceptor revealed by combined structural probes.* J Am Chem Soc, 2011. **133**(24): p. 9395-404.

14. Jung, Y.O., J.H. Lee, J. Kim, M. Schmidt, K. Moffat, V. Srajer, and H. Ihee, *Volume-conserving trans-cis isomerization pathways in photoactive yellow protein visualized by picosecond X-ray crystallography.* Nat Chem, 2013. **5**(3): p. 212-20.

15. Masuda, S. and C.E. Bauer, *AppA Is a blue light photoreceptor that antirepresses photosynthesis gene expression in Rhodobacter sphaeroides.* Cell, 2002. **110**(5): p. 613-623.

16. Laan, W., M. Gauden, S. Yeremenko, R. van Grondelle, J.T.M. Kennis, and K.J. Hellingwerf, *On the mechanism of activation of the BLUF domain of AppA.* Biochemistry, 2006. **45**(1): p. 51-60.

17. Jung, A., J. Reinstein, T. Domratcheva, R.L. Shoeman, and I. Schlichting, *Crystal structures of the AppA BLUF domain photoreceptor provide insights into blue light-mediated signal transduction.* J Mol Biol, 2006. **362**(4): p. 717-732.

18. Anderson, S., V. Dragnea, S. Masuda, J. Ybe, K. Moffat, and C. Bauer, *Structure of a novel photoreceptor, the BLUF domain of AppA from Rhodobacter sphaeroides.* Biochemistry, 2005. **44**(22): p. 7998-8005.

19. Grinstead, J.S., S.-T.D. Hsu, W. Laan, A.M.J.J. Bonvin, K.J. Hellingwerf, R. Boelens, and R. Kaptein, *The solution structure of the AppA BLUF domain: Insight into the mechanism of light-induced signaling.* ChemBioChem, 2006. **7**(1): p. 187-193.

20. Stelling, A.L., K.L. Ronayne, J. Nappa, P.J. Tonge, and S.R. Meech, *Ultrafast structural dynamics in BLUF domains: Transient infrared spectroscopy of AppA and its mutants.* J Am Chem Soc, 2007. **129**(50): p. 15556-15564.

21. Lukacs, A., A. Haigney, R. Brust, R.K. Zhao, A.L. Stelling, I.P. Clark, M. Towrie, G.M. Greetham, S.R. Meech, and P.J. Tonge, *Photoexcitation of the blue light using FAD photoreceptor AppA results in ultrafast changes to the protein matrix.* J Am Chem Soc, 2011. **133**(42): p. 16893-900.

22. Masuda, S., K. Hasegawa, A. Ishii, and T.-a. Ono, *Light-induced structural changes in a putative blue-light receptor with a novel FAD binding fold sensor of blue-light using FAD (BLUF); Slr1694 of Synechocystis sp. PCC6803.* Biochemistry, 2004. **43**(18): p. 5304-5313.

23. Masuda, S., Y. Tomida, H. Ohta, and K.-i. Takamiya, *The critical role of a H-bond between Gln63 and Trp104 in the blue-light sensing BLUF domain that controls AppA activity.* J Mol Biol, 2007. **368**(5): p. 1223-1230.

24. Masuda, S., K. Hasegawa, and T.-a. Ono, *Tryptophan at position 104 is involved in transforming light signal into changes of β-sheet structure for the signaling state in the BLUF domain of AppA.* Plant Cell Physiol, 2005. **46**(12): p. 1894-1901.

25. Unno, M., S. Kikuchi, and S. Masuda, *Structural refinement of a key tryptophan residue in the BLUF photoreceptor AppA by ultraviolet resonance Raman spectroscopy.* Biophys J, 2010. **98**(9): p. 1949-1956.

26. Toh, K.C., I.H.M. van Stokkum, J. Hendriks, M.T.A. Alexandre, J.C. Arents, M.A. Perez, R. van Grondelle, K.J. Hellingwerf, and J.T.M. Kennis, *On the signaling mechanism and the absence of photoreversibility in the AppA BLUF domain.* Biophys J, 2008. **95**(1): p. 312-321.

27. Pandey, R., D. Flockerzi, Marcus J.B. Hauser, and R. Straube, *Modeling the light- and redox-dependent interaction of PpsR/AppA in Rhodobacter sphaeroides.* Biophys J, 2011. **100**(10): p. 2347-2355.

28. Greetham, G.M., P. Burgos, Q.A. Cao, I.P. Clark, P.S. Codd, R.C. Farrow, M.W. George, M. Kogimtzis, P. Matousek, A.W. Parker, M.R. Pollard, D.A. Robinson, Z.J. Xin, and M. Towrie, *ULTRA: A unique instrument for time-resolved spectroscopy.* Appl Spectrosc, 2011. **64**(12): p. 1311-1319.

29. Greetham, G.M., D. Sole, I.P. Clark, A.W. Parker, M.R. Pollard, and M. Towrie, *Time-resolved multiple probe spectroscopy.* Rev Sci Instrum, 2012. **83**(10): p. 103107-5.

30. Greetham, G.M., P. Burgos, Q. Cao, I.P. Clark, P.S. Codd, R.C. Farrow, M.W. George, M. Kogimtzis, P. Matousek, A.W. Parker, M.R. Pollard, D.A. Robinson, Z.-J. Xin, and M. Towrie, *ULTRA: A unique instrument for time-resolved spectroscopy.* Appl Spectrosc, 2009. **64**(12): p. 1311-1319.

31. Laan, W., M.A. van der Horst, I.H. Van Stokkum, and K.J. Hellingwerf, *Initial Characterization of the Primary Photochemistry of AppA, a Blue-light–using Flavin Adenine Dinucleotide–domain Containing Transcriptional Antirepressor Protein from Rhodobacter sphaeroides: A Key Role for Reversible Intramolecular Proton Transfer from the Flavin Adenine Dinucleotide Chromophore to a Conserved Tyrosine?* Photochem. Photobiol., 2003. **78**(3): p. 290-297.

32. Yuan, H., S. Anderson, S. Masuda, V. Dragnea, K. Moffat, and C. Bauer, *Crystal structures of the Synechocystis photoreceptor Slr1694 reveal distinct structural states related to signaling.* Biochemistry, 2006. **45**(42): p. 12687-12694.

33. Haigney, A., A. Lukacs, R.-K. Zhao, A.L. Stelling, R. Brust, R.-R. Kim, M. Kondo, I. Clark, M. Towrie, G.M. Greetham, B. Illarionov, A. Bacher, W. Romisch-Margl, M. Fischer, S.R. Meech, and P.J. Tonge, *Ultrafast infrared spectroscopy of an isotope-labeled photoactivatable flavoprotein.* Biochemistry, 2011. **50**(8): p. 1321-1328.

34. Dragnea, V., A.I. Arunkumar, H. Yuan, D.P. Giedroc, and C.E. Bauer, *Spectroscopic studies of the AppA BLUF domain from Rhodobacter sphaeroides: Addressing movement of tryptophan 104 in the signaling state.* Biochemistry, 2009. **48**(42): p. 9969-9979.

35. Unno, M., R. Sano, S. Masuda, T.-a. Ono, and S. Yamauchi, *Light-Induced Structural Changes in the Active Site of the BLUF Domain in AppA by Raman Spectroscopy.* The Journal of Physical Chemistry B, 2005. **109**(25): p. 12620-12626.

36. Masuda, S., K. Hasegawa, and T.-a. Ono, *Light-induced structural changes of apoprotein and chromophore in the sensor of blue light using FAD (BLUF) domain of AppA for a signaling state* Biochemistry, 2005. **44**(4): p. 1215-1224.

37. Masuda, S., *Light detection and signal transduction in the BLUF photoreceptors.* Plant Cell Physiol, 2013. **54**(2): p. 171-179.

38. Kammler, L. and M. van Gastel, *Electronic structure of the lowest triplet state of flavin mononucleotide.* J Phys Chem A, 2012. **116**(41): p. 10090-10098.

39. Losi, A., E. Polverini, B. Quest, and W. Gärtner, *First evidence for phototropin-related blue-light receptors in prokaryotes.* Biophys J, 2002. **82**(5): p. 2627-2634.

40. Alexandre, M.T.A., T. Domratcheva, C. Bonetti, L.J.G.W. van Wilderen, R. van Grondelle, M.-L. Groot, K.J. Hellingwerf, and J.T.M. Kennis, *Primary reactions of the LOV2 domain of phototropin studied with ultrafast mid-infrared spectroscopy and quantum chemistry.* Biophys J, 2009. **97**(1): p. 227-237.

41. Miura, R., *Versatility and specificity in flavoenzymes: Control mechanisms of flavin reactivity.* Chem Rec, 2001. **1**(3): p. 183-194.

42. Kondo, M., J. Nappa, K.L. Ronayne, A.L. Stelling, P.J. Tonge, and S.R. Meech, *Ultrafast vibrational spectroscopy of the flavin chromophore.* J Phys Chem B, 2006. **110**(41): p. 20107-20110.

43. Haigney, A., A. Lukacs, R. Brust, R.-K. Zhao, M. Towrie, G.M. Greetham, I. Clark, B. Illarionov, A. Bacher, R.-R. Kim, M. Fischer, S.R. Meech, and P.J. Tonge, *Vibrational assignment of the ultrafast infrared spectrum of the photoactivatable flavoprotein AppA.* J Phys Chem B, 2012. **116**(35): p. 10722-10729.

44. Alexandre, M.T.A., L.J.G. van Wilderen, R. van Grondelle, K.J. Hellingwerf, M.L. Groot, and J.T.M. Kennis, *Early steps in blue light reception by plants: an ultrafast mid-infrared spectroscopic study of the LOV2 domain of phototropin.* Biophys J, 2005. **88**(1): p. 509a-509a.

45. Gauden, M., J.S. Grinstead, W. Laan, I.H. van Stokkum, M. Avila-Perez, K.C. Toh, R. Boelens, R. Kaptein, R. van Grondelle, K.J. Hellingwerf, and J.T. Kennis, *On the role of aromatic side chains in the photoactivation of BLUF domains.* Biochemistry, 2007. **46**(25): p. 7405-15.

46. Laan, W., M. Gauden, S. Yeremenko, R. van Grondelle, J.T.M. Kennis, and K.J. Hellingwerf, *On the mechanism of activation of the BLUF domain of AppA.* Biochemistry, 2005. **45**(1): p. 51-60.

47. Mathes, T., I.H. van Stokkum, C. Bonetti, P. Hegemann, and J.T. Kennis, *The hydrogen-bond switch reaction of the Blrb Bluf domain of Rhodobacter sphaeroides.* J Phys Chem B, 2011. **115**(24): p. 7963-71.

48. Bonetti, C., M. Stierl, T. Mathes, I.H.M. van Stokkum, K.M. Mullen, T.A. Cohen-Stuart, R. van Grondelle, P. Hegemann, and J.T.M. Kennis, *The role of key amino acids in the photoactivation pathway of the Synechocystis Slr1694 BLUF domain.* Biochemistry, 2009. **48**(48): p. 11458-11469.

49. Domratcheva, T., B.L. Grigorenko, I. Schlichting, and A.V. Nemukhin, *Molecular models predict light-induced glutamine tautomerization in BLUF photoreceptors.* Biophys J, 2008. **94**(10): p. 3872-3879.

50. Nunthaboot, N., F. Tanaka, and S. Kokpol, *Analysis of photoinduced electron transfer in AppA.* J Photoch Photobio A, 2009. **207**(2-3): p. 274-281.

51. Nunthaboot, N., F. Tanaka, and S. Kokpol, *Simultaneous analysis of photoinduced electron transfer in wild type and mutated AppAs.* J Photoch Photobio A, 2010. **209**(1): p. 79-87.

52. Gauden, M., S. Yeremenko, W. Laan, I.H. van Stokkum, J.A. Ihalainen, R. van Grondelle, K.J. Hellingwerf, and J.T. Kennis, *Photocycle of the flavin-binding photoreceptor AppA, a bacterial transcriptional antirepressor of photosynthesis genes.* Biochemistry, 2005. **44**(10): p. 3653-62.

53. Lin, Y.S., J.M. Shorb, P. Mukherjee, M.T. Zanni, and J.L. Skinner, *Empirical amide I vibrational frequency map: Application to 2D-IR line ahapes for isotope-edited membrane peptide bundles.* J Phys Chem B, 2008. **113**(3): p. 592-602.

54. Strasfeld, D.B., Y.L. Ling, R. Gupta, D.P. Raleigh, and M.T. Zanni, *Strategies for extracting structural information from 2D IR spectroscopy of amyloid: Application to islet amyloid polypeptide.* J Phys Chem B, 2009. **113**(47): p. 15679-15691.

55. Wu, Q., W.H. Ko, and K.H. Gardner, *Structural requirements for key residues and auxiliary portions of a BLUF domain.* Biochemistry, 2008. **47**(39): p. 10271-80.

56. Osvath, S., L. Herenyi, P. Zavodszky, J. Fidy, and G. Kohler, *Hierarchic finite level energy landscape model: to describe the refolding kinetics of phosphoglycerate kinase.* J Biol Chem, 2006. **281**(34): p. 24375-80.

Chapter 5

Structural Dynamics of the Full Length Protein, $AppA_{FULL}$

5.1. Introduction

It is necessary to characterize the mechanism of photoactivation in BLUF protein to unlock their full potential as optogenetic sensors [1]. BLUF proteins are of particular interest as optogenetic tools as a result of the two state, reversible photocycle observed in these systems [2]. AppA, from *Rhodobacter sphaeroides*, is the most commonly studied BLUF protein [2-11], and an ideal candidate for optogenetics [12]. As a multifunctional protein, AppA has evolved to sense two different stimuli (light and O_2), which result inhibition of photosynthetic gene transcription [2]. Photoexcitation of the flavin in low oxygen environments triggers a response of the N-terminal domain that must be transferred to the C-terminal domain in a process that is still poorly understood, and as such there is growing interest to fully characterize this process.

Structural data for the N-terminal domain of AppA revealed an intricate H-bonding network. Surrounding the flavin are key residues such as essential residues Y21 and Q63 [3, 8]. Residues W104 and M106 are found in the β5 strand of the protein and have been shown to adopt different conformations in the two crystal structures solved for N-terminal AppA [3, 8]. Chapter 4 highlighted the importance of W104. The W104A mutation results in a protein that is "short-circuited," suppressing the changes which occur further away from the chromophore while accelerating dynamics close to it.

To date, experiments on the full length protein involve looking at binding of PpsR and AppA [13-16]. PpsR exists as a stable tetramer in solution [2]. Under aerobic conditions ($[O_2]$ = 200 μM) dissolved oxygen concentration), it binds cooperatively to a target promoters of

photosynthetic genes via formation of an intermolecular disulfide bond [2, 17- 19]. At low O_2 concentration (< 3 μM), the disulfide bond is reduced and DNA-binding affinity is lowered. Experiments have also shown that the reduction of PpsR is mediated by the oxygen- and AppA [20, 21]. Under semi-aerobic conditions, photosynthetic genes are repressed by blue light excitation [10, 22].

The C-terminal domain is responsible for oxygen sensing has been proposed to bind heme [23, 24]. Recently, a crystal structure was solved for an AppA construct, $AppA_{\Delta C}$ (1-378), which did not contain the cysteine rich domain, which was shown to not necessary for O_2 sensing [23]. Analysis of the primary sequence indicated the presence of a sensor containing heme in place of cobalamin (SCHIC) domain [23, 24], whose structure can be seen in Figure 5.1. PpsR has also been shown to sense and bind to heme [25], however no cofactor is present in the SCHIC domain, so the importance of heme in AppA is still poorly understood. The position of the side chain of W104, whose role in the photocycle has been established in chapter 4, is shown in the Trp_{out} conformation, in agreement with the crystal structure solved by Jung et al. [8]. The ability of the AppA/PpsR system to regulate gene expression levels in other systems was tested and showed that AppA/PpsR could not introduce blue light sensitivity in other bacterial systems [26]. This result could be attributed to the limited data set for $AppA_{FULL}$. To better elucidate the role of the C-terminal domain, we sought to characterize the full length protein using vibrational spectroscopy and compared the results with what was previously reported in chapters 2 and 4 for $AppA_{BLUF}$.

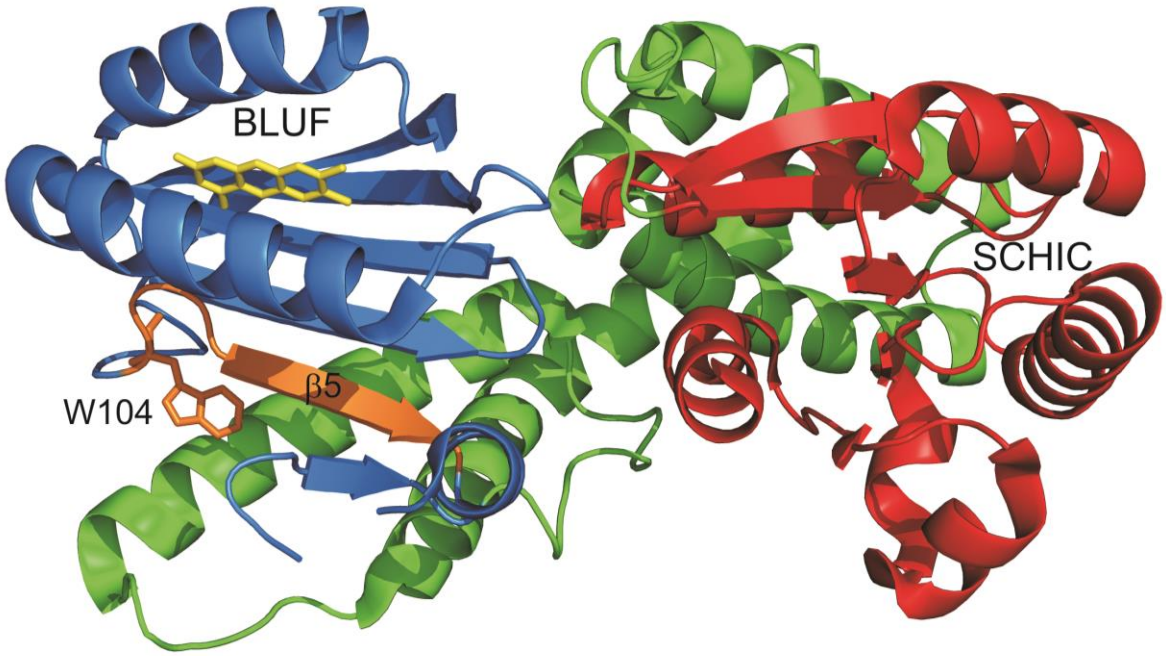

Figure 5.1. Crystal structure of AppA$_{\Delta C}$. X-ray crystal structure of AppA$_{\Delta C}$ (PDB 2HH1 [27]). The BLUF domain is shown in blue, with the isoalloxazine ring of the flavin in yellow. The β5 strand and W104 (in the Trp$_{out}$ conformation) are in orange. The SCHIC domain is shown in red. In green are linker α-helices that connect the two domains.

5.2. Experimental Methods

5.2.1. Cloning of AppA$_{FULL}$

The full length protein was cloned from genomic DNA (ATCC 17023) into pET-15b, encoding for an N-terminal His$_6$ tag. The forward and reverse primers used are shown in Table 5.1.

Table 5.1. Primer Design of AppA$_{FULL}$ cloning.

Primer	Primer Design
Forward Nde1	5'-TCGGAATTCCATATGCAACACGACCTCGAGGCGGACGTC-3'
Reverse Xho1	5'-CCGCTCGAGTCAGGCGCTGCGGCGGCGGTCCTGGCGCGA-3'.

5.2.2. Overexpression and Purification

Plasmids were expressed in BL21(DE3) *E. coli* cells and grown in 10 mL cultures containing LB media with 200 μg/mL ampicillin at 37°C at 250 rpm. Infection of 1 L LB/ampicillin media was performed using these cultures and grown to an OD600 of about 1 at 30°C for 5 hours. The temperature was decreased to 18°C for 30 min and protein expression was induced by adding 0.8 mM IPTG. Protein expression was performed overnight in the dark. Purification of wild type and the various mutants were performed in the dark. Cells were harvested at 5000 rpm at 4°C and stored at -20°C.

Cell pellets were resuspended in 40 mL of wash buffer (400 mM NaCl, 20 mM Tris, pH 8.0), to which 200 μL of 50 mM PMSF was added to inhibit endogenous protease activity. Cells were lysed by sonication and cell debris was removed by ultracentrifugation (33000 rpm for 90 min). The soluble portion was reconstituted with 10 mg of FAD for 45 min on ice. The protein was then purified by Ni-NTA (Novagen) affinity chromatography at 4°C using 20 mM Tris, 400 mM NaCl, pH 8.0 (wash buffer). The bound protein was then washed using the wash buffer and increasing amounts of imidazole and finally eluted with 250 mM imidazole. Size exclusion chromatography was then performed using G-25 resin (GE) in 20 mM Tris, 400 mM NaCl, pH 8.0. Protein purity and yield were determined using UV-Vis spectroscopy and SDS-PAGE.

5.2.3. Photoconversion Experiments

$AppA_{FULL}$ photoconversion experiments were recorded using a Cary 100 UV-Vis spectrometer (Varian) at 25°C. Irradiation of 460 nm high mount LED (Prizmatix) for 3 min was performed at protein concentrations of 50 μM to yield the light adapted state, $lAppA_{FULL}$.

5.2.4. FTIR Spectroscopy

Light minus dark FTIR spectra were obtained on a Vertex 80 FTIR spectrometer (Bruker). For these measurements, 80 µL of 2 mM protein sample was placed between two CaF_2 plates equipped with a 50 µm spacer where 64 scans were accumulated at a 1 cm^{-1} resolution. The light state was generated by 3 min irradiation using a 460 nm high mount LED (Prizmatix) inserted into the sample compartment.

5.2.5. TRIR Spectroscopy

TRIR experiments were performed at STFC Central Laser facility. The TRIR system has been described in greater detail elsewhere [28]. Using the system with a repetition rate of 10 kHz with a high signal to noise, resolution of about 100 fs could be achieved. Excitation pulses were set to 450 nm at 200 nJ with a spot size radius of 100 µm. For dark state measurements, samples were flowed at a rate of 1.5 mL/min to minimize photobleaching. For all measurements samples were performed using 50 µm path length transmission cell using CaF_2 windows and rastered to minimize sample degradation. The IR probe recorded transient difference spectra (pump on-pump off) at time delays between 1 ps and 2000 ps. Photoconversion was shown to be minimal by steady state absorption spectroscopy. The probe beam was measured by two carefully matched 128 pixel CCD detectors, yielding a resolution of 3 cm^{-1} per pixel. Spectra were calibrated relative to the IR transmission of a polystyrene standard. Light-adapted samples were prepared by irradiation at 380 nm high mount LED (Thorlabs). Photoconversion was monitored using UV-Vis absorption spectroscopy and was found to be complete within 3 min. The TRIR setup was operated and maintained by the CLF (Dr. Greg Greetham, Dr. Ian Clark, Dr. Mike Towrie).

5.2.6. TRMPS

The TRMPS method utilizes the impressive signal-to-noise and stable pulse to pulse timing of the ULTRA laser setup described in 5.2.5. [28]. A 1 kHz visible pump laser (450 nm) at 1 μJ is synchronized with the 65 MHz (15×10^{-9} s^{-1}) repetition rate of the titanium sapphire seed laser and is automatically locked to the 10 kHz pulses of the ULTRA amplifier. The delay between 100 ps and 15 ns is achieved by varying an optical stage delay. The times between 10 ns and 100 μs are controlled by using the oscillator seed pulses to add multiple of 15 ns to the pump laser delay. For times between 100 μs and 1 ms the 10 kHz pulses are synchronized with the 1 kHz pump laser, providing a data point every 0.1 ms. In this way the timing is extended but the detection apparatus is identical, allowing transient IR difference data to be recorded every 100 μs with high signal-to-noise. The TRMPS setup was operated and maintained by the CLF (Dr. Greg Greetham, Dr. Ian Clark, and Dr. Mike Towrie).

5.3. Results and Discussion

5.3.1. Photoconversion of $AppA_{FULL}$

Characterization of the photocycle of the full length protein was previously reported [14]. In Figure 6.3A, comparison of the preirradiated ($dAppA_{FULL}$) and post irradiated ($lAppA_{FULL}$) can be seen. A characteristic 10 nm red shift in the absorption of the flavin λ_{max} can be seen and is in good agreement with absorption data for $AppA_{BLUF}$ [2]. Previous work on $AppA_{BLUF}$ looked at the role of the length of the C-terminus: in the two commonly used constructs the length of the C-terminal tail is varied (1-126 and 17-133) [14]. Photorecovery τ of 15.8 min (1-126), 11.8 min (17-133) and 13.25 min ($AppA_{FULL}$) were reported for the various AppA constructs. Here, a τ of 13.0 ± 0.1 min is reported for the photorecovery of $AppA_{FULL}$ at 490 nm (Figure 6.2B), in good

agreement with previous results [14]. Differences in photorecovery were originally proposed to be the result of the position of the conserved tryptophan [14]. The AppA 1-126 construct's crystal structured exhibited the "Trp_{in}" conformation [3] while the 17-133 constructs' crystal structure showed the "Trp_{out}" [8], which suggested that the position of the W104 side chain was a consequence of the construct being used. This was disproven by ultraviolet resonance Raman spectroscopy, which could not differentiate between the two constructs, and concluded a "Trp_{in}" conformation as the dark state [29].

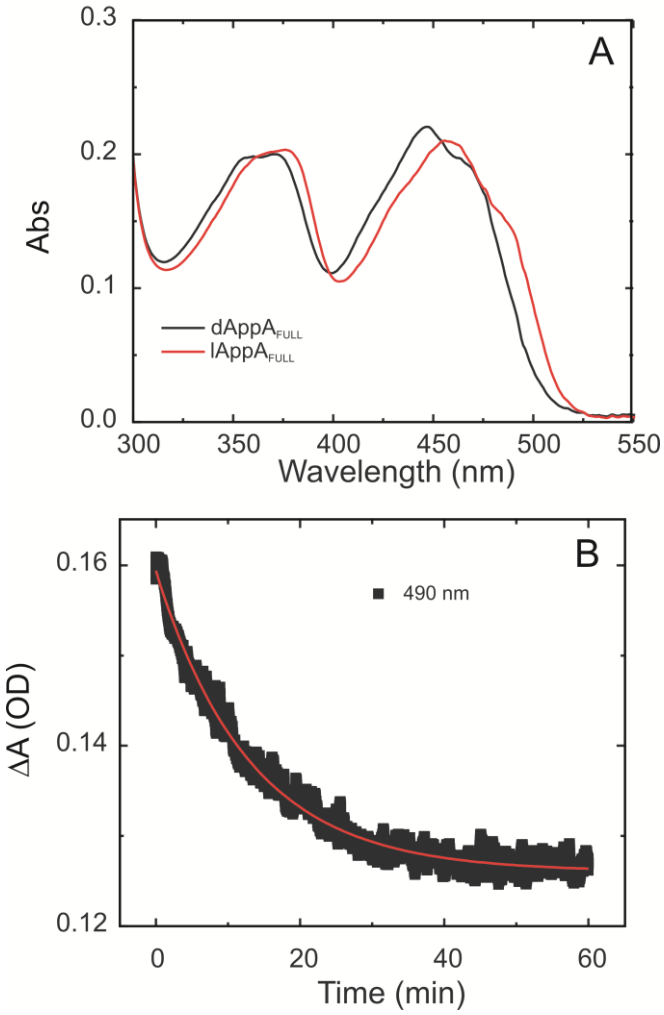

Figure 5.2. Photoconversion of AppA$_{FULL}$. A. Absorption spectra of pre-irradiated (dAppA$_{FULL}$) and post-irradiated (lAppA$_{FULL}$) reveal a characteristic 10 nm red shift upon photoexcitation. **B.** Photorecovery monitored at 490 nm. When fit to a monoexponential, a τ of 13.0 ± 0.1 min is calculated.

5.3.2. FTIR of $AppA_{FULL}$

FTIR spectroscopy has been an invaluable tool for understanding the mechanism of photoactivation in BLUF proteins. Here, we sought to characterize the structural differences between dark and light adapted full length AppA and compared with the results of the N-terminal BLUF domain alone. For $AppA_{BLUF}$ difference modes observed at 1622(-)/1632(+) cm^{-1} and 1688(+)/1700(-) cm^{-1} can be seen (Figure 5.3). The 1688(+)/1700(-) cm^{-1} mode was assigned to an increase in H-bonding from the protein to the C4=O of the flavin as a result of photoexcitation [4]. The difference mode observed at 1622(-)/1632(+) cm^{-1} is assigned to changes of the protein matrix, particularly the β5 strand [30]. These modes are not perturbed in $AppA_{FULL}$, along with no new vibrational modes. A decrease in the intensity of the positive feature at 1665 cm^{-1} is present, in a region of the spectrum where vibrations from α-helices would be observed [31, 32]. The crystal structure solved for $AppA_{\Delta C}$ indicates the presence of multiple α-helices between the N-terminal BLUF domain and the C-terminal SCHIC domain (Figure 5.1). Therefore it is plausible that differences in α-helical structures would be present in the full length protein. The absence of this feature suggests a perturbation is not occurring, presumably due to the additional protein matrix, indicating the addition of the C-terminal domain result in the loss of FTIR signatures, opposite to what was expected.

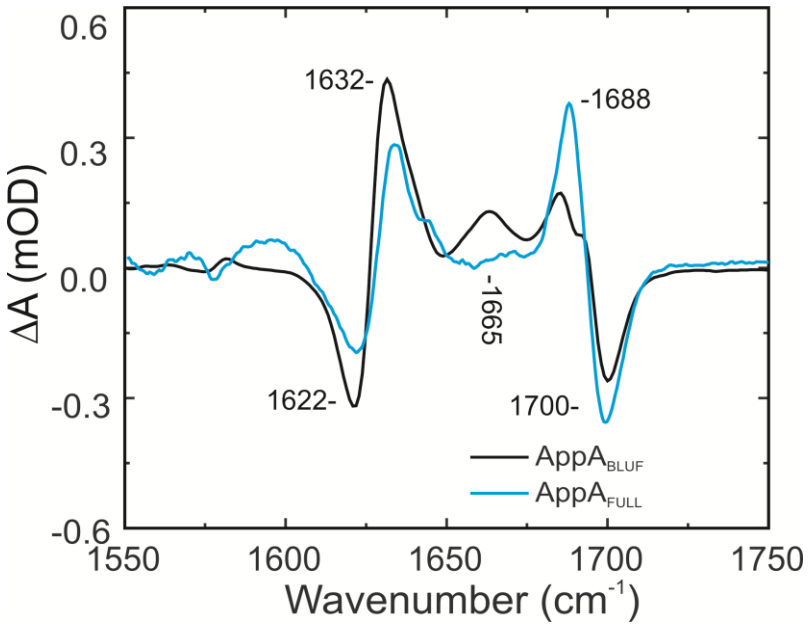

Figure 5.3. FTIR of AppA$_{FULL}$. FTIR light minus dark difference spectra of AppA$_{BLUF}$ (black) and AppA$_{FULL}$ (blue). Light adapted spectra were generated by irradiation of 460 nm light for 3 minutes. Pre-irradiated spectra were subtracted from post-irradiated spectra.

5.3.3. TRIR of AppA$_{FULL}$

Time resolved IR spectroscopy has provided a wealth of knowledge on the photocycle of the BLUF domain of AppA (Figure 5.4). To understand what role the C-terminal domain plays on light excitation TRIR measurements were performed on the full length protein. Extensive work has been performed to assign the vibrational modes present in the TRIR [33]. For the dark state of AppA, there are 4 prominent bleaches at 1547, 1582, 1652, and 1700 cm^{-1}, which were also present in the unbound flavin [34]. The 1547 and 1582 cm^{-1} modes are present in FAD and have been assigned using isotopic labeling to be C=N modes of the flavin in N-terminal AppA [28, 33]. The two high frequency bleaches are assigned to the C2=O carbonyl (1652 cm^{-1}) and C4=O carbonyl (1700 cm^{-1} in dAppA$_{FULL}$, 1688 cm^{-1} in lAppA$_{FULL}$) of the flavin chromophore. A broad transient at 1608 cm^{-1} is assigned to the ES of the flavin, although some contribution of the protein is also likely [11, 28, 33]. A transient at 1670 cm^{-1} is present in dAppA$_{FULL}$ that is

absent in the light adapted state and free flavin [35]; in chapter 2 this mode was tentatively assigned as arising from the amide sides of Q63 and N45. In the light state the most prominent changes are the loss of the 1670 cm^{-1} transient and a 10 cm^{-1} red shift of the high frequency carbonyl to 1688 cm^{-1}. These modes are identical to that observed in the truncated protein.

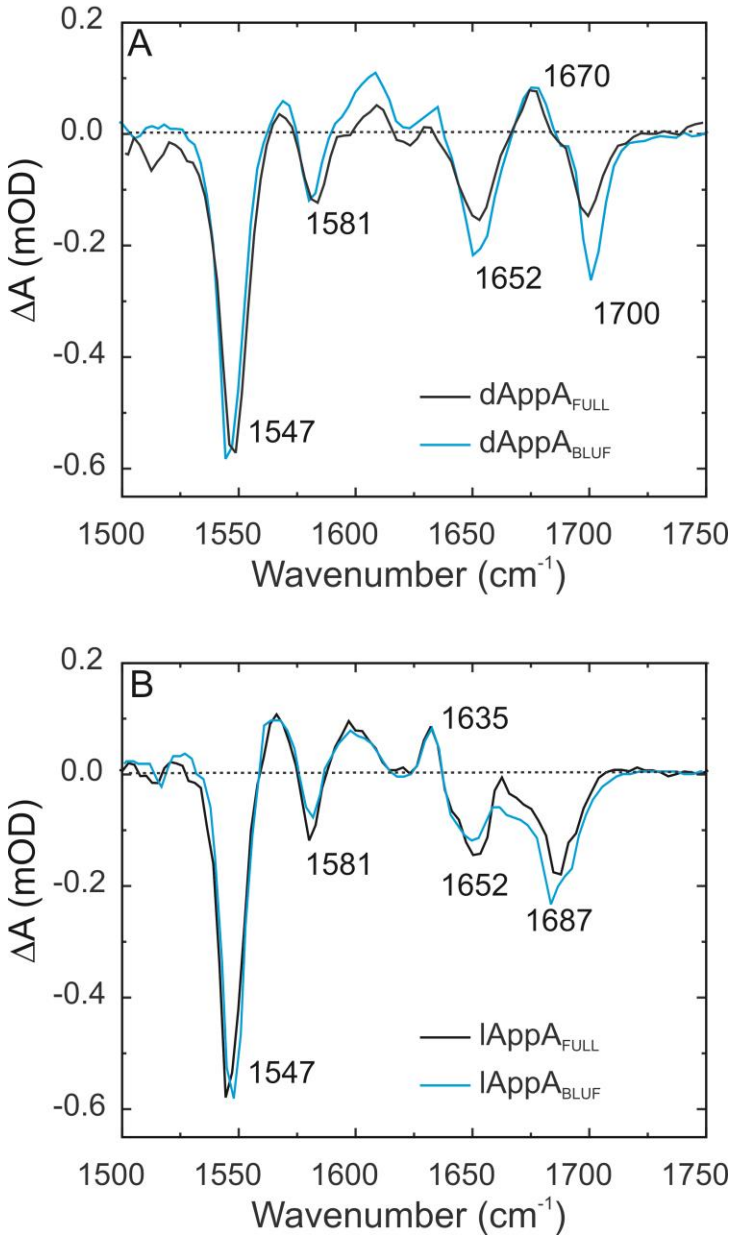

Figure 5.4. TRIR of AppA$_{FULL}$. TRIR spectra of AppA$_{FULL}$ (black) and AppA$_{BLUF}$ (blue) taken 3 ps post excitation. **A.** Spectra of dark states. **B.** Spectra of light states.

Transient absorption spectroscopy previously was used to propose a mechanism where involving electron transfer reaction between excited FAD and tyrosine 21 [5, 36-38]. The change in redox state of the flavin ultimately leads to rearrangement of the H-bonding network prior to recovery of oxidized flavin. Assignment of intermediates in the proposed ET and PT steps were based on analysis of the BLUF protein, PixD [39], and will be discussed in chapter 6. An alternative mechanism was proposed where excitation of FAD itself induced rearrangement of the H-bonding network. This assignment was based on the absence of spectral features consistent with flavin radical states in the sub-nanosecond TRIR spectra of $AppA_{BLUF}$ and the observed perturbation of the protein network on excitation and the quenching rate of FAD [11, 35]. In agreement with those results, no evidence of radical formation is observed in the dark spectra of $AppA_{FULL}$, further suggesting the absence of ET/PT steps in photoactivation of AppA. Vibrational modes consistent with flavin radicals were observed in the TRIR spectra of $lAppA_{BLUF}$ (Chapter 2), however in the photoactivated $lAppA_{FULL}$ spectra, no radicals are observed in the present data set. Further characterization of the full length protein is necessary to fully elucidate the mechanism of photoactivation.

Excited state kinetics were measured for the full length protein and compared to $AppA_{BLUF}$. Plotting the recovery of the bleach at 1547 cm^{-1}, one can see that the rates for full length and N-terminal AppA overlay quite well. Time components are reported in Table 5.2, which indicate that the lifetime of the ES is similar for N-terminal and full length AppA. These results would suggest that the C-terminal domain has little effect on the primary photophysics of the mechanism of light state formation.

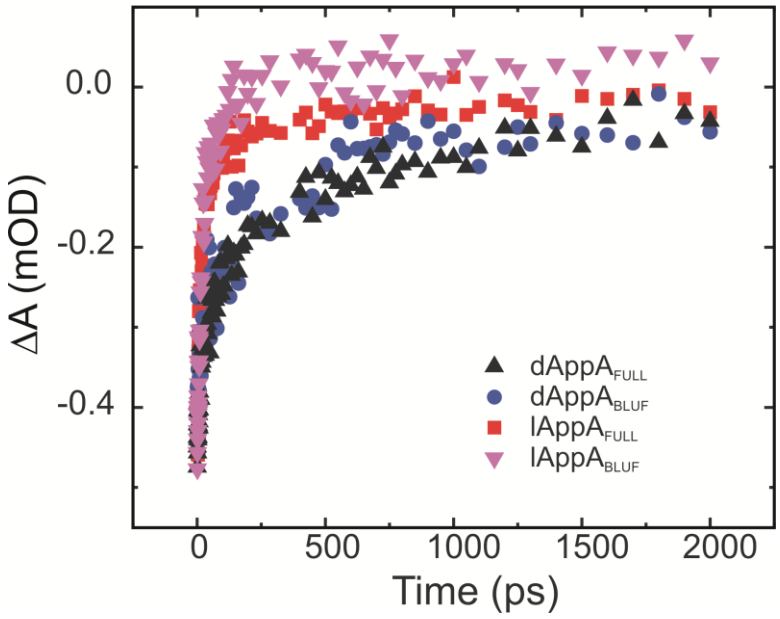

Figure 5.5. Kinetics of GS recovery of AppA$_{FULL}$. Recovery kinetics at 1547 cm^{-1} of dAppA$_{FULL}$ (black), dAppA$_{BLUF}$ (blue), lAppA$_{FULL}$ (red), and dAppA$_{BLUF}$ (magenta).

Table 5.2. Kinetics of ground state recovery of AppA$_{BLUF}$ and AppA$_{FULL}$.

Sample	α1	τ1	α2	τ2	<τ>
dAppA$_{BLUF}$	-0.51	34 ± 4 ps	-0.49	473 ± 73 ps	249 ps
lAppA$_{BLUF}$	-0.78	11 ± 1 ps	-0.28	134 ± 24 ps	45 ps
dAppA$_{FULL}$	-0.45	28 ± 4 ps	-0.55	526 ± 77 ps	301 ps
lAppA$_{FULL}$	-0.64	11 ± 1 ps	-0.28	144 ± 27 ps	48 ps

5.3.4. TRMPS of AppA$_{FULL}$

A considerable amount of effort has been performed on free flavin for the ps to ns time domain [33, 34]; however, to fully understand the mechanism of photoactivation and the role of the C-terminus experiments beyond the ps timescale were necessary. Time resolved multiple probe spectroscopy (TRMPS) allows for measuring transient IR difference spectra from fs to ms, providing key insight into the mechanism of photoactivation in BLUF proteins (chapter 4). Figure 5.5 shows the TRMPS spectra of AppA$_{FULL}$. One can clearly see that by 10 ns the initially

excited singlet state of has completely relaxed as indicated by the 1383 cm^{-1} transient mode of the FAD S_1 state. The ground state has not completely recovered (1547 and 1700 cm^{-1}).

Figure 5.6A shows the temporal evolution of TRIR for $dAppA_{FULL}$ between 20 ps and 10 ns after 450 nm excitation of the flavin chromophore. The dominant sub-nanosecond relaxation is well fit by a biexponential function with components of tens and hundreds of picoseconds consistent with an inhomogeneous distribution of ground state structures leading to a distribution of decay rates [34]. The two highest frequency bleach modes at 1700 and 1652 cm^{-1} are associated with two carbonyl stretches of the FAD ground state, and are sensitive to the H-bond environment [28, 33]. The intense bleach at 1547 cm^{-1} and the weaker one at 1580 cm^{-1} are FAD ring modes. The two positive peaks at 1410 cm^{-1} and 1383 cm^{-1} are not assigned to specific vibrational modes, but are associated with the excited state of the flavin ring rather than shifted protein modes, as shown by comparison with flavin in free solution (chapter 4). The band at 1670 cm^{-1} correlates with the TRIR spectra reported in Figure 5.3A. One can clearly see that by 10 ns the initially excited singlet state of has completely relaxed as indicated by the 1383 cm^{-1} transient mode of the FAD S_1 state. The ground state has not completely recovered (1547 and 1700 cm^{-1}).

While it is clear at least 80 % of the populated ES has returned to the ground state within 10 ns, small signals remain. It is already evident from Figure 5.6A that by 10 ns the FAD excited state has completely relaxed (the 1383 cm^{-1} transient mode of the FAD S_1 state has decayed) but the ground state has not completely recovered (signal is still observed for the FAD localized modes at 1547 and 1700 cm^{-1}). This result immediately proves the existence of intermediate protein structures in the photocycle (Figure 5.6B), as reported for the N-terminal domain in chapter 4. Data beyond the 50 μs measurement (out to 1 ms) showed no further change in the

TRMPS spectra associated with either the chromophore or protein structure. These spectra indicate that conformational changes on the microsecond dynamics are refilling the original ground state and that these features are indicative of formation of light adapted AppA. In addition, a weak band at 1440 cm^{-1} is present in free flavin and $AppA_{BLUF}$ is absent in $AppA_{FULL}$ (figure 5.5B). That is similar to what is observed in free flavin, indicating the possibility of triplet state in the photocycle of AppA. At present time the kinetics are not resolvable, but this appears to be the first reported evidence of flavin triplet state and its importance in the BLUF photocycle.

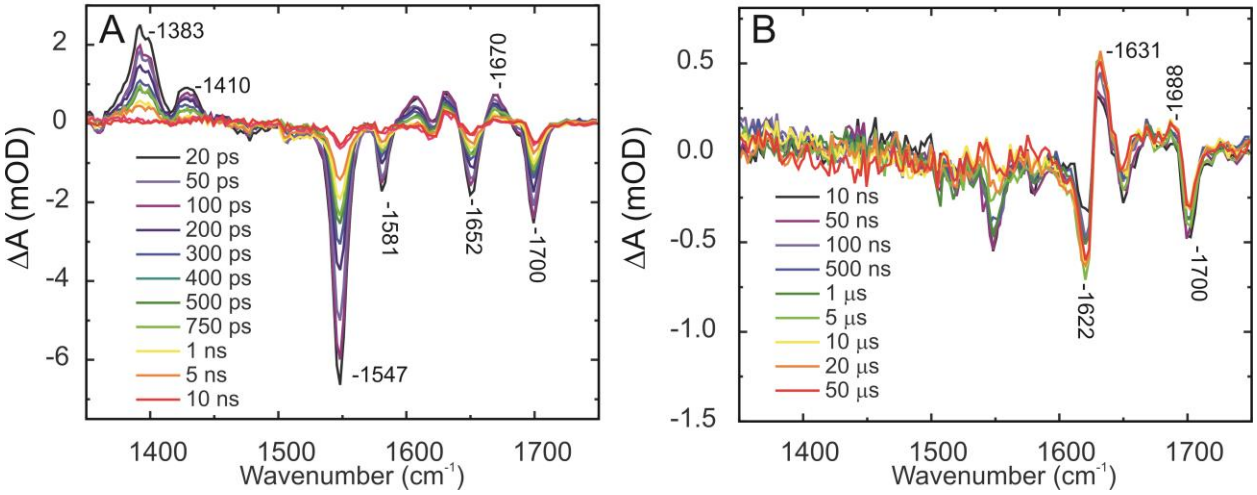

Figure 5.6. TRMPS IR difference spectra for $AppA_{FULL}$. A. TRIR spectra recorded between 20 ps and 10 ns after excitation of the flavin at 450 nm. The fast and complete decay of the singlet excited state is evident in the transient flavin modes at 1383 cm^{-1}. However, the ground state recovery is incomplete; signal from 1547 cm^{-1} is still present. **B.** Relaxation in the $AppA_{FULL}$ TRMPS IR difference spectrum between 10 ns and 50 μs after excitation. The electronic ground state recovers fully (1547 cm^{-1}) but formation of a new environment is indicated by the shift and incomplete recovery in the carbonyl mode at 1700 cm^{-1}. The temporal evolution in the 1622/1631 cm^{-1} pair of protein modes is also evident.

Kinetic analysis of the markers associated with light state formation of $AppA_{FULL}$ was compared to $AppA_{BLUF}$, revealing that these bands are kinetically distinct and not linked by the monotonic blue shift of a single protein mode in the full length and N-terminal BLUF domain.

The transient absorption at 1631 cm^{-1} rises in 1.5 μs for the BLUF domain but in 0.68 μs for the full length protein, which are reproducibly faster than the 2.1 μs development of the 1622 cm^{-1} bleach in the BLUF domain alone and 1.3 μs for the full length protein. While it is not unexpected that the kinetics of the 1622 cm^{-1} and 1631 cm^{-1} modes are distinct from each other, it is surprising that the values reported for the full length protein are faster.

The weak transient feature at 1688 cm^{-1}, assigned as increasing H-bonding to the flavin C4=O carbonyl from the protein in the light adapted state [4, 30], develops on a longer timescale than the protein modes (Table 5.3), but on the same timescale as the partial bleach recovery at 1700 cm^{-1}. As highlighted in chapter 4, the slower structural reorganization occurs in residues near the flavin binding pocket, showing that distance from the flavin does not necessarily correlate with response time. For full length AppA, the 1688 cm^{-1} forms with similar kinetics to the 1700 cm^{-1}, but at a 1.7 fold faster rate.

Table 5.3. TRMPS kinetic analysis of full length AppA.

Peak	$AppA_{BLUF}$	$AppA_{Full}$
1547 cm^{-1}	5.4 ± 0.5 μs	3.8 ± 0.6 μs
1622 cm^{-1}	2.1 ± 0.3 μs	1.3 ± 0.2 μs
1631 cm^{-1}	1.5 ± 0.3 μs	0.68 ± 0.20 μs
1688 cm^{-1}	5.6 ± 0.8 μs	3.9 ± 1.1 μs
1700 cm^{-1}	5.3 ± 0.7 μs	3.0 ± 1.0 μs

5.4. Conclusions

To fully realize the potential of AppA as an optogenetic sensor, characterization of the protein had to be expanded to include the C-terminal domain. It is well understood that

photoexcitation of the N-terminal BLUF domain ultimately leads to signal output in the C-terminal domain. Here, vibrational spectroscopy was used to compare the full length protein with $AppA_{BLUF}$. FTIR light minus dark difference spectroscopy reported subtle differences between full length and the BLUF domain alone; however no new difference mode that could be associated with the C-terminal domain is reported. To further characterize the mechanism of photoactivation, ultrafast IR spectroscopy was performed and revealed spectra for the full length that were similar to $AppA_{BLUF}$ with minimal effect on GS recovery kinetics. Using the TRMPS setup described in detail in chapter 4, kinetic analysis of protein markers associated with light state formation were shown to occur at a 1.4 to 2.3 fold faster rate for $AppA_{FULL}$ compared to $AppA_{BLUF}$, suggesting a possible synergistic effect with the C-terminal domain (Table 5.3).

While these results suggest minimal differences between truncated and full length protein, an important feature of the C-terminal domain is the ability to sense oxygen. These experiments were not performed in the absence of O_2. Under aerobic conditions, transcription of photopigment clusters is shut down in *R. sphaeroides*. Therefore, one could propose that while the N-terminal domain has not yet been activated (e.g. low light conditions); the C-terminal domain is already in its signaling state. In addition, the importance of heme in the C-terminal domain is poorly understood. X-ray crystallography revealed the presence of a SCHIC domain, yet no heme was found in the structure and to date, no vibrational data has been reported where heme was bound to AppA. To fully understand the mechanism of photoactivation in AppA, further characterization involving the C-terminal domain and its function as an oxygen sensor must be carried out. This information will be invaluable to the development of AppA as an optogenetic sensor.

5.5. References

1. Yin, T. and Y. Wu, *Guiding lights: recent developments in optogenetic control of biochemical signals.* Pflugers Archiv, 2013. **465**(3): p. 397-408.
2. Masuda, S. and C.E. Bauer, *AppA Is a blue light photoreceptor that antirepresses photosynthesis gene expression in Rhodobacter sphaeroides.* Cell, 2002. **110**(5): p. 613-623.
3. Anderson, S., V. Dragnea, S. Masuda, J. Ybe, K. Moffat, and C. Bauer, *Structure of a novel photoreceptor, the BLUF domain of AppA from Rhodobacter sphaeroides.* Biochemistry, 2005. **44**(22): p. 7998-8005.
4. Masuda, S., K. Hasegawa, and T.-a. Ono, *Light-induced structural changes of apoprotein and chromophore in the sensor of blue light using FAD (BLUF) domain of AppA for a signaling state* Biochemistry, 2005. **44**(4): p. 1215-1224.
5. Laan, W., M. Gauden, S. Yeremenko, R. van Grondelle, J.T.M. Kennis, and K.J. Hellingwerf, *On the mechanism of activation of the BLUF domain of AppA.* Biochemistry, 2005. **45**(1): p. 51-60.
6. Gauden, M., S. Yeremenko, W. Laan, I.H. van Stokkum, J.A. Ihalainen, R. van Grondelle, K.J. Hellingwerf, and J.T. Kennis, *Photocycle of the flavin-binding photoreceptor AppA, a bacterial transcriptional antirepressor of photosynthesis genes.* Biochemistry, 2005. **44**(10): p. 3653-62.
7. Unno, M., R. Sano, S. Masuda, T.A. Ono, and S. Yamauchi, *Light-induced structural changes in the active site of the BLUF domain in AppA by Raman spectroscopy.* J Phys Chem B, 2005. **109**(25): p. 12620-6.

8. Jung, A., J. Reinstein, T. Domratcheva, R.L. Shoeman, and I. Schlichting, *Crystal structures of the AppA BLUF domain photoreceptor provide insights into blue light-mediated signal transduction.* J Mol Biol, 2006. **362**(4): p. 717-732.

9. Laan, W., M. Gauden, S. Yeremenko, R. van Grondelle, J.T.M. Kennis, and K.J. Hellingwerf, *On the mechanism of activation of the BLUF domain of AppA.* Biochemistry, 2006. **45**(1): p. 51-60.

10. Pandey, R., D. Flockerzi, Marcus J.B. Hauser, and R. Straube, *Modeling the light- and redox-dependent interaction of PpsR/AppA in Rhodobacter sphaeroides.* Biophys J, 2011. **100**(10): p. 2347-2355.

11. Lukacs, A., A. Haigney, R. Brust, R.K. Zhao, A.L. Stelling, I.P. Clark, M. Towrie, G.M. Greetham, S.R. Meech, and P.J. Tonge, *Photoexcitation of the blue light using FAD photoreceptor AppA results in ultrafast changes to the protein matrix.* J Am Chem Soc, 2011. **133**(42): p. 16893-900.

12. Christie, J.M., J. Gawthorne, G. Young, N.J. Fraser, and A.J. Roe, *LOV to BLUF: Flavoprotein contributions to the optogenetic toolkit.* Mol Plant, 2012. **5**(3): p. 533-544.

13. Kim, S.K., J.T. Mason, D.B. Knaff, C.E. Bauer, and A.T. Setterdahl, *Redox properties of the Rhodobacter sphaeroides transcriptional regulatory proteins PpsR and AppA.* Photosynth. Res., 2006. **89**(2-3): p. 89-98.

14. Dragnea, V., A.I. Arunkumar, H. Yuan, D.P. Giedroc, and C.E. Bauer, *Spectroscopic studies of the AppA BLUF domain from Rhodobacter sphaeroides: Addressing movement of tryptophan 104 in the signaling state.* Biochemistry, 2009. **48**(42): p. 9969-9979.

15. Dragnea, V., A.I. Arunkumar, C.W. Lee, D.P. Giedroc, and C.E. Bauer, *A Q63E Rhodobacter sphaeroides AppA BLUF domain mutant is locked in a pseudo-light-excited signaling state.* Biochemistry, 2011. **49**(50): p. 10682-10690.

16. Metz, S., A. Jäger, and G. Klug, *In Vivo sensitivity of blue-light-dependent signaling mediated by AppA/PpsR or PrrB/PrrA in Rhodobacter sphaeroides.* J Bacteriol, 2009. **191**(13): p. 4473-4477.

17. Masuda, S., C. Dong, D. Swem, A.T. Setterdahl, D.B. Knaff, and C.E. Bauer, *Repression of photosynthesis gene expression by formation of a disulfide bond in CrtJ.* Proc Natl Acad Sci U S A, 2002. **99**(10): p. 7078-83.

18. Gomelsky, M. and S. Kaplan, *Genetic evidence that PpsR from Rhodobacter sphaeroides 2.4.1 functions as a repressor of puc and bchF expression.* J Bacteriol, 1995. **177**(6): p. 1634-7.

19. Penfold, R.J. and J.M. Pemberton, *Sequencing, chromosomal inactivation, and functional expression in Escherichia coli of ppsR, a gene which represses carotenoid and bacteriochlorophyll synthesis in Rhodobacter sphaeroides.* J Bacteriol, 1994. **176**(10): p. 2869-76.

20. Gomelsky, M. and S. Kaplan, *AppA, a redox regulator of photosystem formation in Rhodobacter sphaeroides 2.4.1, is a flavoprotein. Identification of a novel fad binding domain.* J Biol Chem, 1998. **273**(52): p. 35319-25.

21. Gomelsky, M. and G. Klug, *BLUF: a novel FAD-binding domain involved in sensory transduction in microorganisms.* Trends Biochem Sci, 2002. **27**(10): p. 497-500.

22. Pandey, R., D. Flockerzi, M.J.B. Hauser, and R. Straube, *An extended model for the repression of photosynthesis genes by the AppA/PpsR system in Rhodobacter sphaeroides.* FEBS J, 2012. **279**(18): p. 3449-3461.

23. Han, Y., M.H. Meyer, M. Keusgen, and G. Klug, *A haem cofactor is required for redox and light signalling by the AppA protein of Rhodobacter sphaeroides.* Mol Microbiol, 2007. **64**(4): p. 1090-104.

24. Metz, S., K. Haberzettl, S. Frühwirth, K. Teich, C. Hasewinkel, and G. Klug, *Interaction of two photoreceptors in the regulation of bacterial photosynthesis genes.* Nucleic Acids Res, 2012. **40**(13): p. 5901-5909.

25. Yin, L., V. Dragnea, and C.E. Bauer, *PpsR, a regulator of heme and bacteriochlorophyll biosynthesis, is a heme-sensing protein.* J Biol Chem, 2012. **287**(17): p. 13850-13858.

26. Jäger, A., S. Braatsch, K. Haberzettl, S. Metz, L. Osterloh, Y. Han, and G. Klug, *The AppA and PpsR proteins from Rhodobacter sphaeroides can establish a redox-dependent signal chain but fail to transmit blue-light signals in other bacteria.* J Bacteriol, 2007. **189**(6): p. 2274-2282.

27. Winkler, A., U. Heintz, R. Lindner, J. Reinstein, R.L. Shoeman, and I. Schlichting, *A ternary AppA–PpsR–DNA complex mediates light regulation of photosynthesis-related gene expression.* Nat Struct Mol Biol, 2013. **20**(7): p. 859-867.

28. Haigney, A., A. Lukacs, R. Brust, R.-K. Zhao, M. Towrie, G.M. Greetham, I. Clark, B. Illarionov, A. Bacher, R.-R. Kim, M. Fischer, S.R. Meech, and P.J. Tonge, *Vibrational assignment of the ultrafast infrared spectrum of the photoactivatable flavoprotein AppA.* J Phys Chem B, 2012. **116**(35): p. 10722-10729.

29. Unno, M., Y. Tsukiji, K. Kubota, and S. Masuda, *N-terminal truncation does not affect the location of a conserved tryptophan in the BLUF domain of AppA from Rhodobacter sphaeroides.* J Phys Chem B, 2012. **116**(30): p. 8974-8980.

30. Masuda, S., K. Hasegawa, and T.-a. Ono, *Tryptophan at position 104 is involved in transforming light signal into changes of β-sheet structure for the signaling state in the BLUF domain of AppA.* Plant Cell Physiol, 2005. **46**(12): p. 1894-1901.

31. Pelton, J.T. and L.R. McLean, *Spectroscopic methods for analysis of protein secondary structure.* Anal Biochem, 2000. **277**(2): p. 167-176.

32. Barth, A., *Infrared spectroscopy of proteins.* Biochim Biophys Acta, 2007. **1767**(9): p. 1073-1101.

33. Haigney, A., A. Lukacs, R.-K. Zhao, A.L. Stelling, R. Brust, R.-R. Kim, M. Kondo, I. Clark, M. Towrie, G.M. Greetham, B. Illarionov, A. Bacher, W. Romisch-Margl, M. Fischer, S.R. Meech, and P.J. Tonge, *Ultrafast infrared spectroscopy of an isotope-labeled photoactivatable flavoprotein.* Biochemistry, 2011. **50**(8): p. 1321-1328.

34. Kondo, M., J. Nappa, K.L. Ronayne, A.L. Stelling, P.J. Tonge, and S.R. Meech, *Ultrafast vibrational spectroscopy of the flavin chromophore.* J Phys Chem B, 2006. **110**(41): p. 20107-20110.

35. Stelling, A.L., K.L. Ronayne, J. Nappa, P.J. Tonge, and S.R. Meech, *Ultrafast structural dynamics in BLUF domains: Transient infrared spectroscopy of AppA and its mutants.* J Am Chem Soc, 2007. **129**(50): p. 15556-15564.

36. Alexandre, M.T.A., L.J.G. van Wilderen, R. van Grondelle, K.J. Hellingwerf, M.L. Groot, and J.T.M. Kennis, *Early steps in blue light reception by plants: an ultrafast mid-*

infrared spectroscopic study of the LOV2 domain of phototropin. Biophys J, 2005. **88**(1): p. 509a-509a.

37. Gauden, M., J.S. Grinstead, W. Laan, I.H. van Stokkum, M. Avila-Perez, K.C. Toh, R. Boelens, R. Kaptein, R. van Grondelle, K.J. Hellingwerf, and J.T. Kennis, *On the role of aromatic side chains in the photoactivation of BLUF domains.* Biochemistry, 2007. **46**(25): p. 7405-15.

38. Mathes, T., I.H.M. van Stokkum, C. Bonetti, P. Hegemann, and J.T.M. Kennis, *The hydrogen-bond switch reaction of the Blrb BLUF domain of Rhodobacter sphaeroides.* J Phys Chem B, 2011. **115**(24): p. 7963-7971.

39. Bonetti, C., M. Stierl, T. Mathes, I.H.M. van Stokkum, K.M. Mullen, T.A. Cohen-Stuart, R. van Grondelle, P. Hegemann, and J.T.M. Kennis, *The role of key amino acids in the photoactivation pathway of the Synechocystis Slr1694 BLUF domain.* Biochemistry, 2009. **48**(48): p. 11458-11469.

Chapter 6

Spectroscopic Studies on the BLUF Protein PixD

6.1. Introduction

Flavin binding photoreceptors represent a unique class of photoreceptors because the flavin chromophore is unable to undergo what is considered large scale structural changes [1]. Instead they undergo subtle changes of their electronic structure, which result in small structural changes of the surrounding matrix. As a result, the proteins in flavin binding photoreceptors must sense and respond to these changes. In the cyanobacterium, *Synechocystis sp.* PCC 6803, positive phototaxic movement is regulated by the BLUF protein, PixD (Slr1694) [2-4]. Similar to what is observed in other BLUF systems, a 10 nm red shift in the λmax of the flavin is observed upon photoexcitation, which relaxes within seconds [5], a much faster rate of recovery when compared to AppA (30 min) or BlsA (12 min).

Structural data for the N-terminal BLUF domain of PixD reveals an intricate H-bonding network surrounding the flavin (Figure 6.1) [6, 7]. Residues where direct contact with the flavin can be observed are Q50, Y8, N31, and N32. Q50 forms an H-bond with the N5 of the flavin ring and a conserved tyrosine (Y8), which are essential for photoactivity [8, 9]. Methionine at this position is conserved in all BLUF proteins and M93 in PixD has been shown to be essential for blue light signaling [4]. The crystal structure reported for PixD revealed that PixD forms a decamer. In the decamer, 9 subunits exhibited a conformation consistent with the Trp_{out} conformation observed in the $AppA_{BLUF}$ crystal structure solved [7]. In one subunit the Trp_{in} conformation is observed, highlighting the mobility of the conserved tryptophan and providing further evidence for its role as signal modulator in BLUF proteins.

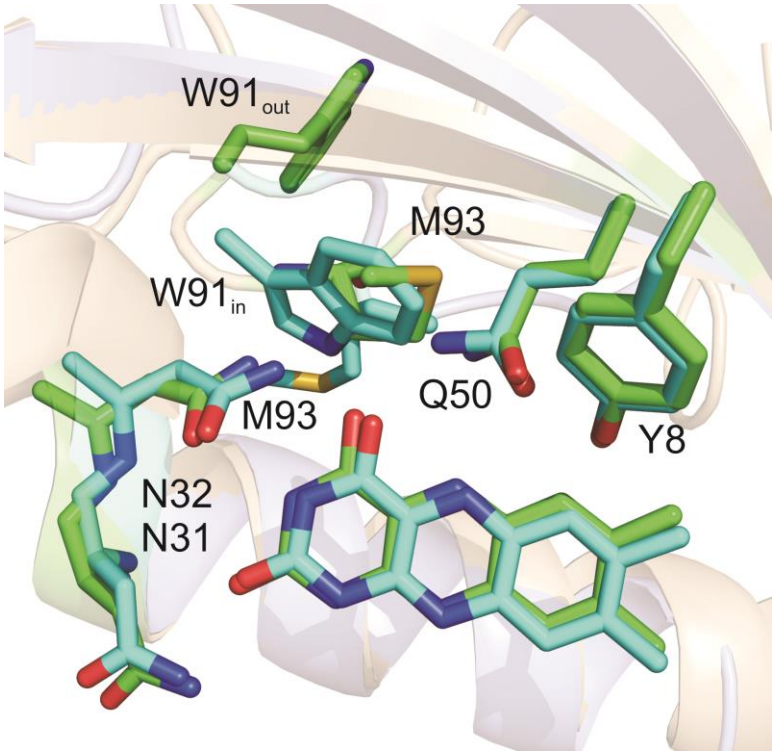

Figure 6.1. Crystal structure of PixD. The position of W91 can be seen either in the "out" conformation (green) or the "in" conformation (blue). In place of W91 is M93 in the "out" conformation.

As a single standalone BLUF protein, PixD has no output domain; only a 50 amino acid tail is present [10]. Based on this observation, it was proposed that PixD must relay its signal via a protein-protein interaction. It was shown that PixD forms a large, oligomeric structure with the response regulator-like protein, PixE (Slr1693) [11-13]. PixE is a PatA-like two-component response regulator that has been shown to interact with PixD *in vivo*, with dissociation of the complex resulting in positive phototaxic response of the bacterium [2, 11, 14, 15]. The PixD-PixE complex is a large oligomeric structure, consisting of 10 PixD monomers and 5 PixE monomers with a mass of 370 kDa [11]. The binding affinity for the PixD-PixE complex is 5 µM [11, 16]. With no structural data currently available for PixE, docking experiments have been performed using a homology model of PixE with the crystal structure for PixD [16]. In this model, an oligomeric structure of only 4 PixE monomers was proposed instead of the more

commonly proposed 5 as a result of BN-PAGE experiments (total mass of 342 kDa) but was in good agreement with a calculated 2.56:1.0 PixD:PixE stoichiometry [11]. Binding was proposed to be on the outer surface of the PixD decamer, in which a potential salt bridge is formed between R80 of PixE and D135 of PixD. Mutational studies in this work highlighted the importance of these residues. Based on this structural information, a model for signal modulation was proposed. In the PixD crystal structure, C-terminal α-helices from two PixD monomers interact with the β-sheet of the intervening PixD monomer in the same ring [10, 14]. The light signal, received by the flavin chromophore, is transmitted to the C-terminal α-helices through a conformational change that involves the conserved Met (M93) and not through the conserved Trp (W91) [4, 12, 17, 18], as was repoted for $AppA_{BLUF}$ in chapter 4. This would perturb the interaction between R80 of PixE and D135 of PixD, ultimately resulting in dissociation of the complex into PixD dimers and PixE monomers [11-13]. It is worth noting that dissociation of the complex is dependent upon photoexcitation of only two PixD subunits [13].

Previous mutational analysis on PixD provided insight into the mechanism of photoactivation. Mutations to the conserved Tyr (Y8), Gln (Q50) and Met (M93) resulted in a protein that exhibited a photoinactive yet exhibited a "light-like" state (i.e. did not bind PixE) [12]. In addition, FTIR spectroscopy revealed that the M93A mutation suppressed protein dynamics associated with photoexcitation [4]. This, in tandem with the crystal structure, led to a model where W91 is found in the "out" state in dPixD, and upon photoexcitation, replaces M93, whose side chain moves from "in" to "out" of the flavin binding pocket [4].

To further elucidate the mechanism of light state formation in PixD the following mutations were generated: Y8F, Y8W, N31H, Q50A, Q50E and M93A. While mutations toY8

result in a photoinactive species [9, 15, 19], recent data suggests a radical pair formation from the Y8 to the flavin as a result of photoexcitation [20-22]. No evidence of PT/ET was observed from W91, presumably due to the greater distance from W91 to the flavin compared to AppA [10, 20, 22]. In comparing the crystal structure of AppA and PixD one can see a difference near the C2=O of the flavin. In AppA, H44 is seen but in PixD and in other BLUF proteins, an asparagine (N31) is in this observed. AppA is known to exhibit the longest observed photocycle [23], so to determine if the histidine in this position is the cause the N31H mutant was generated.

6.2. Experimental Methods

6.2.1. Cloning

Genomic DNA from *Synechocystis* PCC 6803 was purchased from ATCC (27814) and the following primers were used to amplify the *pixD* gene prior to insertion into a pET-15b vector (Invitrogen) with an N-terminal His_6 tag: forward primer – 5'-TGCGGCCATATGAGTTTGTACCGTTTG-3' and reverse primer 5'-GGGATTCTTAGAGGTCGAGGAAAAAG-3'. Site directed mutagenesis was performed using pfu turbo (Agilent). Forward primers are listed in Table 6.1.

Table 6.1. Forward Primers for PixD Mutagenic Studies

Sample	Forward Primer Design
Y8F	5'-AGT TTG TAC CGT TTG ATT TTT AGC AGT CAG GGC ATT CCC-3'
Y8W	5'-AGT TTG TAC CGT TTG ATT TGG AGC AGT CAG GGC ATT CCC-3'
N31H	5'-TTA GAA TCT TCC CAA AGA CAT AAT CCG GCC AAT GGC ATT-3'
Q50A	5'-AAG CCG GCT TTT CTG GCG GTA TTG GAA GGA GAG-3'
Q50E	5'-AAG CCG GCT TTT CTG GAG GTA TTG GAA GGA GAG-3'
M93A	5'-TTC GAG GTT TGG TCT GCG CAA GCG ATC ACG GTG-3'

6.2.2. Protein Expression and Purification

Plasmids were expressed in BL21(DE3) *E. coli* cells and grown in 10 mL cultures containing LB media with 200 μg/mL ampicillin at 37°C at 250 rpm. Inoculation of 1 L LB/ampicillin media was performed using these cultures and grown to an OD600 of about 1 at 30°C (5 hr). The temperature was subsequently decreased to 18°C for 30 min and protein expression was induced by adding 0.8 mM IPTG. Protein expression was performed overnight in the dark. Purification of wild type and the various mutants were performed in the dark. Cells were harvested at 3000 rpm at 4°C. The cell pellets were then resuspended in 40 mL of buffer (10 mM NaCl, 50 mM $Na_2H_2PO_4$, pH 8.0) to which 200 μL of 50 mM PMSF was added to inhibit endogenous protease activity. Cells were lysed by sonication and cell debris was removed by ultracentrifugation (33000 rpm for 90 min). The soluble portion was reconstituted with 1 mL of a 10 mg/mL solution of FAD for 45 min on ice. The protein was then purified by Ni-NTA affinity chromatography using 10 mM NaCl, 50 mM $Na_2H_2PO_4$, pH 8.0 (wash buffer). The bound protein was then washed using the wash buffer and increasing amounts of imidazole and finally eluted with 250 mM imidazole. The fractions were then dialyzed overnight in the dark in the wash buffer. Protein purity and yield were determined using UV-Vis spectroscopy and SDS-PAGE.

6.2.3. FTIR Spectroscopy

FTIR spectroscopy was performed on a Vertex 80 (Bruker) IR spectrometer. The sample chamber and optics were purged with dry air. Protein samples at a concentration of 1.5 mM in deuterated buffer (50 mM sodium phosphate, 10 mM sodium chloride, pD 8) were irradiated

with 20 mW of 460 nm light for 3 min using a high mount LED (Prizmatix). Difference spectra were generated by subtracting the dark state from the light state.

6.2.4. TRIR Spectroscopy

TRIR experiments were performed at STFC Central Laser facility. The TRIR system has been described in detail elsewhere [24]. Excitation pulses were set to 450 nm with a power set to 200 nJ and a spot size radius of 100 μm. Dark state measurements were rastered and flowed at a rate of 1.5 mL/min in a 50 μm path length transmission cell of CaF_2 to minimize photobleaching and sample degradation. The IR probe recorded transient difference spectra (pump on-pump off) at time delays between 1 ps and 2000 ps. After the measurements were recorded, the extent of photoconversion was shown to be negligible using absorption spectroscopy. The probe beam was measured by two carefully matched 128 pixel detectors at a resolution of 3 cm^{-1} per pixel. Spectra were calibrated relative to the IR transmission of a pure polystyrene standard. Light-adapted samples were prepared by irradiation at 380 nm using a high mount LED illuminator (ThorLabs). Protein samples at a concentration of 1.5 mM in deuterated buffer (50 mM sodium phosphate, 10 mM sodium chloride, pD 8). Photoconversion was monitored using UV-vis spectroscopy and was found to be complete within 5 min. Samples were prepared in deuterated buffer (50 mM sodium phosphate, 10 mM sodium chloride, pD 8) at 1.5 mM concentration. The TRIR setup was operated and maintained by the CLF (Dr. Greg Greetham, Dr. Ian Clark, Dr. Mike Towrie).

6.2.5. TRMPS

The TRMPS method expands upon the ULTRA laser setup described above in 6.2.3. A 1 kHz visible pump laser (450 nm) is synchronized with the 65 MHz (15×10^{-9} s^{-1}) repetition rate

of the titanium sapphire seed laser. The seed laser is automatically locked to the 10 kHz pulses of the ULTRA amplifier. The delay between 100 ps and 15 ns is achieved by varying an optical delay. The times between 10 ns and 100 μs is controlled by using the oscillator seed pulses to add multiple of 15 ns to the pump laser delay. For times between 100 μs and 1 ms the 10 kHz pulses of ULTRA are synchronized with the 1 kHz pump laser, allowing for data collection every 0.1 ms. Pump power was set to 1 μJ at 450 nm. The TRMPS setup was operated and maintained by the CLF (Dr. Greg Greetham, Dr. Ian Clark, Dr. Mike Towrie).

6.3. Results and Discussion

6.3.1. FTIR Spectroscopy

Initial characterization of BLUF systems is typically performed using steady state FTIR spectroscopy [5, 25]. BLUF proteins exhibit key differences in their dark and light adapted states that are highlighted in the IR difference spectra. Comparison of the primary sequence of PixD and AppA reveal one key difference in the flavin binding pocket. H44 in AppA is replaced by N31 in PixD. This is a conserved residue in BLUF proteins and proposed to H-bond with the C2=O carbonyl of the flavin. Previous studies revealed that the N31H mutation increases the photocycle of PixD by a factor of 4 [26]. To further investigate the role of this residue, the N31H mutation was performed in PixD and characterized by vibrational spectroscopy. Light minus dark difference FTIR spectra were generated for wild type and N31H PixD (Figure 6.2). Similar to what is observed in AppA [25] and what was previously reported for PixD [4, 27], a shift of a peak at 1700 cm^{-1} is observed, this time of 18 cm^{-1} to 1682 cm^{-1}, in both the wild type and mutant spectra. This can be assigned as the C4=O carbonyl, which exhibits an increase in H-bonding upon light state formation. A difference mode at 1620(-)/1634(+) cm^{-1} can be seen in

both wild type and N31H, and has been assigned to the protein [28]. While the overall shape of the spectra of both wild type and N31H are different than at AppA, the mutation did not affect the difference spectra, suggesting that wild type and N31H PixD adopt similar structures in both dark and light states.

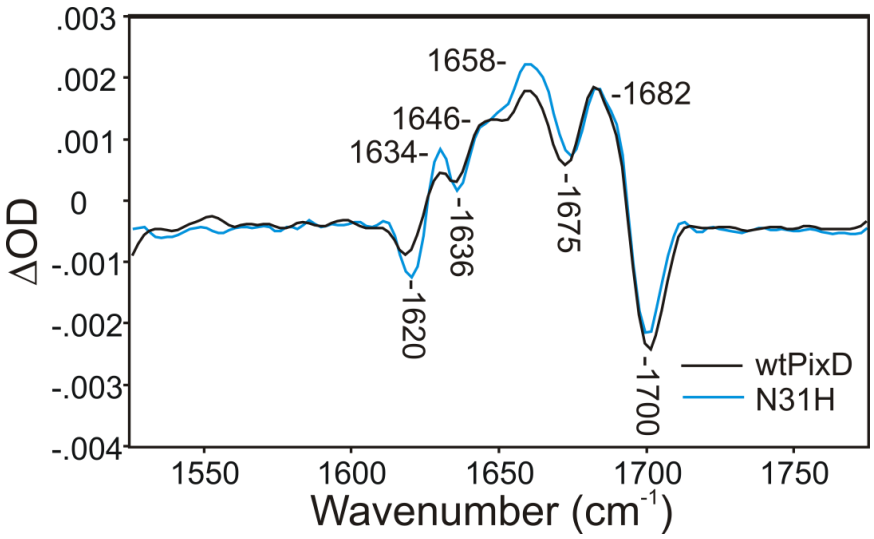

Figure 6.2. FTIR of PixD and N31H. FTIR light minus dark difference spectra of wtPixD (black) and N31H PixD (blue). Light adapted spectra were generated by 3 min irradiation of 460 nm light.

6.3.2. TRIR of PixD

To further investigate the mechanism of photoactivation of PixD, time resolved IR spectroscopy was employed. TRIR has been well established in chapters 2 through 5 as an ideal tool for measuring the primary steps of photoactivation in BLUF proteins. TRIR spectra of d and lPixD are reported in Figure 6.3, which exhibit key flavin modes in the 1500-1620 cm^{-1} region [29]. The main bleach is observed at 1547 cm^{-1}, which was previously assigned in AppA as C=C and C=N vibrations of the isoalloxazine ring of the flavin [24]. A weaker bleach is observed at 1585 cm^{-1}, which was assigned in AppA as C=N vibrations. Absorption and steady state infrared spectra indicate that the flavin is not perturbed in PixD, so assignments previously made in

$AppA_{BLUF}$ should be consistent [24, 30]. A large transient is observed at 1383 cm^{-1}, which is present in free flavin and therefore must be associated with flavin excited state. Moreover, a transient is observed at 1665 cm^{-1} in dPixD only, a feature that was also present only in dAppA [31]. Based on previous assignments, this mode could be tentatively assigned at the amide side chain of the conserved glutamine (Q50), and possibly the conserved asparagine (N32). An environmentally sensitive carbonyl mode is observed at 1700 cm^{-1} is present at the same positions as those observed in our previous studies on AppA [30, 31]. The 1700 cm^{-1} band in dark states shifts to 1685 cm^{-1} in the light states, indicative of an increase in hydrogen bond strength between the flavin C4=O group and the conserved glutamine [5, 31]. These results indicate that the final structure of lPixD is similar to that observed in the N-terminal domain of AppA.

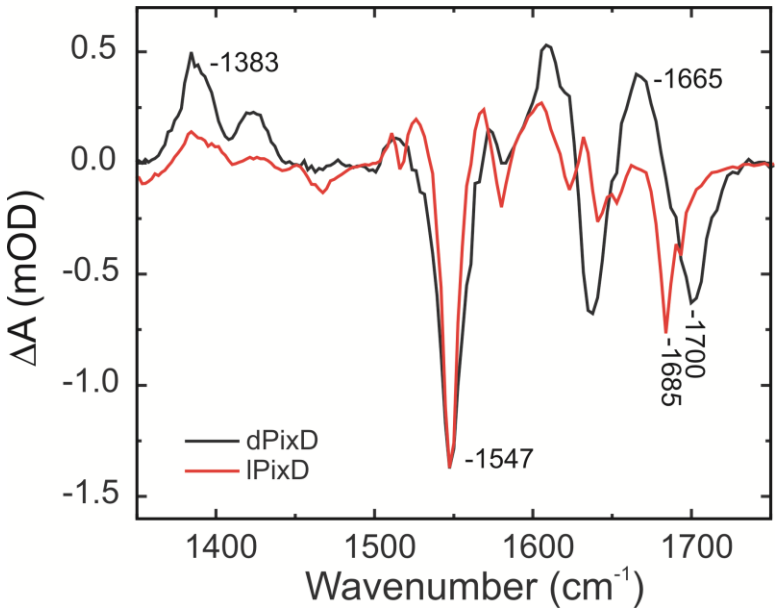

Figure 6.3. TRIR spectra of PixD. TRIR spectra of dPixD (black) and lPixD (red) taken 3 ps post excitation.

Previous characterization of PixD was performed using transient absorption spectroscopy. In these studies, a model was proposed in which proton coupled electron transfer from the conserved tyrosine to the flavin leads to rearrangement of the H-bonding network, ultimately resulting in formation of the signaling state [22, 26, 32]. Key vibrational bands were observed for the fully reduced and semi-reduced flavin TRIR spectra [33, 34]. For the semi reduced neutral flavin, $FAD^{\bullet}$, intense bands were observed at 1514, 1528, 1595, and 1628 cm^{-1}. In addition, a bleach at 1623 cm^{-1} was assigned as the loss of oxidized FAD. If flavin radicals are in fact being formed as a result of photoexcitation, one would expect to see these bands forming as a function of time. Upon further examination of dPixD, one can find a transient forming, followed by decay on a timescale similar to the recovery of the ground state at 1526 cm^{-1} (figure 6.3A) Fitting the rise of this mode to a monoexponential yields a time component of 4.2 ± 0.7 ps while fitting the decay to a monoexponential gave a time component of 221 ± 35 ps.

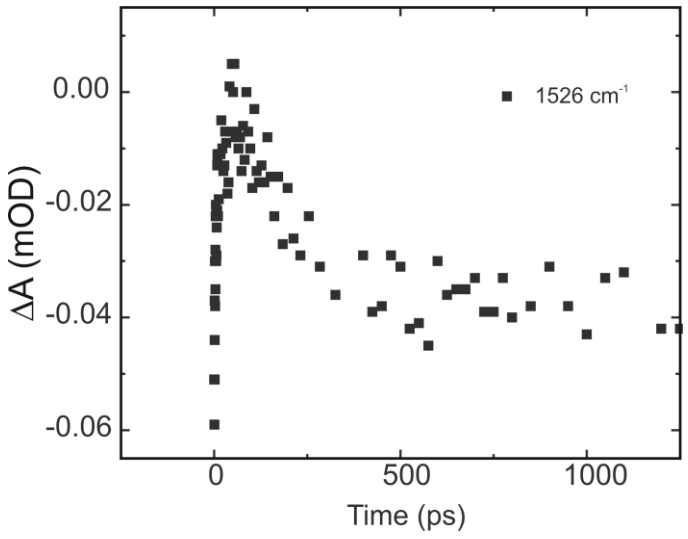

Figure 6.4. Kinetics of radicals in dPixD. Kinetic traces reported at 1526 cm^{-1} reveal a mechanism involving electron transfer.

This mode was previously assigned as C–C stretches of the ring I and C4a-N5, C10a-N1 stretches of $FAD^{\bullet}$ [34]. Since it is observed as a transient, this indicates that a flavin radical is forming during the initial steps of the photocycle.

It has been well established that BLUF proteins are photoirreverisble. In order to recover the dark state, the protein must be kept away from a blue light source for certain amount of time. Upon blue light excitation of light adapted BLUF proteins, the light adapted state is recovered. As a result, it has been proposed that the dark and light adapted states of BLUF proteins exhibit two differing mechanisms [35]. For PixD, two differing mechanisms involving flavin redox states have been proposed. For dPixD, a mechanism involving formation of the anionic semiquinone ($FAD^{\bullet -}$) to the neutral semiquinone ($FADH^{\bullet}$) was proposed, but for lPixD only $FADH^{\bullet}$ is formed [21, 22, 26]. For lPixD, a new feature is observed that is absent in dPixD at 1631 cm^{-1}. This feature has previously been observed in free flavin radical and in the flavin binding enzyme glucose oxidase [34]. Based on these results, one can conclude that this is evidence for formation of $FADH^{\bullet}$ in lPixD. Kinetic analysis of this mode reveals a rise of component of 1.1 ± 0.2 ps and a decay component of 272 ± 26 ps. These results clearly indicate that in lPixD an altered mechanism of radical formation is occurring unrelated to photoactivity, favoring concerted proton coupled electron transfer from the tyrosine to the flavin. Decay of the oxidized flavin can be observed at 1623 cm^{-1}, whose kinetics was calculated to be 3.3 ± 0.2 ps and 266 ± 16 ps. For the 1526 cm^{-1} mode, kinetic components of 1.1 ± 0.1 ps and 52 ± 2 ps are reported (Figure 6.5). These results indicate that the primary event results in formation of the 1526 cm^{-1} mode, which decays and leaves the longer lived $FADH^{\bullet}$ state.

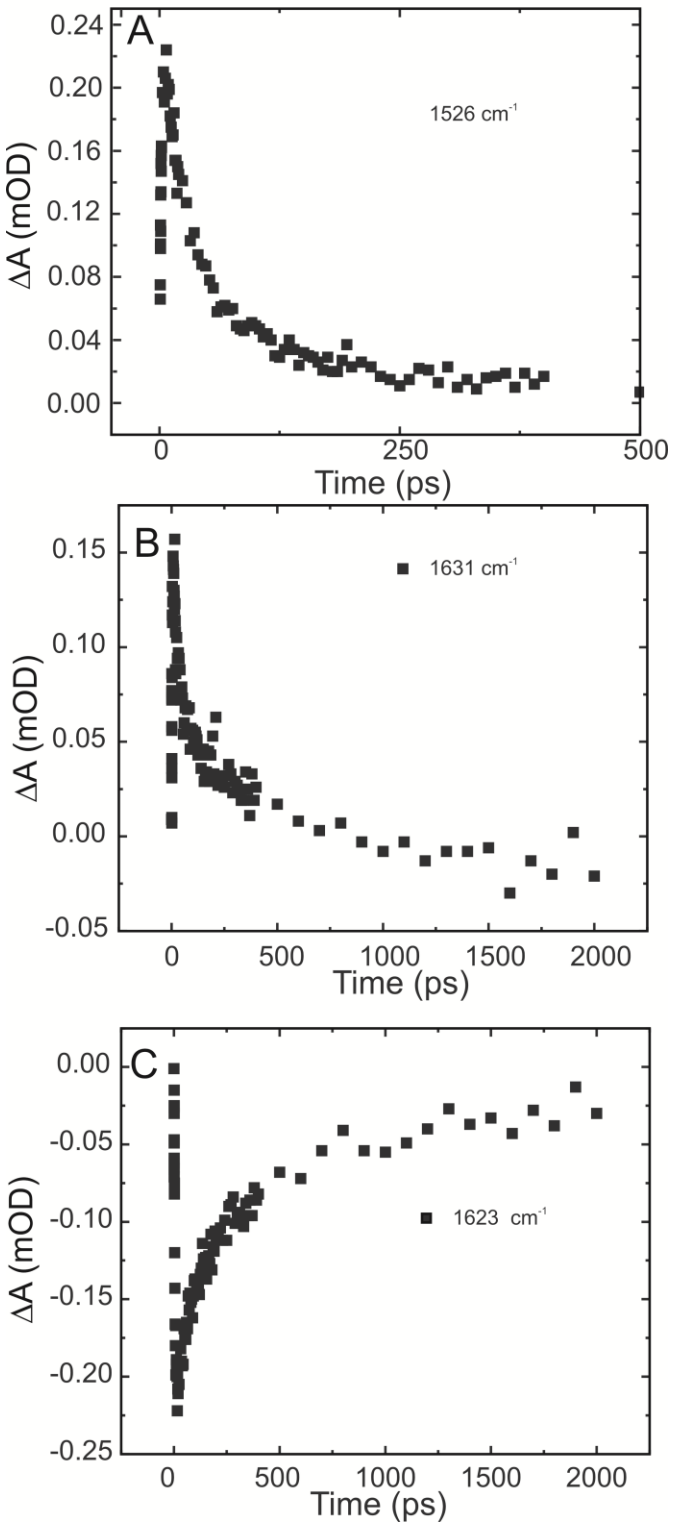

Figure 6.5. Kinetics of radical in lPixD. Kinetics of 1526 cm^{-1} (**A**), 1631 cm^{-1} (**B**) and 1623 cm^{-1} (**C**) indicate the formation of flavin radicals in light adapted PixD.

6.3.3. TRIR of Y8 Mutants

6.3.3.1. Y8F

Mutations to the conserved tyrosine result in an inactive protein, so no light state can be measured. However the C4=O mode can reveal if this mutant is "dark-like" or "light-like." By overlaying the Y8F TRIR spectra with dPixD, we can clearly see that the C4=O carbonyl are near identical, indicating that the Y8 mutants exhibit a "dark-like" C4=O (Figure 6.6). This result contradicts previous structural data, which suggested that the Y8F mutant was in a "light-like" state [12]. The Y8F mutant does not bind PixE, however, which would favor a 'light-like" structure. Here we propose some intermediate structure caused by the Y8F mutation that prevents the protein-protein interactions necessary for complex formation while also leaving the amide side chain of Q50 pointed away from the C4=O of the flavin. Interestingly, in the Y8F mutant there is no transient at 1668 cm^{-1} (Figure 6.6). This mode was tentatively assigned to the conserved Gln (Q50) in the BLUF protein, AppA [31]. This mode is not observed in Y8F, indicating that the initial photochemical process is not occurring. It is important to point out that in addition to the conserved tyrosine which can serve as an electron donor that there is W91. In the Y8F mutant, no evidence of electron transfer is observed, in agreement with previous finding [22]. These results indicate that electron transfer in PixD is responsible for the primary event, which ultimately leads to rotation of the Q50 side chain.

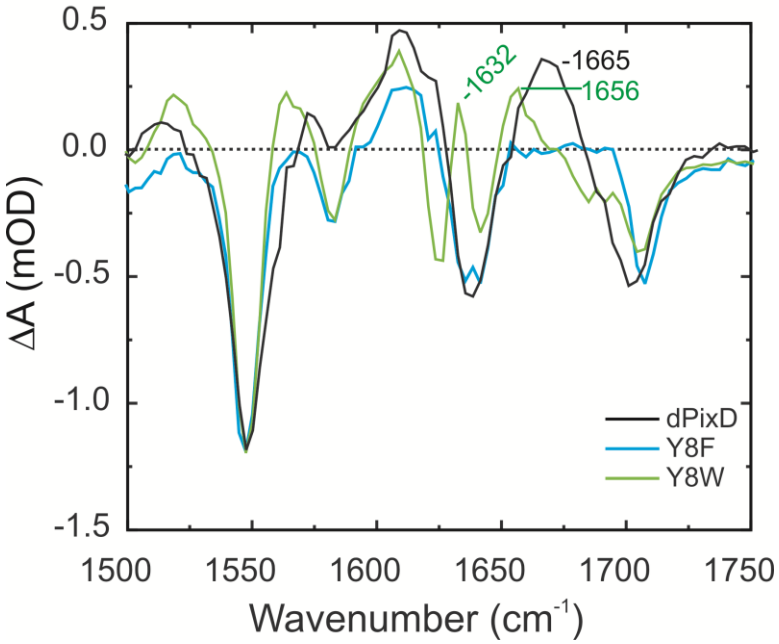

Figure 6.6. TRIR spectra of PixD and Y8 mutants. TRIR spectra of dPixD (black), lPixD (red), Y8F (blue), and Y8W (green), taken 3 ps post-excitation.

6.3.3.2. Y8W

The Y8W mutation results in a photoinactive protein. The TRIR spectra reported for the Y8W mutant is seen in Figure 6.6, and reveals similar features to what was observed in the Y8F mutant, in particular with regards to the C4=O flavin carbonyl. The C4=O carbonyl mode overlays quite well with dPixD, indicating no additional H-bond to the C4=O carbonyl is seen, resulting in a carbonyl vibration that is similar to the dark state. Surprisingly, there is a transient present at 1656 cm^{-1} in Y8W, which is shifted down by 10 cm^{-1} from dPixD. This is particularly interesting in that with the Y8F mutant, no transient is observed yet both are inactive. While being in a similar position, it is possible that position to be arising from a different amide. There are two other potential candidates near the flavin; N31 and N32. Based on band position it is more common to find Gln amides at 1650 cm^{-1} than Asn amides [36, 37]. If in fact this mode arising from Q50 it is surprising result given that Y8W is photoinactive.

By overlaying the TRIR spectra of lPixD with Y8W (Figure 6.7A), one can see that the bands at 1632 cm^{-1} present only in the light adapted PixD spectrum is also seen in Y8W. This indicates that in the Y8W mutant photoexcitation leads directly to formation of $FADH^{\bullet}$. The altered mechanism cannot induce the photoactivated conformational changes that ultimately lead to formation of the light state. These results further emphasize the importance of tyrosine at this position in BLUF proteins, and in particular in PixD. Kinetic analysis of the 1631 cm^{-1} mode reveals a rise of component of 0.8 ± 0.3 ps and a decay component of 54 ± 4 ps (Figure 6.7B). The time components calculated when fitting the kinetics of the 1623 cm^{-1} mode to a monoexponential reveals a rise of component of 0.5 ± 0.2 ps and a decay component of 77 ± 5 ps (Figure 6.7C). These values are faster than those reported for lPixD, suggesting that PCET from the Trp is faster than from Tyr yet also less stable.

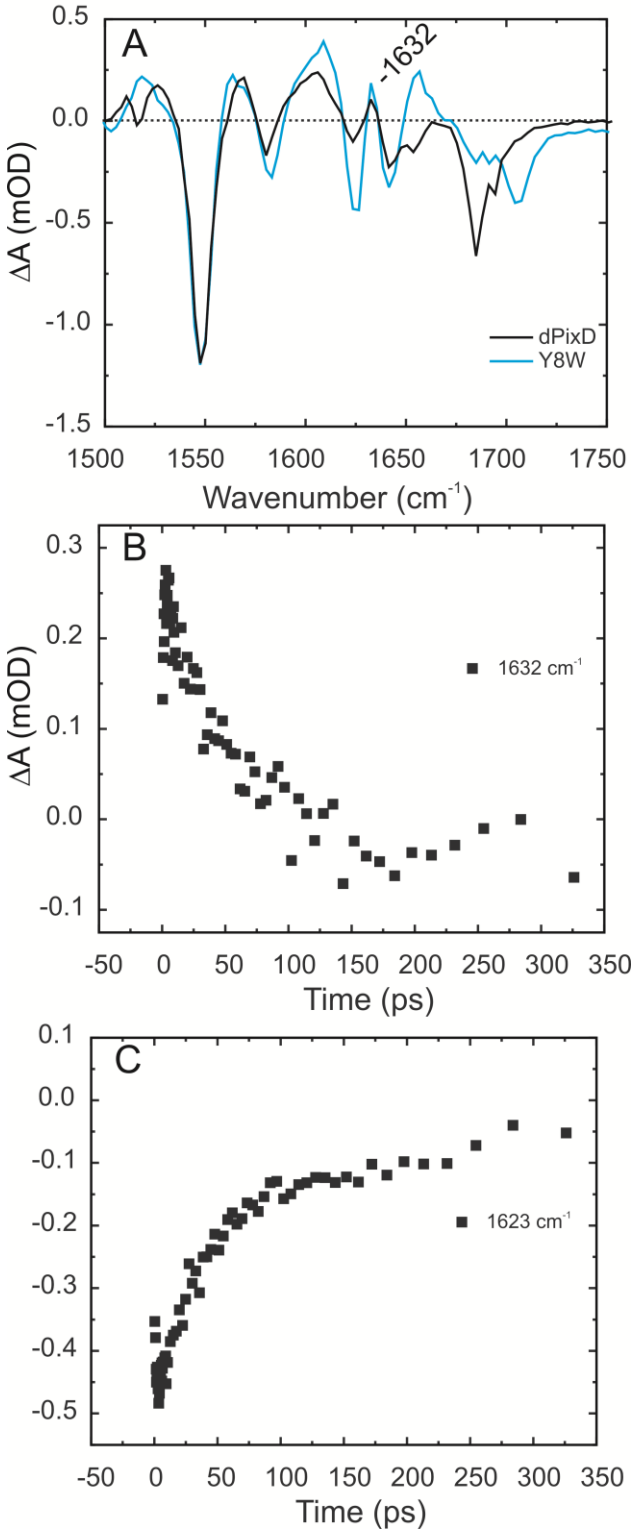

Figure 6.7. Analysis of Y8W mutant. A. TRIR spectra of dPixD (black) and Y8W (blue) taken 3 ps post excitation. **B** and **C.** Kinetic analysis of rise of $FADH^{\bullet}$ (**B**) and decay of FAD_{ox} (**C**).

6.3.4. TRIR of N31H

The 3 ps TRIR spectra for dN31H overlay quite well with wild type (Figure 6.8A). A transient present at 1665 cm^{-1}, which was tentatively been assigned as the side chain of the conserved Gln in AppA [31], however as stated above this assignment is incomplete based on the Q50 mutants described below. Overall the spectra of dN31H overlay well with dPixD, which are in agreement with the FTIR spectra that reveal little structural difference between wild type and N31H.

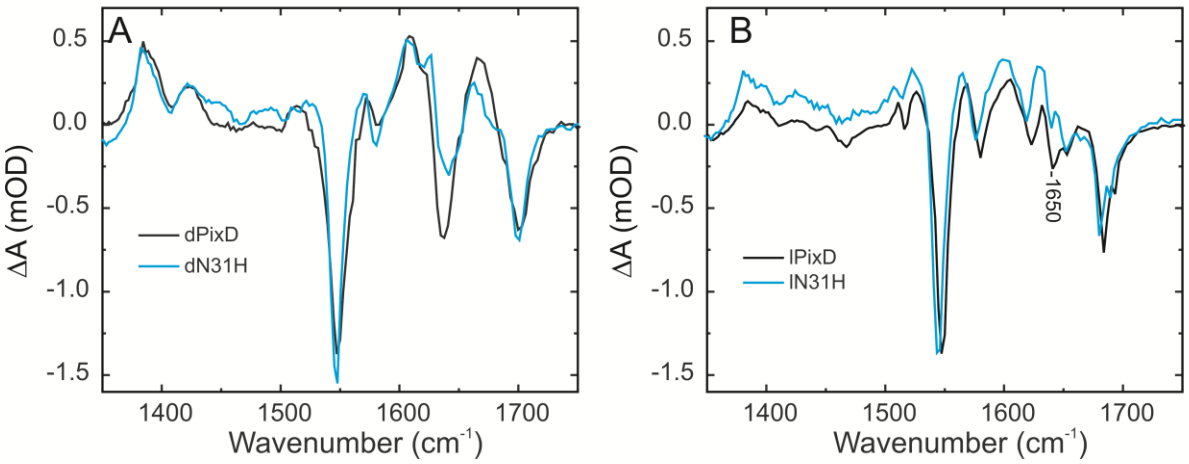

Figure 6.8. TRIR analysis of N31H. TRIR spectra of PixD (black) and N31H (blue) taken 3 ps post excitation. **A.** Spectra of dark adapted states. **B.** Spectra of light adapted states.

In the TRIR spectra of lN31H there is a loss of a defined bleach at 1650 cm^{-1}, assigned to the C2=O carbonyl in AppA(Figure 6.8B) [30]. In PixD, N31 is in a position to H-bond to the C2=O carbonyl whereas in AppA H44 H-bonds to the flavin. This only appears in the light adapted state; in the dark state of N31H the 1650 cm^{-1} bleach is unaffected by the mutation. Based on these results, rearrangement of the protein matrix as a result of photoexcitation disrupts the C2=O carbonyl in the N31H mutant.

Kinetic analysis of the dN31H mutant revealed that like in the wild type protein, a transient forming at 1526 cm^{-1} can be seen (Figure 6.9). Fitting to a monoexponential the rise component yielded a time component of 0.7 ± 0.1 ps, and fitting to a monoexponential the decay of this mode gave a time component of 216 ± 43 ps. While the decay component of this mode is in good agreement with wild type, the rise component reveals that it forms at a 6-fold faster rate.

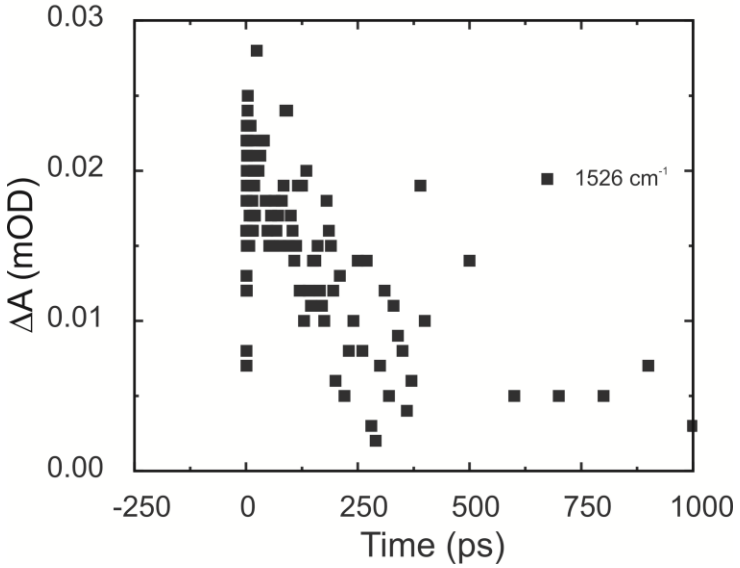

Figure 6.9. Kinetic analysis of flavin radical in dN31H. Formation at 1526 cm^{-1} suggests evidence of ET in the N31H mutant, in agreement with the reported data for wild type.

The kinetics associated with flavin radicals for lN31H are reported in Figure 6.10. Clear rise and decay components can be seen at 1526 and 1636 cm^{-1}. At 1526 cm^{-1}, a rise component of 0.7 ± 0.2 ps and decay component of 36 ± 8 ps were calculated. For the transient at 1636 cm^{-1}, a rise component of 1.5 ± 0.5 ps and decay component of 400 ± 100 ps were calculated. These results are similar to what was reported above for wtPixD. These results indicate that while the N31H mutant increases the rate of ET in the dark adapted state, yet this effect is minimal in the light adapted state.

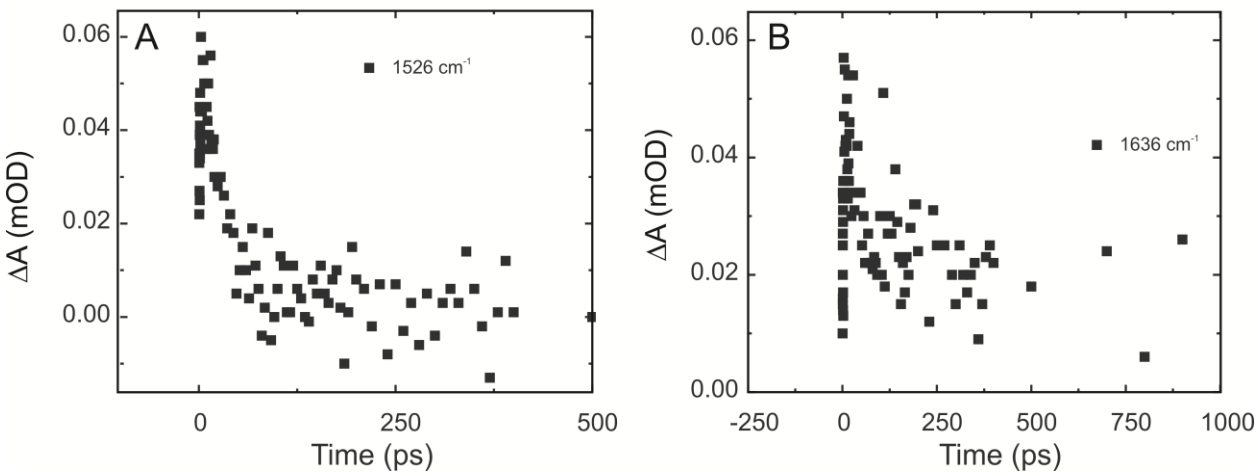

Figure 6.10. Kinetic analysis of flavin radicals in lN31H. A. Kinetics at 1526 cm^{-1}. **B.** Kinetics at 1636 cm^{-1}.

6.3.5. Q50 Mutants

6.3.5.1. Q50A

Mutations of the conserved Gln in BLUF proteins results in an inactive protein yet can provide key information pertaining to the mechanism of light state formation. The Q63E mutant in $AppA_{BLUF}$ was generated and provided important structural information about the initial events following blue light excitation [38]. The Q50A mutant was already shown to be unable to bind PixE and was considered to be in a "light-like" state [12]. However, if one compares the position of the C4=O carbonyl vibrations of Q50A with dPixD, one can see that these bands overlap quite well (Figure 6.11A). This indicates that H-bonding interactions are similar in the Q50A to dPixD. This is to be expected since the methyl side chain of Ala cannot form an H-bond with the flavin C4=O carbonyl. Other key features in the wild type TRIR spectrum overlay well with the Q50A spectrum, indicating minimal perturbations to the structure of the flavin chromophore as a result of the Q50A mutation.

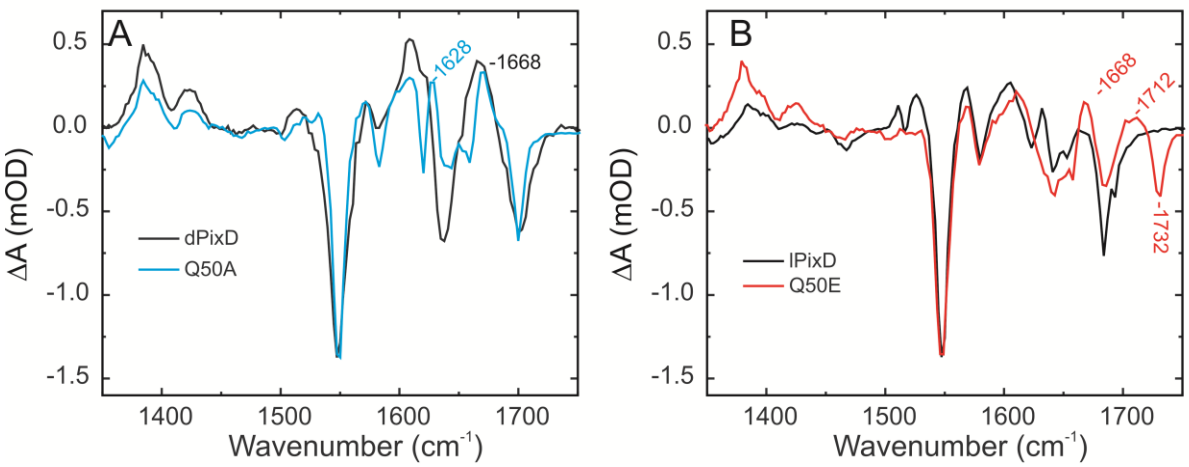

Figure 6.11. TRIR of Q50 mutants. A. TRIR spectra of dPixD (black) and Q50A (blue) taken 3 ps post excitation. **B.** TRIR spectra of lPixD (black) and Q50E (red) taken 3 ps post excitation.

There are two surprising features present in the Q50A mutant spectrum and they both appear as transients: the modes at 1628 cm^{-1} and 1668 cm^{-1}. The 1628 cm^{-1} is interesting in that it is in a similar position to the mode observed in lPixD and Y8W that has been assigned as $FADH^{\bullet}$. In lPixD and Y8W, a mode at 1635 cm^{-1} is tentatively assigned as $FADH^{\bullet}$, yet here this mode shows no characteristic rise and decay but rather this is a mode that forms instantaneously and decays with similar kinetics with the main bleach at 1547 cm^{-1} (Figure 6.12). These results indicate that flavin radical formation is not involved in the Q50A mutant. The appearance of the 1668 cm^{-1} transient indicates that this mode does not arise exclusively from the Q50 side chain. It must be a protein mode as it is absent in the free flavin TRIR, and based on its position one can propose it arises from the amide side chain of N31 in the Q50A mutant.

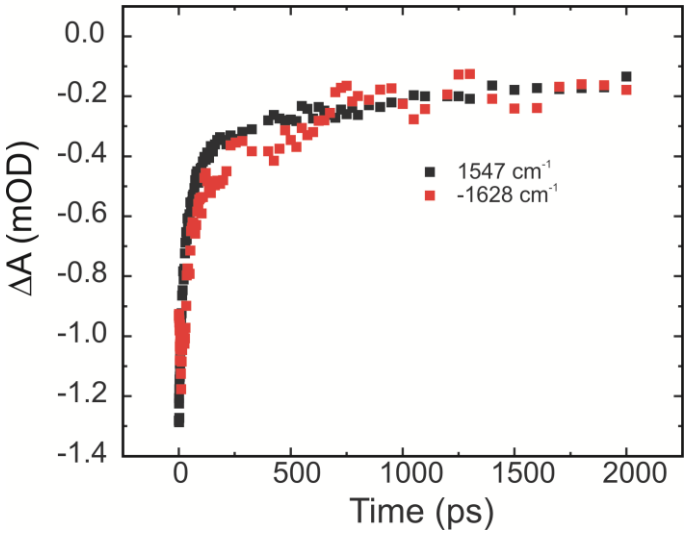

Figure 6.12. **Comparison of 1547 and 1628 cm^{-1} in Q50A.** The kinetics of 1547 and 1628 cm^{-1} overlay. This reveals that formation at 1628 cm^{-1} occurs instantaneously and is not associated with flavin radical formation.

6.3.5.2. Q50E

For comparison, the 3 ps Q50E spectrum has been overlaid with the 3 ps lPixD spectrum (Figure 6.11B). This was performed due to the overlap of what appears to be the C4=O carbonyl of the flavin at 1685 cm^{-1}. Perhaps the most interesting detail in the Q50E spectrum is the presence of a transient at 1707 cm^{-1} and a bleach at 1732 cm^{-1}. Bands at similar position were reported for the Q63E mutant in AppA_{BLUF}, and through isotopic labeling were assigned to the protonated carboxylic side chain of the glutamic acid [38]. This suggests that the pK_a of the Q50E side chain is much higher than the common value for a carboxylic acid (greater than 3 pH units), which has been discussed in detail in the AppA-Q63E mutant [39, 40].

The frequencies of the C4=O flavin carbonyl modes in Q50E and lPixD are quite similar (Figure 6.11B). This was also observed in the Q63E AppA_{BLUF} mutant [38]. As what was previously reported, the protonated carboxylic side chain could serve as an H-bond donor to the C4=O carbonyl and an H-bond acceptor from the conserved Tyr. Direct interaction of the Q50E

side chain with the flavin C4=O carbonyl can also account for the instantaneous response of the protein. Photoexcitation leads to an increase in electron density on the C4=O oxygen in the flavin excited state which would strengthen H-bond interactions between the Q50E side chain and the flavin C4=O carbonyl. Based on the fact that the $AppA_{BLUF}$-Q63E mutant responds instantaneously to blue light excitation, and that the carboxylic acid is isosteric to an enol, a model was proposed in which the light state formation is driven by keto-enol tautomerism that ultimately leads to rotation of the glutamine side chain [38]. This also provides an explanation for the absence of photoactivity in the Q to E mutants in BLUF proteins since Q to E mutants resemble the light activated state. In addition, no transient is observed that could tentatively be assigned to $FADH^{\bullet}$, indicating that Q50 is essential for ET and PT events in PixD.

6.3.6. TRIR of M93A

FTIR light minus dark difference spectroscopy provided key structural insight into the role of M93A in PixD [4]. The primary difference mode associated with the protein in the FTIR difference spectrum was abolished in the M93A mutation, which prevents the protein from undergoing the structural changes necessary to ultimately bind and then PixE upon photoexcitation [4]. For additional insight into how this mutation alters the photochemistry of PixD, the TRIR spectra of dark and light adapted M93A were measured. The spectra reported for the M93A mutant are strikingly similar to the wild type spectra reported (Figure 6.13). There are two distinct TRIR spectra for dark and light adapted M93A, and while the M93A mutation results in a protein that cannot bind PixE, no significant differences are observed in the 3 ps TRIR from wtPixD. A transient can be seen in dM93A at 1668 cm^{-1}, as well as a shift in the C4=O carbonyl from the dark state to the light state.

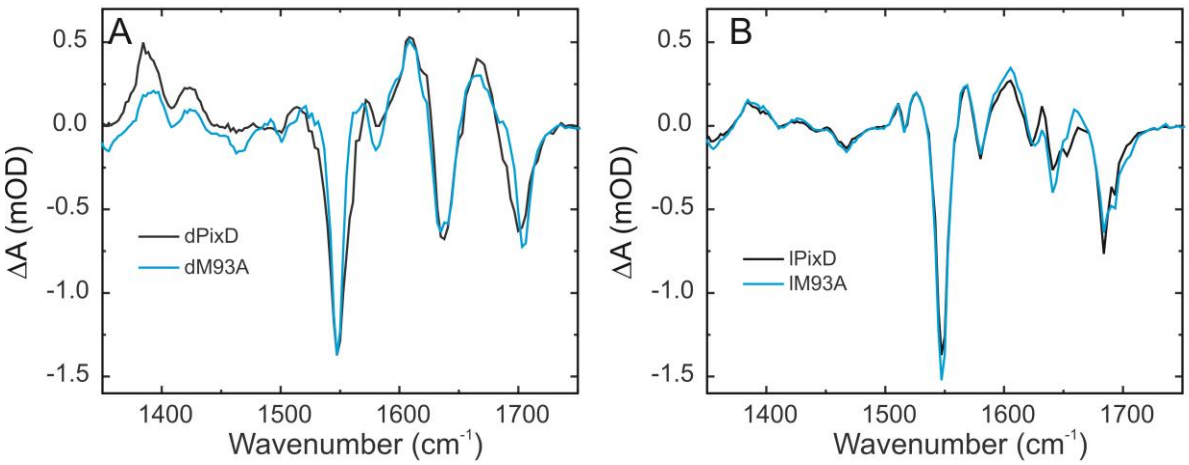

Figure 6.13. TRIR analysis of M93A. TRIR spectra of PixD (black)M93A (blue) taken 3 ps post excitation. **A.** Spectra of dark adapted states. **B.** Spectra of light adapted states.

NMR data on the PixD M93A mutant indicated that the structure exhibited a "pseudo-light" state geometry [12]. Initial observation using TRIR shows that the M93A has two distinct states that are quite similar to wild type. Key flavin modes at 1382, 1547, 1643 cm^{-1} are observed. Comparison of the C4=O mode in d and lM93A shows a 10 cm^{-1} red shift from dark to light, indicative of an increase in H-bonding as a result of photoexcitation.

To better understand what effect the M93A mutant has on PixD, kinetic analysis of key vibrational modes was performed. For dark adapted PixD, kinetics at 1526 and 1623 cm^{-1} indicated the presence of radical intermediates. In dM93A, no radical intermediate was observed (Figure 6.14A). This indicates that the electron transfer observed in PixD is abolished in the M93A mutant. For light adapted M93A (Figure 6.14B-D), we see the appearance of transients at 1526 cm^{-1} (0.8 ± 0.2 ps, 101 ± 8 ps) and 1632 cm^{-1} (1.6. ± 0.2 ps, 636 ± 144 ps) and decay at 1623 cm^{-1} (3.6 ± 0.2 ps, 279 ± 14 ps), all of which are indicative of flavin radical formation with time components in agreement with wtPixD. These results indicate an altered mechanism of light state activation in M93A. The primary step of photoactivation (ET) is disrupted, yet blue light

exciation in M93A results in the characteristic 10 cm^{-1} red shift in the flavin C4=O carbonyl. Therefore, one can conclude that inability to form radical formation is indicative of a disrupted structure that ultimately prevents PixE binding and suggests a mechanism of light state formation similar to $AppA_{BLUF}$ (Chapter 1, 4).

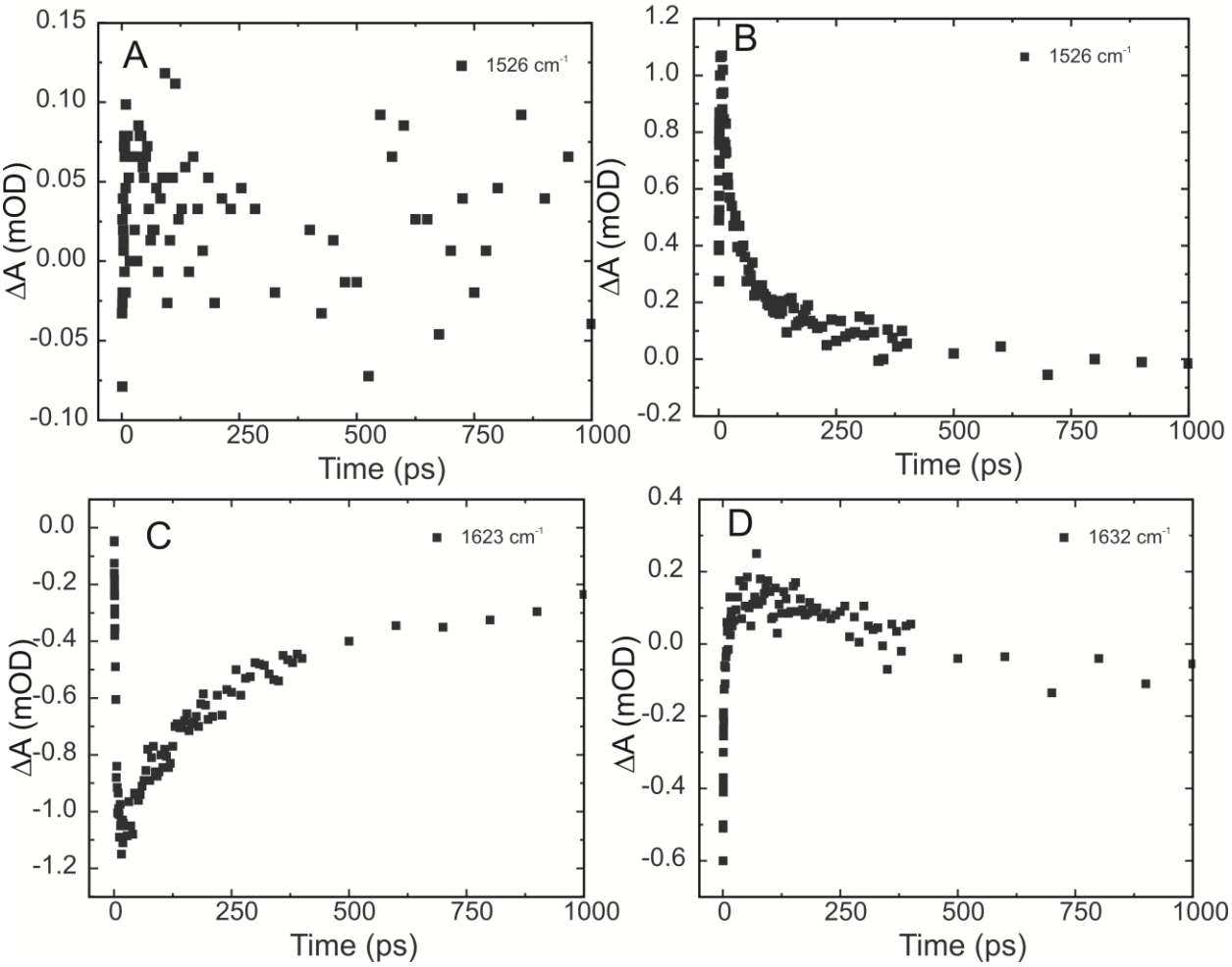

6.14. Kinetic analysis of M93A mutant. A. Kinetics at 1526 cm^{-1} in dM93A, revealing no flavin radical formation. Rise components at 1526 (**B**) and 1632 (**D**) in lM93A, along with decay at 1623 cm^{-1} (**C**) reveal the presence of flavin radicals in lM93A.

6.3.7. Kinetic Analysis

Kinetic analysis was performed for the main bleach at 1547 cm^{-1}, providing insight into the lifetime of the excited state. For the light adapted states, the fast component dominates, while

in the dark adapted states the slow component does. In general, excited state lifetimes reported here for PixD and its mutants are faster than what was previously reported for the N-terminal BLUF domain of AppA [30, 38]. The average ES lifetime, based on the 1547 cm^{-1} recovery for dN31H is longer than wild type, in agreement with previous results and proposed to be the result of an increased redox potential [26]. No difference in ES lifetime is reported for lN31H, indicating that this mutation primarily affects the dark state and its primary events post-photoexcitation. The Y8F mutant exhibits a "dark-like" photorecovery, in agreement with the position of the C4=O carbonyl. In the Y8W mutant, the C4=O carbonyl also overlays with dPixD yet its ES lifetime is more "light-like." The Y8W mutation leads to an increase in the 1631 cm^{-1}, which is only seen in lPixD, indicating that the ES of Y8W is similar to lPixD. The Q50E mutant is also similar to lPixD, which is in agreement with the red-shifted C4=O flavin carbonyl. The Q50A mutant exhibits an ES lifetime that is 1.5 fold longer than dPixD. The TRIR spectra reported for Q50A is unique; the appearance of a 1628 cm^{-1} transient in Q50A is not the result of flavin radical formation. Further characterization of this mode may provide insight into the elongated ES lifetime. For M93A, a ~1.2 fold decrease in the dark state ES and a ~1.2 fold increase in the light adapted ES is reported, however, in agreement with wild-type, the light adapted state recovers faster than the dark state.

Table 6.2. Ground state recovery of PixD and its mutants reported at 1547 cm^{-1}.

Sample	α1	τ1 (ps)	α2	τ2 (ps)	<τ> (ps)
dPixD	0.48	16 ± 2	0.52	159 ± 10	90
lPixD	0.79	12 ± 1	0.21	175 ± 25	46
dN31H	0.49	18 ± 2	0.51	262 ± 18	142
lN31H	0.77	12 ± 1	0.23	170 ± 17	48
Y8F	0.81	28 ± 1	0.19	372 ± 61	93
Y8W	0.66	12 ± 1	0.34	146 ± 12	58
Q50A	0.72	25 ± 1	0.28	425 ± 51	137
Q50E	0.44	9 ± 1	0.56	65 ± 4	40
dM93A	0.57	24 ± 2	0.43	138 ± 15	73
lM93A	0.72	10 ± 1	0.28	167 ± 20	53

6.3.8. TRMPS of PixD

Thus far, a substantial amount of work has been shown characterizing the early (ps to ns) structural events of PixD photoexcitation. However, biological processes occur over a multitude of timescales [41]. To better understand the mechanism of photoactivation, measurements of time resolved IR spectra beyond 1 ns had to be performed. TRMPS is a powerful tool that allows for measurements from pico- to milliseconds, allowing for a complete analysis of all biological processes [42]. The ability of TRMPS to characterize the mechanism of photoactivation for BLUF proteins was highlighted in chapter 4.

Figure 6.15A shows the temporal evolution of PixD from 5 ps to 10 ns. The two highest frequency bleach modes at 1700 and 1650 cm^{-1} are associated with two carbonyl stretches of the FAD ground state, and have been shown to be sensitive to the H-bond environment [24, 30]. The intense bleach at 1547 cm^{-1} and the weaker one at 1580 cm^{-1} are FAD ring modes. The two positive peaks at 1423 cm^{-1} and 1383 cm^{-1} are present in free flavin (Chapter 4) and are

associated with the excited state of the flavin ring but cannot be assigned to specific vibrational modes at this time.

Unlike what was previously reported for AppA, formation of the transient at 1690 cm^{-1} appears to be complete within the first 10 ns. This is further emphasized in Figure 6.14B; no spectral evolution is observed from 10 ns to 20 µs at 1690 cm^{-1} or any mode associated with light state formation. This is in stark contrast to AppA; where evolutions of bands associated with light state formation occur on a microsecond timescale (Chapter 4). For PixD, formation of the light adapted state is on a nanosecond timescale, reaching completion at greater than 1000 fold faster than AppA. A weak band observed at 1438 cm^{-1} was proposed to be possible flavin triplet state based on its presence in the free flavin and is seen in the PixD spectra, again highlighting the possibility of flavin triplet state in the BLUF photocycle.

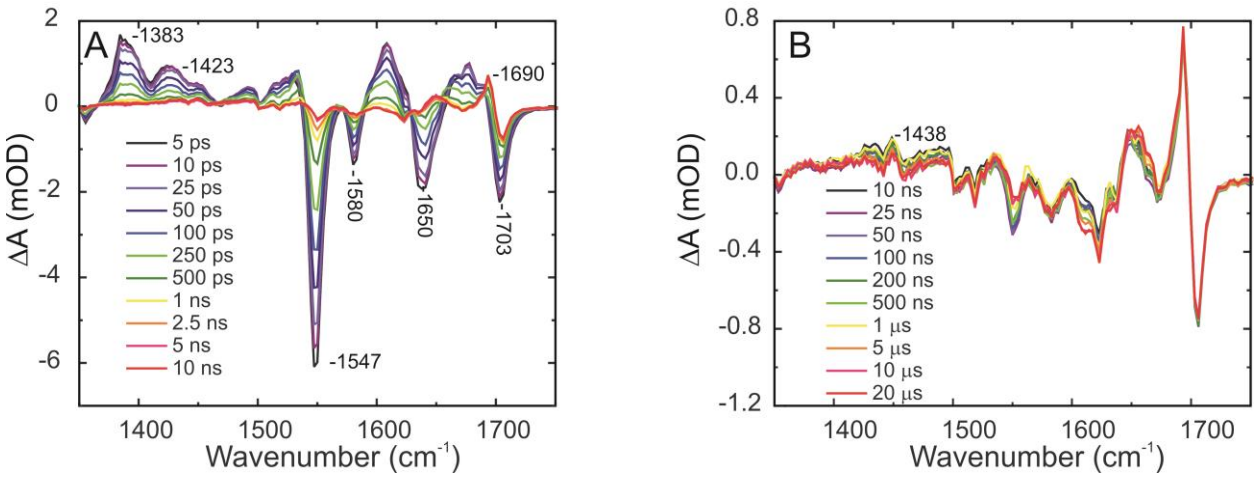

Figure 6.15. TRMPS spectra of PixD. **A.** TRMPS spectra recorded between 2 ps and 10 ns after excitation of the flavin at 450 nm. The fast and complete decay of the singlet excited state is evident in the transient flavin modes at 1383 cm^{-1} and 1423 cm^{-1}. However, the ground state recovery is incomplete e.g. at 1547 cm^{-1} and some transient (probably triplet) state is formed. Bands which previously formed in microseconds in $AppA_{BLUF}$ are now complete within 10 ns. **B.** Relaxation in the PixD spectrum between 10 ns and 20 µs after excitation. The electronic ground state recovers fully (1547 cm^{-1}). No new evolution is observed from 10 ns to 20 µs.

Fitting the kinetics of the main peaks associated with light state formation to an exponential yielded the time components reported in table 6.3, and clearly indicate much faster rate of formation than what was observed for $AppA_{BLUF}$ (Chapter 4). The time components reported are in picoseconds, which is ~10^6 times faster than $AppA_{BLUF}$. The decay of the 1547 cm^{-1} bleach on the nanosecond timescale suggests the possibility of flavin triplet state. At present signal to noise, kinetics associated with the 1438 cm^{-1} transient are unresolvable. The two bands associated with the protein (1622 cm^{-1}, 1652 cm^{-1}) are kinetically distinct from each other; the transient absorption at 1631 cm^{-1} rises in *ca.* 53 ps, which is reproducibly faster than the 35 ps development of the 1622 cm^{-1} bleach (Table 6.3). This result is not unexpected, as the structural changes between the light and dark states are spread over a number of residues that may have slightly different vibrational frequencies [43]. The kinetics associated with changes occurring on more than one residue will be both more complex than a simple first order process and hierarchical in nature.

The weak transient feature at 1690 cm^{-1} develops on a longer timescale than the protein modes (Table 6.3). The 1690 cm^{-1} feature is well resolved in the light minus dark difference spectrum (Figure 6.2). In agreement with $AppA_{BLUF}$, slower structural reorganization occurs in protein residues sufficiently close to the flavin chromophore to be involved in H-bonding with it. This contrasts with the faster changes assigned to the more remote residues in the β-sheet. This again shows that there is no simple relationship between the timescale of the protein response to electronic excitation and distance from the chromophore. Surprisingly, the kinetics associated with the bleach at 1700 cm^{-1} are faster than at 1690 cm^{-1} (Table 6.3.) One probably explanation lies with the timescale. Formation of these bands appears on a similar timescale to GS recovery,

indicating that there are two competing events occurring at the same time, making the kinetics difficult to differentiate between GS recovery and light state formation.

Table 6.3. Kinetic analysis of PixD TRMPS spectra.

Sample	Time (ns)
1547 cm^{-1}	413 ± 107
1622 cm^{-1}	0.035 ± 0.001
1652 cm^{-1}	0.053 ± 0.002
1690 cm^{-1}	0.235 ± 0.005
1700 cm^{-1}	0.085 ± 0.003

6.3.9. Complex Formation

6.3.9.1.FTIR

Positive phototaxic movement of *Synechocystis* is regulated by PixD. *In vivo*, PixD and PixE form a large oligomeric complex that dissociates upon photoexcitation of blue light. Therefore, in order to fully understand the mechanism of blue light sensing in PixD, analysis must be expanded to include the binding partner, PixE. Initial characterization was performed by FTIR spectroscopy. PixE does not contain any functional group that absorbs visible blue light, so any conformational change as a result from blue light excitation must arise from PixD. The FTIR light minus dark difference spectra of PixD in the presence and absence of PixE are reported in Figure 6.15, revealing no spectral difference. This result indicates that the final structure formed as a result of photoexcitation is independent of PixE.

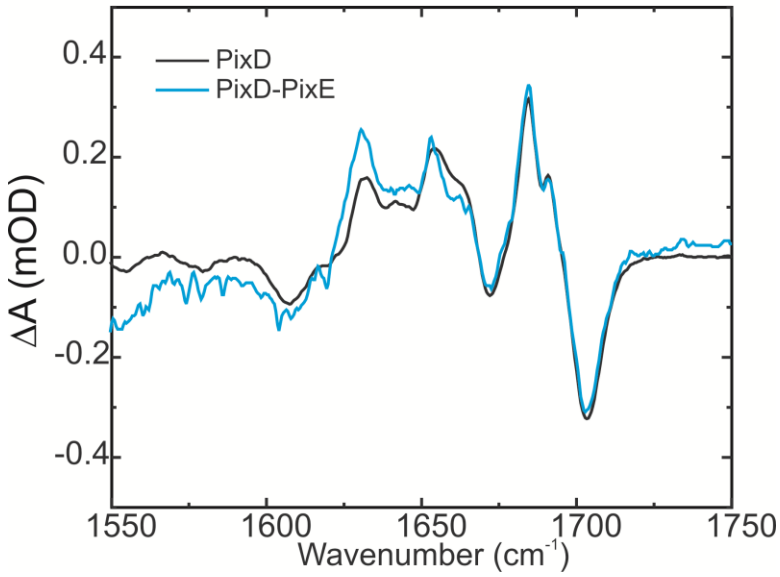

Figure 6.16. FTIR of PixD-PixE complex. Light minus dark difference spectra of PixD (black) overlaid with PixD-PixE complex. Light states were generated by irradiation of 460 nm light for 3 min.

6.3.9.2. TRIR of PixD-PixE

Stationary state FTIR spectroscopy did not reveal structural differences between PixD in the presence and absence of PixE. To investigate the primary steps post-excitation, ultrafast infrared spectra were generated for the PixD-PixE complex. Figure 6.16 shows the TRIR spectra of PixD with PixE at 3 ps post excitation and are overlaid with the spectra of PixD in the absence of PixE. The main bleaches associated with the flavin 1547 cm^{-1}, 1585 cm^{-1}, 1650 cm^{-1} and 1700 cm^{-1} are all not perturbed by binding of PixE. Photoactive markers at 1665 cm^{-1} and the 10 cm^{-1} red shift in the C4=O carbonyl flavin mode (1700 to 1690 cm^{-1}), all suggest a similar mechanism for photoexcitation of PixD with PixE. A large transient is observed at 1382 cm^{-1}, which is present in free flavin and therefore must be associated with flavin excited state. The binding site of PixE is proposed to be near the C-terminus of PixD, away from the flavin binding pocket, and these results suggest that the binding of the cofactor is relatively unaffected by PixE binding.

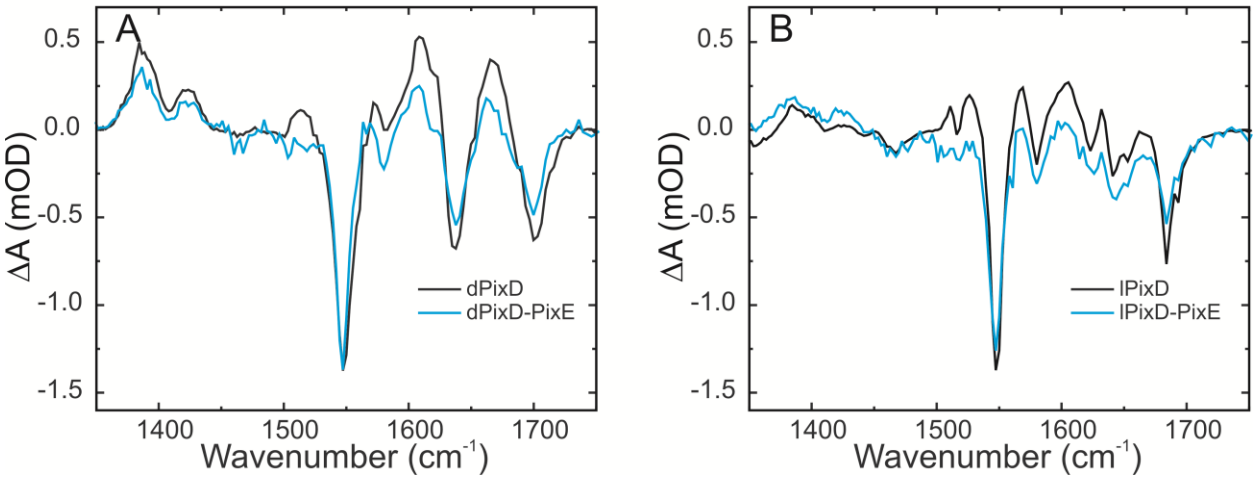

Figure 6.17. TRIR of PixD-PixE complex. TRIR spectra taken 3 ps post-excitation of PixD (black) and the PixD-PixE complex (blue). **A.** Spectra of dark states. **B.** Spectra of light adapted states.

In this chapter, it has been well established that PixD undergoes an electron transfer event upon photoexcitation, which ultimately results in rotation of the amide side chain of Q50. This was observed by the formation of a transient at 1526 cm^{-1} in d and lPixD as well as a transient at 1631 cm^{-1} in lPixD, only. Based on previous findings, it has been proposed that these modes correspond to two unique flavin radical states and can thusly explain the absence of photoreversility in PixD. In the TRIR spectra reported for the complex, characteristic modes associated with light state formation are observed. Further examination of the TRIR spectra was performed, in particular with these modes associated with flavin radical formation. Plotting the kinetics at 1526 cm^{-1} for d and l PixD-PixE as well as 1631 cm^{-1} in lPixD-PixE revealed the absence of any formation dynamics.

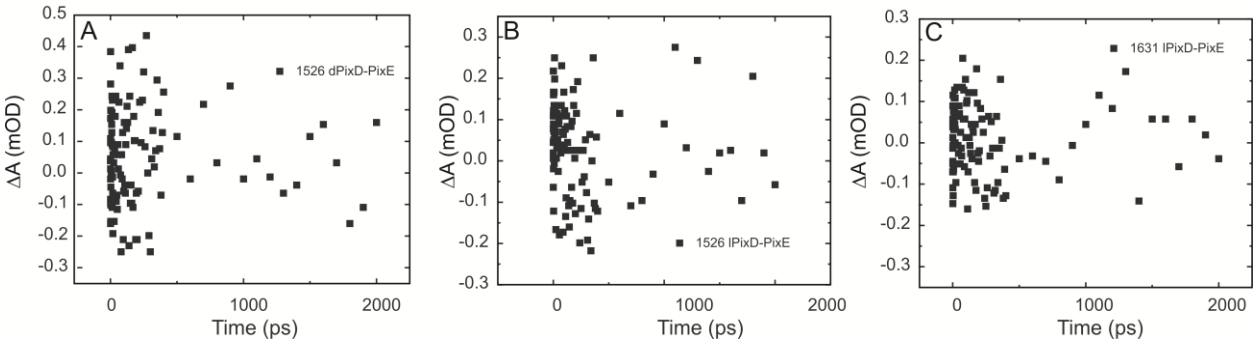

Figure 6.18. Kinetics associated with flavin radicals in PixD-PixE complex. Kinetics at 1526 cm^{-1} for dPixD-PixE (**A**) and lPixD-PixE (**B**), as well as at 1631 cm^{-1} in lPixD-PixE (**C**) are unresolvable at this time.

The absence of these modes can be attributed to two hypotheses; at present time the kinetics are unresolvable or that flavin radicals are an artifact of PixD photoexcitation in the absence of PixE. If the data of the main bleach is plotted for the complex (table 6.4), one can see the introduction of higher degrees of error, in particular with the long-lived component in the light adapted measurement. This suggests a signal to noise concern, which would explain the absence of resolvable flavin radical kinetics. At the present time, it is difficult to draw a significant conclusion giving these data.

Table 6.4. TRIR kinetics of PixD and PixD-PixE complex.

Sample	α1	τ1 (ps)	α2	t2 (ps)	<τ> (ps)
dPixD	0.48	16 ± 2	0.52	159 ±10	90
lPixD	0.79	12 ± 1	0.21	175 ± 25	46
dPixD-PixE	0.47	20 ± 11	0.53	163 ± 55	96
lPixD-PixE	0.75	15 ± 2	0.25	800 ± 600	N.D.

6.4. Conclusions

PixD is a standalone BLUF protein that binds a partner protein in order to relay the signal produced by irradiation, in contrast to the multidomain protein, AppA. To further investigate the mechanism of photoactivation in BLUF proteins PixD was chosen as a model standalone BLUF protein. In stark contrast to the reported TRIR spectra for $AppA_{BLUF}$, the presence of flavin radical intermediates were observed in dPixD. These results indicate that ET is the primary mechanism of photoactivation in PixD. Initial analysis was conducted on the tyrosine mutants, Y8F and Y8W. In the Y8F mutant, no transient at ~1670 cm^{-1} was observed, revealing the necessity of tyrosine at this position to initiate the protein's response to flavin excitation. No ET intermediates were observed in the Q50 mutants, indicating that Q50 functions as a "wire" from the conserved tyrosine to the flavin, thus initiating flavin radical formation. Expanding the analysis to longer timescales revealed that the photocycle of PixD is complete on the nanosecond timescale, in stark contrast to $AppA_{BLUF}$ (microseconds). These data suggest differing mechanisms for multidomain and standalone BLUF proteins.

6.5. References

1. Losi, A. and W. Gärtner, *Old chromophores, new photoactivation paradigms, trendy applications: Flavins in blue light-sensing photoreceptors.* Photochem Photobiol, 2011. **87**(3): p. 491-510.
2. Okajima, K., S. Yoshihara, Y. Fukushima, X. Geng, M. Katayama, S. Higashi, M. Watanabe, S. Sato, S. Tabata, Y. Shibata, S. Itoh, and M. Ikeuchi, *Biochemical and functional characterization of BLUF-type flavin-binding proteins of two species of Cyanobacteria.* J Biochem, 2005. **137**(6): p. 741-750.

3. Fiedler, B., T. Börner, and A. Wilde, *Phototaxis in the cyanobacterium synechocystis sp. PCC 6803: Role of different photoreceptors.* Photochem Photobiol, 2005. **81**(6): p. 1481-1488.

4. Masuda, S., K. Hasegawa, H. Ohta, and T.-a. Ono, *Crucial role in light signal transduction for the conserved Met93 of the BLUF protein PixD/Slr1694.* Plant Cell Physiol, 2008. **49**(10): p. 1600-1606.

5. Masuda, S., K. Hasegawa, A. Ishii, and T.-a. Ono, *Light-induced structural changes in a putative blue-light receptor with a novel FAD binding fold sensor of blue-light using FAD (BLUF); Slr1694 of Synechocystis sp. PCC6803.* Biochemistry, 2004. **43**(18): p. 5304-5313.

6. Anderson, S., V. Dragnea, S. Masuda, J. Ybe, K. Moffat, and C. Bauer, *Structure of a novel photoreceptor, the BLUF domain of AppA from Rhodobacter sphaeroides.* Biochemistry, 2005. **44**(22): p. 7998-8005.

7. Jung, A., J. Reinstein, T. Domratcheva, R.L. Shoeman, and I. Schlichting, *Crystal structures of the AppA BLUF domain photoreceptor provide insights into blue light-mediated signal transduction.* J Mol Biol, 2006. **362**(4): p. 717-732.

8. Grinstead, J.S., M. Avila-Perez, K.J. Hellingwerf, R. Boelens, and R. Kaptein, *Light-induced flipping of a conserved glutamine sidechain and its orientation in the AppA BLUF domain.* J Am Chem Soc, 2006. **128**(47): p. 15066-15067.

9. Laan, W., M.A. van der Horst, I.H. van Stokkum, and K.J. Hellingwerf, *Initial characterization of the primary photochemistry of AppA, a blue-light-using flavin adenine dinucleotide-domain containing transcriptional antirepressor protein from Rhodobacter sphaeroides: a key role for reversible intramolecular proton transfer from*

the flavin adenine dinucleotide chromophore to a conserved tyrosine? Photochem Photobiol, 2003. **78**(3): p. 290-7.

10. Yuan, H., S. Anderson, S. Masuda, V. Dragnea, K. Moffat, and C. Bauer, *Crystal structures of the Synechocystis photoreceptor Slr1694 reveal distinct structural states related to signaling.* Biochemistry, 2006. **45**(42): p. 12687-12694.
11. Yuan, H. and C.E. Bauer, *PixE promotes dark oligomerization of the BLUF photoreceptor PixD.* Proc. Nat. Acad. Sci., 2008. **105**(33): p. 11715-11719.
12. Yuan, H., V. Dragnea, Q. Wu, K.H. Gardner, and C.E. Bauer, *Mutational and structural studies of the PixD BLUF output signal that affects light-regulated interactions with PixE.* Biochemistry, 2011. **50**(29): p. 6365-6375.
13. Tanaka, K., Y. Nakasone, K. Okajima, M. Ikeuchi, S. Tokutomi, and M. Terazima, *Time-resolved tracking of interprotein signal transduction: Synechocystis PixD–PixE complex as a sensor of light Intensity.* J Am Chem Soc, 2012. **134**(20): p. 8336-8339.
14. Kita, A., K. Okajima, Y. Morimoto, M. Ikeuchi, and K. Miki, *Structure of a cyanobacterial BLUF protein, Tll0078, containing a novel FAD-binding blue light sensor domain.* J Mol Biol, 2005. **349**(1): p. 1-9.
15. Okajima, K., Y. Fukushima, H. Suzuki, A. Kita, Y. Ochiai, M. Katayama, Y. Shibata, K. Miki, T. Noguchi, S. Itoh, and M. Ikeuchi, *Fate determination of the flavin photoreceptions in the cyanobacterial blue light receptor TePixD (Tll0078).* J Mol Biol, 2006. **363**(1): p. 10-8.
16. Ren, S., R. Sato, K. Hasegawa, H. Ohta, and S. Masuda, *A predicted structure for the PixD–PixE complex determined by homology modeling, docking simulations, and a mutagenesis study.* Biochemistry, 2013. **52**(7): p. 1272-1279.

17. Ren, S., M. Sawada, K. Hasegawa, Y. Hayakawa, H. Ohta, and S. Masuda, *A PixD—PapB Chimeric Protein Reveals the Function of the BLUF Domain C-Terminal α-Helices for Light Signal Transduction.* Plant Cell Physiol, 2012. **53**(9): p. 1638-1647.

18. Barends, T.R.M., E. Hartmann, J.J. Griese, T. Beitlich, N.V. Kirienko, D.A. Ryjenkov, J. Reinstein, R.L. Shoeman, M. Gomelsky, and I. Schlichting, *Structure and mechanism of a bacterial light-regulated cyclic nucleotide phosphodiesterase.* Nature, 2009. **459**(7249): p. 1015-1018.

19. Berthomieu, C. and R. Hienerwadel, *Vibrational spectroscopy to study the properties of redox-active tyrosines in photosystem II and other proteins.* Biochim Biophys Acta, 2005. **1707**(1): p. 51-66.

20. Gauden, M., J.S. Grinstead, W. Laan, I.H. van Stokkum, M. Avila-Perez, K.C. Toh, R. Boelens, R. Kaptein, R. van Grondelle, K.J. Hellingwerf, and J.T. Kennis, *On the role of aromatic side chains in the photoactivation of BLUF domains.* Biochemistry, 2007. **46**(25): p. 7405-15.

21. Bonetti, C., T. Mathes, I.H.M. van Stokkum, K.M. Mullen, M.-L. Groot, R. van Grondelle, P. Hegemann, and J.T.M. Kennis, *Hydrogen bond switching among flavin and amino acid side chains in the BLUF photoreceptor observed by ultrafast infrared spectroscopy.* Biophys J, 2008. **95**(10): p. 4790-4802.

22. Bonetti, C., M. Stierl, T. Mathes, I.H.M. van Stokkum, K.M. Mullen, T.A. Cohen-Stuart, R. van Grondelle, P. Hegemann, and J.T.M. Kennis, *The role of key amino acids in the photoactivation pathway of the Synechocystis Slr1694 BLUF domain.* Biochemistry, 2009. **48**(48): p. 11458-11469.

23. Masuda, S. and C.E. Bauer, *AppA Is a blue light photoreceptor that antirepresses photosynthesis gene expression in Rhodobacter sphaeroides.* Cell, 2002. **110**(5): p. 613-623.

24. Haigney, A., A. Lukacs, R. Brust, R.-K. Zhao, M. Towrie, G.M. Greetham, I. Clark, B. Illarionov, A. Bacher, R.-R. Kim, M. Fischer, S.R. Meech, and P.J. Tonge, *Vibrational assignment of the ultrafast infrared spectrum of the photoactivatable flavoprotein AppA.* J Phys Chem B, 2012. **116**(35): p. 10722-10729.

25. Masuda, S., K. Hasegawa, and T.-a. Ono, *Light-induced structural changes of apoprotein and chromophore in the sensor of blue light using FAD (BLUF) domain of AppA for a signaling state* Biochemistry, 2005. **44**(4): p. 1215-1224.

26. Mathes, T., I.H.M. van Stokkum, M. Stierl, and J.T.M. Kennis, *Redox modulation of flavin and tyrosine determines photoinduced proton-coupled electron transfer and photoactivation of BLUF photoreceptors.* J Biol Chem, 2012. **287**(38): p. 31725-31738.

27. Hasegawa, K., S. Masuda, and T.-a. Ono, *Spectroscopic analysis of the dark relaxation process of a photocycle in a sensor of blue light using FAD (BLUF) protein Slr1694 of the cyanobacterium Synechocystis sp. PCC6803.* Plant Cell Physiol, 2005. **46**(1): p. 136-146.

28. Masuda, S., K. Hasegawa, and T.-a. Ono, *Tryptophan at position 104 is involved in transforming light signal into changes of β-sheet structure for the signaling state in the BLUF domain of AppA.* Plant Cell Physiol, 2005. **46**(12): p. 1894-1901.

29. Kondo, M., J. Nappa, K.L. Ronayne, A.L. Stelling, P.J. Tonge, and S.R. Meech, *Ultrafast vibrational spectroscopy of the flavin chromophore.* J Phys Chem B, 2006. **110**(41): p. 20107-20110.

30. Haigney, A., A. Lukacs, R.-K. Zhao, A.L. Stelling, R. Brust, R.-R. Kim, M. Kondo, I. Clark, M. Towrie, G.M. Greetham, B. Illarionov, A. Bacher, W. Romisch-Margl, M. Fischer, S.R. Meech, and P.J. Tonge, *Ultrafast infrared spectroscopy of an isotope-labeled photoactivatable flavoprotein.* Biochemistry, 2011. **50**(8): p. 1321-1328.

31. Stelling, A.L., K.L. Ronayne, J. Nappa, P.J. Tonge, and S.R. Meech, *Ultrafast structural dynamics in BLUF domains: Transient infrared spectroscopy of AppA and its mutants.* J Am Chem Soc, 2007. **129**(50): p. 15556-15564.

32. Kennis, J.T. and M.L. Groot, *Ultrafast spectroscopy of biological photoreceptors.* Curr Opin Struct Biol, 2007. **17**(5): p. 623-30.

33. Zhao, R.-K., A. Lukacs, A. Haigney, R. Brust, G.M. Greetham, M. Towrie, P.J. Tonge, and S.R. Meech, *Ultrafast transient mid IR to visible spectroscopy of fully reduced flavins.* Phys Chem Chem Phys, 2011. **13**(39): p. 17642-17648.

34. Lukacs, A., R.K. Zhao, A. Haigney, R. Brust, G.M. Greetham, M. Towrie, P.J. Tonge, and S.R. Meech, *Excited state structure and dynamics of the neutral and anionic flavin radical revealed by ultrafast transient mid-IR to visible spectroscopy.* J Phys Chem B, 2012. **116**(20): p. 5810-8.

35. Toh, K.C., I.H.M. van Stokkum, J. Hendriks, M.T.A. Alexandre, J.C. Arents, M.A. Perez, R. van Grondelle, K.J. Hellingwerf, and J.T.M. Kennis, *On the signaling mechanism and the absence of photoreversibility in the AppA BLUF domain.* Biophys J, 2008. **95**(1): p. 312-321.

36. Barth, A., *The infrared absorption of amino acid side chains.* Prog Biophys Mol Biol, 2000. **74**(3–5): p. 141-173.

37. Barth, A., *Infrared spectroscopy of proteins.* Biochim Biophys Acta, 2007. **1767**(9): p. 1073-1101.

38. Lukacs, A., A. Haigney, R. Brust, R.K. Zhao, A.L. Stelling, I.P. Clark, M. Towrie, G.M. Greetham, S.R. Meech, and P.J. Tonge, *Photoexcitation of the blue light using FAD photoreceptor AppA results in ultrafast changes to the protein matrix.* J Am Chem Soc, 2011. **133**(42): p. 16893-900.

39. Tonge, P., G.R. Moore, and C.W. Wharton, *Fourier-transform infra-red studies of the alkaline isomerization of mitochondrial cytochrome c and the ionization of carboxylic acids.* Biochem J, 1989. **258**(2): p. 599-605.

40. Kottke, T., A. Batschauer, M. Ahmad, and J. Heberle, *Blue-Light-Induced Changes in Arabidopsis Cryptochrome 1 Probed by FTIR Difference Spectroscopy.* Biochemistry, 2006. **45**(8): p. 2472-2479.

41. Henzler-Wildman, K.A., M. Lei, V. Thai, S.J. Kerns, M. Karplus, and D. Kern, *A hierarchy of timescales in protein dynamics is linked to enzyme catalysis.* Nature, 2007. **450**(7171): p. 913-916.

42. Greetham, G.M., D. Sole, I.P. Clark, A.W. Parker, M.R. Pollard, and M. Towrie, *Time-resolved multiple probe spectroscopy.* Rev Sci Instrum, 2012. **83**(10): p. 103107-5.

43. Wu, Q., W.H. Ko, and K.H. Gardner, *Structural requirements for key residues and auxiliary portions of a BLUF domain.* Biochemistry, 2008. **47**(39): p. 10271-80.

Bibliography

Chapter 1

1. Losi, A. and W. Gärtner, *The evolution of flavin-binding photoreceptors: An ancient chromophore serving trendy blue-light sensors.* Annu Rev Plant Biol, 2012. **63**(1): p. 49-72.
2. Losi, A. and W. Gartner, *Bacterial bilin- and flavin-binding photoreceptors.* Photochem Photobiol Sci, 2008. **7**(10): p. 1168-1178.
3. Losi, A., *The bacterial counterparts of plant phototropins.* Photochem. Photobiol. Sci., 2004. **3**(6): p. 566-574.
4. Losi, A. and W. Gärtner, *Old chromophores, new photoactivation paradigms, trendy applications: Flavins in blue light-sensing photoreceptors.* Photochem Photobiol, 2011. **87**(3): p. 491-510.
5. van der Horst, M.A. and K.J. Hellingwerf, *Photoreceptor proteins, "star actors of modern times": a review of the functional dynamics in the structure of representative members of six different photoreceptor families.* Acc Chem Res, 2004. **37**(1): p. 13-20.
6. Kort, R., W.D. Hoff, M. Van West, A.R. Kroon, S.M. Hoffer, K.H. Vlieg, W. Crielaand, J.J. Van Beeumen, and K.J. Hellingwerf, *The xanthopsins: a new family of eubacterial blue-light photoreceptors.* EMBO J, 1996. **15**(13): p. 3209-18.
7. Rockwell, N.C., Y.S. Su, and J.C. Lagarias, *Phytochrome structure and signaling mechanisms.* Annu Rev Plant Biol, 2006. **57**: p. 837-58.
8. Losi, A., E. Polverini, B. Quest, and W. Gärtner, *First evidence for phototropin-related blue-light receptors in prokaryotes.* Biophys J, 2002. **82**(5): p. 2627-2634.

9. Kottke, T., P. Hegemann, B. Dick, and J. Heberle, *The photochemistry of the light-, oxygen-, and voltage-sensitive domains in the algal blue light receptor phot.* Biopolymers, 2006. **82**(4): p. 373-378.

10. Chaves, I., R. Pokorny, M. Byrdin, N. Hoang, T. Ritz, K. Brettel, L.-O. Essen, G.T.J. van der Horst, A. Batschauer, and M. Ahmad, *The cryptochromes: Blue light photoreceptors in plants and animals.* Annu Rev Plant Biol, 2011. **62**(1): p. 335-364.

11. Li, Q.-H. and H.-Q. Yang, *Cryptochrome signaling in plants.* Photochem Photobiol, 2007. **83**(1): p. 94-101.

12. Gomelsky, M. and G. Klug, *BLUF: a novel FAD-binding domain involved in sensory transduction in microorganisms.* Trends Biochem Sci, 2002. **27**(10): p. 497-500.

13. Kao, Y.-T., C. Saxena, T.-F. He, L. Guo, L. Wang, A. Sancar, and D. Zhong, *Ultrafast dynamics of flavins in five redox states.* J Am Chem Soc, 2008. **130**(39): p. 13132-13139.

14. Rieff, B., S. Bauer, G. Mathias, and P. Tavan, *IR Spectra of flavins in solution: DFT/MM description of redox effects.* J Phys Chem B, 2011. **115**(9): p. 2117-2123.

15. Briggs, W.R., *The LOV domain: a chromophore module servicing multiple photoreceptors.* J Biomed Sci, 2007. **14**(4): p. 499-504.

16. Masuda, S., *Light detection and signal transduction in the BLUF photoreceptors.* Plant Cell Physiol, 2013. **54**(2): p. 171-179.

17. Christie, J.M., J. Gawthorne, G. Young, N.J. Fraser, and A.J. Roe, *LOV to BLUF: Flavoprotein contributions to the optogenetic toolkit.* Mol Plant, 2012. **5**(3): p. 533-544.

18. Yin, T. and Y. Wu, *Guiding lights: recent developments in optogenetic control of biochemical signals.* Pflugers Archiv, 2013. **465**(3): p. 397-408.

19. Iseki, M., S. Matsunaga, A. Murakami, K. Ohno, K. Shiga, K. Yoshida, M. Sugai, T. Takahashi, T. Hori, and M. Watanabe, *A blue-light-activated adenylyl cyclase mediates photoavoidance in Euglena gracilis.* Nature, 2002. **415**(6875): p. 1047-51.

20. Okajima, K., Y. Fukushima, H. Suzuki, A. Kita, Y. Ochiai, M. Katayama, Y. Shibata, K. Miki, T. Noguchi, S. Itoh, and M. Ikeuchi, *Fate determination of the flavin photoreceptions in the cyanobacterial blue light receptor TePixD (Tll0078).* J Mol Biol, 2006. **363**(1): p. 10-8.

21. Tanaka, K., Y. Nakasone, K. Okajima, M. Ikeuchi, S. Tokutomi, and M. Terazima, *A way to sense light intensity: Multiple-excitation of the BLUF photoreceptor TePixD suppresses conformational change.* FEBS Lett, 2011. **585**(5): p. 786-790.

22. Zirak, P., A. Penzkofer, T. Schiereis, P. Hegemann, A. Jung, and I. Schlichting, *Photodynamics of the small BLUF protein BlrB from Rhodobacter sphaeroides.* J Photochem Photobiol B, 2006. **83**(3): p. 180-194.

23. Mathes, T., I.H.M. van Stokkum, C. Bonetti, P. Hegemann, and J.T.M. Kennis, *The hydrogen-bond switch reaction of the Blrb BLUF domain of Rhodobacter sphaeroides.* J Phys Chem B, 2011. **115**(24): p. 7963-7971.

24. Okajima, K., S. Yoshihara, Y. Fukushima, X. Geng, M. Katayama, S. Higashi, M. Watanabe, S. Sato, S. Tabata, Y. Shibata, S. Itoh, and M. Ikeuchi, *Biochemical and functional characterization of BLUF-type flavin-binding proteins of two species of Cyanobacteria.* J Biochem, 2005. **137**(6): p. 741-750.

25. Yuan, H., V. Dragnea, Q. Wu, K.H. Gardner, and C.E. Bauer, *Mutational and structural studies of the PixD BLUF output signal that affects light-regulated interactions with PixE.* Biochemistry, 2011. **50**(29): p. 6365-6375.

26. Anderson, S., V. Dragnea, S. Masuda, J. Ybe, K. Moffat, and C. Bauer, *Structure of a novel photoreceptor, the BLUF domain of AppA from Rhodobacter sphaeroides.* Biochemistry, 2005. **44**(22): p. 7998-8005.

27. Jung, A., J. Reinstein, T. Domratcheva, R.L. Shoeman, and I. Schlichting, *Crystal structures of the AppA BLUF domain photoreceptor provide insights into blue light-mediated signal transduction.* J Mol Biol, 2006. **362**(4): p. 717-732.

28. Wu, Q. and K.H. Gardner, *Structure and insight into blue light-induced changes in the BlrP1 BLUF domain.* Biochemistry, 2009. **48**(12): p. 2620-2629.

29. Yuan, H., S. Anderson, S. Masuda, V. Dragnea, K. Moffat, and C. Bauer, *Crystal structures of the Synechocystis photoreceptor Slr1694 reveal distinct structural states related to signaling.* Biochemistry, 2006. **45**(42): p. 12687-12694.

30. Laan, W., M.A. van der Horst, I.H. van Stokkum, and K.J. Hellingwerf, *Initial characterization of the primary photochemistry of AppA, a blue-light-using flavin adenine dinucleotide-domain containing transcriptional antirepressor protein from Rhodobacter sphaeroides: a key role for reversible intramolecular proton transfer from the flavin adenine dinucleotide chromophore to a conserved tyrosine?* Photochem Photobiol, 2003. **78**(3): p. 290-7.

31. Grinstead, J.S., M. Avila-Perez, K.J. Hellingwerf, R. Boelens, and R. Kaptein, *Light-induced flipping of a conserved glutamine sidechain and its orientation in the AppA BLUF domain.* J Am Chem Soc, 2006. **128**(47): p. 15066-15067.

32. Masuda, S., K. Hasegawa, A. Ishii, and T.-a. Ono, *Light-induced structural changes in a putative blue-light receptor with a novel FAD binding fold sensor of blue-light using*

FAD (BLUF); Slr1694 of Synechocystis sp. PCC6803. Biochemistry, 2004. **43**(18): p. 5304-5313.

33. Laan, W., M. Gauden, S. Yeremenko, R. van Grondelle, J.T.M. Kennis, and K.J. Hellingwerf, *On the mechanism of activation of the BLUF domain of AppA.* Biochemistry, 2005. **45**(1): p. 51-60.

34. Kita, A., K. Okajima, Y. Morimoto, M. Ikeuchi, and K. Miki, *Structure of a cyanobacterial BLUF protein, Tll0078, containing a novel FAD-binding blue light sensor domain.* J Mol Biol, 2005. **349**(1): p. 1-9.

35. Masuda, S. and C.E. Bauer, *AppA Is a blue light photoreceptor that antirepresses photosynthesis gene expression in Rhodobacter sphaeroides.* Cell, 2002. **110**(5): p. 613-623.

36. Pandey, R., D. Flockerzi, Marcus J.B. Hauser, and R. Straube, *Modeling the light- and redox-dependent interaction of PpsR/AppA in Rhodobacter sphaeroides.* Biophys J, 2011. **100**(10): p. 2347-2355.

37. Kim, S.K., J.T. Mason, D.B. Knaff, C.E. Bauer, and A.T. Setterdahl, *Redox properties of the Rhodobacter sphaeroides transcriptional regulatory proteins PpsR and AppA.* Photosynth. Res., 2006. **89**(2-3): p. 89-98.

38. Pandey, R., D. Flockerzi, M.J.B. Hauser, and R. Straube, *An extended model for the repression of photosynthesis genes by the AppA/PpsR system in Rhodobacter sphaeroides.* FEBS J, 2012. **279**(18): p. 3449-3461.

39. Gauden, M., S. Yeremenko, W. Laan, I.H. van Stokkum, J.A. Ihalainen, R. van Grondelle, K.J. Hellingwerf, and J.T. Kennis, *Photocycle of the flavin-binding*

photoreceptor AppA, a bacterial transcriptional antirepressor of photosynthesis genes. Biochemistry, 2005. **44**(10): p. 3653-62.

40. Masuda, S., K. Hasegawa, and T.-a. Ono, *Tryptophan at position 104 is involved in transforming light signal into changes of β-sheet structure for the signaling state in the BLUF domain of AppA.* Plant Cell Physiol, 2005. **46**(12): p. 1894-1901.

41. Masuda, S., K. Hasegawa, H. Ohta, and T.-a. Ono, *Crucial role in light signal transduction for the conserved Met93 of the BLUF protein PixD/Slr1694.* Plant Cell Physiol, 2008. **49**(10): p. 1600-1606.

42. Dragnea, V., A.I. Arunkumar, H. Yuan, D.P. Giedroc, and C.E. Bauer, *Spectroscopic studies of the AppA BLUF domain from Rhodobacter sphaeroides: Addressing movement of tryptophan 104 in the signaling state.* Biochemistry, 2009. **48**(42): p. 9969-9979.

43. Grinstead, J.S., S.-T.D. Hsu, W. Laan, A.M.J.J. Bonvin, K.J. Hellingwerf, R. Boelens, and R. Kaptein, *The solution structure of the AppA BLUF domain: Insight into the mechanism of light-induced signaling.* ChemBioChem, 2006. **7**(1): p. 187-193.

44. Unno, M., R. Sano, S. Masuda, T.A. Ono, and S. Yamauchi, *Light-induced structural changes in the active site of the BLUF domain in AppA by Raman spectroscopy.* J Phys Chem B, 2005. **109**(25): p. 12620-6.

45. Unno, M., S. Kikuchi, and S. Masuda, *Structural refinement of a key tryptophan residue in the BLUF photoreceptor AppA by ultraviolet resonance Raman spectroscopy.* Biophys J, 2010. **98**(9): p. 1949-1956.

46. Kondo, M., J. Nappa, K.L. Ronayne, A.L. Stelling, P.J. Tonge, and S.R. Meech, *Ultrafast vibrational spectroscopy of the flavin chromophore.* J Phys Chem B, 2006. **110**(41): p. 20107-20110.

47. Bowman, W.D. and T.G. Spiro, *Normal mode analysis of lumiflavin and interpretation of resonance Raman spectra of flavoproteins.* Biochemistry, 1981. **20**(11): p. 3313-3318.

48. Venyaminov, S.Y. and N.N. Kalnin, *Quantitative IR spectrophotometry of peptide compounds in water (H2O) solutions. II. Amide absorption bands of polypeptides and fibrous proteins in α-, β-, and random coil conformations.* Biopolymers, 1990. **30**(13-14): p. 1259-1271.

49. Barth, A., *Infrared spectroscopy of proteins.* Biochim Biophys Acta, 2007. **1767**(9): p. 1073-1101.

50. Masuda, S., K. Hasegawa, and T.-a. Ono, *Light-induced structural changes of apoprotein and chromophore in the sensor of blue light using FAD (BLUF) domain of AppA for a signaling state* Biochemistry, 2005. **44**(4): p. 1215-1224.

51. Stelling, A.L., K.L. Ronayne, J. Nappa, P.J. Tonge, and S.R. Meech, *Ultrafast structural dynamics in BLUF domains: Transient infrared spectroscopy of AppA and its mutants.* J Am Chem Soc, 2007. **129**(50): p. 15556-15564.

52. Haigney, A., A. Lukacs, R.-K. Zhao, A.L. Stelling, R. Brust, R.-R. Kim, M. Kondo, I. Clark, M. Towrie, G.M. Greetham, B. Illarionov, A. Bacher, W. Romisch-Margl, M. Fischer, S.R. Meech, and P.J. Tonge, *Ultrafast infrared spectroscopy of an isotope-labeled photoactivatable flavoprotein.* Biochemistry, 2011. **50**(8): p. 1321-1328.

53. Haigney, A., A. Lukacs, R. Brust, R.-K. Zhao, M. Towrie, G.M. Greetham, I. Clark, B. Illarionov, A. Bacher, R.-R. Kim, M. Fischer, S.R. Meech, and P.J. Tonge, *Vibrational assignment of the ultrafast infrared spectrum of the photoactivatable flavoprotein AppA.* J Phys Chem B, 2012. **116**(35): p. 10722-10729.

54. Toh, K.C., I.H.M. van Stokkum, J. Hendriks, M.T.A. Alexandre, J.C. Arents, M.A. Perez, R. van Grondelle, K.J. Hellingwerf, and J.T.M. Kennis, *On the signaling mechanism and the absence of photoreversibility in the AppA BLUF domain.* Biophys J, 2008. **95**(1): p. 312-321.

55. Lukacs, A., A. Haigney, R. Brust, R.K. Zhao, A.L. Stelling, I.P. Clark, M. Towrie, G.M. Greetham, S.R. Meech, and P.J. Tonge, *Photoexcitation of the blue light using FAD photoreceptor AppA results in ultrafast changes to the protein matrix.* J Am Chem Soc, 2011. **133**(42): p. 16893-900.

56. Domratcheva, T., B.L. Grigorenko, I. Schlichting, and A.V. Nemukhin, *Molecular models predict light-induced glutamine tautomerization in BLUF photoreceptors.* Biophys J, 2008. **94**(10): p. 3872-3879.

57. Sadeghian, K., M. Bocola, and M. Schultz, *A conclusive mechanism of the photoinduced reaction cascade in blue light using dlavin photoreceptors.* J Am Chem Soc, 2008. **130**(37): p. 12501-12513.

58. Dragnea, V., A.I. Arunkumar, C.W. Lee, D.P. Giedroc, and C.E. Bauer, *A Q63E Rhodobacter sphaeroides AppA BLUF domain mutant is locked in a pseudo-light-excited signaling state.* Biochemistry, 2011. **49**(50): p. 10682-10690.

59. Greetham, G.M., P. Burgos, Q. Cao, I.P. Clark, P.S. Codd, R.C. Farrow, M.W. George, M. Kogimtzis, P. Matousek, A.W. Parker, M.R. Pollard, D.A. Robinson, Z.-J. Xin, and M. Towrie, *ULTRA: A unique instrument for time-resolved spectroscopy.* Appl Spectrosc, 2009. **64**(12): p. 1311-1319.

60. Fenno, L., O. Yizhar, and K. Deisseroth, *The development and application of optogenetics.* Annu Rev Neurosci, 2011. **34**(1): p. 389-412.

61. Boyden, E.S., F. Zhang, E. Bamberg, G. Nagel, and K. Deisseroth, *Millisecond-timescale, genetically targeted optical control of neural activity.* Nat Neurosci, 2005. **8**(9): p. 1263-1268.

62. Gradinaru, V., M. Mogri, K.R. Thompson, J.M. Henderson, and K. Deisseroth, *Optical deconstruction of Parkinsonian neural circuitry.* Science, 2009. **324**(5925): p. 354-359.

63. Zemelman, B.V., G.A. Lee, M. Ng, and G. Miesenböck, *Selective photostimulation of genetically chARGed neurons.* Neuron, 2002. **33**(1): p. 15-22.

64. Berthold, P., S.P. Tsunoda, O.P. Ernst, W. Mages, D. Gradmann, and P. Hegemann, *Channelrhodopsin-1 initiates phototaxis and photophobic responses in Chlamydomonas by iImmediate light-induced depolarization.* Plant Cell, 2008. **20**(6): p. 1665-1677.

65. Schroder-Lang, S., M. Schwarzel, R. Seifert, T. Strunker, S. Kateriya, J. Looser, M. Watanabe, U.B. Kaupp, P. Hegemann, and G. Nagel, *Fast manipulation of cellular cAMP level by light in vivo.* Nat Meth, 2007. **4**(1): p. 39-42.

Chapter 2

1. Losi, A., *The bacterial counterparts of plant phototropins.* Photochem. Photobiol. Sci., 2004. **3**(6): p. 566-574.

2. Losi, A. and W. Gartner, *Bacterial bilin- and flavin-binding photoreceptors.* Photochem Photobiol Sci, 2008. **7**(10): p. 1168-1178.

3. Losi, A. and W. Gärtner, *Old chromophores, new photoactivation paradigms, trendy applications: Flavins in blue light-sensing photoreceptors.* Photochem Photobiol, 2011. **87**(3): p. 491-510.

4. Losi, A. and W. Gärtner, *The evolution of flavin-binding photoreceptors: An ancient chromophore serving trendy blue-light sensors.* Annu Rev Plant Biol, 2012. **63**(1): p. 49-72.

5. Christie, J.M., J. Gawthorne, G. Young, N.J. Fraser, and A.J. Roe, *LOV to BLUF: Flavoprotein contributions to the optogenetic toolkit.* Mol Plant, 2012. **5**(3): p. 533-544.

6. Yin, T. and Y. Wu, *Guiding lights: recent developments in optogenetic control of biochemical signals.* Pflugers Archiv, 2013. **465**(3): p. 397-408.

7. Mitra, D., X. Yang, and K. Moffat, *Crystal structures of aureochrome1 LOV suggest new design strategies for optogenetics.* Structure, 2012. **20**(4): p. 698-706.

8. Gomelsky, M. and G. Klug, *BLUF: a novel FAD-binding domain involved in sensory transduction in microorganisms.* Trends Biochem Sci, 2002. **27**(10): p. 497-500.

9. Masuda, S., *Light detection and signal transduction in the BLUF photoreceptors.* Plant Cell Physiol, 2013. **54**(2): p. 171-179.

10. Masuda, S. and C.E. Bauer, *AppA Is a blue light photoreceptor that antirepresses photosynthesis gene expression in Rhodobacter sphaeroides.* Cell, 2002. **110**(5): p. 613-623.

11. Pandey, R., D. Flockerzi, Marcus J.B. Hauser, and R. Straube, *Modeling the light- and redox-dependent interaction of PpsR/AppA in Rhodobacter sphaeroides.* Biophys J, 2011. **100**(10): p. 2347-2355.

12. Kim, S.K., J.T. Mason, D.B. Knaff, C.E. Bauer, and A.T. Setterdahl, *Redox properties of the Rhodobacter sphaeroides transcriptional regulatory proteins PpsR and AppA.* Photosynth. Res., 2006. **89**(2-3): p. 89-98.

13. Pandey, R., D. Flockerzi, M.J.B. Hauser, and R. Straube, *An extended model for the repression of photosynthesis genes by the AppA/PpsR system in Rhodobacter sphaeroides.* FEBS J, 2012. **279**(18): p. 3449-3461.

14. Masuda, S., K. Hasegawa, and T.-a. Ono, *Light-induced structural changes of apoprotein and chromophore in the sensor of blue light using FAD (BLUF) domain of AppA for a signaling state* Biochemistry, 2005. **44**(4): p. 1215-1224.

15. Haigney, A., A. Lukacs, R.-K. Zhao, A.L. Stelling, R. Brust, R.-R. Kim, M. Kondo, I. Clark, M. Towrie, G.M. Greetham, B. Illarionov, A. Bacher, W. Romisch-Margl, M. Fischer, S.R. Meech, and P.J. Tonge, *Ultrafast infrared spectroscopy of an isotope-labeled photoactivatable flavoprotein.* Biochemistry, 2011. **50**(8): p. 1321-1328.

16. Stelling, A.L., K.L. Ronayne, J. Nappa, P.J. Tonge, and S.R. Meech, *Ultrafast structural dynamics in BLUF domains: Transient infrared spectroscopy of AppA and its mutants.* J Am Chem Soc, 2007. **129**(50): p. 15556-15564.

17. Unno, M., R. Sano, S. Masuda, T.-a. Ono, and S. Yamauchi, *Light-Induced Structural Changes in the Active Site of the BLUF Domain in AppA by Raman Spectroscopy.* J. Phys. Chem. B, 2005. **109**(25): p. 12620-12626.

18. Lukacs, A., A. Haigney, R. Brust, R.-K. Zhao, A.L. Stelling, I.P. Clark, M. Towrie, G.M. Greetham, S.R. Meech, and P.J. Tonge, *Photoexcitation of the blue Light Using FAD Photoreceptor AppA results in ultrafast changes to the protein matrix.* J Am Chem Soc, 2011. **133**(42): p. 16893–16900.

19. *The PyMOL molecular graphics system, Version 1.2r3pre, Schrödinger, LLC.*

20. Anderson, S., V. Dragnea, S. Masuda, J. Ybe, K. Moffat, and C. Bauer, *Structure of a novel photoreceptor, the BLUF domain of AppA from Rhodobacter sphaeroides.* Biochemistry, 2005. **44**(22): p. 7998-8005.

21. Götze, J. and P. Saalfrank, *Serine in BLUF domains displays spectral importance in computational models.* J Photochem Photobiol B, 2009. **94**(2): p. 87-95.

22. Grinstead, J.S., S.-T.D. Hsu, W. Laan, A.M.J.J. Bonvin, K.J. Hellingwerf, R. Boelens, and R. Kaptein, *The solution structure of the AppA BLUF domain: Insight into the mechanism of light-induced signaling.* ChemBioChem, 2006. **7**(1): p. 187-193.22.

23. Bonetti, C., M. Stierl, T. Mathes, I.H.M. van Stokkum, K.M. Mullen, T.A. Cohen-Stuart, R. van Grondelle, P. Hegemann, and J.T.M. Kennis, *The role of key amino acids in the photoactivation pathway of the Synechocystis Slr1694 BLUF domain.* Biochemistry, 2009. **48**(48): p. 11458-11469.

24. Bell, A.F., X. He, R.M. Wachter, and P.J. Tonge, *Probing the ground state structure of the green fluorescent protein chromophore using Raman spectroscopy.* Biochemistry, 2000. **39**(15): p. 4423-31.

25. Greetham, G.M., P. Burgos, Q. Cao, I.P. Clark, P.S. Codd, R.C. Farrow, M.W. George, M. Kogimtzis, P. Matousek, A.W. Parker, M.R. Pollard, D.A. Robinson, Z.-J. Xin, and M. Towrie, *ULTRA: A unique instrument for time-resolved spectroscopy.* Appl Spectrosc, 2010. **64**(12): p. 1311-1319.

26. Unno, M., R. Sano, S. Masuda, T.A. Ono, and S. Yamauchi, *Light-induced structural changes in the active site of the BLUF domain in AppA by Raman spectroscopy.* J Phys Chem B, 2005. **109**(25): p. 12620-6.

27. Masuda, S., K. Hasegawa, and T.-a. Ono, *Tryptophan at position 104 is involved in transforming light signal into changes of β-sheet structure for the signaling state in the BLUF domain of AppA.* Plant Cell Physiol, 2005. **46**(12): p. 1894-1901.

28. Unno, M., S. Kikuchi, and S. Masuda, *Structural refinement of a key tryptophan residue in the BLUF photoreceptor AppA by ultraviolet resonance Raman spectroscopy.* Biophys J, 2010. **98**(9): p. 1949-1956.

29. Masuda, S., Y. Tomida, H. Ohta, and K.-i. Takamiya, *The critical role of a H-bond between Gln63 and Trp104 in the blue-light sensing BLUF domain that controls AppA activity.* J Mol Biol, 2007. **368**(5): p. 1223-1230.

30. Barth, A., *Infrared spectroscopy of proteins.* Biochim Biophys Acta, 2007. **1767**(9): p. 1073-1101.

31. Kennis, J.T. and M.L. Groot, *Ultrafast spectroscopy of biological photoreceptors.* Curr Opin Struct Biol, 2007. **17**(5): p. 623-30.

32. Kim, M. and P.R. Carey, *Observation of a carbonyl feature for riboflavin bound to riboflavin-binding protein in the red-excited raman spectrum.* J Am Chem Soc, 1993. **115**(15): p. 7015-7016.

33. Bowman, W.D. and T.G. Spiro, *Normal mode analysis of lumiflavin and interpretation of resonance Raman spectra of flavoproteins.* Biochemistry, 1981. **20**(11): p. 3313-3318.

34. Pelton, J.T. and L.R. McLean, *Spectroscopic methods for analysis of protein secondary structure.* Anal Biochem, 2000. **277**(2): p. 167-176.

35. Maiti, N.C., M.M. Apetri, M.G. Zagorski, P.R. Carey, and V.E. Anderson, *Raman spectroscopic characterization of secondary structure in natively unfolded proteins: α-synuclein.* J Am Chem Soc, 2004. **126**(8): p. 2399-2408.

36. Barron, L.D., *Structure and behaviour of biomolecules from Raman optical activity.* Curr Opin Struct Biol, 2006. **16**(5): p. 638-643.

37. Roach, C.A., J.V. Simpson, and R.D. JiJi, *Evolution of quantitative methods in protein secondary structure determination via deep-ultraviolet resonance Raman spectroscopy.* Analyst, 2012. **137**(3): p. 555-562.

38. Measey, T., A. Hagarman, F. Eker, K. Griebenow, and R. Schweitzer-Stenner, *Side chain dependence of intensity and wavenumber position of amide I' in IR and visible Raman spectra of XA and AX dipeptides.* J Phys Chem B, 2005. **109**(16): p. 8195-8205.

39. Kondo, M., J. Nappa, K.L. Ronayne, A.L. Stelling, P.J. Tonge, and S.R. Meech, *Ultrafast vibrational spectroscopy of the flavin chromophore.* J Phys Chem B, 2006. **110**(41): p. 20107-20110.

40. Haigney, A., A. Lukacs, R. Brust, R.-K. Zhao, M. Towrie, G.M. Greetham, I. Clark, B. Illarionov, A. Bacher, R.-R. Kim, M. Fischer, S.R. Meech, and P.J. Tonge, *Vibrational assignment of the ultrafast infrared spectrum of the photoactivatable flavoprotein AppA.* J Phys Chem B, 2012. **116**(35): p. 10722-10729.

41. Venyaminov, S.Y. and N.N. Kalnin, *Quantitative IR spectrophotometry of peptide compounds in water (H2O) solutions. I. Spectral parameters of amino acid residue absorption bands.* Biopolymers, 1990. **30**(13-14): p. 1243-1257.

42. Barth, A., *The infrared absorption of amino acid side chains.* Prog Biophys Mol Biol, 2000. **74**(3–5): p. 141-173.

43. Laan, W., M. Gauden, S. Yeremenko, R. van Grondelle, J.T.M. Kennis, and K.J. Hellingwerf, *On the mechanism of activation of the BLUF domain of AppA.* Biochemistry, 2006. **45**(1): p. 51-60.

Chapter 3

1. Giamarellou, H., A. Antoniadou, and K. Kanellakopoulou, *Acinetobacter baumannii: a universal threat to public health?* Int J Androl, 2008. **32**(2): p. 106-119.
2. Tomaras, A.P., M.J. Flagler, C.W. Dorsey, J.A. Gaddy, and L.A. Actis, *Characterization of a two-component regulatory system from Acinetobacter baumannii that controls biofilm formation and cellular morphology.* Microbiol, 2008. **154**(11): p. 3398-3409.
3. Kallen, Alexander J.M.D.M.P.H., M.D. Alicia I. Hidron, J.P. Patel, and A.M.D. Srinivasan, *Multidrug Resistance among Gram-Negative Pathogens That Caused Healthcare-Associated Infections Reported to the National Healthcare Safety Network, 2006–2008* •. Infect. Control Hosp. Epidemiol., 2010. **31**(5): p. 528-531.
4. Sebeny, P.J., M.S. Riddle, and K. Petersen, *Acinetobacter baumannii skin and soft-tissue infection associated with war trauma.* Clin Infect Dis, 2008. **47**(4): p. 444-449.
5. Howard, A., M. O'Donoghue, A. Feeney, and R.D. Sleator, Acinetobacter baumanni*: An emerging opportunistic pathogen.* Virulence, 2012. **3**(3): p. 243-250.
6. *Acinetobacter baumannii infections among patients at military medical facilities treating injured U.S. service members, 2002-2004.* MMWR Morb Mortal Wkly Rep, 2004. **53**(45): p. 1063-6.
7. Peleg, A.Y., H. Seifert, and D.L. Paterson, *Acinetobacter baumannii: Emergence of a successful pathogen.* Clin Microbiol Rev, 2008. **21**(3): p. 538-582.
8. Zimbler, D., W. Penwell, J. Gaddy, S. Menke, A. Tomaras, P. Connerly, and L. Actis, *Iron acquisition functions expressed by the human pathogen Acinetobacter baumannii.* BioMetals, 2009. **22**(1): p. 23-32.

9. Daniel, C., S. Haentjens, M.-C. Bissinger, and R.J. Courcol, *Characterization of the Acinetobacter baumannii Fur regulator: cloning and sequencing of the fur homolog gene.* FEMS Microbiol Lett, 1999. **170**(1): p. 199-209.

10. Charnot-Katsikas, A., A.H. Dorafshar, J.K. Aycock, M.Z. David, S.G. Weber, and K.M. Frank, *Two cases of necrotizing fasciitis due to Acinetobacter baumannii.* J Clin Microbiol, 2009. **47**(1): p. 258-263.

11. McQueary, C. and L. Actis, *Acinetobacter baumannii biofilms: Variations among strains and correlations with other cell properties.* J Microbiol, 2011. **49**(2): p. 243-250.

12. Mah, T.-F.C. and G.A. O'Toole, *Mechanisms of biofilm resistance to antimicrobial agents.* Trends Microbiol., 2001. **9**(1): p. 34-39.

13. Thurlow, L.R., M.L. Hanke, T. Fritz, A. Angle, A. Aldrich, S.H. Williams, I.L. Engebretsen, K.W. Bayles, A.R. Horswill, and T. Kielian, *Staphylococcus aureus biofilms prevent macrophage phagocytosis and attenuate inflammation in vivo.* J Immunol, 2011. **186**(11): p. 6585-6596.

14. Schommer, N.N., M. Christner, M. Hentschke, K. Ruckdeschel, M. Aepfelbacher, and H. Rohde, *Staphylococcus epidermidis uses distinct mechanisms of biofilm formation to interfere with phagocytosis and activation of mouse macrophage-like cells 774A.1.* Infect Immun, 2011. **79**(6): p. 2267-2276.

15. Gaddy, J.A., A.P. Tomaras, and L.A. Actis, *The Acinetobacter baumannii 19606 OmpA protein plays a role in biofilm formation on abiotic surfaces and in the interaction of this pathogen with eukaryotic cells.* Infect Immun, 2009. **77**(8): p. 3150-3160.

16. Gaddy, J.A. and L.A. Actis, *Regulation of Acinetobacter baumannii biofilm formation.* Future Microbiol, 2009. **4**(3): p. 273-278.

17. Marc S. Hoffmann, M.D., B.S.E. Michael R. Eber, and P.M.P.H. Ramanan Laxminarayan, *Increasing resistance of Acinetobacter species to imipenem in United States hospitals, 1999–2006* Infect Control Hosp Epidemiol, 2010. **31**(2): p. 196-197.

18. Lin, L., B. Tan, P. Pantapalangkoor, T. Ho, B. Baquir, A. Tomaras, J.I. Montgomery, U. Reilly, E.G. Barbacci, K. Hujer, R.A. Bonomo, L. Fernandez, R.E.W. Hancock, M.D. Adams, S.W. French, V.S. Buslon, and B. Spellberg, *Inhibition of LpxC protects mice from resistant Acinetobacter baumannii by modulating inflammation and enhancing phagocytosis.* mBio, 2012. **3**(5).

19. Mussi, M.A., J.A. Gaddy, M. Cabruja, B.A. Arivett, A.M. Viale, R. Rasia, and L.A. Actis, *The opportunistic human pathogen Acinetobacter baumannii senses and responds to Llight.* J Bacteriol, 2010. **192**(24): p. 6336-6345.

20. Golic, A., M. Vaneechoutte, A. Nemec, A.M. Viale, L.A. Actis, and M.A. Mussi, *Staring at the cold sun: Blue light regulation is distributed within the genus Acinetobacter.* PLoS ONE, 2013. **8**(1): p. e55059.

21. Mussi, M.A., J.A. Gaddy, M. Cabruja, B.A. Arivett, A.M. Viale, R. Rasia, and L.A. Actis, *The Opportunistic Human Pathogen Acinetobacter baumannii Senses and Responds to Light.* J. Bacteriol. **192**(24): p. 6336-6345.

22. Clemmer, K.M., R.A. Bonomo, and P.N. Rather, *Genetic analysis of surface motility in Acinetobacter baumannii*. Microbiology, 2011. **157**(9): p. 2534-2544.

23. Losi, A. and W. Gartner, *Bacterial bilin- and flavin-binding photoreceptors.* Photochem Photobiol Sci, 2008. **7**(10): p. 1168-1178.

24. Masuda, S., *Light detection and signal transduction in the BLUF photoreceptors.* Plant Cell Physiol, 2013. **54**(2): p. 171-179.

25. Losi, A. and W. Gärtner, *Old chromophores, new photoactivation paradigms, trendy applications: Flavins in blue light-sensing photoreceptors.* Photochem Photobiol, 2011. **87**(3): p. 491-510.

26. Losi, A. and W. Gärtner, *The evolution of flavin-binding photoreceptors: An ancient chromophore serving trendy blue-light sensors.* Annu Rev Plant Biol, 2012. **63**(1): p. 49-72.

27. Tonge, P., G.R. Moore, and C.W. Wharton, *Fourier-transform infra-red studies of the alkaline isomerization of mitochondrial cytochrome c and the ionization of carboxylic acids.* Biochem J, 1989. **258**(2): p. 599-605.

28. Stelling, A.L., K.L. Ronayne, J. Nappa, P.J. Tonge, and S.R. Meech, *Ultrafast structural dynamics in BLUF domains: Transient infrared spectroscopy of AppA and its mutants.* J Am Chem Soc, 2007. **129**(50): p. 15556-15564.

29. Haigney, A., A. Lukacs, R.-K. Zhao, A.L. Stelling, R. Brust, R.-R. Kim, M. Kondo, I. Clark, M. Towrie, G.M. Greetham, B. Illarionov, A. Bacher, W. Romisch-Margl, M. Fischer, S.R. Meech, and P.J. Tonge, *Ultrafast infrared spectroscopy of an isotope-labeled photoactivatable flavoprotein.* Biochemistry, 2011. **50**(8): p. 1321-1328.

30. Lukacs, A., A. Haigney, R. Brust, R.K. Zhao, A.L. Stelling, I.P. Clark, M. Towrie, G.M. Greetham, S.R. Meech, and P.J. Tonge, *Photoexcitation of the blue light using FAD photoreceptor AppA results in ultrafast changes to the protein matrix.* J Am Chem Soc, 2011. **133**(42): p. 16893-900.

31. Haigney, A., A. Lukacs, R. Brust, R.-K. Zhao, M. Towrie, G.M. Greetham, I. Clark, B. Illarionov, A. Bacher, R.-R. Kim, M. Fischer, S.R. Meech, and P.J. Tonge, *Vibrational assignment of the ultrafast infrared spectrum of the photoactivatable flavoprotein AppA.* J Phys Chem B, 2012. **116**(35): p. 10722-10729.

32. Zirak, P., A. Penzkofer, T. Schiereis, P. Hegemann, A. Jung, and I. Schlichting, *Photodynamics of the small BLUF protein BlrB from Rhodobacter sphaeroides.* J Photochem Photobiol B, 2006. **83**(3): p. 180-194.

33. Masuda, S., K. Hasegawa, A. Ishii, and T.-a. Ono, *Light-induced structural changes in a putative blue-light receptor with a novel FAD binding fold sensor of blue-light using FAD (BLUF); Slr1694 of Synechocystis sp. PCC6803.* Biochemistry, 2004. **43**(18): p. 5304-5313.

34. Hasegawa, K., S. Masuda, and T.-a. Ono, *Spectroscopic analysis of the dark relaxation process of a photocycle in a sensor of blue light using FAD (BLUF) protein Slr1694 of the cyanobacterium Synechocystis sp. PCC6803.* Plant Cell Physiol, 2005. **46**(1): p. 136-146.

35. Yuan, H., S. Anderson, S. Masuda, V. Dragnea, K. Moffat, and C. Bauer, *Crystal structures of the Synechocystis photoreceptor Slr1694 reveal distinct structural states related to signaling.* Biochemistry, 2006. **45**(42): p. 12687-12694.

36. Clamp, M., J. Cuff, S.M. Searle, and G.J. Barton, *The Jalview Java alignment editor.* Bioinformatics, 2004. **20**(3): p. 426-427.

37. Waterhouse, A.M., J.B. Procter, D.M.A. Martin, M. Clamp, and G.J. Barton, *Jalview Version 2—a multiple sequence alignment editor and analysis workbench.* Bioinformatics, 2009. **25**(9): p. 1189-1191.

38. Lukacs, A., A. Haigney, R. Brust, R.-K. Zhao, A.L. Stelling, I.P. Clark, M. Towrie, G.M. Greetham, S.R. Meech, and P.J. Tonge, *Photoexcitation of the Blue Light Using FAD Photoreceptor AppA Results in Ultrafast Changes to the Protein Matrix.* J. Am. Chem. Soc., 2011. **133**(42): p. 16893–16900.

39. Tishler, M., K. Pfister, R.D. Babson, K. Ladenburg, and A.J. Fleming, *The Reaction between o-aminoazo compounds and barbituric acid. A new synthesis of riboflavin.* J Am Chem Soc, 1947. **69**(6): p. 1487-1492.

40. Arnold, K., L. Bordoli, J.r. Kopp, and T. Schwede, *The SWISS-MODEL workspace: a web-based environment for protein structure homology modelling.* Bioinformatics, 2006. **22**(2): p. 195-201.

41. Geux, N., Peitsch, Manuel C., *SWISS-MODEL and the Swiss-PdbViewer: An environment for comparative protein modelling.* Electrophoresis, 1997. **18**: p. 2714-2723.

42. Kiefer, F., K. Arnold, M. KÃ¼nzli, L. Bordoli, and T. Schwede, *The SWISS-MODEL epository and associated resources.* Nuc Acids Res, 2009. **37**(suppl 1): p. D387-D392.

43. Schwede, T., J. Kopp, N. Guex, and M.C. Peitsch, *SWISS-MODEL: an automated protein homology-modeling server.* Nucl. Acids Res., 2003. **31**(13): p. 3381-3385.

44. Götze, J. and P. Saalfrank, *Serine in BLUF domains displays spectral importance in computational models.* J Photochem Photobiol B, 2009. **94**(2): p. 87-95.

45. Masuda, S. and C.E. Bauer, *AppA Is a blue light photoreceptor that antirepresses photosynthesis gene expression in Rhodobacter sphaeroides.* Cell, 2002. **110**(5): p. 613-623.

46. Decatur, S.M., *Elucidation of residue-level structure and dynamics of polypeptides via isotope-edited infrared spectroscopy.* Acc Chem Res, 2006. **39**(3): p. 169-175.

47. Strasfeld, D.B., Y.L. Ling, R. Gupta, D.P. Raleigh, and M.T. Zanni, *Strategies for extracting structural information from 2D IR spectroscopy of amyloid: Application to islet amyloid polypeptide.* J Phys Chem B, 2009. **113**(47): p. 15679-15691.

48. Masuda, S., K. Hasegawa, and T.-a. Ono, *Tryptophan at position 104 is involved in transforming light signal into changes of β-sheet structure for the signaling state in the BLUF domain of AppA.* Plant Cell Physiol, 2005. **46**(12): p. 1894-1901.

49. Grinstead, J.S., M. Avila-Perez, K.J. Hellingwerf, R. Boelens, and R. Kaptein, *Light-induced flipping of a conserved glutamine sidechain and its orientation in the AppA BLUF domain.* J Am Chem Soc, 2006. **128**(47): p. 15066-15067.

50. Masuda, S., K. Hasegawa, and T.-a. Ono, *Light-induced structural changes of apoprotein and chromophore in the sensor of blue light using FAD (BLUF) domain of AppA for a signaling state* Biochemistry, 2005. **44**(4): p. 1215-1224.

51. Kondo, M., J. Nappa, K.L. Ronayne, A.L. Stelling, P.J. Tonge, and S.R. Meech, *Ultrafast vibrational spectroscopy of the flavin chromophore.* J Phys Chem B, 2006. **110**(41): p. 20107-20110.

52. Jung, A., J. Reinstein, T. Domratcheva, R.L. Shoeman, and I. Schlichting, *Crystal structures of the AppA BLUF domain photoreceptor provide insights into blue light-mediated signal transduction.* J Mol Biol, 2006. **362**(4): p. 717-732.

53. Yuan, H. and C.E. Bauer, *PixE promotes dark oligomerization of the BLUF photoreceptor PixD.* Proc. Nat. Acad. Sci., 2008. **105**(33): p. 11715-11719.

54. Masuda, S., K. Hasegawa, H. Ohta, and T.-a. Ono, *Crucial role in light signal transduction for the conserved Met93 of the BLUF protein PixD/Slr1694.* Plant Cell Physiol, 2008. **49**(10): p. 1600-1606.

Chapter 4

1. Agarwal, P.K., S.R. Billeter, P.T. Rajagopalan, S.J. Benkovic, and S. Hammes-Schiffer, *Network of coupled promoting motions in enzyme catalysis.* Proc Natl Acad Sci U.S.A., 2002. **99**(5): p. 2794-9.
2. Yang, H., G. Luo, P. Karnchanaphanurach, T.M. Louie, I. Rech, S. Cova, L. Xun, and X.S. Xie, *Protein conformational dynamics probed by single-molecule electron transfer.* Science, 2003. **302**(5643): p. 262-6.
3. Lange, O.F., N.A. Lakomek, C. Fares, G.F. Schroder, K.F. Walter, S. Becker, J. Meiler, H. Grubmuller, C. Griesinger, and B.L. de Groot, *Recognition dynamics up to microseconds revealed from an RDC-derived ubiquitin ensemble in solution.* Science, 2008. **320**(5882): p. 1471-5.
4. Mulder, F.A.A., N.R. Skrynnikov, B. Hon, F.W. Dahlquist, and L.E. Kay, *Measurement of slow (μs−ms) time scale dynamics in protein side chains by 15N relaxation dispersion NMR spectroscopy: Application to Asn and Gln residues in a cavity mutant of T4 lysozyme.* J Am Chem Soc, 2001. **123**(5): p. 967-975.
5. Boehr, D.D., H.J. Dyson, and P.E. Wright, *An NMR perspective on enzyme dynamics.* Chem Rev, 2006. **106**(8): p. 3055-3079.
6. Henzler-Wildman, K.A., M. Lei, V. Thai, S.J. Kerns, M. Karplus, and D. Kern, *A hierarchy of timescales in protein dynamics is linked to enzyme catalysis.* Nature, 2007. **450**(7171): p. 913-916.
7. Cho, H.S., N. Dashdorj, F. Schotte, T. Graber, R. Henning, and P. Anfinrud, *Protein structural dynamics in solution unveiled via 100-ps time-resolved x-ray scattering.* Proc Natl Acad Sci U S A, 2010. **107**(16): p. 7281-6.

8. Ihee, H., S. Rajagopal, V. Srajer, R. Pahl, S. Anderson, M. Schmidt, F. Schotte, P.A. Anfinrud, M. Wulff, and K. Moffat, *Visualizing reaction pathways in photoactive yellow protein from nanoseconds to seconds.* Proc Natl Acad Sci U S A, 2005. **102**(20): p. 7145-50.

9. Schotte, F., H.S. Cho, V.R. Kaila, H. Kamikubo, N. Dashdorj, E.R. Henry, T.J. Graber, R. Henning, M. Wulff, G. Hummer, M. Kataoka, and P.A. Anfinrud, *Watching a signaling protein function in real time via 100-ps time-resolved Laue crystallography.* Proc Natl Acad Sci U S A, 2012. **109**(47): p. 19256-61.

10. Ihee, H., M. Lorenc, T.K. Kim, Q.Y. Kong, M. Cammarata, J.H. Lee, S. Bratos, and M. Wulff, *Ultrafast x-ray diffraction of transient molecular structures in solution.* Science, 2005. **309**(5738): p. 1223-7.

11. Kim, K.H., S. Muniyappan, K.Y. Oang, J.G. Kim, S. Nozawa, T. Sato, S.Y. Koshihara, R. Henning, I. Kosheleva, H. Ki, Y. Kim, T.W. Kim, J. Kim, S. Adachi, and H. Ihee, *Direct observation of cooperative protein structural dynamics of homodimeric hemoglobin from 100 ps to 10 ms with pump-probe X-ray solution scattering.* J Am Chem Soc, 2012. **134**(16): p. 7001-8.

12. Kim, T.W., J.H. Lee, J. Choi, K.H. Kim, L.J. van Wilderen, L. Guerin, Y. Kim, Y.O. Jung, C. Yang, J. Kim, M. Wulff, J.J. van Thor, and H. Ihee, *Protein structural dynamics of photoactive yellow protein in solution revealed by pump-probe X-ray solution scattering.* J Am Chem Soc, 2012. **134**(6): p. 3145-53.

13. Ramachandran, P.L., J.E. Lovett, P.J. Carl, M. Cammarata, J.H. Lee, Y.O. Jung, H. Ihee, C.R. Timmel, and J.J. van Thor, *The short-lived signaling state of the photoactive yellow*

protein photoreceptor revealed by combined structural probes. J Am Chem Soc, 2011. **133**(24): p. 9395-404.

14. Jung, Y.O., J.H. Lee, J. Kim, M. Schmidt, K. Moffat, V. Srajer, and H. Ihee, *Volume-conserving trans-cis isomerization pathways in photoactive yellow protein visualized by picosecond X-ray crystallography.* Nat Chem, 2013. **5**(3): p. 212-20.
15. Masuda, S. and C.E. Bauer, *AppA Is a blue light photoreceptor that antirepresses photosynthesis gene expression in Rhodobacter sphaeroides.* Cell, 2002. **110**(5): p. 613-623.
16. Laan, W., M. Gauden, S. Yeremenko, R. van Grondelle, J.T.M. Kennis, and K.J. Hellingwerf, *On the mechanism of activation of the BLUF domain of AppA.* Biochemistry, 2006. **45**(1): p. 51-60.
17. Jung, A., J. Reinstein, T. Domratcheva, R.L. Shoeman, and I. Schlichting, *Crystal structures of the AppA BLUF domain photoreceptor provide insights into blue light-mediated signal transduction.* J Mol Biol, 2006. **362**(4): p. 717-732.
18. Anderson, S., V. Dragnea, S. Masuda, J. Ybe, K. Moffat, and C. Bauer, *Structure of a novel photoreceptor, the BLUF domain of AppA from Rhodobacter sphaeroides.* Biochemistry, 2005. **44**(22): p. 7998-8005.
19. Grinstead, J.S., S.-T.D. Hsu, W. Laan, A.M.J.J. Bonvin, K.J. Hellingwerf, R. Boelens, and R. Kaptein, *The solution structure of the AppA BLUF domain: Insight into the mechanism of light-induced signaling.* ChemBioChem, 2006. **7**(1): p. 187-193.
20. Stelling, A.L., K.L. Ronayne, J. Nappa, P.J. Tonge, and S.R. Meech, *Ultrafast structural dynamics in BLUF domains: Transient infrared spectroscopy of AppA and its mutants.* J Am Chem Soc, 2007. **129**(50): p. 15556-15564.

21. Lukacs, A., A. Haigney, R. Brust, R.K. Zhao, A.L. Stelling, I.P. Clark, M. Towrie, G.M. Greetham, S.R. Meech, and P.J. Tonge, *Photoexcitation of the blue light using FAD photoreceptor AppA results in ultrafast changes to the protein matrix.* J Am Chem Soc, 2011. **133**(42): p. 16893-900.

22. Masuda, S., K. Hasegawa, A. Ishii, and T.-a. Ono, *Light-induced structural changes in a putative blue-light receptor with a novel FAD binding fold sensor of blue-light using FAD (BLUF); Slr1694 of Synechocystis sp. PCC6803.* Biochemistry, 2004. **43**(18): p. 5304-5313.

23. Masuda, S., Y. Tomida, H. Ohta, and K.-i. Takamiya, *The critical role of a hydrogen bond between Gln63 and Trp104 in the blue-light sensing BLUF domain that controls AppA activity.* J Mol Biol, 2007. **368**(5): p. 1223-1230.

24. Masuda, S., K. Hasegawa, and T.-a. Ono, *Tryptophan at position 104 is involved in transforming light signal into changes of β-sheet structure for the signaling state in the BLUF domain of AppA.* Plant Cell Physiol, 2005. **46**(12): p. 1894-1901.

25. Unno, M., S. Kikuchi, and S. Masuda, *Structural refinement of a key tryptophan residue in the BLUF photoreceptor AppA by ultraviolet resonance Raman spectroscopy.* Biophys J, 2010. **98**(9): p. 1949-1956.

26. Toh, K.C., I.H.M. van Stokkum, J. Hendriks, M.T.A. Alexandre, J.C. Arents, M.A. Perez, R. van Grondelle, K.J. Hellingwerf, and J.T.M. Kennis, *On the signaling mechanism and the absence of photoreversibility in the AppA BLUF domain.* Biophys J, 2008. **95**(1): p. 312-321.

27. Pandey, R., D. Flockerzi, Marcus J.B. Hauser, and R. Straube, *Modeling the light- and redox-dependent interaction of PpsR/AppA in Rhodobacter sphaeroides.* Biophys J, 2011. **100**(10): p. 2347-2355.

28. Greetham, G.M., P. Burgos, Q.A. Cao, I.P. Clark, P.S. Codd, R.C. Farrow, M.W. George, M. Kogimtzis, P. Matousek, A.W. Parker, M.R. Pollard, D.A. Robinson, Z.J. Xin, and M. Towrie, *ULTRA: A unique instrument for time-resolved spectroscopy.* Appl Spectrosc, 2011. **64**(12): p. 1311-1319.

29. Greetham, G.M., D. Sole, I.P. Clark, A.W. Parker, M.R. Pollard, and M. Towrie, *Time-resolved multiple probe spectroscopy.* Rev Sci Instrum, 2012. **83**(10): p. 103107-5.

30. Greetham, G.M., P. Burgos, Q. Cao, I.P. Clark, P.S. Codd, R.C. Farrow, M.W. George, M. Kogimtzis, P. Matousek, A.W. Parker, M.R. Pollard, D.A. Robinson, Z.-J. Xin, and M. Towrie, *ULTRA: A unique instrument for time-resolved spectroscopy.* Appl Spectrosc, 2009. **64**(12): p. 1311-1319.

31. Laan, W., M.A. van der Horst, I.H. Van Stokkum, and K.J. Hellingwerf, *Initial Characterization of the Primary Photochemistry of AppA, a Blue-light–using Flavin Adenine Dinucleotide–domain Containing Transcriptional Antirepressor Protein from Rhodobacter sphaeroides: A Key Role for Reversible Intramolecular Proton Transfer from the Flavin Adenine Dinucleotide Chromophore to a Conserved Tyrosine?* Photochem. Photobiol., 2003. **78**(3): p. 290-297.

32. Yuan, H., S. Anderson, S. Masuda, V. Dragnea, K. Moffat, and C. Bauer, *Crystal structures of the Synechocystis photoreceptor Slr1694 reveal distinct structural states related to signaling.* Biochemistry, 2006. **45**(42): p. 12687-12694.

33. Haigney, A., A. Lukacs, R.-K. Zhao, A.L. Stelling, R. Brust, R.-R. Kim, M. Kondo, I. Clark, M. Towrie, G.M. Greetham, B. Illarionov, A. Bacher, W. Romisch-Margl, M. Fischer, S.R. Meech, and P.J. Tonge, *Ultrafast infrared spectroscopy of an isotope-labeled photoactivatable flavoprotein.* Biochemistry, 2011. **50**(8): p. 1321-1328.

34. Dragnea, V., A.I. Arunkumar, H. Yuan, D.P. Giedroc, and C.E. Bauer, *Spectroscopic studies of the AppA BLUF domain from Rhodobacter sphaeroides: Addressing movement of tryptophan 104 in the signaling state.* Biochemistry, 2009. **48**(42): p. 9969-9979.

35. Unno, M., R. Sano, S. Masuda, T.-a. Ono, and S. Yamauchi, *Light-Induced Structural Changes in the Active Site of the BLUF Domain in AppA by Raman Spectroscopy.* The Journal of Physical Chemistry B, 2005. **109**(25): p. 12620-12626.

36. Masuda, S., K. Hasegawa, and T.-a. Ono, *Light-induced structural changes of apoprotein and chromophore in the sensor of blue light using FAD (BLUF) domain of AppA for a signaling state* Biochemistry, 2005. **44**(4): p. 1215-1224.

37. Masuda, S., *Light detection and signal transduction in the BLUF photoreceptors.* Plant Cell Physiol, 2013. **54**(2): p. 171-179.

38. Kammler, L. and M. van Gastel, *Electronic structure of the lowest triplet state of flavin mononucleotide.* J Phys Chem A, 2012. **116**(41): p. 10090-10098.

39. Losi, A., E. Polverini, B. Quest, and W. Gärtner, *First evidence for phototropin-related blue-light receptors in prokaryotes.* Biophys J, 2002. **82**(5): p. 2627-2634.

40. Alexandre, M.T.A., T. Domratcheva, C. Bonetti, L.J.G.W. van Wilderen, R. van Grondelle, M.-L. Groot, K.J. Hellingwerf, and J.T.M. Kennis, *Primary reactions of the LOV2 domain of phototropin studied with ultrafast mid-infrared spectroscopy and quantum chemistry.* Biophys J, 2009. **97**(1): p. 227-237.

41. Miura, R., *Versatility and specificity in flavoenzymes: Control mechanisms of flavin reactivity.* Chem Rec, 2001. **1**(3): p. 183-194.

42. Kondo, M., J. Nappa, K.L. Ronayne, A.L. Stelling, P.J. Tonge, and S.R. Meech, *Ultrafast vibrational spectroscopy of the flavin chromophore.* J Phys Chem B, 2006. **110**(41): p. 20107-20110.

43. Haigney, A., A. Lukacs, R. Brust, R.-K. Zhao, M. Towrie, G.M. Greetham, I. Clark, B. Illarionov, A. Bacher, R.-R. Kim, M. Fischer, S.R. Meech, and P.J. Tonge, *Vibrational assignment of the ultrafast infrared spectrum of the photoactivatable flavoprotein AppA.* J Phys Chem B, 2012. **116**(35): p. 10722-10729.

44. Alexandre, M.T.A., L.J.G. van Wilderen, R. van Grondelle, K.J. Hellingwerf, M.L. Groot, and J.T.M. Kennis, *Early steps in blue light reception by plants: an ultrafast mid-infrared spectroscopic study of the LOV2 domain of phototropin.* Biophys J, 2005. **88**(1): p. 509a-509a.

45. Gauden, M., J.S. Grinstead, W. Laan, I.H. van Stokkum, M. Avila-Perez, K.C. Toh, R. Boelens, R. Kaptein, R. van Grondelle, K.J. Hellingwerf, and J.T. Kennis, *On the role of aromatic side chains in the photoactivation of BLUF domains.* Biochemistry, 2007. **46**(25): p. 7405-15.

46. Laan, W., M. Gauden, S. Yeremenko, R. van Grondelle, J.T.M. Kennis, and K.J. Hellingwerf, *On the mechanism of activation of the BLUF domain of AppA.* Biochemistry, 2005. **45**(1): p. 51-60.

47. Mathes, T., I.H. van Stokkum, C. Bonetti, P. Hegemann, and J.T. Kennis, *The hydrogen-bond switch reaction of the Blrb Bluf domain of Rhodobacter sphaeroides.* J Phys Chem B, 2011. **115**(24): p. 7963-71.

48. Bonetti, C., M. Stierl, T. Mathes, I.H.M. van Stokkum, K.M. Mullen, T.A. Cohen-Stuart, R. van Grondelle, P. Hegemann, and J.T.M. Kennis, *The role of key amino acids in the photoactivation pathway of the Synechocystis Slr1694 BLUF domain.* Biochemistry, 2009. **48**(48): p. 11458-11469.

49. Domratcheva, T., B.L. Grigorenko, I. Schlichting, and A.V. Nemukhin, *Molecular models predict light-induced glutamine tautomerization in BLUF photoreceptors.* Biophys J, 2008. **94**(10): p. 3872-3879.

50. Nunthaboot, N., F. Tanaka, and S. Kokpol, *Analysis of photoinduced electron transfer in AppA.* J Photoch Photobio A, 2009. **207**(2-3): p. 274-281.

51. Nunthaboot, N., F. Tanaka, and S. Kokpol, *Simultaneous analysis of photoinduced electron transfer in wild type and mutated AppAs.* J Photoch Photobio A, 2010. **209**(1): p. 79-87.

52. Gauden, M., S. Yeremenko, W. Laan, I.H. van Stokkum, J.A. Ihalainen, R. van Grondelle, K.J. Hellingwerf, and J.T. Kennis, *Photocycle of the flavin-binding photoreceptor AppA, a bacterial transcriptional antirepressor of photosynthesis genes.* Biochemistry, 2005. **44**(10): p. 3653-62.

53. Lin, Y.S., J.M. Shorb, P. Mukherjee, M.T. Zanni, and J.L. Skinner, *Empirical amide I vibrational frequency map: Application to 2D-IR line ahapes for isotope-edited membrane peptide bundles.* J Phys Chem B, 2008. **113**(3): p. 592-602.

54. Strasfeld, D.B., Y.L. Ling, R. Gupta, D.P. Raleigh, and M.T. Zanni, *Strategies for extracting structural information from 2D IR spectroscopy of amyloid: Application to islet amyloid polypeptide.* J Phys Chem B, 2009. **113**(47): p. 15679-15691.

55. Wu, Q., W.H. Ko, and K.H. Gardner, *Structural requirements for key residues and auxiliary portions of a BLUF domain.* Biochemistry, 2008. **47**(39): p. 10271-80.

56. Osvath, S., L. Herenyi, P. Zavodszky, J. Fidy, and G. Kohler, *Hierarchic finite level energy landscape model: to describe the refolding kinetics of phosphoglycerate kinase.* J Biol Chem, 2006. **281**(34): p. 24375-80.

Chapter 5

1. Yin, T. and Y. Wu, *Guiding lights: recent developments in optogenetic control of biochemical signals.* Pflugers Archiv, 2013. **465**(3): p. 397-408.

2. Masuda, S. and C.E. Bauer, *AppA Is a blue light photoreceptor that antirepresses photosynthesis gene expression in Rhodobacter sphaeroides.* Cell, 2002. **110**(5): p. 613-623.

3. Anderson, S., V. Dragnea, S. Masuda, J. Ybe, K. Moffat, and C. Bauer, *Structure of a novel photoreceptor, the BLUF domain of AppA from Rhodobacter sphaeroides.* Biochemistry, 2005. **44**(22): p. 7998-8005.

4. Masuda, S., K. Hasegawa, and T.-a. Ono, *Light-induced structural changes of apoprotein and chromophore in the sensor of blue light using FAD (BLUF) domain of AppA for a signaling state* Biochemistry, 2005. **44**(4): p. 1215-1224.

5. Laan, W., M. Gauden, S. Yeremenko, R. van Grondelle, J.T.M. Kennis, and K.J. Hellingwerf, *On the mechanism of activation of the BLUF domain of AppA.* Biochemistry, 2005. **45**(1): p. 51-60.

6. Gauden, M., S. Yeremenko, W. Laan, I.H. van Stokkum, J.A. Ihalainen, R. van Grondelle, K.J. Hellingwerf, and J.T. Kennis, *Photocycle of the flavin-binding*

photoreceptor AppA, a bacterial transcriptional antirepressor of photosynthesis genes. Biochemistry, 2005. **44**(10): p. 3653-62.

7. Unno, M., R. Sano, S. Masuda, T.A. Ono, and S. Yamauchi, *Light-induced structural changes in the active site of the BLUF domain in AppA by Raman spectroscopy.* J Phys Chem B, 2005. **109**(25): p. 12620-6.
8. Jung, A., J. Reinstein, T. Domratcheva, R.L. Shoeman, and I. Schlichting, *Crystal structures of the AppA BLUF domain photoreceptor provide insights into blue light-mediated signal transduction.* J Mol Biol, 2006. **362**(4): p. 717-732.
9. Laan, W., M. Gauden, S. Yeremenko, R. van Grondelle, J.T.M. Kennis, and K.J. Hellingwerf, *On the mechanism of activation of the BLUF domain of AppA.* Biochemistry, 2006. **45**(1): p. 51-60.
10. Pandey, R., D. Flockerzi, Marcus J.B. Hauser, and R. Straube, *Modeling the light- and redox-dependent interaction of PpsR/AppA in Rhodobacter sphaeroides.* Biophys J, 2011. **100**(10): p. 2347-2355.
11. Lukacs, A., A. Haigney, R. Brust, R.K. Zhao, A.L. Stelling, I.P. Clark, M. Towrie, G.M. Greetham, S.R. Meech, and P.J. Tonge, *Photoexcitation of the blue light using FAD photoreceptor AppA results in ultrafast changes to the protein matrix.* J Am Chem Soc, 2011. **133**(42): p. 16893-900.
12. Christie, J.M., J. Gawthorne, G. Young, N.J. Fraser, and A.J. Roe, *LOV to BLUF: Flavoprotein contributions to the optogenetic toolkit.* Mol Plant, 2012. **5**(3): p. 533-544.
13. Kim, S.K., J.T. Mason, D.B. Knaff, C.E. Bauer, and A.T. Setterdahl, *Redox properties of the Rhodobacter sphaeroides transcriptional regulatory proteins PpsR and AppA.* Photosynth. Res., 2006. **89**(2-3): p. 89-98.

14. Dragnea, V., A.I. Arunkumar, H. Yuan, D.P. Giedroc, and C.E. Bauer, *Spectroscopic studies of the AppA BLUF domain from Rhodobacter sphaeroides: Addressing movement of tryptophan 104 in the signaling state.* Biochemistry, 2009. **48**(42): p. 9969-9979.

15. Dragnea, V., A.I. Arunkumar, C.W. Lee, D.P. Giedroc, and C.E. Bauer, *A Q63E Rhodobacter sphaeroides AppA BLUF domain mutant is locked in a pseudo-light-excited signaling state.* Biochemistry, 2011. **49**(50): p. 10682-10690.

16. Metz, S., A. Jäger, and G. Klug, *In Vivo sensitivity of blue-light-dependent signaling mediated by AppA/PpsR or PrrB/PrrA in Rhodobacter sphaeroides.* J Bacteriol, 2009. **191**(13): p. 4473-4477.

17. Masuda, S., C. Dong, D. Swem, A.T. Setterdahl, D.B. Knaff, and C.E. Bauer, *Repression of photosynthesis gene expression by formation of a disulfide bond in CrtJ.* Proc Natl Acad Sci U S A, 2002. **99**(10): p. 7078-83.

18. Gomelsky, M. and S. Kaplan, *Genetic evidence that PpsR from Rhodobacter sphaeroides 2.4.1 functions as a repressor of puc and bchF expression.* J Bacteriol, 1995. **177**(6): p. 1634-7.

19. Penfold, R.J. and J.M. Pemberton, *Sequencing, chromosomal inactivation, and functional expression in Escherichia coli of ppsR, a gene which represses carotenoid and bacteriochlorophyll synthesis in Rhodobacter sphaeroides.* J Bacteriol, 1994. **176**(10): p. 2869-76.

20. Gomelsky, M. and S. Kaplan, *AppA, a redox regulator of photosystem formation in Rhodobacter sphaeroides 2.4.1, is a flavoprotein. Identification of a novel fad binding domain.* J Biol Chem, 1998. **273**(52): p. 35319-25.

21. Gomelsky, M. and G. Klug, *BLUF: a novel FAD-binding domain involved in sensory transduction in microorganisms.* Trends Biochem Sci, 2002. **27**(10): p. 497-500.

22. Pandey, R., D. Flockerzi, M.J.B. Hauser, and R. Straube, *An extended model for the repression of photosynthesis genes by the AppA/PpsR system in Rhodobacter sphaeroides.* FEBS J, 2012. **279**(18): p. 3449-3461.

23. Han, Y., M.H. Meyer, M. Keusgen, and G. Klug, *A haem cofactor is required for redox and light signalling by the AppA protein of Rhodobacter sphaeroides.* Mol Microbiol, 2007. **64**(4): p. 1090-104.

24. Metz, S., K. Haberzettl, S. Frühwirth, K. Teich, C. Hasewinkel, and G. Klug, *Interaction of two photoreceptors in the regulation of bacterial photosynthesis genes.* Nucleic Acids Res, 2012. **40**(13): p. 5901-5909.

25. Yin, L., V. Dragnea, and C.E. Bauer, *PpsR, a regulator of heme and bacteriochlorophyll biosynthesis, is a heme-sensing protein.* J Biol Chem, 2012. **287**(17): p. 13850-13858.

26. Jäger, A., S. Braatsch, K. Haberzettl, S. Metz, L. Osterloh, Y. Han, and G. Klug, *The AppA and PpsR proteins from Rhodobacter sphaeroides can establish a redox-dependent signal chain but fail to transmit blue-light signals in other bacteria.* J Bacteriol, 2007. **189**(6): p. 2274-2282.

27. Winkler, A., U. Heintz, R. Lindner, J. Reinstein, R.L. Shoeman, and I. Schlichting, *A ternary AppA–PpsR–DNA complex mediates light regulation of photosynthesis-related gene expression.* Nat Struct Mol Biol, 2013. **20**(7): p. 859-867.

28. Haigney, A., A. Lukacs, R. Brust, R.-K. Zhao, M. Towrie, G.M. Greetham, I. Clark, B. Illarionov, A. Bacher, R.-R. Kim, M. Fischer, S.R. Meech, and P.J. Tonge, *Vibrational*

assignment of the ultrafast infrared spectrum of the photoactivatable flavoprotein AppA. J Phys Chem B, 2012. **116**(35): p. 10722-10729.

29. Unno, M., Y. Tsukiji, K. Kubota, and S. Masuda, *N-terminal truncation does not affect the location of a conserved tryptophan in the BLUF domain of AppA from Rhodobacter sphaeroides.* J Phys Chem B, 2012. **116**(30): p. 8974-8980.

30. Masuda, S., K. Hasegawa, and T.-a. Ono, *Tryptophan at position 104 is involved in transforming light signal into changes of β-sheet structure for the signaling state in the BLUF domain of AppA.* Plant Cell Physiol, 2005. **46**(12): p. 1894-1901.

31. Pelton, J.T. and L.R. McLean, *Spectroscopic methods for analysis of protein secondary structure.* Anal Biochem, 2000. **277**(2): p. 167-176.

32. Barth, A., *Infrared spectroscopy of proteins.* Biochim Biophys Acta, 2007. **1767**(9): p. 1073-1101.

33. Haigney, A., A. Lukacs, R.-K. Zhao, A.L. Stelling, R. Brust, R.-R. Kim, M. Kondo, I. Clark, M. Towrie, G.M. Greetham, B. Illarionov, A. Bacher, W. Romisch-Margl, M. Fischer, S.R. Meech, and P.J. Tonge, *Ultrafast infrared spectroscopy of an isotope-labeled photoactivatable flavoprotein.* Biochemistry, 2011. **50**(8): p. 1321-1328.

34. Kondo, M., J. Nappa, K.L. Ronayne, A.L. Stelling, P.J. Tonge, and S.R. Meech, *Ultrafast vibrational spectroscopy of the flavin chromophore.* J Phys Chem B, 2006. **110**(41): p. 20107-20110.

35. Stelling, A.L., K.L. Ronayne, J. Nappa, P.J. Tonge, and S.R. Meech, *Ultrafast structural dynamics in BLUF domains: Transient infrared spectroscopy of AppA and its mutants.* J Am Chem Soc, 2007. **129**(50): p. 15556-15564.

36. Alexandre, M.T.A., L.J.G. van Wilderen, R. van Grondelle, K.J. Hellingwerf, M.L. Groot, and J.T.M. Kennis, *Early steps in blue light reception by plants: an ultrafast mid-infrared spectroscopic study of the LOV2 domain of phototropin.* Biophys J, 2005. **88**(1): p. 509a-509a.

37. Gauden, M., J.S. Grinstead, W. Laan, I.H. van Stokkum, M. Avila-Perez, K.C. Toh, R. Boelens, R. Kaptein, R. van Grondelle, K.J. Hellingwerf, and J.T. Kennis, *On the role of aromatic side chains in the photoactivation of BLUF domains.* Biochemistry, 2007. **46**(25): p. 7405-15.

38. Mathes, T., I.H.M. van Stokkum, C. Bonetti, P. Hegemann, and J.T.M. Kennis, *The hydrogen-bond switch reaction of the Blrb BLUF domain of Rhodobacter sphaeroides.* J Phys Chem B, 2011. **115**(24): p. 7963-7971.

39. Bonetti, C., M. Stierl, T. Mathes, I.H.M. van Stokkum, K.M. Mullen, T.A. Cohen-Stuart, R. van Grondelle, P. Hegemann, and J.T.M. Kennis, *The role of key amino acids in the photoactivation pathway of the Synechocystis Slr1694 BLUF domain.* Biochemistry, 2009. **48**(48): p. 11458-11469.

Chapter 6

1. Losi, A. and W. Gärtner, *Old chromophores, new photoactivation paradigms, trendy applications: Flavins in blue light-sensing photoreceptors.* Photochem Photobiol, 2011. **87**(3): p. 491-510.

2. Okajima, K., S. Yoshihara, Y. Fukushima, X. Geng, M. Katayama, S. Higashi, M. Watanabe, S. Sato, S. Tabata, Y. Shibata, S. Itoh, and M. Ikeuchi, *Biochemical and functional characterization of BLUF-type flavin-binding proteins of two species of Cyanobacteria.* J Biochem, 2005. **137**(6): p. 741-750.

3. Fiedler, B., T. Börner, and A. Wilde, *Phototaxis in the cyanobacterium synechocystis sp. PCC 6803: Role of different photoreceptors.* Photochem Photobiol, 2005. **81**(6): p. 1481-1488.

4. Masuda, S., K. Hasegawa, H. Ohta, and T.-a. Ono, *Crucial role in light signal transduction for the conserved Met93 of the BLUF protein PixD/Slr1694.* Plant Cell Physiol, 2008. **49**(10): p. 1600-1606.

5. Masuda, S., K. Hasegawa, A. Ishii, and T.-a. Ono, *Light-induced structural changes in a putative blue-light receptor with a novel FAD binding fold sensor of blue-light using FAD (BLUF); Slr1694 of Synechocystis sp. PCC6803.* Biochemistry, 2004. **43**(18): p. 5304-5313.

6. Anderson, S., V. Dragnea, S. Masuda, J. Ybe, K. Moffat, and C. Bauer, *Structure of a novel photoreceptor, the BLUF domain of AppA from Rhodobacter sphaeroides.* Biochemistry, 2005. **44**(22): p. 7998-8005.

7. Jung, A., J. Reinstein, T. Domratcheva, R.L. Shoeman, and I. Schlichting, *Crystal structures of the AppA BLUF domain photoreceptor provide insights into blue light-mediated signal transduction.* J Mol Biol, 2006. **362**(4): p. 717-732.

8. Grinstead, J.S., M. Avila-Perez, K.J. Hellingwerf, R. Boelens, and R. Kaptein, *Light-induced flipping of a conserved glutamine sidechain and its orientation in the AppA BLUF domain.* J Am Chem Soc, 2006. **128**(47): p. 15066-15067.

9. Laan, W., M.A. van der Horst, I.H. van Stokkum, and K.J. Hellingwerf, *Initial characterization of the primary photochemistry of AppA, a blue-light-using flavin adenine dinucleotide-domain containing transcriptional antirepressor protein from Rhodobacter sphaeroides: a key role for reversible intramolecular proton transfer from*

the flavin adenine dinucleotide chromophore to a conserved tyrosine? Photochem Photobiol, 2003. **78**(3): p. 290-7.

10. Yuan, H., S. Anderson, S. Masuda, V. Dragnea, K. Moffat, and C. Bauer, *Crystal structures of the Synechocystis photoreceptor Slr1694 reveal distinct structural states related to signaling.* Biochemistry, 2006. **45**(42): p. 12687-12694.
11. Yuan, H. and C.E. Bauer, *PixE promotes dark oligomerization of the BLUF photoreceptor PixD.* Proc. Nat. Acad. Sci., 2008. **105**(33): p. 11715-11719.
12. Yuan, H., V. Dragnea, Q. Wu, K.H. Gardner, and C.E. Bauer, *Mutational and structural studies of the PixD BLUF output signal that affects light-regulated interactions with PixE.* Biochemistry, 2011. **50**(29): p. 6365-6375.
13. Tanaka, K., Y. Nakasone, K. Okajima, M. Ikeuchi, S. Tokutomi, and M. Terazima, *Time-resolved tracking of interprotein signal transduction: Synechocystis PixD–PixE complex as a sensor of light Intensity.* J Am Chem Soc, 2012. **134**(20): p. 8336-8339.
14. Kita, A., K. Okajima, Y. Morimoto, M. Ikeuchi, and K. Miki, *Structure of a cyanobacterial BLUF protein, Tll0078, containing a novel FAD-binding blue light sensor domain.* J Mol Biol, 2005. **349**(1): p. 1-9.
15. Okajima, K., Y. Fukushima, H. Suzuki, A. Kita, Y. Ochiai, M. Katayama, Y. Shibata, K. Miki, T. Noguchi, S. Itoh, and M. Ikeuchi, *Fate determination of the flavin photoreceptions in the cyanobacterial blue light receptor TePixD (Tll0078).* J Mol Biol, 2006. **363**(1): p. 10-8.
16. Ren, S., R. Sato, K. Hasegawa, H. Ohta, and S. Masuda, *A predicted structure for the PixD–PixE complex determined by homology modeling, docking simulations, and a mutagenesis study.* Biochemistry, 2013. **52**(7): p. 1272-1279.

17. Ren, S., M. Sawada, K. Hasegawa, Y. Hayakawa, H. Ohta, and S. Masuda, *A PixD—PapB Chimeric Protein Reveals the Function of the BLUF Domain C-Terminal α-Helices for Light Signal Transduction.* Plant Cell Physiol, 2012. **53**(9): p. 1638-1647.

18. Barends, T.R.M., E. Hartmann, J.J. Griese, T. Beitlich, N.V. Kirienko, D.A. Ryjenkov, J. Reinstein, R.L. Shoeman, M. Gomelsky, and I. Schlichting, *Structure and mechanism of a bacterial light-regulated cyclic nucleotide phosphodiesterase.* Nature, 2009. **459**(7249): p. 1015-1018.

19. Berthomieu, C. and R. Hienerwadel, *Vibrational spectroscopy to study the properties of redox-active tyrosines in photosystem II and other proteins.* Biochim Biophys Acta, 2005. **1707**(1): p. 51-66.

20. Gauden, M., J.S. Grinstead, W. Laan, I.H. van Stokkum, M. Avila-Perez, K.C. Toh, R. Boelens, R. Kaptein, R. van Grondelle, K.J. Hellingwerf, and J.T. Kennis, *On the role of aromatic side chains in the photoactivation of BLUF domains.* Biochemistry, 2007. **46**(25): p. 7405-15.

21. Bonetti, C., T. Mathes, I.H.M. van Stokkum, K.M. Mullen, M.-L. Groot, R. van Grondelle, P. Hegemann, and J.T.M. Kennis, *Hydrogen bond switching among flavin and amino acid side chains in the BLUF photoreceptor observed by ultrafast infrared spectroscopy.* Biophys J, 2008. **95**(10): p. 4790-4802.

22. Bonetti, C., M. Stierl, T. Mathes, I.H.M. van Stokkum, K.M. Mullen, T.A. Cohen-Stuart, R. van Grondelle, P. Hegemann, and J.T.M. Kennis, *The role of key amino acids in the photoactivation pathway of the Synechocystis Slr1694 BLUF domain.* Biochemistry, 2009. **48**(48): p. 11458-11469.

23. Masuda, S. and C.E. Bauer, *AppA Is a blue light photoreceptor that antirepresses photosynthesis gene expression in Rhodobacter sphaeroides.* Cell, 2002. **110**(5): p. 613-623.

24. Haigney, A., A. Lukacs, R. Brust, R.-K. Zhao, M. Towrie, G.M. Greetham, I. Clark, B. Illarionov, A. Bacher, R.-R. Kim, M. Fischer, S.R. Meech, and P.J. Tonge, *Vibrational assignment of the ultrafast infrared spectrum of the photoactivatable flavoprotein AppA.* J Phys Chem B, 2012. **116**(35): p. 10722-10729.

25. Masuda, S., K. Hasegawa, and T.-a. Ono, *Light-induced structural changes of apoprotein and chromophore in the sensor of blue light using FAD (BLUF) domain of AppA for a signaling state* Biochemistry, 2005. **44**(4): p. 1215-1224.

26. Mathes, T., I.H.M. van Stokkum, M. Stierl, and J.T.M. Kennis, *Redox modulation of flavin and tyrosine determines photoinduced proton-coupled electron transfer and photoactivation of BLUF photoreceptors.* J Biol Chem, 2012. **287**(38): p. 31725-31738.

27. Hasegawa, K., S. Masuda, and T.-a. Ono, *Spectroscopic analysis of the dark relaxation process of a photocycle in a sensor of blue light using FAD (BLUF) protein Slr1694 of the cyanobacterium Synechocystis sp. PCC6803.* Plant Cell Physiol, 2005. **46**(1): p. 136-146.

28. Masuda, S., K. Hasegawa, and T.-a. Ono, *Tryptophan at position 104 is involved in transforming light signal into changes of β-sheet structure for the signaling state in the BLUF domain of AppA.* Plant Cell Physiol, 2005. **46**(12): p. 1894-1901.

29. Kondo, M., J. Nappa, K.L. Ronayne, A.L. Stelling, P.J. Tonge, and S.R. Meech, *Ultrafast vibrational spectroscopy of the flavin chromophore.* J Phys Chem B, 2006. **110**(41): p. 20107-20110.

30. Haigney, A., A. Lukacs, R.-K. Zhao, A.L. Stelling, R. Brust, R.-R. Kim, M. Kondo, I. Clark, M. Towrie, G.M. Greetham, B. Illarionov, A. Bacher, W. Romisch-Margl, M. Fischer, S.R. Meech, and P.J. Tonge, *Ultrafast infrared spectroscopy of an isotope-labeled photoactivatable flavoprotein.* Biochemistry, 2011. **50**(8): p. 1321-1328.

31. Stelling, A.L., K.L. Ronayne, J. Nappa, P.J. Tonge, and S.R. Meech, *Ultrafast structural dynamics in BLUF domains: Transient infrared spectroscopy of AppA and its mutants.* J Am Chem Soc, 2007. **129**(50): p. 15556-15564.

32. Kennis, J.T. and M.L. Groot, *Ultrafast spectroscopy of biological photoreceptors.* Curr Opin Struct Biol, 2007. **17**(5): p. 623-30.

33. Zhao, R.-K., A. Lukacs, A. Haigney, R. Brust, G.M. Greetham, M. Towrie, P.J. Tonge, and S.R. Meech, *Ultrafast transient mid IR to visible spectroscopy of fully reduced flavins.* Phys Chem Chem Phys, 2011. **13**(39): p. 17642-17648.

34. Lukacs, A., R.K. Zhao, A. Haigney, R. Brust, G.M. Greetham, M. Towrie, P.J. Tonge, and S.R. Meech, *Excited state structure and dynamics of the neutral and anionic flavin radical revealed by ultrafast transient mid-IR to visible spectroscopy.* J Phys Chem B, 2012. **116**(20): p. 5810-8.

35. Toh, K.C., I.H.M. van Stokkum, J. Hendriks, M.T.A. Alexandre, J.C. Arents, M.A. Perez, R. van Grondelle, K.J. Hellingwerf, and J.T.M. Kennis, *On the signaling mechanism and the absence of photoreversibility in the AppA BLUF domain.* Biophys J, 2008. **95**(1): p. 312-321.

36. Barth, A., *The infrared absorption of amino acid side chains.* Prog Biophys Mol Biol, 2000. **74**(3–5): p. 141-173.

37. Barth, A., *Infrared spectroscopy of proteins.* Biochim Biophys Acta, 2007. **1767**(9): p. 1073-1101.

38. Lukacs, A., A. Haigney, R. Brust, R.K. Zhao, A.L. Stelling, I.P. Clark, M. Towrie, G.M. Greetham, S.R. Meech, and P.J. Tonge, *Photoexcitation of the blue light using FAD photoreceptor AppA results in ultrafast changes to the protein matrix.* J Am Chem Soc, 2011. **133**(42): p. 16893-900.

39. Tonge, P., G.R. Moore, and C.W. Wharton, *Fourier-transform infra-red studies of the alkaline isomerization of mitochondrial cytochrome c and the ionization of carboxylic acids.* Biochem J, 1989. **258**(2): p. 599-605.

40. Kottke, T., A. Batschauer, M. Ahmad, and J. Heberle, *Blue-Light-Induced Changes in Arabidopsis Cryptochrome 1 Probed by FTIR Difference Spectroscopy.* Biochemistry, 2006. **45**(8): p. 2472-2479.

41. Henzler-Wildman, K.A., M. Lei, V. Thai, S.J. Kerns, M. Karplus, and D. Kern, *A hierarchy of timescales in protein dynamics is linked to enzyme catalysis.* Nature, 2007. **450**(7171): p. 913-916.

42. Greetham, G.M., D. Sole, I.P. Clark, A.W. Parker, M.R. Pollard, and M. Towrie, *Time-resolved multiple probe spectroscopy.* Rev Sci Instrum, 2012. **83**(10): p. 103107-5.

43. Wu, Q., W.H. Ko, and K.H. Gardner, *Structural requirements for key residues and auxiliary portions of a BLUF domain.* Biochemistry, 2008. **47**(39): p. 10271-80.

Chapter 6

1. Losi, A. and W. Gärtner, *Old chromophores, new photoactivation paradigms, trendy applications: Flavins in blue light-sensing photoreceptors.* Photochem Photobiol, 2011. **87**(3): p. 491-510.
2. Okajima, K., S. Yoshihara, Y. Fukushima, X. Geng, M. Katayama, S. Higashi, M. Watanabe, S. Sato, S. Tabata, Y. Shibata, S. Itoh, and M. Ikeuchi, *Biochemical and functional characterization of BLUF-type flavin-binding proteins of two species of Cyanobacteria.* J Biochem, 2005. **137**(6): p. 741-750.
3. Fiedler, B., T. Börner, and A. Wilde, *Phototaxis in the cyanobacterium synechocystis sp. PCC 6803: Role of different photoreceptors.* Photochem Photobiol, 2005. **81**(6): p. 1481-1488.
4. Masuda, S., K. Hasegawa, H. Ohta, and T.-a. Ono, *Crucial role in light signal transduction for the conserved Met93 of the BLUF protein PixD/Slr1694.* Plant Cell Physiol, 2008. **49**(10): p. 1600-1606.
5. Masuda, S., K. Hasegawa, A. Ishii, and T.-a. Ono, *Light-induced structural changes in a putative blue-light receptor with a novel FAD binding fold sensor of blue-light using FAD (BLUF); Slr1694 of Synechocystis sp. PCC6803.* Biochemistry, 2004. **43**(18): p. 5304-5313.
6. Anderson, S., V. Dragnea, S. Masuda, J. Ybe, K. Moffat, and C. Bauer, *Structure of a novel photoreceptor, the BLUF domain of AppA from Rhodobacter sphaeroides.* Biochemistry, 2005. **44**(22): p. 7998-8005.

7. Jung, A., J. Reinstein, T. Domratcheva, R.L. Shoeman, and I. Schlichting, *Crystal structures of the AppA BLUF domain photoreceptor provide insights into blue light-mediated signal transduction.* J Mol Biol, 2006. **362**(4): p. 717-732.

8. Grinstead, J.S., M. Avila-Perez, K.J. Hellingwerf, R. Boelens, and R. Kaptein, *Light-induced flipping of a conserved glutamine sidechain and its orientation in the AppA BLUF domain.* J Am Chem Soc, 2006. **128**(47): p. 15066-15067.

9. Laan, W., M.A. van der Horst, I.H. van Stokkum, and K.J. Hellingwerf, *Initial characterization of the primary photochemistry of AppA, a blue-light-using flavin adenine dinucleotide-domain containing transcriptional antirepressor protein from Rhodobacter sphaeroides: a key role for reversible intramolecular proton transfer from the flavin adenine dinucleotide chromophore to a conserved tyrosine?* Photochem Photobiol, 2003. **78**(3): p. 290-7.

10. Yuan, H., S. Anderson, S. Masuda, V. Dragnea, K. Moffat, and C. Bauer, *Crystal structures of the Synechocystis photoreceptor Slr1694 reveal distinct structural states related to signaling.* Biochemistry, 2006. **45**(42): p. 12687-12694.

11. Yuan, H. and C.E. Bauer, *PixE promotes dark oligomerization of the BLUF photoreceptor PixD.* Proc. Nat. Acad. Sci., 2008. **105**(33): p. 11715-11719.

12. Yuan, H., V. Dragnea, Q. Wu, K.H. Gardner, and C.E. Bauer, *Mutational and structural studies of the PixD BLUF output signal that affects light-regulated interactions with PixE.* Biochemistry, 2011. **50**(29): p. 6365-6375.

13. Tanaka, K., Y. Nakasone, K. Okajima, M. Ikeuchi, S. Tokutomi, and M. Terazima, *Time-resolved tracking of interprotein signal transduction: Synechocystis PixD–PixE complex as a sensor of light Intensity.* J Am Chem Soc, 2012. **134**(20): p. 8336-8339.

14. Kita, A., K. Okajima, Y. Morimoto, M. Ikeuchi, and K. Miki, *Structure of a cyanobacterial BLUF protein, Tll0078, containing a novel FAD-binding blue light sensor domain.* J Mol Biol, 2005. **349**(1): p. 1-9.

15. Okajima, K., Y. Fukushima, H. Suzuki, A. Kita, Y. Ochiai, M. Katayama, Y. Shibata, K. Miki, T. Noguchi, S. Itoh, and M. Ikeuchi, *Fate determination of the flavin photoreceptions in the cyanobacterial blue light receptor TePixD (Tll0078).* J Mol Biol, 2006. **363**(1): p. 10-8.

16. Ren, S., R. Sato, K. Hasegawa, H. Ohta, and S. Masuda, *A predicted structure for the PixD–PixE complex determined by homology modeling, docking simulations, and a mutagenesis study.* Biochemistry, 2013. **52**(7): p. 1272-1279.

17. Ren, S., M. Sawada, K. Hasegawa, Y. Hayakawa, H. Ohta, and S. Masuda, *A PixD—PapB Chimeric Protein Reveals the Function of the BLUF Domain C-Terminal α-Helices for Light Signal Transduction.* Plant Cell Physiol, 2012. **53**(9): p. 1638-1647.

18. Barends, T.R.M., E. Hartmann, J.J. Griese, T. Beitlich, N.V. Kirienko, D.A. Ryjenkov, J. Reinstein, R.L. Shoeman, M. Gomelsky, and I. Schlichting, *Structure and mechanism of a bacterial light-regulated cyclic nucleotide phosphodiesterase.* Nature, 2009. **459**(7249): p. 1015-1018.

19. Berthomieu, C. and R. Hienerwadel, *Vibrational spectroscopy to study the properties of redox-active tyrosines in photosystem II and other proteins.* Biochim Biophys Acta, 2005. **1707**(1): p. 51-66.

20. Gauden, M., J.S. Grinstead, W. Laan, I.H. van Stokkum, M. Avila-Perez, K.C. Toh, R. Boelens, R. Kaptein, R. van Grondelle, K.J. Hellingwerf, and J.T. Kennis, *On the role of*

aromatic side chains in the photoactivation of BLUF domains. Biochemistry, 2007. **46**(25): p. 7405-15.

21. Bonetti, C., T. Mathes, I.H.M. van Stokkum, K.M. Mullen, M.-L. Groot, R. van Grondelle, P. Hegemann, and J.T.M. Kennis, *Hydrogen bond switching among flavin and amino acid side chains in the BLUF photoreceptor observed by ultrafast infrared spectroscopy*. Biophys J, 2008. **95**(10): p. 4790-4802.
22. Bonetti, C., M. Stierl, T. Mathes, I.H.M. van Stokkum, K.M. Mullen, T.A. Cohen-Stuart, R. van Grondelle, P. Hegemann, and J.T.M. Kennis, *The role of key amino acids in the photoactivation pathway of the Synechocystis Slr1694 BLUF domain.* Biochemistry, 2009. **48**(48): p. 11458-11469.
23. Masuda, S. and C.E. Bauer, *AppA Is a blue light photoreceptor that antirepresses photosynthesis gene expression in Rhodobacter sphaeroides.* Cell, 2002. **110**(5): p. 613-623.
24. Haigney, A., A. Lukacs, R. Brust, R.-K. Zhao, M. Towrie, G.M. Greetham, I. Clark, B. Illarionov, A. Bacher, R.-R. Kim, M. Fischer, S.R. Meech, and P.J. Tonge, *Vibrational assignment of the ultrafast infrared spectrum of the photoactivatable flavoprotein AppA.* J Phys Chem B, 2012. **116**(35): p. 10722-10729.
25. Masuda, S., K. Hasegawa, and T.-a. Ono, *Light-induced structural changes of apoprotein and chromophore in the sensor of blue light using FAD (BLUF) domain of AppA for a signaling state* Biochemistry, 2005. **44**(4): p. 1215-1224.
26. Mathes, T., I.H.M. van Stokkum, M. Stierl, and J.T.M. Kennis, *Redox modulation of flavin and tyrosine determines photoinduced proton-coupled electron transfer and photoactivation of BLUF photoreceptors.* J Biol Chem, 2012. **287**(38): p. 31725-31738.

27. Hasegawa, K., S. Masuda, and T.-a. Ono, *Spectroscopic analysis of the dark relaxation process of a photocycle in a sensor of blue light using FAD (BLUF) protein Slr1694 of the cyanobacterium Synechocystis sp. PCC6803.* Plant Cell Physiol, 2005. **46**(1): p. 136-146.

28. Masuda, S., K. Hasegawa, and T.-a. Ono, *Tryptophan at position 104 is involved in transforming light signal into changes of β-sheet structure for the signaling state in the BLUF domain of AppA.* Plant Cell Physiol, 2005. **46**(12): p. 1894-1901.

29. Kondo, M., J. Nappa, K.L. Ronayne, A.L. Stelling, P.J. Tonge, and S.R. Meech, *Ultrafast vibrational spectroscopy of the flavin chromophore.* J Phys Chem B, 2006. **110**(41): p. 20107-20110.

30. Haigney, A., A. Lukacs, R.-K. Zhao, A.L. Stelling, R. Brust, R.-R. Kim, M. Kondo, I. Clark, M. Towrie, G.M. Greetham, B. Illarionov, A. Bacher, W. Romisch-Margl, M. Fischer, S.R. Meech, and P.J. Tonge, *Ultrafast infrared spectroscopy of an isotope-labeled photoactivatable flavoprotein.* Biochemistry, 2011. **50**(8): p. 1321-1328.

31. Stelling, A.L., K.L. Ronayne, J. Nappa, P.J. Tonge, and S.R. Meech, *Ultrafast structural dynamics in BLUF domains: Transient infrared spectroscopy of AppA and its mutants.* J Am Chem Soc, 2007. **129**(50): p. 15556-15564.

32. Kennis, J.T. and M.L. Groot, *Ultrafast spectroscopy of biological photoreceptors.* Curr Opin Struct Biol, 2007. **17**(5): p. 623-30.

33. Zhao, R.-K., A. Lukacs, A. Haigney, R. Brust, G.M. Greetham, M. Towrie, P.J. Tonge, and S.R. Meech, *Ultrafast transient mid IR to visible spectroscopy of fully reduced flavins.* Phys Chem Chem Phys, 2011. **13**(39): p. 17642-17648.

34. Lukacs, A., R.K. Zhao, A. Haigney, R. Brust, G.M. Greetham, M. Towrie, P.J. Tonge, and S.R. Meech, *Excited state structure and dynamics of the neutral and anionic flavin radical revealed by ultrafast transient mid-IR to visible spectroscopy.* J Phys Chem B, 2012. **116**(20): p. 5810-8.

35. Toh, K.C., I.H.M. van Stokkum, J. Hendriks, M.T.A. Alexandre, J.C. Arents, M.A. Perez, R. van Grondelle, K.J. Hellingwerf, and J.T.M. Kennis, *On the signaling mechanism and the absence of photoreversibility in the AppA BLUF domain.* Biophys J, 2008. **95**(1): p. 312-321.

36. Barth, A., *The infrared absorption of amino acid side chains.* Prog Biophys Mol Biol, 2000. **74**(3–5): p. 141-173.

37. Barth, A., *Infrared spectroscopy of proteins.* Biochim Biophys Acta, 2007. **1767**(9): p. 1073-1101.

38. Lukacs, A., A. Haigney, R. Brust, R.K. Zhao, A.L. Stelling, I.P. Clark, M. Towrie, G.M. Greetham, S.R. Meech, and P.J. Tonge, *Photoexcitation of the blue light using FAD photoreceptor AppA results in ultrafast changes to the protein matrix.* J Am Chem Soc, 2011. **133**(42): p. 16893-900.

39. Tonge, P., G.R. Moore, and C.W. Wharton, *Fourier-transform infra-red studies of the alkaline isomerization of mitochondrial cytochrome c and the ionization of carboxylic acids.* Biochem J, 1989. **258**(2): p. 599-605.

40. Kottke, T., A. Batschauer, M. Ahmad, and J. Heberle, *Blue-Light-Induced Changes in Arabidopsis Cryptochrome 1 Probed by FTIR Difference Spectroscopy.* Biochemistry, 2006. **45**(8): p. 2472-2479.

41. Henzler-Wildman, K.A., M. Lei, V. Thai, S.J. Kerns, M. Karplus, and D. Kern, *A hierarchy of timescales in protein dynamics is linked to enzyme catalysis.* Nature, 2007. **450**(7171): p. 913-916.

42. Greetham, G.M., D. Sole, I.P. Clark, A.W. Parker, M.R. Pollard, and M. Towrie, *Time-resolved multiple probe spectroscopy.* Rev Sci Instrum, 2012. **83**(10): p. 103107-5.

43. Wu, Q., W.H. Ko, and K.H. Gardner, *Structural requirements for key residues and auxiliary portions of a BLUF domain.* Biochemistry, 2008. **47**(39): p. 10271-80.